Foundations and Trends® in Communications and Information Theory
Vol. 11, No. 3-4 (2014) 185–396

DOI: 10.1561/0100000088

now
the essence of knowledge

Energy Efficiency in Wireless Networks via Fractional Programming Theory

Alessio Zappone
TU Dresden
alessio.zappone@tu-dresden.de

Eduard Jorswieck
TU Dresden
eduard.jorswieck@tu-dresden.de

Contents

List of Acronyms **186**

Notation **189**

1 Introduction **190**
1.1 Energy efficiency of a point-to-point system 193
1.2 Energy efficiency of a communication network 203
1.3 Fractional programming for energy efficiency 208
1.4 State of the art and future directions 210

2 Fractional Programming Theory **215**
2.1 Generalized concavity 217
2.2 Generalized concavity of ratios 228
2.3 A taxonomy of fractional problems 231

3 Algorithms for Fractional Programming **236**
3.1 Linear fractional problems 236
3.2 Concave-convex fractional problems 238
3.3 Max-Min fractional programming 248
3.4 Sum and product of ratios 250
3.5 Global optimality in fractional programming 251

4 Energy efficiency in wireless networks: centralized approaches 255
4.1 Power allocation in wireless networks 256
4.2 Resource allocation in MIMO wireless networks 279
4.3 Resource allocation in multi-carrier wireless networks . . . 307
4.4 Summary 325

5 Energy efficiency in wireless networks: distributed approaches 327
5.1 Power allocation in wireless networks 328
5.2 Resource allocation in MIMO wireless networks 336
5.3 Resource allocation in multi-carrier wireless networks . . . 349
5.4 Summary 353

6 Extensions and future lines of research 354
6.1 Global optimality in energy efficiency problems 354
6.2 Resource allocation with imperfect CSI 356
6.3 Energy efficiency in networks with stochastic topologies . . 357

Appendices 359

A Fundamentals of linear algebra 360

B Fundamentals of optimization theory 363
B.1 Convex optimization 363
B.2 Monotonic optimization 368

C Fundamentals of game theory 375
C.1 Games in strategic normal form 375

Acknowledgments 379

References 380

Abstract

This monograph presents a unified framework for energy efficiency maximization in wireless networks via fractional programming theory.

The definition of energy efficiency is introduced, with reference to single-user and multi-user wireless networks, and it is observed how the problem of resource allocation for energy efficiency optimization is naturally cast as a fractional program. An extensive review of the state-of-the-art in energy efficiency optimization by fractional programming is provided, with reference to centralized and distributed resource allocation schemes.

A solid background on fractional programming theory is provided. The key-notion of generalized concavity is presented and its strong connection with fractional functions described. A taxonomy of fractional problems is introduced, and for each class of fractional problem, general solution algorithms are described, discussing their complexity and convergence properties.

The described theoretical and algorithmic framework is applied to solve energy efficiency maximization problems in practical wireless networks. A general system and signal model is developed which encompasses many relevant special cases, such as one-hop and two-hop heterogeneous networks, multi-cell networks, small-cell networks, device-to-device systems, cognitive radio systems, and hardware-impaired networks, wherein multiple-antennas and multiple subcarriers are (possibly) employed. Energy-efficient resource allocation algorithms are developed, considering both centralized, cooperative schemes, as well as distributed approaches for self-organizing networks.

Finally, some remarks on future lines of research are given, stating some open problems that remain to be studied. It is shown how the described framework is general enough to be extended in these directions, proving useful in tackling future challenges that may arise in the design of energy-efficient future wireless networks.

A. Zappone and E. A. Jorswieck . *Energy Efficiency in Wireless Networks via Fractional Programming Theory*. Foundations and Trends® in Communications and Information Theory, vol. 11, no. 3-4, pp. 185–396, 2014.
DOI: 10.1561/0100000088.

List of Acronyms

AF: amplify-and-forward

BC: broadcast channel

BER: bit error rate

BR: best-response

BRD: best-response dynamics

CCFP: concave-convex fractional problem

CLFP: concave-linear fractional problem

CoMP: coordinated multi-point

CSI: channel state information

D2D: device-to-device

DPC: Dirty paper coding

EVD: eigenvalue decomposition

GEE: global energy efficiency

GNE: generalized Nash equilibrium

IBC: interference broadcast channel

IC: interference channel

IMAC: interference multiple-access-channel

KKT: Karush-Kuhn-Tucker

LFP: linear fractional problem

LHS: left-hand-side

LMMSE: linear minimum mean squared error

MAC: multiple-access-channel

MC: multi-carrier

MIMO: multiple-input multiple-output

MMFP: max-min fractional problem

NE: Nash equilibrium

OFDMA: orthogonal frequency division multiple-access

P2P: point-to-point

PC: pseudo-concave

PL: pseudo-linear

PoRP: product-of-ratios problem

PPP: Poisson point process

QC: quasi-concave

QL: quasi-linear

QoS: quality-of-service

RHS: right-hand-side

RMT: random matrix theory

SC: single-carrier

SG: stochastic geometry

SIC: successive interference cancellation

SINR: signal-to-interference-plus-noise-ratio

SISO: single-input single-output

SNR: signal-to-noise-ratio

SoRP: sum-of-ratios problem

SPC: strictly pseudo-concave

SQC: strictly quasi-concave

SVD: singular value decomposition

WMEE: weighted minimum energy efficiency

WPEE: weighted product energy efficiency

WSEE: weighted sum energy efficiency

ZF: zero-forcing

Notation

Boldface upper-case and lower-case letters denote matrices and vectors, respectively.

$\|\boldsymbol{x}\|$, $\boldsymbol{x}^T$, $\boldsymbol{x}^H$ denote Euclidean norm, transpose, and conjugate transpose of the n-dimensional column vector $\boldsymbol{x} = \{x_i\}_{i=1}^n$. $\mathbf{0}_n$ and $\mathbf{1}_n$ denote an all zero and an all one n-dimensional vector, respectively. Component-wise vector ordering is used, i.e. $\boldsymbol{x} \succeq \boldsymbol{y}$ means $x_i \geq y_i$, for all $i = 1, \ldots, N$.

$\mathrm{tr}(\boldsymbol{X})$, $\boldsymbol{X}^T$, $\boldsymbol{X}^H$, $|\boldsymbol{X}|$, $\boldsymbol{X}^{-1}$, $\boldsymbol{X}^+$, $\|\boldsymbol{X}\|$ denote trace, transpose, conjugate transpose, determinant, inverse, pseudo-inverse, and Frobenius norm of the matrix $\boldsymbol{X}$. $\boldsymbol{I}_n$, $\boldsymbol{O}_{m,n}$, and $\mathrm{diag}(\boldsymbol{x})$ denote the identity matrix of order n, an all zero $m \times n$ matrix, and a diagonal matrix with $\boldsymbol{x}$ on the diagonal, respectively. Löwner matrix order is used, i.e. $\boldsymbol{X} \succeq \boldsymbol{Y}$ means $\boldsymbol{X} - \boldsymbol{Y}$ is positive semidefinite. $\otimes$ denotes the Kronecker matrix product.

When applied to a set $\mathcal{S}$, the symbol $|\mathcal{S}|$ denotes the cardinality of $\mathcal{S}$.

$\mathbb{E}$, $\mathbb{R}$, and $\mathbb{C}$ denote statistical expectation, the field of real numbers, and the field of complex numbers. $\mathbb{R}_+$ and $\mathbb{R}_{++}$ denote the set of nonnegative real numbers and the set of positive real numbers, respectively. We say that a function $f(p)$ is $o(p)$ if $\lim_{p \to +\infty} \dfrac{f(p)}{p} = 0$.

1

Introduction

Over the last years, energy-aware optimization of wireless communication networks has become a very popular research topic [194, 74, 104], due to at least three main reasons:

- The exponential increase of connected devices that wireless communications have been experiencing, poses serious sustainable growth concerns. The number of devices connected to the internet is larger than the size of the world population. By 2020, there might be more than 50 Billion devices or more than 6 devices per person connected to the internet. The IP traffic forecast for 2014 is more than 60 Exabytes (1000^6 Bytes) per month. Most connections will be wireless because most devices are small and mobile. In 5G networks, the goal is set to 1000 times higher data rates compared to present systems, but it is clear that trying to achieve this goal by a proportional increase of the transmit power would soon lead to an unmanageable energy demand. The 1000x data-rate increase should be achieved at a similar energy consumption as today's networks, which calls for a 1000x increase of the energy efficiency.

- The rapid expansion of wireless networks causes also environmental concerns. Even nowadays, information and communication technology (ICT) infrastructures consume more than 3% of the world-wide energy, out of which about 60% is consumed by base stations, which causes about 2% of the world-wide CO_2 emissions. Given the rate at which wireless connected devices are increasing, the situation will eventually escalate, if no countermeasure is taken. This is acknowledged as key-issue by GSMA (green manifesto), which demands a reduction of CO_2 emissions per connection by 40% until 2020, and by NGMN, which also declares energy saving as a top priority. In addition to CO_2 emissions, electromagnetic pollution is also another concern to be dealt with.

- Besides sustainable growth and ecological concerns, economical reasons drive the development of novel energy-efficient ICT, too. Reducing energy consumptions allows network operators to save on electricity bills and maintenance costs, which makes energy efficiency a very popular topic not only in the academic world but also among industries. As an example, many leading telecommunication companies have formed the GreenTouch consortium (http://www.greentouch.org), whose goal is an increase of energy efficiency by a factor 1000 compared to 2010.

The numbers for the breakdown of the conventional cellular system base station power consumption differ between vendors, base station types, and location. More than 50% are consumed by the power amplifier including feeder, about 10% by the digital and analog signal processing, and about 20% by the cooling system. In general, energy efficiency can be improved on all technology layers including the network deployment strategies: hardware components and RF front-ends, physical layer with link adaptation, adaptive multiple access and resource allocation, and adaptive network management.

This monograph focuses on energy-efficient wireless network design including resource allocation, scheduling, precoding, relaying, and decoding. Starting from simple point-to-point (P2P) systems and then gradually moving towards more complex interference networks, the energy efficiency is defined and its properties characterized. It is shown

how the energy efficiency is naturally defined by fractional functions, thus establishing that a key-role in the modeling, analysis, and optimization of energy efficiency is played by *fractional programming*, a branch of optimization theory specifically concerned with the properties and optimization of fractional functions. The monograph introduces fractional programming theory, illustrating how it can be used to formulate and handle energy efficiency optimization problems. More in detail, the monograph is divided into three main parts.

The first part provides a solid description of fractional programming theory and generalized concavity. The classes of quasi-concave and pseudo-concave functions are characterized, detailing their properties and highlighting the key role they play in fractional programming theory. The connection between fractional programming and generalized concavity is described in detail, and a taxonomy of fractional problems is introduced. We consider the classes of fractional problems that have proved most useful in the energy-efficient design of wireless networks: linear fractional problem (LFP), concave-convex fractional problem (CCFP), max-min fractional problem (MMFP), sum-of-ratios problem (SoRP), and product-of-ratios problem (PoRP).

After illustrating the theoretical aspects of fractional programming, the second part of the monograph focuses on the algorithmic side of fractional programming. For each class of introduced fractional problems, general solution algorithms are presented, which are able to solve any generic instance of the corresponding problem class. The analysis provides both intuitive insights into the algorithms and a mathematically rigorous treatment, including complexity/performance trade offs and sub-optimal algorithm development.

Finally, the third part of the monograph deals with practical applications, in which we show how the developed framework is used to optimize the energy efficiency of practical wireless networks. In particular, we show how fractional programming is extremely useful for the optimization of the energy efficiency of multiuser, multi-hop, multiple antenna, multi-carrier (MC), and multi-cell networks, which will all be key technologies in future wireless networks such as 5G. Both cooperative schemes to be centrally implemented and decentralized algorithms

which allow for self-organizing networks are discussed, clearly pointing out advantages and disadvantages of the two approaches. In the decentralized setting, it is shown how fractional programming is used together with game theory to analyze the existence and uniqueness of stable equilibria of the resource allocation problem, and to devise distributed resource allocation algorithms.

We should mention that as far as applications to wireless systems are concerned, the focus will be on networks with deterministic topology, which are more well-established at this point in time, as opposed to stochastic topologies which have started to emerge recently and in which the position of the nodes and the interference levels are treated as random processes. However, we stress that fractional programming is not restricted only to deterministic topologies, but can be applied to stochastic networks, too. However, in this case, additional mathematical tools like random matrix theory (RMT) [165, 47] and stochastic geometry (SG) [11, 175] are required to statistically characterize the network interference levels. More details on this issue will be reported in Chapter 6.

1.1 Energy efficiency of a point-to-point system

A general definition of the efficiency with which a system uses a given resource, is the benefit-cost ratio. The ratio between the goods produced by using a given resource and the corresponding incurred cost naturally measures the income per unit cost. This general definition of efficiency applies to all fields of science, from physics to economics, and wireless communication is no exception.

As far as wireless communications are concerned, the cost is represented by the amount of energy consumed to operate the system. To elaborate, let us consider a P2P link, and as a first introductory example assume a single-input single-output (SISO), single-carrier (SC) system. The transmit power is p and the signal-to-noise ratio (SNR) at the receiver is γ. If the transmission takes T seconds to complete, the consumed energy will be

$$\mathrm{E}(p) = T(\mu p + P_c) \text{ [Joule]} , \tag{1.1}$$

wherein $\mu = 1/\eta$, with η the efficiency of the transmit power amplifier, while P_c includes the power dissipated in all other circuit blocks of the transmitter and receiver to operate the terminals. We should remark that the two underlying assumptions in (1.1) are that the transmit amplifier operates in its linear region, and that the circuit power P_c is a fixed power cost which depends neither on the transmit power p, nor on the communication rate R. Both assumptions are typically met in wireless communication systems, which are operated so as to ensure the amplifiers operate in the linear region of their transfer function, and in which the hardware-dissipated power is a constant power offset [8]. Indeed, the energy model in (1.1) has become a canonical choice in wireless network design [105, 84, 60] and for this reason in this monograph we will focus on the model in (1.1). Nevertheless a more general energy consumption model can be written as

$$\mathrm{E}(p, R) = T \left(\mu p + \sum_{n=2}^{N} c_n p^n + P_c(p, R) \right) \text{ [Joule]} , \qquad (1.2)$$

wherein $\mu p + \sum_{n=2}^{N} c_n p^n$ is the transfer function of the amplifier, also including non-linear terms, whereas $P_c(p, R)$ models the functional relationship between the hardware-dissipated power and the transmit power and communication rate. We remark that here R is the fixed rate at which communication is taking place, and is not a function of the transmit power. This more general model can be useful in specific scenarios. Some examples are:

- Very high peak-to-average power ratio of the transmit signals, or very narrow linear region of the transmit amplifier, which make it difficult to guarantee the absence of higher-order distortions.

- Resource allocation schemes in which the modulation order is one optimization variable, which would make P_c dependent on R through the allocation of the modulation scheme. Some examples in this sense can be found in [119, 46].

- In multiple-antenna systems, if the transmit radio-frequency chains can be adaptively switched-off and on, it would be possible to reduce the power consumption by switching off the in-

active transmit chains. This would cause the circuit power P_c to depend on the rank of the transmit covariance matrix, and so on the transmit power. However, this not a typical operation condition in communication networks, in which instead the inactive transmit chains are usually left in idle mode, thereby leaving the per-chain hardware power consumption unaltered.

As a final remark on the choice of the energy consumption model, we stress that the theory of fractional optimization to be described in the sequel, applies to the more general model in (1.2), too. However, when (1.2) is used, we might have to deal with computational complexity issues. As it will become clear after Chapter 3, energy efficiency optimization problems can be globally solved with limited complexity, only if the function $E(p, R)$ is convex. If this requirement does not hold, then the complexity required for resource allocation is in general exponential.

As for the income resulting from the use of a given amount of energy, it can be measured by many different metrics, and the choice depends on the particular system to design, but also on subjective considerations regarding the particular physical quantity which needs to be optimized [181, 78]. For example, if the goal is to have a system with a large coverage, then the income is well-represented by the system coverage radius. Instead, if the goal is to serve as many users as possible, than the number of serviced users should be taken as system benefit. Many similar examples can be made, and in all cases we would be left with a ratio to optimize, which can be managed by fractional programming. However, in this monograph we will focus our attention on the communication aspect of a wireless network, measuring the income of the system as the amount of data that can be reliably transmitted to the receiver in the time interval T. Even restricting our focus to this scenario, more than one performance function can be used to measure the system income, each one with advantages and disadvantages. A first approach is to use the system capacity, defining the income in the interval T as $TW \log_2(1+\gamma)$, with W the communication bandwidth. However, this metric does not account for the actual communication bit error rate (BER). For this reason, another proposed function is $TR(1-e^{-\gamma})$,

with R the communication rate and $(1-e^{-\gamma})$ an approximation of the BER. If the channel h is rapidly varying, these two functions can be replaced by their ergodic counterpart, obtained by averaging with respect to the channel. Instead, in scenarios with a slowly-varying channel h, a meaningful performance function is $TR(1-p_{out}(\gamma))$, with p_{out} the communication outage probability. A common feature of all presented metrics, is that they depend on the SNR γ. Then, we can include all of these special cases by considering a generic function $Tf(\gamma)$, with f the so-called efficiency function, to be specified according to the particular considered system.

Finally, we can give the following definition.

Definition 1.1. SISO SC Energy Efficiency
The energy efficiency of a P2P SISO SC system is

$$\mathrm{EE} = \frac{Tf(\gamma)}{T(\mu p + P_c)} = \frac{f(\gamma)}{\mu p + P_c}[\text{bit/Joule}] \,. \tag{1.3}$$

The energy efficiency (1.3) is measured in bit/Joule, thereby measuring the amount of data that can be reliably transmitted per Joule of consumed energy. Fig. 1.1 shows the shape of (1.3) when the efficiency function is chosen as the achievable rate.

It is seen that the energy efficiency is not monotone in p, but instead is a unimodal function that increases up to a point, and then decreases to zero. This is the key feature which allows us to save energy by energy-efficient resource allocation. Indeed, unlike traditional performance measures such as achievable rate, BER, mean square error, which are typically optimized by using all of the available power, the transmit power level that maximizes the energy efficiency is in general lower than the maximum feasible power. For example, in Fig. 1.1 the energy efficiency is maximized for $p = 0.48\,\mathrm{W}$ and the transmitter will use exactly this power level even if it is lower than the maximum feasible power. This optimum power level represents the best trade-off between achieving fast and reliable communication and saving energy. These consideration also hold for the other mentioned efficiency functions, which result in similar shapes of the energy efficiency.

However, it is clear that not all functions $f(\gamma)$ yield a similar energy efficiency as in Fig.1.1. More in general, what are the properties that

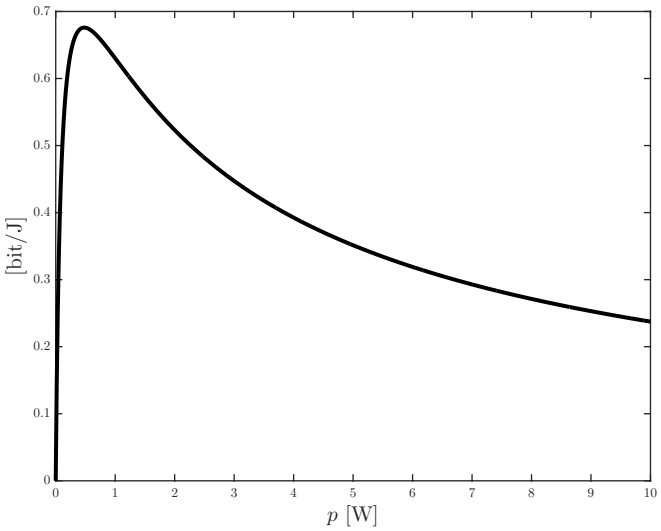

Figure 1.1: Energy efficiency with $f(\gamma(p)) = \log_2(1+p)$ [bit/s], $\mu = 1$, $P_c = 0.1$ [W]. The optimum power level is $p = 0.48$ [W].

$f(\gamma)$ should enjoy to obtain a physically meaningful energy efficiency? We have already implicitly introduced the first property, when we expressed the energy efficiency in bit/Joule. Indeed, for this to be true, we should require the following.

Property 1. *The efficiency function $f(\gamma)$ is measured in [bit/s].*

We have also intuitively already introduced the second property. For energy efficiency optimization to result in energy savings, we require that the energy efficiency must decrease for growing p, approaching 0 as $p \to \infty$. Moreover, clearly the efficiency should be zero if we do not transmit at all. This translates into the following requirements for f.

Property 2. *$f(\gamma)$ must be such that $f(0) = 0$ and $f(\gamma(p)) = o(p)$.*

The third and final property derives by the consideration that a meaningful f must reflect the fact that the benefit obtained from the system increases with the SNR γ.

Property 3. *$f(\gamma)$ must be increasing with γ.*

Equipped with this framework, we can move on and extend our definition to slightly more complex scenarios. We always consider a P2P system, but now we assume the optimization variable is not a scalar power but rather an N-dimensional matrix $\boldsymbol{P}$. For example, this could be the case of a multiple-input multiple-output (MIMO) system with $\boldsymbol{P}$ being the transmit covariance matrix. Considering the capacity as efficiency function, denoting by σ^2 the noise power at the receiver, and by $\boldsymbol{H}$ the MIMO channel matrix, the following definition should be clear.

Definition 1.2. MIMO Energy Efficiency
The energy efficiency of a MIMO P2P system is

$$\mathrm{EE} = \frac{W \log_2 \left| \boldsymbol{I}_N + \frac{1}{\sigma^2} \boldsymbol{H}\boldsymbol{P}\boldsymbol{H}^H \right|}{\mu \mathrm{tr}(\boldsymbol{P}) + P_c} [\text{bit/Joule}] \, . \tag{1.4}$$

If instead, we have a MC P2P system with N orthogonal subcarriers, the matrix $\boldsymbol{P}$ reduces to its diagonal vector $\boldsymbol{p} = \{p_n\}_{n=1}^N$. Then, denoting by γ_n the SNR on subcarrier n, Definition 1.2 simplifies as follows

Definition 1.3. MC Energy Efficiency
The energy efficiency of a MC P2P system is

$$\mathrm{EE} = \frac{W \sum_{n=1}^N \log_2(1+\gamma_n)}{\mu \sum_{n=1}^N p_n + P_c} [\text{bit/Joule}] \, . \tag{1.5}$$

Typically, an energy efficiency optimization problem is formulated as the maximization of the energy efficiency with respect to $\boldsymbol{P} \in \mathcal{S}$ where the set $\mathcal{S}$ of feasible power allocations models all constraints including power constraints $\mathrm{tr}(\boldsymbol{P}) \leq P_{max}$, quality of service (QoS) constraints $\log_2 \left| \boldsymbol{I}_N + 1/\sigma^2 \boldsymbol{H}\boldsymbol{P}\boldsymbol{H}^H \right| \geq R_{min}$, or other constraints.

Before closing this section, we should mention that another popular approach to energy efficiency does not consider the fractional approach, but rather takes a difference-based approach. More specifically, denoting by $R(p)$ the system achievable data-rate, another possible definition of energy efficiency is the function [143]

$$u(p) = R(p) - \mu(p + P_c) \text{ [bits/s]} \, , \tag{1.6}$$

with μ a constant term with dimensions bit/s/W. This approach is typically used in conjunction with pricing techniques and is not directly related to ratios. However, in the following we will not consider the difference-based approach, focusing instead on the fractional definition of energy efficiency. The motivation for this choice is based on both physical and mathematical arguments:

- As already mentioned, an efficiency is intrinsically a ratio, and in particular the ratio between the *output of the system* over the *consumed goods by the system*. This definition is well-established in communication theory, too. For example, the spectral efficiency of a communication system is defined as the number of transmitted bits per unit of bandwidth. Replacing spectrum with energy yields the definition of energy efficiency as the number of transmitted bits per unit of energy.

- In the difference-based approach, the energy efficiency is defined as $R(p) - \mu p$. This quantity is measured in bit/s and represents the difference between the rate minus a term which measures the cost in bit/s associated to the use of the transmit power. Thus, this definition of energy efficiency lacks the strong physical interpretation of *output of the system* over *consumed goods by the system*, being instead more related to the net gain in bit/s resulting from the use of the system, rather than to the efficiency with which the available Joules of energy are used to transmit information bits.

- Finally, from a mathematical point of view, the difference-based approach is closely connected to the fractional-based approach. More in detail, the maximization of the ratio $f(p)/g(p)$ is mathematically equivalent to the maximization of the difference $f(p) - \mu g(p)$ for a specific choice of the parameter μ. In order to elaborate further on this point, we need to introduce a second, more mathematical, approach to energy efficiency, based on multi-objective optimization. This is done in the coming section.

1.1.1 Bi-objective energy-efficient optimization

Leveraging the theory of multi-objective optimization, we can mathematically capture the trade-off between achieving a reliable communication and saving power, by formulating a bi-objective optimization problem in which the objectives to maximize are the benefit of the system $f(\gamma(p))$, and the negative of the power consumption, namely,

$$\max_{p\in\mathcal{P}}\{f(\gamma(p)); -(p+P_c)\}\ , \tag{1.7}$$

with $\mathcal{P}$ the set of admissible transmit powers, which can account for constraints such as a maximum feasible power constraint as well as QoS constraints. Employing the scalarization technique [20, 28], (1.7) can be converted into the scalar problem

$$\max_{p\in\mathcal{P}} w_1 f(\gamma(p)) - w_2(p+P_c)\ , \tag{1.8}$$

wherein the scalar objective is given by the linear combination of the two objectives in (1.7) and the non-negative weights w_1 and w_2 weigh the priority given to the two contrasting objectives. For any choice of the weights, the solution of (1.8) is on the Pareto-boundary of (1.7), and we see that the two extreme points of the boundary are obtained when either $w_2 = 0$, and (1.8) reduces to the maximization of $f(\gamma(p))$ (e.g. rate maximization), or when $w_1 = 0$, and (1.8) reduces to power minimization.

Using this approach, the critical question is how to choose the weights in order to obtain a meaningful point on the Pareto-boundary. The answer is obtained by considering the maximization of the ratio $f(\gamma(p))/(p+P_c)$. Indeed, in Chapter 3 we will show that maximizing the ratio $f(\gamma(p))/(p+P_c)$ also yields a point on the Pareto-boundary of (1.7), which corresponds to a specific choice of the weights w_1 and w_2. Such a Pareto-optimal point corresponds to the maximum benefit-cost ratio of the system, which, in light of the physical consideration described in the previous section, is the most meaningful operating point as far as energy efficiency maximization is concerned.

1.1.2 Energy-spectral efficiency trade-off

Some more insight on the operational meaning of the energy efficiency in (1.3) can be gained considering an additive white Gaussian noise (AWGN) channel with band B, noise spectral density N_0, and channel power gain h^2. In this context, taking the channel capacity as the measure of the system benefit, the spectral efficiency and energy efficiency can be written as

$$\mathrm{EE} = \frac{B \log_2\left(1 + \frac{ph^2}{N_0 B}\right)}{\mu p + P_c} = \frac{B\eta_B}{\mu p + P_c} \tag{1.9}$$

$$\eta_B = \log_2\left(1 + \frac{ph^2}{N_0 B}\right) . \tag{1.10}$$

The energy efficiency in (1.9) can be expressed as a function of the energy per bit E_b, by observing that $p = \eta_B E_b$, which yields

$$\mathrm{EE} = \frac{B \log_2\left(1 + h^2 \eta_B \frac{E_b}{N_0}\right)}{\mu E_b \eta_B + \frac{P_c}{B}} , \tag{1.11}$$

which shows the connection between the energy efficiency and the energy contrast E_b/N_0. We see that in AWGN channels, the energy contrast plays a similar role as the SNR γ in (1.3). Indeed, in AWGN channels, the energy contrast is proportional to the SNR $\frac{h^2 p}{N_0 B}$ through the spectral efficiency η_B [173].

Elaborating again on equations (1.9) and (1.10) we can gain more insight on the fundamental trade-off between energy efficiency and spectral efficiency. From (1.10) we obtain the transmit power as

$$p = (2^{\eta_B} - 1)\frac{N_0 B}{h^2} , \tag{1.12}$$

which plugged into (1.9) yields the energy efficiency as a function of the spectral efficeincy

$$\mathrm{EE} = \frac{\eta_B}{\mu(2^{\eta_B} - 1)\frac{N_0}{h^2} + \frac{P_c}{B}} . \tag{1.13}$$

The functional relation in (1.13) is reported in Fig. 1.2, showing that the energy efficiency is unimodal with respect to η_B.

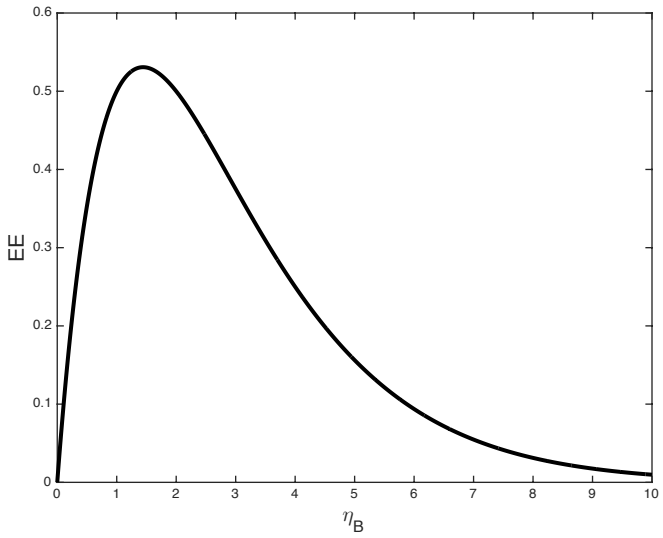

Figure 1.2: EE vs. η_B, for $\mu = 1$,$N_0/h^2 = P_c/B = 1$ [W/Hz].

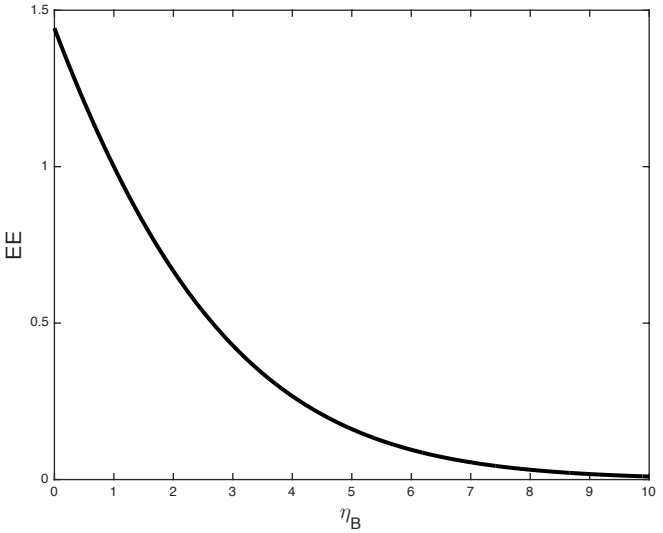

Figure 1.3: EE vs. η_B, for $\mu = 1$, $N_0/h^2 = 1$, $P_c/B = 0$ [W/Hz].

Instead, if $P_c = 0$, the energy efficiency becomes strictly decreasing in η_B, as shown in Fig. 1.3. It is interesting to observe that a similar behavior is observed for the energy efficiency versus the transmit

power, which is unimodal if $P_c > 0$, as shown in Fig. 1.1, but which becomes strictly decreasing if $P_c = 0$. Before closing this section, we remark that by similar elaborations on (1.9) and (1.10), it is possible to analyze other energy-related trade-offs, such as the energy-delay and bandwidth-power trade-offs [42, 78].

1.2 Energy efficiency of a communication network

After learning how to define the energy efficiency of a P2P system, a natural question is how to extend such definition to a network composed of multiple nodes. It is intuitively clear that we should somehow combine the energy efficiencies of the single links, but what is the best way to do so? As we will see, there is no objective answer. Several different choices are possible, each with advantages and disadvantages, and the best choice depends on our subjective goals or on the particular constraints of the network to optimize.

In this section we introduce the most common performance metrics that have been proposed, describing merits and drawbacks of each approach. To elaborate, let us denote by L the number of links in the networks, and by γ_ℓ and P_ℓ the signal to interference plus noise ratio (SINR) and power consumption experienced by the ℓ-th link. Accordingly, we can define the energy efficiency of the ℓ-th link as $\mathrm{EE}_\ell = f(\gamma_\ell)/P_\ell$, with $f(\cdot)$ any meaningful efficiency function.

1.2.1 Global energy efficiency

A first approach is to stick to the physical meaning of energy efficiency as benefit-cost ratio, where now the benefit and cost should be related to the whole network, rather than to a single link. Following this approach leads to the following definition.

Definition 1.4. GEE
The global energy efficiency (GEE) of a network is defined as

$$\mathrm{GEE} = \frac{\sum_{\ell=1}^{L} f(\gamma_\ell)}{\sum_{\ell=1}^{L} \mu_\ell p_\ell + P_{c,\ell}} \,. \tag{1.14}$$

The GEE is the ratio between the total amount of data that can be reliably transmitted per unit of time and the total amount of consumed power, thus representing the efficiency with which the network resources are being used to produce the necessary goods. Otherwise stated, the GEE is exactly the total benefit produced by the network, divided by the total incurred cost.

However, while having a clear and strong physical interpretation, the GEE does not allow to tune the individual energy efficiencies of the different links. This is a drawback in heterogeneous networks where terminals with different features and specifications coexist and possibly have different energy-efficient requirements. As an example, consider a multi-cell system in which regular base stations are deployed together with small access points operated by renewable sources of energy. Clearly, the energy-harvesting nodes require a higher energy efficiency than regular terminals which are plugged to the electrical network.

A second observation regarding GEE concerns fairness issues, in terms of an unbalanced distribution of the energy efficiency among the different communication links. More formally, we define fairness according to the Max-Min fairness concept[1] [123], considering unfair those resource allocations which result in some links experiencing very low energy efficiency with respect to some other links. This might be the case when maximizing the GEE, which is a sum-based performance metric and therefore tends to favor the links with better propagation channels. Moreover, the GEE does not explicitly depend on the energy efficiencies of the different links. Therefore, maximizing the GEE makes it difficult to adjust the individual energy efficiencies according to specific needs.

For these reasons, we also describe a second approach to network energy efficiency, based on multi-objective optimization, which allows more flexibility in the choice of the network operating point.

[1] A resource allocation is said to be max-min fair if it is not possible to increase the energy efficiency EE_i of link i, without decreasing the energy efficiency EE_j of link j which is smaller than or equal to EE_i.

1.2.2 Multi-objective network energy efficiency

An alternative approach to defining the network energy efficiency is based on a multi-objective formulation, in which the objectives to optimize are the L energy efficiencies of the network $\{\mathrm{EE}_\ell\}_{\ell=1}^{L}$. This leads to considering the network energy-efficient region as the set of all feasible vectors $\{\mathrm{EE}_\ell\}_{\ell=1}^{L}$, and to defining the network energy efficiency as a performance measure whose maximization yields a point on the Pareto boundary of the energy-efficient region. This can be accomplished by defining the network energy efficiency as

$$\phi(\mathrm{EE}_1, \ldots, \mathrm{EE}_L) \ , \tag{1.15}$$

wherein $\phi : \mathbb{R}^L \to \mathbb{R}$ is an increasing function of each argument. The choice of the particular function ϕ to employ depends on the particular point on the Pareto boundary that needs to be achieved. In the following we list the most widely used choices, describing advantages and disadvantages of each approach.

Weighted sum of the energy efficiencies

If the function ϕ is set to the weighted sum of the energy efficiencies, (1.15) becomes the weighted arithmetic mean of the energy efficiencies.

Definition 1.5. WSEE
The weighted sum energy efficiency (WSEE) of a network is defined as

$$\mathrm{WSEE} = \sum_{\ell=1}^{L} w_\ell \frac{f(\gamma_\ell)}{\mu_\ell p_\ell + P_{c,\ell}} \ . \tag{1.16}$$

This choice results in the point where the hyperplane $y = \sum_{\ell=1}^{L} w_\ell \mathrm{EE}_\ell$ is tangent to the Pareto boundary. In the multi-objective jargon such a point is called utilitarian point. Similarly to the GEE, the WSEE is a sum-based metric and therefore still tends to favor links with better propagation channels. However, unlike the GEE, the WSEE allows one to counteract this effect because it explicitly depend on the individual energy efficiencies, which can be assigned different priorities through the choice of the weights.

Weighted product of the energy efficiencies

If the function ϕ is set to the exponentially weighted product of the energy efficiencies, (1.15) becomes the weighted geometric mean of the energy efficiencies.

Definition 1.6. WPEE
The weighted product energy efficiency (WPEE) of a network is defined as

$$\mathrm{WPEE} = \prod_{\ell=1}^{L} \left(\frac{f(\gamma_\ell)}{\mu_\ell p_\ell + P_{c,\ell}} \right)^{w_\ell} . \tag{1.17}$$

This choice yields the point where the hyperbola $y = \prod_{\ell=1}^{L} \mathrm{EE}_\ell^{w_\ell}$ is tangent to the Pareto boundary. Unlike previous performance measures, WPEE allows a more balanced resource allocation, thanks to its product-based definition. In particular, it is known that maximizing the product of given utility functions yields the point on the Pareto-boundary corresponding to the Nash Bargaining solution [138]. Moreover, just as WSEE, also WPEE enables the possibility to assign priorities to the individual energy efficiencies through the choice of the weights. However, even though WPEE maximization ensures that no link will experience a near-zero energy efficiency, it can not guarantee to achieve the max-min fair allocation.

Weighted minimum of the energy efficiencies

In order to obtain the max-min fair resource allocation, we set the function ϕ in (1.15) to the weighted minimum of the energy efficiencies. This leads to the following definition.

Definition 1.7. WMEE
The weighted minimum energy efficiency (WMEE) of a network is defined as

$$\mathrm{WMEE} = \min_{\ell \in \{1,\ldots,L\}} \left(w_\ell \frac{f(\gamma_\ell)}{\mu_\ell p_\ell + P_{c,\ell}} \right) . \tag{1.18}$$

This choice results in the point where the hyperplane through the origin and in the direction $[w_1, \ldots, w_L]$ intersects the Pareto boundary.

In the multi-objective jargon such a point is called egalitarian point, and it has the property to make $w_\ell \mathrm{EE}_\ell$ the same for all $\ell = 1, \ldots, L$. Hence, if the weights are all equal, maximizing the WMEE results in all of the energy efficiencies to be equal.

Fig. 1.4 summarizes the global-performance/fairness trade-off for the mentioned metrics and shows an example of energy-efficient Pareto region with the points on the boundary achieved by the different metrics. It should be remarked that by varying the weights, it is possible to describe the whole Pareto region by considering the maximization of any metric among WSEE, WPEE, and WMEE.

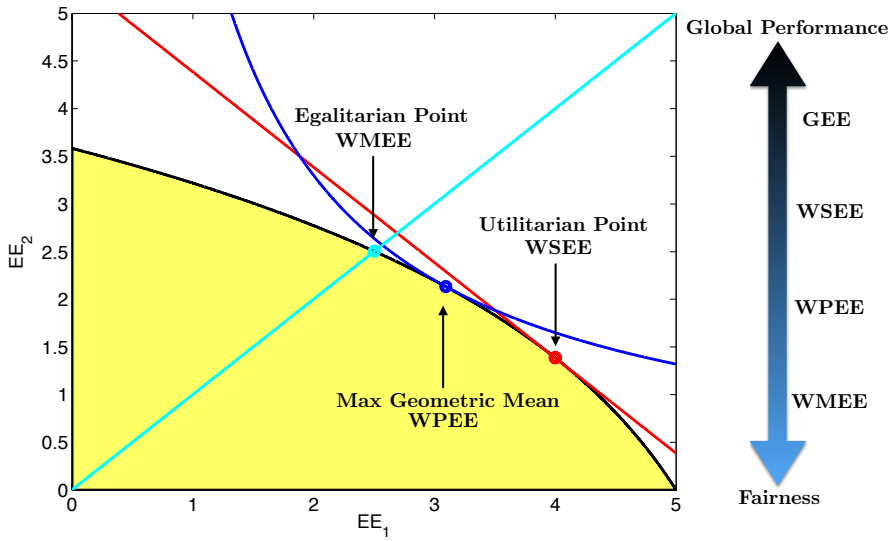

Figure 1.4: Different operating point for multi-objective network energy efficiency optimization. In all performance measures, weights are assumed all equal.

However, none of the functions that fall within the described multi-objective framework can be interpreted as the network benefit-cost ratio, as the GEE. Indeed, although the GEE will be in general inside the Pareto region, not depending directly on the links' energy efficiencies, it still retains the strongest physical meaning among the discussed performance functions.

1.3 Fractional programming for energy efficiency

Fractional programming theory is the branch of optimization theory that is concerned with the properties and optimization of fractional functions [153]. From previous sections it should appear clear the strong link between fractional programming and energy efficiency optimization. Be it a single link or a network, and regardless of the particular performance measure that is adopted, the energy efficiency of a communication system is always expressed through fractional functions and the energy-efficient resource allocation problem is naturally cast as a fractional program. Thus, fractional programming represents a fundamental tool in the energy-efficient modeling and design of wireless networks, and of communication systems in general.

Fractional programming studies problems of the form

$$\max_{\boldsymbol{x}} \frac{f(\boldsymbol{x})}{g(\boldsymbol{x})} \tag{1.19a}$$

$$\text{s.t. } \boldsymbol{x} \in \mathcal{X} \tag{1.19b}$$

with $f : \mathcal{C} \subseteq \mathbb{R}^n \to \mathbb{R}$, $g : \mathcal{C} \subseteq \mathbb{R}^n \to \mathbb{R}_+$ and $\mathcal{X} \subseteq \mathcal{C} \subseteq \mathbb{R}^n$. The challenge in tackling Problem (1.19) is that the objective is generally not concave, even making very restrictive assumptions on f and g. For example, even assuming f and g are both affine functions, in general (1.19a) is not concave. An immediate consequence of this fact is that the strong results of convex optimization theory in general do not apply for fractional problems, and Karush Kuhn Tucker (KKT) optimality conditions are only necessary for a generic fractional problem. However, under specific assumptions on f and g, the objective (1.19a), although not concave, falls into the class of generalized concave functions. In this case, it is possible to develop computationally-efficient methods and algorithms to find the global solution of (1.19). This will be described in detail in Chapters 2 and 3.

In the field of resource allocation for energy efficiency, while (1.19a) represents the energy-efficient metric to optimize, the set $\mathcal{X}$ models the constraints typically enforced in wireless communication systems. The most common constraint is the maximum feasible power constraint, related to the fact that the power which can be used for transmission is

upper bounded by the power amplifier characteristics. Other common constraints are QoS constraints, which ensure that the result of the energy-efficient resource allocation fulfills specific service requirements to the network subscribers. Many different kinds of QoS constraints can be formulated in connection to energy-efficient problems, with two of the most common being minimum rate constraints [12] and maximum delay constraints [119, 51].

In the former case, the resource vector $\boldsymbol{x}$ must be such that each subscriber of the network enjoys at least a minimum achievable rate, or such that the global sum-rate is above a given threshold. Enforcing minimum rate constraints might degrade the resulting energy efficiency, if the target rates are large, because in this case it is necessary to increase the transmit power beyond the unconstrained maximizer of the energy efficiency, in order to ensure that each subscriber achieves his target achievable rate.

In the latter case, the resource vector $\boldsymbol{x}$ must be such that each subscriber experiences a transmission and/or queuing delay below a threshold. Employing a lower transmit power might result in decoding errors at the receiver, and hence in retransmission requests. Therefore, a maximum delay constraint requires each user's SINR to be above a certain threshold and this may again require the use of a transmit power beyond the unconstrained maximizer of the energy efficiency.

In both cases, and in general regardless of the particular constraints which define the set $\mathcal{X}$, the fractional programming framework to be described can always be applied and is always guaranteed to yield the global solution. The critical issue is about the required complexity. As it will be formally shown in Chapters 2 and 3, in order to solve (1.19) with polynomial complexity, $\mathcal{X}$ needs to be convex, while f and g need to be concave and convex, respectively. However, in Chapter 4 a technique will be introduced, to obtain a point fulfilling the KKT conditions of (1.19) with polynomial complexity, also when one of these assumptions is not met.

1.4 State of the art and future directions

Over the last years, fractional programming has become a well-established mathematical tool to solve energy-efficient resource allocation problems in wireless networks.

Paper [141] represents, to the best of authors' knowledge, the first application of fractional programming theory to the optimization of wireless networks. In particular, a set of parallel non-interfering channels is considered, and, using Dinkelbach's algorithm, the power allocation profile for energy efficiency maximization is derived. Since then, fractional programming has been largely used in the field of energy-efficient optimization of wireless systems, and some fractional programming methods and applications are outlined in [84].

Papers [137, 174, 112, 193, 142, 109] employ fractional programming to optimize the energy efficiency of cognitive radio systems. [137] considers a sensing scenario in which secondary (unlicensed) users are allowed to use licensed frequency bands that are temporarily not used by the primary (licensed) users. In [174] an underlay approach is used in which secondary users are allowed to use licensed subcarriers provided this does not cause too much interference to the primary users. Underlay approaches are also used in [112], where a MIMO broadcast channel is considered, in [193], which includes QoS requirements in the optimization process, in [142] which provides energy-efficient resource allocation algorithms for ad-hoc cognitive networks, and in [109], where fractional programming together with the rate-splitting technique is employed in cognitive MIMO systems.

In [45, 41, 29, 52, 72, 131, 169, 177] fractional programming is used for energy-efficient resource allocation in wireless MIMO systems. In [45] a single-user system with time-varying channel is considered. In [41] fractional programming is used to minimize the energy consumption per transmitted bit, while in [29] energy and outage probability optimization are considered. The energy-spectral efficiency trade-off is analyzed via fractional programming in [131]. In [169] optimal, energy-efficient precoding design in a single-user MIMO system is performed. In [177] a full-duplex multi-user system is considered in which uplink and downlink communications take place on the same frequency band.

Instead [178, 72] focus on MIMO broadcast channels. Also, applications of fractional programming in systems with a large number of antennas are considered in [128, 80, 40, 25], thus showing that fractional optimization proves useful in massive and large MIMO systems, too.

Fractional programming in MC and orthogonal frequency division multiple access (OFDMA) systems is employed in [176, 73, 97, 68, 179, 107]. In [176, 107, 179] energy-efficient resource allocation is performed subject to QoS constraints. In [97] energy per bit minimization is performed by fractional programming, while in [68] fractional programming is applied for energy efficiency optimization subject to proportional fairness constraints.

Fractional programming has been applied to relay-assisted systems, too, in [43, 160, 98, 185, 186, 71, 184]. In [43] an OFMDA network with multiple relays is considered, while in [160] the energy efficiency of a two-way relay system is discussed. In [98] the trade-off between spectral and energy efficiency is analyzed for relay-systems, while in [185, 186] a relay-assisted multi-stream MIMO system is considered, for different channel state information (CSI) assumptions. A MIMO system is also considered in [71], where low-complexity algorithms are provided for energy efficiency optimization with perfect CSI. In [184], a multi-user relay-assisted MIMO system is considered and fractional programming is employed to perform joint transceiver and relay allocation.

The papers [127, 69, 171, 55, 70] consider the issue of energy-efficient resource allocation in a coordinated multi-point (CoMP) system in which a cluster of base stations coordinate their resource allocations via backhaul connection. Fractional programming is employed to optimize different energy-efficient performance metrics, including the global energy efficiency of the cluster [127, 171], the sum of the individual energy efficiencies [69, 171], the product of the individual energy efficiencies [171], and the minimum of the energy efficiencies [55]. In [70], fractional programming is used to come up with beamforming allocation in single-stream MIMO systems.

Fractional programming has also been used to optimize the energy efficiency of systems with secure communications. In [39, 126] secure OFDMA networks are considered, while in [191] secure communication

in multiple-antenna systems is studied.

The above works mainly consider centralized resource allocation approaches. However, a key-feature of future cellular systems is anticipated to be self-organization, given the sheer amount of nodes to manage. In particular, the study of energy-efficient resource allocation problems in wireless networks has started considering power control algorithms for competitive scenarios in single-cell and multi-cell networks [63, 148], where a game-theoretic approach is taken. The results in [63, 148] paved the way to many following contributions, which also employed game theory to devise competitive resource allocation algorithms. In [120, 121, 32], the algorithms provided in [63, 148] are extended considering also transceiver design, whereas [118] and [119] consider competitive power control in MC systems and in presence of maximum communication delay constraints. In [101] a hierarchical power control algorithm is proposed, using a Stackelberg game formulation. The results indicate that the equilibrium point is more efficient that in [148]. A further improvement can be obtained using a repeated-game formulation, as done in [162]. In [16], energy-efficient precoding matrix allocation in single-user MIMO systems is studied. In [13] and [31] competitive power control algorithms have been proposed for ultra-wide-band systems and for networks subject to frequency-selective fading, respectively. In [33] competitive resource allocation for multi-user wireless systems is performed, while [35] considers competitive resource allocation in cognitive systems. In [34] the impact of widely linear signaling on competitive, energy-efficient resource allocation algorithms is analyzed for multi-user wireless networks, while [30, 182] consider competitive power and subcarrier allocation in MC and multiple-antenna wireless networks. Fractional programming in competitive resource allocation problems has been used also in [122] for OFDMA networks, in [183, 187, 12, 190] for relay-assisted systems, and in [89, 189] for multiple-antenna systems.

The common denominator to all the mentioned contributions in the area of competitive resource allocation, is that they use game theory to analyze the competition among the network nodes. As it will be explained in more detail in Chapter 5, fractional programming proves

very useful in this context, too, because it allows one to analyze the generalized concavity properties of the individual utility functions, thereby leading to the optimal resource allocation for each node and to determining the existence of equilibria points.

It is thus seen that fractional programming is a general theory that has been widely applied in recent years to the design of resource allocation protocols for wireless networks. It is clearly anticipated that fractional programming will continue to be a valuable tool also for the design and optimization of future wireless networks such as 5G cellular networks. In particular, the following technologies appear among the most promising candidates to meet the requirements of future cellular networks [3, 27, 83].

- *Densely deployed small cells* [79, 4, 82], which try to cope with the sheer number of connected nodes by an extensive use of small-cells and relay stations to be placed in critical areas that would be otherwise difficult to serve. From an energy-efficient point-of-view, network densification is particularly attractive because it reduces the distances between nodes, thus leading to higher data-rates at lower transmit powers. However, deploying more infrastructure nodes results in increased inter-cell interference and leads to an heterogeneous network where nodes with different features and specifications should co-exist.

- *Device-to-device communications* [197], which aim at increasing a cellular system resource reuse factor and reducing the infrastructure load by allowing neighboring mobiles wishing to communicate with each other, to establish a direct communication link, bypassing the network infrastructure. device-to-device (D2D) communications in cellular networks can be either operator-controlled [103], or opportunistically activated by the devices, thus underlaying the regular cellular system [139]. In the former case, the system resources are centrally optimized by the network operator, which dictates what resource blocks can be used for D2D communications. In the latter, neighboring devices can autonomously decide to directly communicate, reusing the same resource blocks

used by the cellular system, provided the interference caused to the cellular users remains under a predetermined threshold.

- *Massive MIMO systems* [147, 99], which deal with the large number of connected nodes by drastically increasing the amount of deployed antennas. Owing to the law of large numbers, using many antennas has the potential to average out multi-user interference, provided the so-called *favorable propagation condition* holds [116]. However, deploying a number of antennas much larger than the mobiles to serve, has some drawbacks, too, among which we mention pilot contamination effects that complicate channel estimation, and more significant hardware impairments due to the fact that low-cost hardware must be used in practical systems, given the large amount of circuitry required to feed hundreds of antennas.

The debate as to what candidate technology is the most suited to the implementation of 5G networks is still ongoing in the wireless community, and it is common opinion that the final selected technology will not be based on a single approach, but rather on a combination of different approaches. However, even if it is not clear yet, what 5G networks will look like, it is clear that they will have to be energy-efficient in order to meet the exponentially increasing rate demands, while at the same time guaranteeing a sustainable growth and affordable costs. This makes energy efficiency one enabler of 5G networks, and fractional programming an invaluable mathematical tool for the energy-efficient analysis and optimization of future wireless networks.

2

Fractional Programming Theory

As the name implies, fractional programming is the branch of optimization theory that studies the optimization of fractional functions. Early works in this field focused on the optimization of a single ratio, devising either parametric approaches [86], [54], [152], or parameter-free methods [38], [149]. These works showed that while in regular optimization theory the complexity divide is between convex and non-convex problems, in single-ratio maximization it is between fractions with concave numerator and convex denominator, and fractions with a different structure. Later it was shown that this clear distinction is present also as far as the maximization of the minimum of a family of ratios is concerned, a problem which is commonly referred to as generalized fractional programming [50], [48]. Single-ratio and max-min fractional optimization have also been analyzed by means of duality approaches, [87], [150], [151]. More recent results have focused on the optimization of a sum or product of ratios [56, 18, 17, 19, 140] for which however no low-complexity method has been devised to date, even assuming the simpler concave-convex structure for each ratio.

In its more general form, a fractional program has the form

$$\max_{\boldsymbol{x}} r(\boldsymbol{x}) = \frac{f(\boldsymbol{x})}{g(\boldsymbol{x})} \tag{2.1a}$$

$$\text{s.t. } \boldsymbol{x} \in \mathcal{X} \tag{2.1b}$$

with $f : \mathcal{C} \subseteq \mathbb{R}^n \to \mathbb{R}$, $g : \mathcal{C} \subseteq \mathbb{R}^n \to \mathbb{R}_{++}$ and $\mathcal{X} \subseteq \mathcal{C}$. Due to the fractional nature of the objective, (2.1) can not be guaranteed to be always convex, even if both f and g are assumed to be affine functions. As a simple counter-example, consider the case $\mathcal{X} = \mathbb{R}_+$, $f(\boldsymbol{x}) = ax+b$, $g(x) = cx + d$, with $a, b, c, d \in \mathbb{R}_+$. Then, (2.1a) will be concave only if $ad \geq cb$.

This simple counter-example shows that due to the fractional nature of the objective, fractional problems do not inherit the properties and results which hold for convex problems. Fractional functions might have stationary points which are not global optima, and the KKT conditions of a fractional problem are only necessary conditions for optimality[1]. At this point, a natural question to ask is whether there exist a class of functions which includes (at least some) non-concave fractional functions, but that at the same time enjoys the *most useful* properties of concave functions. In particular, being interested in solving maximization problems, given a non-concave function r, the *most useful* properties we are concerned with are:

1. any stationary point of r is a global maximum.

2. the KKT conditions resulting from the maximization of r subject to convex constraints are necessary and sufficient for global optimality.

The answer is affirmative, and leads to the class of generalized concave functions, which is the topic of this chapter. Section 2.1 is devoted to the characterization of generalized concave functions and their properties in relation to optimization, while Section 2.2 formally establishes the connection between generalized concavity and fractional functions.

[1]We assume that a constraint qualification condition is fulfilled.

2.1 Generalized concavity

Several extensions of concavity have been proposed over the years. Here, the focus will be on two notable classes of generalized concave functions, namely quasi-concave (QC) functions [6] and pseudo-concave (PC) functions [111], which are the most useful as far as maximizing ratios is concerned. For a more in-depth treatment of generalized concavity, we refer to [9, 10, 37, 49]. We should also remark that in the following the focus will be on generalized concavity, because our ultimate goal is to solve maximization problems. However, this entails no loss of generality, and all the concepts and results to be described, apply to generalized convex functions and to minimization problems with straightforward modifications.

2.1.1 Quasi-concavity

The definition of concavity can be relaxed by requiring that the restriction of a function to a line joining two points of the domain should be above at least one of the endpoints of the line. Formally, we have the following definition.

Definition 2.1 (Quasi-concavity)**.** Let $\mathcal{C} \subseteq \mathbb{R}^n$ be a convex set. Then $r : \mathcal{C} \to \mathbb{R}$ is QC if

$$r(\lambda \boldsymbol{x}_1 + (1-\lambda)\boldsymbol{x}_2) \geq \min\{r(\boldsymbol{x}_1), r(\boldsymbol{x}_2)\} , \tag{2.2}$$

for all $\boldsymbol{x}_1, \boldsymbol{x}_2 \in \mathcal{C}$ and $\lambda \in [0; 1]$.

By enforcing a strict inequality, we can define strict quasi-concavity.

Definition 2.2 (Strict quasi-concavity)**.** Let $\mathcal{C} \subseteq \mathbb{R}^n$ be a convex set. Then $r : \mathcal{C} \to \mathbb{R}$ is strictly quasi-concave (SQC) if

$$r(\lambda \boldsymbol{x}_1 + (1-\lambda)\boldsymbol{x}_2) > \min\{r(\boldsymbol{x}_1), r(\boldsymbol{x}_2)\} , \tag{2.3}$$

for all $\boldsymbol{x}_1, \boldsymbol{x}_2 \in \mathcal{C}$, $\boldsymbol{x}_1 \neq \boldsymbol{x}_2$ and $\lambda \in (0; 1)$.

Remark 2.1. In a similar way it is possible to introduce the definition of quasi-convexity. In particular, if r is QC, then $-r$ is quasi-convex. Moreover, if r is both QC and quasi-convex, then it is called quasi-linear.

The following result proves that quasi-concavity is indeed an extension of concavity.

Proposition 2.1. Let $\mathcal{C} \subseteq \mathbb{R}^n$ be a convex set and $r : \mathcal{C} \to \mathbb{R}$.

(a) If r is concave, then r is QC.

(b) If r is strictly concave, then r is SQC.

(c) If r is SQC, then r is QC.

Proof. (a) follows directly from the definition of concavity,

$$r(\lambda \boldsymbol{x}_1 + (1-\lambda)\boldsymbol{x}_2) \geq \lambda r(\boldsymbol{x}_1) + (1-\lambda) r(\boldsymbol{x}_2) \geq \min\{r(\boldsymbol{x}_1), r(\boldsymbol{x}_2)\} \ . \quad (2.4)$$

Similarly we can prove (b),

$$r(\lambda \boldsymbol{x}_1 + (1-\lambda)\boldsymbol{x}_2) > \lambda r(\boldsymbol{x}_1) + (1-\lambda) r(\boldsymbol{x}_2) > \min\{r(\boldsymbol{x}_1), r(\boldsymbol{x}_2)\} \ , \quad (2.5)$$

while (c) is obvious from Definitions 2.1 and 2.2. □

We should remark that no inclusion can be established between the classes of concave and SQC functions.

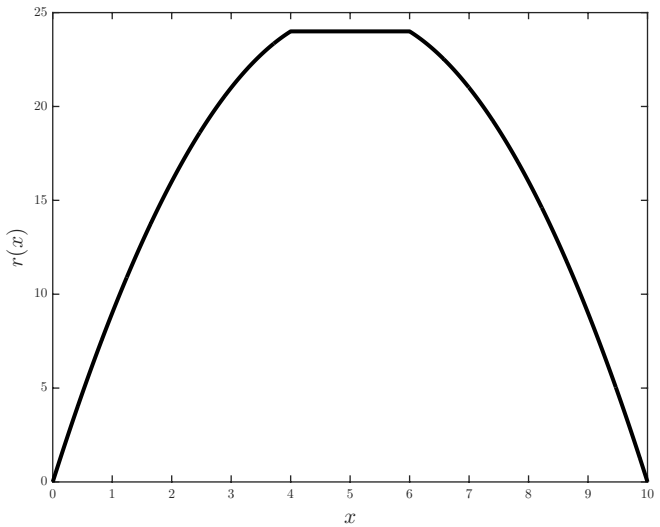

Figure 2.1: Example of a concave function which is not SQC.

As counterexamples, the function shown in Fig. 2.1 is concave, but not SQC, as can be verified by taking any $\boldsymbol{x}_1$ and $\boldsymbol{x}_2$ in the constant part of the function. On the other hand, consider the function $r(x) = x^3$, with $x \in \mathbb{R}$. It can be easily seen that $r(x)$ is SQC, even though it is not concave.

More examples of QC and SQC functions are illustrated in Figs. 2.2-2.4. The intuition we gain is that QC functions must not *oscillate too much*, or, more formally, that the function be unimodal. In particular, (strictly) monotone functions of scalar variable are (strictly) QC. As a consequence, convex functions can also be QC. Moreover, QC functions might have discontinuities in the interior of their domain as well as stationary points that are not global optima. Regarding this last point, the following proposition holds.

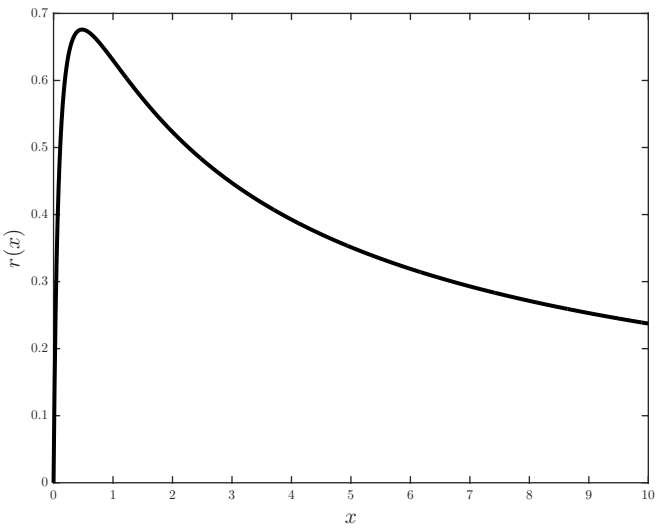

Figure 2.2: Example of a QC, but not concave function.

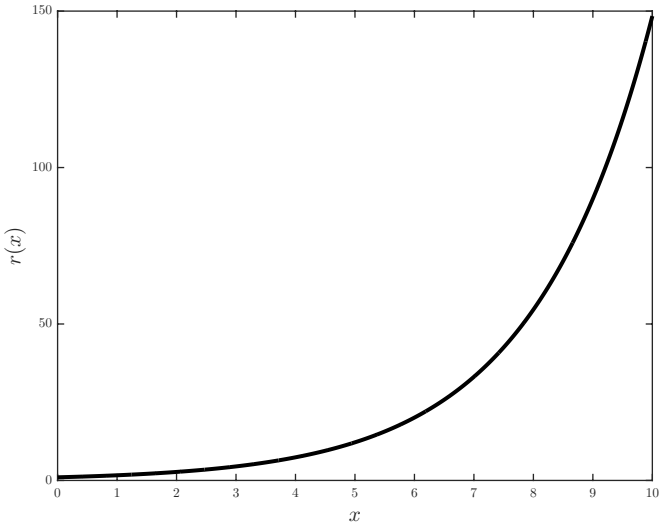

Figure 2.3: Convex function can be QC. An example is shown.

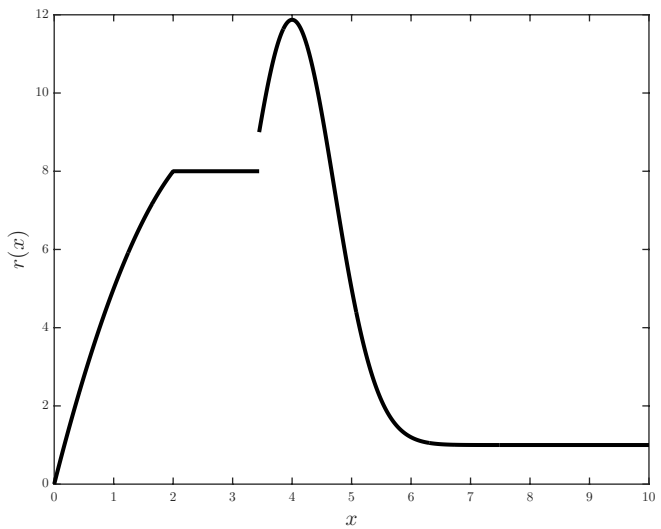

Figure 2.4: QC functions can be non-continuous in the interior of their domain. Moreover, stationary points may exist which are not global maximizers. An example of both points is shown.

Proposition 2.2. Let $r : \mathcal{C} \to \mathbb{R}$ be a QC function.

(a) If $\boldsymbol{x}^* \in \mathcal{C}$ is a strict local maximum, then it is also global.

(b) If r is SQC, then a unique local maximizer exists, and it is also global.

Proof. (a). Define the set $I_\delta = \{\boldsymbol{x} \in \mathcal{C} : \|\boldsymbol{x} - \boldsymbol{x}^*\| < \delta\}$. Since $\boldsymbol{x}^*$ is a strict local maximum, we have that it exists $\delta > 0$ such that

$$r(\boldsymbol{x}) < r(\boldsymbol{x}^*) \ , \forall \ x \in I_\delta \ . \tag{2.6}$$

Now, assume that $\boldsymbol{x}^*$ is not a global maximum. Then it exists $\tilde{\boldsymbol{x}} \in \mathcal{C}$, with $\tilde{\boldsymbol{x}} \neq \boldsymbol{x}^*$, such that $r(\tilde{\boldsymbol{x}}) > r(\boldsymbol{x})$, and from the definition of quasi-concavity it follows

$$r(\lambda\tilde{\boldsymbol{x}} + (1-\lambda)\boldsymbol{x}^*) \geq r(\boldsymbol{x}^*) \ , \forall \ \lambda \in [0;1] \tag{2.7}$$

Taking the limit for $\lambda \to 0$, we see that there exists $\lambda > 0$ such that $(\lambda\tilde{\boldsymbol{x}} + (1-\lambda)\boldsymbol{x}^*) \in I_\delta$, which contradicts (2.6), thus proving (a).

(b). Since SQC functions are also QC, (a) holds, and we have that any local maximum is also global. Finally, the uniqueness of the global maximum follows by contradiction from the definition of strict quasi-concavity. Assume r admits two global maxima $\boldsymbol{x}_1^*$ and $\boldsymbol{x}_2^*$, with $\boldsymbol{x}_1^* \neq \boldsymbol{x}_2^*$. Then,

$$r(\lambda\boldsymbol{x}_1^* + (1-\lambda)\boldsymbol{x}_2^*) > r(\boldsymbol{x}_1^*) = r(\boldsymbol{x}_2^*) \ , \tag{2.8}$$

which contradicts the fact that $\boldsymbol{x}_1^*$ and $\boldsymbol{x}_2^*$ are global maxima. □

We stress that Proposition 2.2 holds only for local maxima, and does not imply that any stationary point of a QC function is also a global maximum. For example, a QC function can have saddle points where the gradient vanishes, which are not global optima. However, many useful properties which hold for concave functions continue to hold in the quasi-concave case.

Proposition 2.3. Let $r : \mathcal{C} \to \mathbb{R}$, with $\mathcal{C} \subseteq \mathbb{R}^n$, convex. Then, r is QC if and only if its super-level set $\mathcal{S}_t = \{\boldsymbol{x} \in \mathcal{C} : r(\boldsymbol{x}) \geq t\}$ are convex for all $t \in \mathbb{R}$.

Proof. Take any $\boldsymbol{x}_1, \boldsymbol{x}_2 \in \mathcal{S}_t$. So, $r(\boldsymbol{x}_1) \geq t$ and $r(\boldsymbol{x}_2) \geq t$. Then, if r is QC we have

$$r(\lambda \boldsymbol{x}_1 + (1-\lambda)\boldsymbol{x}_2) \geq \min\{r(\boldsymbol{x}_1), r(\boldsymbol{x}_2)\} \geq t \ , \tag{2.9}$$

which shows that $(\lambda \boldsymbol{x}_1 + (1-\lambda)\boldsymbol{x}_2) \in \mathcal{S}_t$.

Conversely, assume without loss of generality that $r(\boldsymbol{x}_1) \leq r(\boldsymbol{x}_2)$, and consider $\mathcal{S}_t$, with $t = r(\boldsymbol{x}_1)$. Then, both $\boldsymbol{x}_1$ and $\boldsymbol{x}_2$ belong to $\mathcal{S}_t$, and since $\mathcal{S}_t$ is convex, it also contains $\lambda \boldsymbol{x}_1 + (1-\lambda)\boldsymbol{x}_2$. Hence we have

$$r(\lambda \boldsymbol{x}_1 + (1-\lambda)\boldsymbol{x}_2) \geq r(\boldsymbol{x}_1) = \min\{r(\boldsymbol{x}_1), r(\boldsymbol{x}_2)\} \tag{2.10}$$

□

One immediate consequence of this result is that the global maximizers of a QC function define a convex set. Another useful property of concave functions which extends to QC functions is the characterization in terms of quasi-concavity of the restrictions to an arbitrary line. Specifically, $r : \mathcal{C} \to \mathbb{R}$, with $\mathcal{C} \subseteq \mathbb{R}^n$, is (strictly) QC if and only if its restriction to any line in $\mathcal{C}$ is (strictly) QC, which directly follows applying the definition of (strict) quasi-concavity.

First-order conditions

Quasi-concavity for differentiable functions can be characterized in terms of first-order derivatives, similarly to what happens for differentiable concave functions.

Proposition 2.4. Let $\mathcal{C}$ be an open, convex set. Then, a differentiable function $r : \mathcal{C} \to \mathbb{R}$ is QC if and only if

$$r(\boldsymbol{x}_2) \leq r(\boldsymbol{x}_1) \Rightarrow \nabla r(\boldsymbol{x}_2)^T (\boldsymbol{x}_1 - \boldsymbol{x}_2) \geq 0 \ , \ \forall \ \boldsymbol{x}_1, \boldsymbol{x}_2 \in \mathcal{C} \tag{2.11}$$

Proof. If r is QC, and since $r(\boldsymbol{x}_2) \leq r(\boldsymbol{x}_1)$, then it holds

$$r(\boldsymbol{x}_2 + \lambda(\boldsymbol{x}_1 - \boldsymbol{x}_2)) \geq r(\boldsymbol{x}_2) \ , \ \forall \ \lambda \in [0; 1] \ . \tag{2.12}$$

Let us consider the direction $\boldsymbol{y} = \boldsymbol{x}_1 - \boldsymbol{x}_2$. The directional derivative of r with respect to $\boldsymbol{y}$ is

$$\frac{\partial r}{\partial \boldsymbol{y}} = \lim_{\lambda \to 0^+} \frac{r(\boldsymbol{x}_2 + \lambda(\boldsymbol{x}_1 - \boldsymbol{x}_2)) - r(\boldsymbol{x}_2)}{\lambda} = \nabla r(\boldsymbol{x}_2)^T (\boldsymbol{x}_1 - \boldsymbol{x}_2) \ , \tag{2.13}$$

which is non-negative due to (2.12).

Conversely, assume that (2.11) holds, but r is not QC. Then, there exist $\boldsymbol{x}_1$, $\boldsymbol{x}_2$, and $\lambda > 0$ such that $r(\lambda \boldsymbol{x}_1 + (1-\lambda)\boldsymbol{x}_2) < r(\boldsymbol{x}_2)$, which, defining $\boldsymbol{y} = \lambda \boldsymbol{x}_1 + (1-\lambda)\boldsymbol{x}_2$, is rewritten as $r(\boldsymbol{y}) < r(\boldsymbol{x}_2)$. Next, applying (2.11) first to $(\boldsymbol{x}_2, \boldsymbol{y})$, and then to $(\boldsymbol{x}_1, \boldsymbol{y})$, we obtain

$$\begin{cases} \nabla r(\boldsymbol{y})^T(\boldsymbol{x}_2 - \boldsymbol{y}) = \lambda \nabla r(\boldsymbol{y})^T(\boldsymbol{x}_2 - \boldsymbol{x}_1) \geq 0 \\ \nabla r(\boldsymbol{y})^T(\boldsymbol{x}_1 - \boldsymbol{y}) = (1-\lambda)\nabla r(\boldsymbol{y})^T(\boldsymbol{x}_1 - \boldsymbol{x}_2) \geq 0 \end{cases}, \tag{2.14}$$

from which we conclude that $\nabla r(\boldsymbol{y})^T(\boldsymbol{x}_1 - \boldsymbol{x}_2) = 0$. Next, let us consider the set of all convex combinations $\boldsymbol{z}$ of $\boldsymbol{x}_2$ and $\boldsymbol{y}$ such that $r(\boldsymbol{z}) \geq r(\boldsymbol{x}_2)$, namely

$$\mathcal{S} = \{(\mu, \boldsymbol{z}) \in [0;1] \times \mathcal{C} : \boldsymbol{z} = \mu \boldsymbol{x}_2 + (1-\mu)\boldsymbol{y}, r(\boldsymbol{z}) \geq r(\boldsymbol{x}_2)\} \,. \tag{2.15}$$

By the Mean Value Theorem [14], there exist $(\boldsymbol{z}_0, \mu_0) \in \mathcal{S}$ with $\mu_0 > 0$ and $(\tilde{\boldsymbol{z}}, \tilde{\mu}) \notin \mathcal{S}$, with $\tilde{\mu} \in [0,1]$ and $\tilde{\boldsymbol{z}} = \tilde{\mu}\boldsymbol{z}_0 + (1-\tilde{\mu})\boldsymbol{y}$, such that

$$r(\boldsymbol{y}) = r(\boldsymbol{z}_0) + \nabla r(\tilde{\boldsymbol{z}})^T(\boldsymbol{y} - \boldsymbol{z}_0) = r(\boldsymbol{z}_0) + \mu_0 \lambda \nabla r(\tilde{\boldsymbol{z}})^T(\boldsymbol{x}_1 - \boldsymbol{x}_2) \tag{2.16}$$

Since $(\tilde{\boldsymbol{z}}, \tilde{mu}) \notin \mathcal{S}$, we have $r(\tilde{\boldsymbol{z}}) < r(\boldsymbol{x}_2)$. Moreover, $\tilde{\boldsymbol{z}}$ can be written as a convex combination of $\boldsymbol{x}_1$ and $\boldsymbol{x}_2$ (with parameter $\lambda(1-\tilde{\mu}\mu_0)$). Then, by the same steps that led to (2.14) we find that $\nabla r(\tilde{\boldsymbol{z}})^T(\boldsymbol{x}_1 - \boldsymbol{x}_2) = 0$, from which by (2.16) it follows $r(\boldsymbol{y}) = r(\boldsymbol{z}_0) \geq r(\boldsymbol{x}_2)$, which is a contradiction. □

Two remarks are in order.

Remark 2.2. A condition equivalent to (2.11) can be written as[2]

$$\nabla r(\boldsymbol{x}_2)^T(\boldsymbol{x}_1 - \boldsymbol{x}_2) < 0 \Rightarrow r(\boldsymbol{x}_2) > r(\boldsymbol{x}_1) \;,\; \forall\, \boldsymbol{x}_1, \boldsymbol{x}_2 \in \mathcal{C} \,. \tag{2.17}$$

Equation (2.17) implies that if we can find $\boldsymbol{x}_2 \in \mathcal{C}$ such that $\nabla r(\boldsymbol{x}_2)^T(\boldsymbol{x}_1 - \boldsymbol{x}_2) < 0$ for all $\boldsymbol{x}_1 \in \mathcal{C}$, then $\boldsymbol{x}_2$ is a global maximizer for r. However, we can see that no stationary point of r can fulfill (2.17), due to the strict inequality at the left-hand side (LHS). Therefore, condition (2.17) provides no insight regarding whether a stationary point of a QC function is a global maximizer.

[2]Recall that by the transposition law we have that for any couple of propositions $\mathcal{P}_1$ and $\mathcal{P}_2$, if $\mathcal{P}_1$ implies $\mathcal{P}_2$, then $\overline{\mathcal{P}_2}$ implies $\overline{\mathcal{P}_1}$, with $\overline{\mathcal{P}_1}$ and $\overline{\mathcal{P}_2}$ denoting the negation of $\mathcal{P}_1$ and $\mathcal{P}_2$.

Remark 2.3. It would be reasonable to think that a stronger condition than (2.11) holds for SQC functions, with a strict inequality at the right-hand side (RHS). Unfortunately this is not the case, and no stronger condition than (2.11) is available for SQC functions. Indeed, if the RHS of (2.11) held with a strict inequality, it would be possible to obtain a similar condition as in (2.17), but with a non-strict inequality at the LHS, and this would imply that any stationary point of a SQC function is a global maximizer. However, as already remarked after Proposition 2.2 this is not true in general. As a counterexample, consider the SQC function $r : x \in \mathbb{R} \to r(x) = x^3$, which has a stationary point in $x = 0$, which is not a global maximizer. Indeed, if we take $x_1 = 1$ and $x_2 = 0$, we can see that (2.11) is verified, but with an equality at the RHS.

In order to strengthen (2.11) into a condition that allows one to prove that any stationary point is a global maximizer, we need to strengthen the definition of quasi-concavity. This leads to defining the concept of pseudo-concavity.

2.1.2 Pseudo-concavity

The class of PC functions plays a key role in the theory of generalized concavity, especially in connection with optimization theory. Roughly speaking, pseudo-concavity and concavity are equivalent as far as optimization is concerned. In this section we formalize and clarify this statement. To begin with, let us give the definition of PC and strictly pseudo-concave (SPC) functions.

Definition 2.3 (Pseudo-concavity)**.** Let $\mathcal{C} \subseteq \mathbb{R}^n$ be a convex set. Then $r : \mathcal{C} \to \mathbb{R}$ is PC if it is differentiable and, for all $\boldsymbol{x}_1, \boldsymbol{x}_2 \in \mathcal{C}$, it holds

$$r(\boldsymbol{x}_2) < r(\boldsymbol{x}_1) \Rightarrow \nabla(r(\boldsymbol{x}_2))^T(\boldsymbol{x}_1 - \boldsymbol{x}_2) > 0 \tag{2.18}$$

Remark 2.4. In a similar way it is possible to define pseudo-convexity. In particular, if r is PC, then $-r$ is pseudo-convex. Moreover, if r is both PC and pseudo-convex, then it is called pseudo-linear.

Definition 2.4 (Strict pseudo-concavity)**.** Let $\mathcal{C} \subseteq \mathbb{R}^n$ be a convex set. Then $r : \mathcal{C} \to \mathbb{R}$ is SPC if it is differentiable and, for all $\boldsymbol{x}_1, \boldsymbol{x}_2 \in \mathcal{C}$, with $\boldsymbol{x}_1 \neq \boldsymbol{x}_2$, it holds

$$r(\boldsymbol{x}_2) \leq r(\boldsymbol{x}_1) \Rightarrow \nabla(r(\boldsymbol{x}_2))^T(\boldsymbol{x}_1 - \boldsymbol{x}_2) > 0 \tag{2.19}$$

The following proposition states that, as anticipated, pseudo-concavity implies quasi-concavity, but at the same time it is implied by concavity.

Proposition 2.5. Let $\mathcal{C} \subseteq \mathbb{R}^n$ be a convex set and $r : \mathcal{C} \to \mathbb{R}$.

(a) If r is differentiable and concave, then r is PC.

(b) If r is differentiable and strictly concave, then r is SQC.

(c) If r is PC, then r is QC.

(d) If r is SPC, then r is SQC and PC.

Proof. Take $\boldsymbol{x}_1$ and $\boldsymbol{x}_2$ such that $r(\boldsymbol{x}_2) < r(\boldsymbol{x}_1)$. Then, (a) follows from the first-order concavity conditions for r,

$$\nabla r(\boldsymbol{x}_2)^T(\boldsymbol{x}_1 - \boldsymbol{x}_2) \geq r(\boldsymbol{x}_1) - r(\boldsymbol{x}_2) > 0 \,. \tag{2.20}$$

In a similar way we can prove (b).

Assertion (c) follows by contradiction. Assume r is PC, but not QC. Then, there exist $\boldsymbol{x}_1, \boldsymbol{x}_2 \in \mathcal{C}$ such that $r(\boldsymbol{x}_2) \leq r(\boldsymbol{x}_1)$, and $\nabla r(\boldsymbol{x}_2)^T(\boldsymbol{x}_1 - \boldsymbol{x}_2) < 0$. Then, consider the restriction of r to the line joining $\boldsymbol{x}_1$ and $\boldsymbol{x}_2$, namely $\phi(\lambda) = r(\lambda\boldsymbol{x}_1 + (1-\lambda)\boldsymbol{x}_2)$, with $\lambda \in [0;1]$. Since $r(\boldsymbol{x}_2) \leq r(\boldsymbol{x}_1)$, it holds $\phi(0) = r(\boldsymbol{x}_2) \leq r(\boldsymbol{x}_1) = \phi(1)$. Moreover,

$$\frac{\partial \phi}{\partial \lambda}\Big|_{\lambda=0} = \nabla r(\boldsymbol{x}_2)^T(\boldsymbol{x}_1 - \boldsymbol{x}_2) < 0 \,. \tag{2.21}$$

Therefore, $\phi(\lambda)$ is minimized for some $\lambda_0 \in (0;1)$, to which it corresponds $\boldsymbol{x}_0 = \lambda_0\boldsymbol{x}_1 + (1-\lambda_0)\boldsymbol{x}_2$. This implies that $r(\boldsymbol{x}_0) < r(\boldsymbol{x}_1)$ and

$$\frac{\partial \phi}{\partial \lambda}\Big|_{\lambda=\lambda_0} = \nabla r(\boldsymbol{x}_0)^T(\boldsymbol{x}_1 - \boldsymbol{x}_2) = 0 \,. \tag{2.22}$$

Finally, since r is PC, we have

$$\nabla r(\boldsymbol{x}_0)^T(\boldsymbol{x}_1 - \boldsymbol{x}_0) = (1 - \lambda_0)\nabla r(\boldsymbol{x}_0)^T(\boldsymbol{x}_1 - \boldsymbol{x}_2) > 0 \,, \tag{2.23}$$

which is a contradiction.

In a similar way we can show the first part of (d), while the last part is obvious from Definitions 2.3 and 2.4. □

We should remark that no inclusion can be established between the classes of concave and SPC functions. The same is true between PC and SQC functions, since we have already observed that not even concavity implies strict quasi-concavity.

The next proposition formally establishes the equivalence between stationary points and global maximizers for PC functions.

Proposition 2.6. Let $r : \mathcal{C} \to \mathbb{R}$ be a PC function.

(a) If $\boldsymbol{x}^* \in \mathcal{C}$ is a stationary point of r, then it is a global maximizer of r.

(b) If r is SPC and $\boldsymbol{x}^* \in \mathcal{C}$ is a stationary point of r, then it is the unique global maximizer of r.

Proof. (a). By a similar reasoning as in Remark 2.2, we can see that Definition 2.3 is equivalent to

$$\nabla r(\boldsymbol{x}_2)^T(\boldsymbol{x}_1 - \boldsymbol{x}_2) \leq 0 \Rightarrow r(\boldsymbol{x}_2) \geq r(\boldsymbol{x}_1) \,, \forall \boldsymbol{x}_1, \boldsymbol{x}_2 \in \mathcal{C} \,. \tag{2.24}$$

Then, if $\boldsymbol{x}_2$ is a stationary point, the LHS of (2.24) is fulfilled, and we have $r(\boldsymbol{x}_2) \geq r(\boldsymbol{x}_1)$ for all $\boldsymbol{x}_1 \in \mathcal{C}$, thus implying that $\boldsymbol{x}_2$ must be a global maximizer for r.

(b). Similarly, if r is SPC, we obtain

$$\nabla r(\boldsymbol{x}_2)^T(\boldsymbol{x}_1 - \boldsymbol{x}_2) \leq 0 \Rightarrow r(\boldsymbol{x}_2) > r(\boldsymbol{x}_1) \,, \forall \boldsymbol{x}_1, \boldsymbol{x}_2 \in \mathcal{C} \,, \tag{2.25}$$

showing that if $\nabla r(\boldsymbol{x}_2) = 0$, then $\boldsymbol{x}_2$ is the unique maximizer of r. □

Comparing the proof of Proposition 2.6 with the argument of Remark 2.2, we notice that the difference between quasi-concavity and pseudo-concavity is the possibility to include stationary points in the optimality conditions (2.24) and (2.17). This fact can be formalized in the following proposition.

Proposition 2.7. Let $\mathcal{C} \subseteq \mathbb{R}^n$ and $r : \mathcal{C} \to \mathbb{R}$, differentiable. Then, r is (strictly) PC if and only if r is QC and any stationary point of r is a (strict) local maximum.

As stated by Proposition 2.7, a QC function whose stationary points are local maximizer is also PC. However, this immediately implies that stationary points are actually global maximizers, due to the properties of PC functions. This is consistent with Proposition 2.2, which showed that the local maximizers of a QC functions are also global maximizers.

Generalized concavity and optimality conditions

By virtue of Proposition 2.6, one can maximize a PC function by simply looking for the points where the gradient vanishes, as one would do with concave functions. Moreover, if the function is SPC, we are guaranteed that the maximizer is unique, as it happens for strictly concave functions. Therefore, all gradient-based methods commonly employed for concave functions maximization can also be employed to maximize PC functions. This is true for constrained maximizations, too, because it turns out that KKT conditions are necessary and sufficient for PC functions, as formalized in the following proposition.

Proposition 2.8. Consider the following optimization problem:

$$\max_{\boldsymbol{x}} r(\boldsymbol{x}) \tag{2.26a}$$

$$\text{s.t. } c_i(\boldsymbol{x}) \geq 0 \ , \forall i = 1, \ldots, I \tag{2.26b}$$

with $r, c_i : \mathcal{C} \subseteq \mathbb{R}^n \to \mathbb{R}$, differentiable functions. Assume r is PC while c_i is QC, for all $i = 1, \ldots, I$. Then, assuming a constraint qualification holds, the KKT conditions of Problem (2.26) are necessary and sufficient conditions for optimality[3].

[3]The result can be straightforwardly extended to the case in which also quasi-linear equality constraints are included.

Proof. The KKT conditions of (2.26) are expressed as

$$\nabla r(\boldsymbol{x}) + \sum_{i=1}^{I} \lambda_i \nabla c_i(\boldsymbol{x}) = 0 \tag{2.27a}$$

$$\lambda_i c_i(\boldsymbol{x}) = 0 \ , \forall i = 1, \ldots, I \tag{2.27b}$$

$$\lambda_i \geq 0 \ , \ c_i(\boldsymbol{x}_i) \geq 0 \ , \ \forall i = 1, \ldots, I \tag{2.27c}$$

The necessity of (2.27) is a standard result of optimization theory, which holds under the constraint qualification assumption. In the following we report the proof for the sufficiency part.

Let $\boldsymbol{x}^*$ be a solution of (2.27), with corresponding multipliers $\{\lambda_i^*\}_{i=1}^I$. Assume by contradiction that there exist a feasible $\tilde{\boldsymbol{x}}$ such that $r(\tilde{\boldsymbol{x}}) > r(\boldsymbol{x}^*)$. Then, by the pseudo-concavity of r we have

$$\nabla r(\boldsymbol{x}^*)^T (\tilde{\boldsymbol{x}} - \boldsymbol{x}^*) > 0 \ . \tag{2.28}$$

Next, let us define $\mathcal{I} = \{i : \lambda_i > 0\}$. Then, by (2.27b) we have that for all $i \in \mathcal{I}$, $c_i(\boldsymbol{x}^*) = 0$. As a consequence, for all $i \in \mathcal{I}$, $c_i(\tilde{\boldsymbol{x}}) \geq 0 = c_i(\boldsymbol{x}^*)$, and, by the quasi-concavity of c_i,

$$\nabla c_i(\boldsymbol{x}^*)^T (\tilde{\boldsymbol{x}} - \boldsymbol{x}^*) \geq 0 \ , \ \forall \ i \in \mathcal{I} \tag{2.29}$$

Exploiting (2.28) and (2.29), and since $\lambda_i = 0$ for $i \notin \mathcal{I}$, we obtain

$$\left[\nabla r(\boldsymbol{x}^*) + \sum_{i=1}^{I} \lambda_i \nabla c_i(\boldsymbol{x}) \right]^T (\tilde{\boldsymbol{x}} - \boldsymbol{x}^*) > 0 \ , \tag{2.30}$$

which contradicts (2.27a). □

Fig. 2.5 summarizes the different classes of generalized concave functions which we have introduced, with their inclusion relationships and properties.

2.2 Generalized concavity of ratios

After presenting the framework of generalized concavity theory, we can come back to Problem (2.1), finally providing a complete answer to the question about the properties enjoyed by its fractional objective.

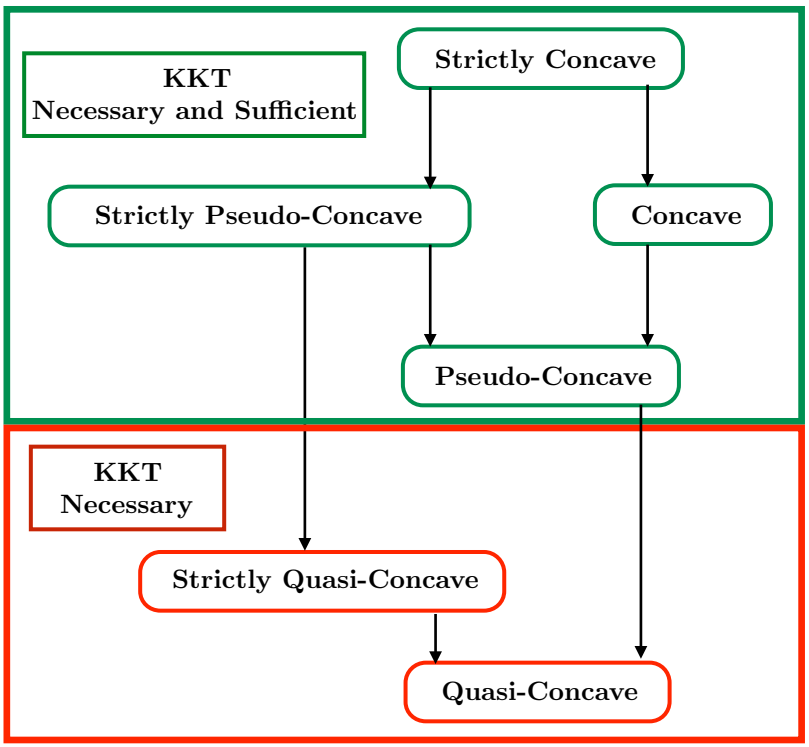

Figure 2.5: Inclusion relationships and optimality of KKT conditions for different classes of generalized concave functions.

Proposition 2.9. Let $r(\boldsymbol{x}) = \dfrac{f(\boldsymbol{x})}{g(\boldsymbol{x})}$, with $f : \mathcal{C} \subseteq \mathbb{R}^n \to \mathbb{R}$ and $g : \mathcal{C} \subseteq \mathbb{R}^n \to \mathbb{R}_{++}$. Then:

(a) If f is non-negative and concave, while g is convex, then r is QC.
If g is affine, the non-negativity of f can be relaxed.

(b) If f is non-negative, differentiable, and concave, while g is differentiable and convex, then r is PC.
If g is affine, the non-negativity of f can be relaxed.

(c) If f and g are affine, then r is pseudo-linear.

Proof. (a). The first part of Assertion (a) follows by showing that the super-level sets of r, $\mathcal{S}_t = \{\boldsymbol{x} \in \mathcal{C} : r(\boldsymbol{x}) \geq t\}$, with $t \in \mathbb{R}$, are convex

sets. First of all, we observe that if $t < 0$, $\mathcal{S}_t$ is the empty set, because $f(\boldsymbol{x}) \geq 0$ and $g(\boldsymbol{x}) > 0$. Thus, we only need to consider $t \geq 0$. Then, we express $\mathcal{S}$ in the equivalent form $\mathcal{S}_t = \{\boldsymbol{x} \in \mathcal{C} : f(\boldsymbol{x}) - tg(\boldsymbol{x}) \geq 0\}$, which is a convex set because f and g are respectively concave and convex, and $t \geq 0$. The second part of (a) follows by observing that if g is affine, $f(\boldsymbol{x}) - tg(\boldsymbol{x})$ is always a concave function, regardless the sign of t.

(b). We have that r is QC, by virtue of (a). In order to show that r is also PC, we exploit Proposition 2.7. Accordingly, (b) follows if we can show that if r admits a stationary point, then it is a local maximizer. A stationary point $\boldsymbol{x}^*$ of r must satisfy the equation

$$\nabla f(\boldsymbol{x}^*)g(\boldsymbol{x}^*) = \nabla g(\boldsymbol{x}^*)f(\boldsymbol{x}^*) \;\Leftrightarrow\; \nabla f(\boldsymbol{x}^*) = r(\boldsymbol{x}^*)\nabla g(\boldsymbol{x}^*) \tag{2.31}$$

Next, by the convexity and differentiability of g we obtain

$$\nabla g(\boldsymbol{x}^*)^T(\boldsymbol{x} - \boldsymbol{x}^*) \leq g(\boldsymbol{x}) - g(\boldsymbol{x}^*) \;, \forall\; \boldsymbol{x} \in \mathcal{C} \;. \tag{2.32}$$

Moreover, by the concavity and differentiability of f we obtain

$$f(\boldsymbol{x}) \leq f(\boldsymbol{x}^*) + \nabla f(\boldsymbol{x}^*)^T(\boldsymbol{x} - \boldsymbol{x}^*) \;, \forall\; \boldsymbol{x} \in \mathcal{C} \;. \tag{2.33}$$

Plugging (2.31) into (2.33), and exploiting (2.32) plus the non-negativity of f which implies $r(\boldsymbol{x}^*) \geq 0$, we obtain

$$\begin{aligned} f(\boldsymbol{x}) &\leq f(\boldsymbol{x}^*) + \nabla f(\boldsymbol{x}^*)^T(\boldsymbol{x} - \boldsymbol{x}^*) \\ &\leq f(\boldsymbol{x}^*) + r(\boldsymbol{x}^*)(g(\boldsymbol{x}) - g(\boldsymbol{x}^*)) = r(\boldsymbol{x}^*)g(\boldsymbol{x}) \;, \end{aligned} \tag{2.34}$$

and rearranging terms we finally have $r(\boldsymbol{x}) \leq r(\boldsymbol{x}^*)$, for all $\boldsymbol{x} \in \mathcal{C}$. The last part of Assertion (b), follows by noticing that if g is affine, the last inequality in (2.34) holds with equality regardless the sign of f, because $g(\boldsymbol{x}^*)^T(\boldsymbol{x} - \boldsymbol{x}^*) = g(\boldsymbol{x}) - g(\boldsymbol{x}^*)$.

(c). Assertion (c) follows by observing that if both f and g are affine, then both the super-level sets and the sub-level sets of r are convex, thus showing that r is quasi-linear (QL). Next, pseudo-linearity follows observing that in this case r has no stationary point in its domain. □

The concavity assumption on f can be partially relaxed for functions on $\mathbb{R}$.

Proposition 2.10. Let $f : \mathbb{R}_+ \to \mathbb{R}_+$ be a differentiable, increasing, and (strictly) S-shaped function[4], with $f(0) = 0$. Then, $r(x) = \dfrac{f(x)}{ax+b}$, with a, b positive coefficients, is (strictly) PC.

Proof. Since r is strictly S-shaped, there exists $x^* \in \mathbb{R}_+$ such that r is strictly convex for $x \leq x^*$, and strictly concave for $x \geq x^*$. We will prove the result by separately showing that r is strictly pseudo-concave for $x \geq x^*$ and strictly increasing for $x < x^*$, which in turn implies strict pseudo-concavity of r, since r is also differentiable in x^*.

For $x \geq x^*$, r is the ratio of a strictly concave function over an affine function, and therefore it is strictly pseudo-concave. Next, we have to show that for $x < x^*$, r is strictly increasing. To see this let us compute the first derivative of r, which yields

$$\frac{dr}{dx} = \frac{(ax+b)f'(x) - af(x)}{(ax+b)^2} = \frac{a(xf'(x) - f(x)) + f'(x)b}{(ax+b)^2}\,. \quad (2.35)$$

Now, for $x < x^*$, f is strictly convex, thus implying that $(y-x)\,f'(x) < f(y) - f(x)$, for all $x, y < x^*$. Setting $y = 0$, we obtain the condition $xf'(x) > f(x)$, for all $x < x^*$. Moreover, f' is non-negative because f is increasing by assumption. Thus, we obtain that (2.35) is strictly positive, and hence that $r(x)$ is strictly increasing. □

2.3 A taxonomy of fractional problems

The rest of this chapter is devoted to the description of a taxonomy of fractional problems. Starting from the simplest case of linear fractional problems, we continue with concave-affine and concave-convex fractional problems, ending the chapter with max-min fractional problems, and with the hardest case of sum-of-ratios and product-of-ratios problems. Solution algorithms for each class of fractional problems will be discussed in Chapter 3.

[4] An increasing, positive function g is said to be (strictly) S-shaped if it is exists a point $x^* \in \mathbb{R}_+$ such that g is (strictly) convex for $x \leq x^*$, and (strictly) concave for $x \geq x^*$

2.3.1 Linear fractional problems

A LFP in canonical form is the optimization problem[5]

$$\max_{\boldsymbol{x}} \frac{\boldsymbol{a}^T\boldsymbol{x}+b}{\boldsymbol{c}^T\boldsymbol{x}+d} \tag{2.36a}$$

$$\text{s.t. } \boldsymbol{M}\boldsymbol{x}=\boldsymbol{\beta}\ ,\ \boldsymbol{x}\geq\boldsymbol{0}\ , \tag{2.36b}$$

with $\boldsymbol{a},\boldsymbol{c}\in\mathbb{R}^n$, $b,d\in\mathbb{R}$, $\boldsymbol{M}\in\mathbb{R}^{m\times n}$ and $\text{rank}(\boldsymbol{M})=m<n$, $\boldsymbol{\beta}\in\mathbb{R}^m$, $\boldsymbol{c}^T\boldsymbol{x}+d>0$, $\boldsymbol{c}\neq\boldsymbol{0}$, $d\neq 0$. By virtue of Proposition 2.9, the objective of Problem (2.36) is pseudo-linear, thus implying that KKT conditions are necessary and sufficient for optimality. Moreover, similarly to what happens for linear problems, a LFP enjoys the property that if it admits a solution, then at least one solution must lie on one vertex of the polyhedron defining the feasible set. As we will see in Chapter 3, this will allow to solve a LFP with a simplex-like algorithm, similarly to what happens for linear problems.

2.3.2 Concave-linear fractional problems

A concave-linear fractional problem (CLFP) is the optimization problem

$$\max_{\boldsymbol{x}} \frac{f(\boldsymbol{x})}{\boldsymbol{c}^T\boldsymbol{x}+d} \tag{2.37a}$$

$$\text{s.t. } c_i(\boldsymbol{x})\leq 0\ ,\forall\ i=1,\dots,I \tag{2.37b}$$

$$h_j(\boldsymbol{x})=0\ ,\forall\ j=1,\dots,J\ , \tag{2.37c}$$

with f concave and differentiable, $\boldsymbol{c}^T\boldsymbol{x}+d>0$, c_i convex for all $i=1,\dots,I$, and h_j affine for all $j=1,\dots,J$. The objective of (2.37) is PC by virtue of Proposition 2.9, and, as a consequence, each stationary point of the objective is a global maximizer. Moreover, by Proposition 2.8, KKT conditions are necessary and sufficient for optimality.

[5]Any LFP with linear inequality constraints can be restated in the form (2.36) by introducing slack variables.

2.3.3 Concave-convex fractional problems

A CCFP is stated as the optimization problem

$$\max_{\boldsymbol{x}} \frac{f(\boldsymbol{x})}{g(\boldsymbol{x})} \tag{2.38a}$$

$$\text{s.t. } c_i(\boldsymbol{x}) \leq 0 \ , \forall \ i = 1, \ldots, I \tag{2.38b}$$

$$h_j(\boldsymbol{x}) = 0 \ , \forall \ j = 1, \ldots, J \ , \tag{2.38c}$$

with f concave, differentiable, and non-negative, g convex, differentiable, and positive, c_i convex for all $i = 1, \ldots, I$, and h_j affine for all $j = 1, \ldots, J$. A CCFP enjoys similar properties as a CLFP, but, in addition, the numerator f of the objective is required to be non-negative[6].

2.3.4 Max-Min fractional programming

A MMFP is stated as the optimization problem

$$\max_{\boldsymbol{x}} \min_{1 \leq k \leq K} \frac{f_k(\boldsymbol{x})}{g_k(\boldsymbol{x})} \tag{2.39a}$$

$$\text{s.t. } c_i(\boldsymbol{x}) \leq 0 \ , \forall \ i = 1, \ldots, I \tag{2.39b}$$

$$h_j(\boldsymbol{x}) = 0 \ , \forall \ j = 1, \ldots, J \ , \tag{2.39c}$$

with f_k, concave and non-negative for all $k = 1, \ldots, K$, g_k convex, and positive for all $k = 1, \ldots, K$, c_i convex for all $i = 1, \ldots, I$, and h_j affine for all $j = 1, \ldots, J$. Proposition 2.9 guarantees that each ratio in (2.39) is QC. Exploiting this fact, the following proposition shows that the objective of Problem (2.39) is QC, too.

Proposition 2.11. Let $\underline{r}(\boldsymbol{x}) = \min\limits_{1 \leq k \leq K} \{r_k(\boldsymbol{x})\}$, with $r_k : \mathcal{C} \subseteq \mathbb{R}^n \to \mathbb{R}$, QC for all $k = 1, \ldots, K$. Then, $\underline{r}(\boldsymbol{x})$ is QC.

Proof. By the definition of quasi-concavity, we have to show that

$$\underline{r}(\lambda \boldsymbol{x}_1 + (1 - \lambda)\boldsymbol{x}_2) \geq \min\{\underline{r}(\boldsymbol{x}_1), \underline{r}(\boldsymbol{x}_2)\} \ , \tag{2.40}$$

[6] In Chapter 3 we will see that this condition can be partially relaxed into requiring that only the maximum of f over the feasible set is positive.

for any $\boldsymbol{x}_1, \boldsymbol{x}_2$ in the domain of $\underline{r}(\boldsymbol{x})$, and $\lambda \in [0;1]$. Then,

$$\underline{r}(\lambda\boldsymbol{x}_1 + (1-\lambda)\boldsymbol{x}_2) = \min_{1\leq k\leq K}\{r_k(\lambda\boldsymbol{x}_1 + (1-\lambda)\boldsymbol{x}_2)\} \geq$$
$$\min_{1\leq k\leq K}\Big\{\min\{r_k(\boldsymbol{x}_1), r_k(\boldsymbol{x}_2)\}\Big\} \geq \min\Big\{\min_{1\leq k\leq K}\{r_k(\boldsymbol{x}_1)\}, \min_{1\leq k\leq K}\{r_k(\boldsymbol{x}_2)\}\Big\}$$
$$= \min\{\underline{r}(\boldsymbol{x}_1), \underline{r}(\boldsymbol{x}_2)\}\ , \tag{2.41}$$

where the assumption of quasi-concavity of $r_k(\boldsymbol{x})$ for all $k = 1, \ldots, K$, has been used to obtain the first inequality. □

Remark 2.5. It is not possible to strengthen Proposition 2.11 to show the pseudo-concavity of $\underline{r}(\boldsymbol{x})$ by assuming that each $r_k(\boldsymbol{x})$ is PC. Indeed, the $\min(\cdot)$ function is not differentiable, even if each $r_k(\boldsymbol{x})$ is PC.

Since the objective of (2.39) is not PC, it is possible to have stationary points which are not global maximizers. Moreover, KKT conditions do not apply to (2.39), since the objective is not differentiable. However, in Chapter 3 we will see that (2.39) can still be globally solved with affordable complexity.

2.3.5 Sum and product of ratios

A SoRP is stated as the optimization problem

$$\max_{\boldsymbol{x}} \sum_{k=1}^{K} \frac{f_k(\boldsymbol{x})}{g_k(\boldsymbol{x})} \tag{2.42a}$$
$$\text{s.t. } c_i(\boldsymbol{x}) \leq 0\ , \forall\ i = 1, \ldots, I \tag{2.42b}$$
$$h_j(\boldsymbol{x}) = 0\ , \forall\ j = 1, \ldots, J \tag{2.42c}$$

with f_k, concave and non-negative for all $k = 1, \ldots, K$, g_k convex, and positive for all $k = 1, \ldots, K$, c_i convex for all $i = 1, \ldots, I$, and h_j affine for all $j = 1, \ldots, J$.

In a similar way, a PoRP is stated as the optimization problem

$$\max_{\boldsymbol{x}} \prod_{k=1}^{K} \frac{f_k(\boldsymbol{x})}{g_k(\boldsymbol{x})} \tag{2.43a}$$

$$\text{s.t. } c_i(\boldsymbol{x}) \leq 0 \,, \forall\, i = 1, \ldots, I \tag{2.43b}$$

$$h_j(\boldsymbol{x}) = 0 \,, \forall\, j = 1, \ldots, J \tag{2.43c}$$

with similar assumptions on the objective and constraints[7]. We observe that a PoRP can be recast as the maximization of the sum of PC functions, by taking the logarithm of the objective. This does not affect the maximizers because the logarithm is increasing, and yields $\sum_{k=1}^{K} \ln\left(\frac{f_k(\boldsymbol{x})}{g_k(\boldsymbol{x})}\right)$. Moreover, the logarithm of a positive PC function is still a PC function, as implied by the following result.

Proposition 2.12. Let $r : \mathcal{C} \subseteq \mathbb{R}^n \to \mathcal{S}$, with $\mathcal{S} \subseteq \mathbb{R}$, be PC, and let $f : \mathcal{S} \to \mathbb{R}$, be strictly increasing and differentiable. Then, $f(r(\boldsymbol{x}))$ is PC.

Proof. Take $\boldsymbol{x}_1, \boldsymbol{x}_2 \in \mathcal{C}$ such that $r(\boldsymbol{x}_2) < r(\boldsymbol{x}_1)$, which implies $f(r(\boldsymbol{x}_2)) < f(r(\boldsymbol{x}_1))$, because f is strictly increasing. Next, denoting by $f^{'}(y)$ the first derivative of f evaluated at y, it holds

$$\nabla f(r(\boldsymbol{x}_2))^T(\boldsymbol{x}_1 - \boldsymbol{x}_2) = f^{'}(r(\boldsymbol{x}_2))(\nabla r(\boldsymbol{x}_2))^T(\boldsymbol{x}_1 - \boldsymbol{x}_2) > 0 \,, \tag{2.44}$$

where the inequality follows because f is strictly increasing and r is PC. □

As will be discussed in Chapter 3, globally solving the optimization programs (2.42) and (2.43) with affordable complexity is still an open problem, the main difficulty lying in the fact that summation does not preserve pseudo-concavity, as instead happens for concavity. Moreover, while applying the logarithmic function to a product of concave functions leads to a sum of concave functions, following this approach does not make things simpler in the PC case, as already observed.

[7]Without loss of optimality, $\{f_k\}_{k=1}^{K}$ can be assumed to be strictly positive. Indeed, if $\boldsymbol{x}$ is such that $f_k(\boldsymbol{x}) = 0$ for some k, then the resulting objective value will be zero. Therefore, these points cannot be the solution of the problem and can be excluded from our analysis.

3

Algorithms for Fractional Programming

The last chapter focused on the notion of generalized concavity and on its strong connection to fractional programming. A classification of fractional problems was introduced and their theoretical properties were shown. This chapter focuses on the algorithmic aspect of fractional programming. For each class of fractional problems introduced in Chapter 2, solution algorithms will be presented and discussed.

3.1 Linear fractional problems

A LFP has the form, or can be reformulated as,

$$\max_{\boldsymbol{x}} \frac{\boldsymbol{a}^T\boldsymbol{x} + b}{\boldsymbol{c}^T\boldsymbol{x} + d} \tag{3.1a}$$

$$\text{s.t. } \boldsymbol{M}\boldsymbol{x} = \boldsymbol{\beta}\ ,\ \boldsymbol{x} \geq \boldsymbol{0}\ , \tag{3.1b}$$

Let us denote by $\mathcal{P}$ the polyhedron defining the feasible set of (3.1). Similarly to what happens for linear problems, if an LFP admits a solution, then it can be shown to lie on one of the vertices of $\mathcal{P}$. This result makes it possible to modify the well-known simplex algorithm used for linear problems, to work also with LFPs. The resulting algorithm is

known as *Martos' Algorithm* [115], and is described in the following section.

3.1.1 Martos' Algorithm

Martos' algorithm starts from a basic solution of the system $\boldsymbol{M}\boldsymbol{x} = \boldsymbol{\eta}$, say $\boldsymbol{x}^{(0)}$, which is a vertex of $\mathcal{P}$. Then, the optimality of the current vertex is tested by computing the directional derivatives of the objective (3.1a) in the directions from $\boldsymbol{x}^{(0)}$ towards all other vertices of $\mathcal{P}$. If all directional derivatives are non-positive, then $\boldsymbol{x}^{(0)}$ is a solution of (3.1). Otherwise we have a feasible direction along which (3.1a) is increasing and we update the current vertex with the vertex associated to the direction of maximal increase. The process is iterated until no feasible directions exist along which the objective function is increasing. The algorithm can be formally stated as follows.

Algorithm 1 Martos' algorithm

Compute a basic feasible solution $\tilde{\boldsymbol{x}}$;
$\tilde{\boldsymbol{a}} = \boldsymbol{a}$; $\tilde{\boldsymbol{c}} = \boldsymbol{c}$; $\tilde{b} = b$; $\tilde{d} = d$;
$\boldsymbol{y} = \tilde{d}\tilde{\boldsymbol{a}} - \tilde{b}\tilde{\boldsymbol{c}}$;
$y_{max} = \max_j y_j$; $\tilde{j} = \arg\max_j y_j$;
while $y_{max} > 0$ **do**
    The non basic variable $x_{\tilde{j}}$ enters the basis;
    Update $\tilde{\boldsymbol{a}}$, $\tilde{\boldsymbol{c}}$, $\tilde{b}$, $\tilde{d}$ by a simplex iteration;
    $\boldsymbol{y} = \tilde{d}\tilde{\boldsymbol{a}} - \tilde{b}\tilde{\boldsymbol{c}}$;
    $y_{max} = \max_j y_j$; $\tilde{j} = \arg\max_j y_j$;
end while

We can see that the algorithm resembles the well-known simplex algorithm for linear optimization, the only difference being the rule which is used to test the optimality of a given vertex, which takes into account the fractional nature of the objective function. Specifically, in stating Algorithm 1, we have used the fact that in each iteration, the condition for the optimality of the current vertex can be equivalently stated as $y_{max} \leq 0$ [37].

3.2 Concave-convex fractional problems

This section focuses at the same time on CLFP and CCFP. Solution methods for the more general CCFP case will be presented and the peculiarities of their specialization to the CLFP case will be highlighted.

Let us consider the CCFP

$$\max_{\boldsymbol{x}} \frac{f(\boldsymbol{x})}{g(\boldsymbol{x})} \tag{3.2a}$$

$$\text{s.t. } c_i(\boldsymbol{x}) \leq 0 \ , \forall \ i = 1, \ldots, I \tag{3.2b}$$

$$h_j(\boldsymbol{x}) = 0 \ , \forall \ j = 1, \ldots, J \ . \tag{3.2c}$$

Two solution methods will be discussed in Sections 3.2.1 and 3.2.2. Although employing different approaches, a connection can be established between these two methods, which will be shown in Section 3.2.3 by means of duality theory.

3.2.1 Dinkelbach's algorithm

Dinkelbach's algorithm has been introduced in [86] and [54]. It belongs to the class of parametric algorithms, whose basic idea is to tackle a CCFP by solving a sequence of easier problems which converges to the global solution of the CCFP. For ease of notation, let us denote by $\mathcal{S}$ the set defined by the constraints (3.2b) and (3.2c). The fundamental result upon which Dinkelbach's algorithm is built is the relation between the CCFP (3.2) and the function of real variable

$$F(\lambda) = \max_{\boldsymbol{x} \in \mathcal{S}} \{ f(\boldsymbol{x}) - \lambda g(\boldsymbol{x}) \} \ . \tag{3.3}$$

Before presenting this main result, some more insight on the function F is necessary. We can see that F exists and is continuous, provided f and g are continuous and $\mathcal{S}$ is compact. Moreover, we have the following result.

Lemma 3.1. Assume f and g are continuous, g is positive, and $\mathcal{S}$ is compact. Then, the function F enjoys the following properties.

(a) F is on $\mathbb{R}$.

(b) F is strictly monotone decreasing on $\mathbb{R}$.

(c) $F(\lambda)$ has a unique root λ_0.

(d) For any $\tilde{\boldsymbol{x}} \in \mathcal{S}$, $F(\lambda_{\tilde{x}}) \geq 0$, with $\lambda_{\tilde{x}} = \dfrac{f(\tilde{\boldsymbol{x}})}{g(\tilde{\boldsymbol{x}})}$, with equality when $\tilde{\boldsymbol{x}} = \arg\max_{\boldsymbol{x}\in\mathcal{S}}\{f(\boldsymbol{x}) - \lambda_{\tilde{x}} g(\boldsymbol{x})\}$.

Proof. Let $t \in [0;1]$. Then, Assertion (a) is obtained as follows.

$$\begin{aligned}
&F(t\lambda_1 + (1-t)\lambda_2) = \\
&\max_{\boldsymbol{x}\in\mathcal{S}}\{f(\boldsymbol{x}) - t\lambda_1 g(\boldsymbol{x}) - (1-t)\lambda_2 g(\boldsymbol{x})\} = \\
&\max_{\boldsymbol{x}\in\mathcal{S}}\{t[f(\boldsymbol{x}) - \lambda_1 g(\boldsymbol{x})] + (1-t)[f(\boldsymbol{x}) - \lambda_2 g(\boldsymbol{x})]]\} \leq \\
&t\max_{\boldsymbol{x}\in\mathcal{S}}\{[f(\boldsymbol{x}) - \lambda_1 g(\boldsymbol{x})]\} + (1-t)\max_{\boldsymbol{x}\in\mathcal{S}}\{[f(\boldsymbol{x}) - \lambda_2 g(\boldsymbol{x})]]\} = \\
&tF(\lambda_1) + (1-t)F(\lambda_2)
\end{aligned} \tag{3.4}$$

Let $\lambda_2 > \lambda_1$ and $\boldsymbol{x}_2 = \arg\max_{\boldsymbol{x}\in\mathcal{S}}\{f(\boldsymbol{x}) - \lambda_2 g(\boldsymbol{x})\}$. Then, Assertion (b) is obtained as follows.

$$\begin{aligned}
F(\lambda_2) &= f(\boldsymbol{x}_2) - \lambda_2 g(\boldsymbol{x}_2) < f(\boldsymbol{x}_2) - \lambda_1 g(\boldsymbol{x}_2) \\
&\leq \max_{\boldsymbol{x}\in\mathcal{S}}\{f(\boldsymbol{x}) - \lambda_1 g(\boldsymbol{x})\} = F(\lambda_1)
\end{aligned} \tag{3.5}$$

Assertion (c) follows from (b), together with the observation that $\lim_{\lambda\to-\infty} F(\lambda) = +\infty$ and that $\lim_{\lambda\to+\infty} F(\lambda) = -\infty$.

Take $\boldsymbol{x} \in \mathcal{S}$. Then, Assertion (d) is obtained as follows.

$$F(\lambda_{\tilde{x}}) = \max_{\boldsymbol{x}\in\mathcal{S}}\left\{f(\boldsymbol{x}) - \frac{f(\tilde{\boldsymbol{x}})}{g(\tilde{\boldsymbol{x}})}g(\boldsymbol{x})\right\} \geq f(\tilde{\boldsymbol{x}}) - \frac{f(\tilde{\boldsymbol{x}})}{g(\tilde{\boldsymbol{x}})}g(\tilde{\boldsymbol{x}}) = 0\,, \tag{3.6}$$

with equality holding if $\tilde{x}$ is the maximizer of $\left\{f(\boldsymbol{x}) - \frac{f(\tilde{\boldsymbol{x}})}{g(\tilde{\boldsymbol{x}})}g(\boldsymbol{x})\right\}$ over $\mathcal{S}$. □

The connection between (3.3) and (3.2) is stated next.

Proposition 3.1. Consider $\boldsymbol{x}^* \in \mathcal{S}$ and $\lambda^* = \dfrac{f(\boldsymbol{x}^*)}{g(\boldsymbol{x}^*)}$. Then, $\boldsymbol{x}^*$ is a solution of (3.2) if and only if

$$\boldsymbol{x}^* = \arg\max_{\boldsymbol{x}\in\mathcal{S}}\{f(\boldsymbol{x}) - \lambda^* g(\boldsymbol{x})\} \tag{3.7}$$

Proof. Assume $\boldsymbol{x}^*$ solves (3.2). Then,

$$\lambda^* = \frac{f(\boldsymbol{x}^*)}{g(\boldsymbol{x}^*)} \geq \frac{f(\boldsymbol{x})}{g(\boldsymbol{x})} \,, \forall \boldsymbol{x} \in \mathcal{S} \,. \tag{3.8}$$

This in turn implies

$$\begin{aligned} f(\boldsymbol{x}) - \lambda^* g(\boldsymbol{x}) \leq 0 \,, \ \forall \boldsymbol{x} \in \mathcal{S} \\ f(\boldsymbol{x}^*) - \lambda^* g(\boldsymbol{x}^*) = 0 \end{aligned} \tag{3.9}$$

Thus, $\boldsymbol{x}^*$ fulfills (3.7) and $F(\lambda^*) = 0$.

Conversely, let $\boldsymbol{x}^* = \arg\max_{\boldsymbol{x} \in \mathcal{S}} \{f(\boldsymbol{x}) - \lambda^* g(\boldsymbol{x})\}$. This implies

$$f(\boldsymbol{x}) - \lambda^* g(\boldsymbol{x}) \leq f(\boldsymbol{x}^*) - \lambda^* g(\boldsymbol{x}^*) = F(\lambda^*) = 0 \,, \ \forall x \in \mathcal{S} \,, \tag{3.10}$$

which in turn can be rewritten as the two conditions

$$\begin{aligned} \lambda^* \geq \frac{f(\boldsymbol{x})}{g(\boldsymbol{x})} \,, \ \forall x \in \mathcal{S} \\ \lambda^* = \frac{f(\boldsymbol{x}^*)}{g(\boldsymbol{x}^*)} \,. \end{aligned} \tag{3.11}$$

Hence, the thesis. □

As a consequence of Proposition 3.1, solving a fractional problem is equivalent to finding the unique zero of the auxiliary function $F(\lambda)$. Dinkelbach's algorithm allows one to accomplish this.

Algorithm 2 Dinkelbach's algorithm

1: $\epsilon > 0$; $n = 0$; $\lambda_n = 0$;
2: **while** $F(\lambda_n) > \epsilon$ **do**
3: $\quad \boldsymbol{x}_n^* = \arg\max_{\boldsymbol{x} \in \mathcal{S}} \{f(\boldsymbol{x}) - \lambda_n g(\boldsymbol{x})\}$;
4: $\quad F(\lambda_n) = f(\boldsymbol{x}_n^*) - \lambda_n g(\boldsymbol{x}_n^*)$;
5: $\quad \lambda_{n+1} = \dfrac{f(\boldsymbol{x}_n^*)}{g(\boldsymbol{x}_n^*)}$;
6: $\quad n = n + 1$;
7: **end while**

A formal proof of convergence and optimality will be provided in Proposition 3.2, but assuming for a moment that convergence to the

solution of (3.2) holds, we see that the parameter λ upon convergence is by construction the maximum value of the objective of (3.2). A second important observation, is to come back to the discussion of Section 1.1.1, showing the connection between fractional programming and multi-objective optimization.

Bi-objective interpretation

Assume that rather than maximizing the ratio $f(\boldsymbol{x})/g(\boldsymbol{x})$, our goal is to solve the bi-objective optimization problem

$$\max_{\boldsymbol{x}\in\mathcal{S}} \{f(\boldsymbol{x}); -g(\boldsymbol{x})\} . \tag{3.12}$$

Employing the scalarization approach with weights w_1 and w_2, we obtain the problem

$$\max_{\boldsymbol{x}\in\mathcal{S}} \; w_1 f(\boldsymbol{x}) - w_2 g(\boldsymbol{x}) . \tag{3.13}$$

For any fixed w_1 and w_2, the solutions of (3.13) is guaranteed to lie on (the convex hull of) the Pareto-boundary of (3.12). Moreover, if f and g are respectively concave and convex, the Pareto-boundary of (3.12) can be completely described by the solutions of (3.13) for different choice of the weights [28]. The two extreme points on the boundary correspond to the cases in which one of the weights is zero, and (3.12) reduces to a scalar problem in which only one of the two objectives is maximized.

Observing (3.13) we learn that the parametric problem to be solved in each iteration of Dinkelbach's algorithm can be seen as the scalarized version of the bi-objective problem with objectives $f(\boldsymbol{x})$ and $-g(\boldsymbol{x})$ and scalarization coefficients 1 and λ. This implies that the maximization of the fractional function $f(\boldsymbol{x})/g(\boldsymbol{x})$ yields a particular point on the Pareto boundary of the bi-objective problem (3.12), and in particular the point which represents the best trade-off between f and g, in terms of their ratio.

Computational complexity

Dinkelbach's algorithm converts the original fractional problem into a sequence of auxiliary problems, indexed by the parameter λ. Then, the overall computational complexity depends on both the convergence

rate of the sub-problem sequence, and the complexity of each individual subproblem.

In order to learn the convergence rate of the sub-problem sequence, we proceed by rewriting the update rule for λ as

$$\lambda_{n+1} = \frac{f(\boldsymbol{x}_n^*)}{g(\boldsymbol{x}_n^*)} = \lambda_n - \frac{f(\boldsymbol{x}_n^*) - \lambda_n g(\boldsymbol{x}_n^*)}{-g(\boldsymbol{x}_n^*)} = \lambda_n - \frac{F(\lambda_n)}{F'(\lambda_n)} \,, \qquad (3.14)$$

thereby observing that Dinkelbach's algorithm follows Newton's method as far as updating λ is concerned. This means that Algorithm 2 can be interpreted as Newton's method applied to the convex function $F(\lambda)$. An immediate consequence of this fact is that Dinkelbach's algorithm exhibits a super-linear convergence rate in the sub-problem sequence.

As for the complexity of each sub-problem, it is difficult to make general statements, as it depends on the specific expression of the auxiliary function F and on the number of constraints. Focusing on the more practical case in which the auxiliary problem is convex, we can employ standard convex analysis results to state that the computational complexity of the auxiliary problem is polynomial in the number of variables and constraints [20, 28].

Let us now formally prove the convergence and optimality of Dinkelbach's algorithm.

Proposition 3.2. Algorithm 2 converges to the global solution of (3.2).

Proof. Given the update rule for λ in (3.14), and recalling Lemma 3.1-(d), we have

$$F(\lambda_n) = f(\boldsymbol{x}_n^*) - \lambda_n g(\boldsymbol{x}_n^*) = (\lambda_{n+1} - \lambda_n) g(\boldsymbol{x}_n^*) \geq 0 \,. \qquad (3.15)$$

Since g is positive, this implies $\lambda_{n+1} > \lambda_n$, unless we are already at convergence. Therefore, the succession $\{\lambda_n\}_n$ is increasing, which implies that the succession $\{F(\lambda_n)\}_n$ is decreasing by Lemma 3.1-(b), and by the continuity of F and compactness of $\mathcal{S}$. Thus, Algorithm 2 converges.

Convergence to the optimum is obtained by contradiction. Assume the limit point of $\{\lambda_n\}_n$ is some $\tilde{\lambda} < \lambda^*$, to which it corresponds

some $\tilde{\boldsymbol{x}}$ which is not the optimal solution. Then, since F is decreasing, this implies $F(\tilde{\lambda}) > F(\lambda^*)$. On the other hand, by Lemma 3.1-(d), $F(\tilde{\lambda}) = 0$, because upon convergence we have $\tilde{\lambda} = f(\tilde{\boldsymbol{x}})/g(\tilde{\boldsymbol{x}})$ and $\tilde{\boldsymbol{x}} = \arg\max_{\boldsymbol{x}\in\mathcal{S}}\{f(\boldsymbol{x}) - \tilde{\lambda}g(\boldsymbol{x})\}$. But from Proposition 3.1 we also know that $F(\lambda^*) = 0$, which is a contradiction. □

A very important observation is that so far we have not actually exploited any concavity/convexity assumption on the numerator and denominator of the objective function. Similarly, we have not exploited the non-negativity of the numerator, but only the positivity of the denominator. This means that Dinkelbach's algorithm is guaranteed to converge to the global solution of any fractional problem under milder assumptions than those required for a CCFP, namely that f and g are continuous, real-valued functions, that $\mathcal{S}$ is a compact set, and that g is positive. The critical point in this reasoning is that in order to implement Dinkelbach's algorithm, we need to compute $F(\lambda_n)$ in each iteration of the algorithm, which, in general, requires to globally solve a non-convex optimization problem. One case when this can be accomplished with limited complexity is if the problem is a CCFP. Indeed, in this case $\mathcal{S}$ is a convex set and $f(\boldsymbol{x}) - \lambda g(\boldsymbol{x})$ is a concave function, provided $\lambda \geq 0$. Regarding this last point, the non-negativity of λ is also ensured for any CCFP, thanks to the non-negativity of f and to the positivity of g. More in detail, it also possible to partially relax the non-negativity condition of f into requiring only that $F(0) = \max_{\boldsymbol{x}\in\mathcal{S}}\{f(\boldsymbol{x})\} \geq 0$. If this holds, then λ_0 will be non-negative and this guarantees that each $\lambda_n \geq 0$ because the succession $\{\lambda_n\}_n$ is increasing.

However, it is possible that for some specific instances of fractional problems, one can compute the auxiliary function $F(\lambda)$ even if the problem is not a CCFP. In this case, it is possible to employ Dinkelbach's algorithm to solve the problem [144].

Remark 3.1. Clearly, Dinkelbach's algorithm can be implemented with limited complexity also when g is affine. Moreover, in this case we can relax the assumption on the non-negativity of f, because if g is affine, then $f(\boldsymbol{x}) - \lambda g(\boldsymbol{x})$ is a convex problem regardless of the sign of λ. Then, the non-negativity of f is not required as far as solving CLFPs

with limited complexity is concerned. It is interesting to observe that a similar circumstance was observed in the proof of Proposition 2.9, in which the pseudo-concavity of $f(\boldsymbol{x})/g(\boldsymbol{x})$ could be proved regardless of the sign of f, assuming a concave f and an affine g.

3.2.2 Charnes-Cooper Transform

Charnes-Cooper Transform has been introduced in [38] for LFP, and was extended to CCFP in [149]. If Dinkelbach's algorithm is a parametric approach which converts the original CCFP into a sequence of convex problems indexed by the parameter λ, the idea of Charnes-Cooper Transform is to apply a suitable variable transformation to reformulate a CCFP into an equivalent convex problem. In particular, consider Problem (3.2) and apply the transformation

$$\boldsymbol{y} = \frac{\boldsymbol{x}}{g(\boldsymbol{x})} \ , \ t = \frac{1}{g(\boldsymbol{x})} \ . \tag{3.16}$$

Noticing that from (3.16) it follows $\boldsymbol{x} = \boldsymbol{y}/t$, we have the equivalent problem

$$\max_{t,\boldsymbol{y}/t} \ tf\left(\frac{\boldsymbol{y}}{t}\right) \tag{3.17a}$$

$$\text{s.t. } tg\left(\frac{\boldsymbol{y}}{t}\right) = 1 \tag{3.17b}$$

$$tc_i\left(\frac{\boldsymbol{y}}{t}\right) \leq 0 \ , \forall \ i = 1, \ldots, I \tag{3.17c}$$

$$h_j\left(\frac{\boldsymbol{y}}{t}\right) = 0 \ , \forall \ j = 1, \ldots, J \ . \tag{3.17d}$$

The objective (3.17a) and the LHS of the constraints (3.17c) are the perspective of the functions f and c_i, respectively. Therefore, (3.17a) is concave and (3.17c) are convex constraints, since the perspective operation preserves concavity/convexity [28]. Constraints (3.17d) can also be seen to be convex constraints, detailing the affine structure of h_j as $h_j(\boldsymbol{x}) = a_j^T \boldsymbol{x} + b$, upon which (3.17d) becomes $a_j^T \boldsymbol{y} + bt = 0$. If also (3.17b) were a convex constraint, then (3.17) would be a convex problem and could be solved by means of any convex programming algorithm.

Remark 3.2. If we consider CLFPs, then (3.17b) is a convex constraint. Indeed, in this case g can be specified as the affine function $g(\boldsymbol{x}) = c^T\boldsymbol{x} + d$, and (3.17b) becomes $c^T\boldsymbol{y} + dt - 1 = 0$. Thus, CLFPs can be reformulated as convex problems and can be solved by standard convex programming approaches.

However, when dealing with the more general case of CCFPs, g is convex but not affine, and therefore the equality constraint (3.17b) is not convex. In this case, let us consider the relaxed problem obtained relaxing (3.17b) to an inequality constraint.

$$\max_{t,\boldsymbol{y}/t} \; tf\left(\frac{\boldsymbol{y}}{t}\right) \tag{3.18a}$$

$$\text{s.t. } tg\left(\frac{\boldsymbol{y}}{t}\right) \leq 1 \tag{3.18b}$$

$$tc_i\left(\frac{\boldsymbol{y}}{t}\right) \leq 0 \;, \forall\, i = 1, \ldots, I \tag{3.18c}$$

$$h_j\left(\frac{\boldsymbol{y}}{t}\right) = 0 \;, \forall\, j = 1, \ldots, J \;. \tag{3.18d}$$

The following result guarantees that no loss of optimality is incurred by solving (3.18) in place of (3.17).

Proposition 3.3. Assume f is non-negative. Then, Problems (3.2) and (3.18) are equivalent.

Proof. Let $\mathcal{S}$ denote the feasible set of Problem (3.2), which is equivalent to (3.17). We also denote by $\mathcal{S}_1$ the feasible set of Problem (3.17) and by $\mathcal{S}_2$ the feasible set of Problem (3.18), namely

$$\begin{aligned} \mathcal{S}_1 &= \left\{ (\boldsymbol{y}_1, t_1) \in \mathbb{R}^n \times \mathbb{R}_{++} : \frac{\boldsymbol{y}_1}{t_1} \in \mathcal{S},\; t_1 g\left(\frac{\boldsymbol{y}_1}{t_1}\right) = 1 \right\} \\ \mathcal{S}_2 &= \left\{ (\boldsymbol{y}_2, t_2) \in \mathbb{R}^n \times \mathbb{R}_{++} : \frac{\boldsymbol{y}_2}{t_2} \in \mathcal{S},\; t_2 g\left(\frac{\boldsymbol{y}_2}{t_2}\right) \leq 1 \right\} \end{aligned} \tag{3.19}$$

Clearly $\mathcal{S}_1 \subseteq \mathcal{S}_2$ and in order to prove the result we need to show that all elements in $\mathcal{S}_2 \setminus \mathcal{S}_1$ are suboptimal for (3.18). To this end, observe that for any $(\boldsymbol{y}_2, t_2) \in \mathcal{S}_2$ we have

$$t_2 g\left(\frac{\boldsymbol{y}_2}{t_2}\right) = \tau \in (0; 1] \;, \tag{3.20}$$

and we can construct and element of $\mathcal{S}_1$ as $\boldsymbol{y}_1 = \boldsymbol{y}_2/\tau$ and $t_1 = t_2/\tau$. This means that for any $(\boldsymbol{y}_2, t_2) \in \mathcal{S}_2$, there exist $(\boldsymbol{y}_1, t_1) \in \mathcal{S}_1$ and $\tau \in (0; 1]$, such that $(\boldsymbol{y}_2, t_2) = (\tau \boldsymbol{y}_1, \tau t_1)$, with $\tau < 1$ if $(\boldsymbol{y}_2, t_2) \in \mathcal{S}_2 \backslash \mathcal{S}_1$. Then, exploiting the non-negativity of f we obtain

$$t_2 f\left(\frac{\boldsymbol{y}_2}{t_2}\right) = \tau t_1 f\left(\frac{\boldsymbol{y}_1}{t_1}\right) \leq t_1 f\left(\frac{\boldsymbol{y}_1}{t_1}\right) , \tag{3.21}$$

where the inequality is strict if $(\boldsymbol{y}_2, t_2) \in \mathcal{S}_2 \setminus \mathcal{S}_1$. Hence, all elements in $\mathcal{S}_2 \setminus \mathcal{S}_1$ are suboptimal for Problem (3.18). □

Thus, any CCFP can be equivalently reformulated as the convex problem (3.18) and solved by means of well-established convex programming algorithms. Before closing the section, we should remark that once again we have obtained that the sign of the numerator f is not relevant as long as the denominator is affine, whereas the numerator should be restricted in sign if the denominator is convex, but not affine.

3.2.3 Duality in fractional programming

In Section 3.2.2 we have reformulated Problem (3.2) into the convex Problem (3.18). In this section, we analyze (3.18) by a Lagrangian duality approach. This will lead to establishing a connection between the Charnes-Cooper Transform and Dinkelbach's algorithm, allowing us to obtain the optimality condition derived in Proposition 3.1 from the KKT optimality conditions of (3.18).

In order not to make the notation too cumbersome, we do not consider the equality constraints (3.18d). Then, denoting by λ and μ_i the Lagrange multipliers for (3.18b) and (3.18c), for all $i = 1, \ldots, I$, the Lagrangian function of (3.18) is written as

$$\mathcal{L}(\boldsymbol{y}, t, \lambda, \{\mu_i\}_{i=1}^I) = -tf\left(\frac{\boldsymbol{y}}{t}\right) + \lambda t\left(g\left(\frac{\boldsymbol{y}}{t}\right) - 1\right) + t\sum_{i=1}^{I} \mu_i c_i\left(\frac{\boldsymbol{y}}{t}\right) , \tag{3.22}$$

and the KKT conditions of (3.18) are expressed as

$$-f\left(\frac{\boldsymbol{y}}{t}\right)+\lambda g\left(\frac{\boldsymbol{y}}{t}\right)+\sum_{i=1}^{I}\mu_i c_i\left(\frac{\boldsymbol{y}}{t}\right)- \frac{\boldsymbol{y}^T}{t}\left[-\nabla f\left(\frac{\boldsymbol{y}}{t}\right)+\lambda\nabla g\left(\frac{\boldsymbol{y}}{t}\right)+\sum_{i=1}^{I}\mu_i\nabla c_i\left(\frac{\boldsymbol{y}}{t}\right)\right]=0 \tag{3.23a}$$

$$-\nabla f\left(\frac{\boldsymbol{y}}{t}\right)+\lambda\nabla g\left(\frac{\boldsymbol{y}}{t}\right)+\sum_{i=1}^{I}\mu_i\nabla c_i\left(\frac{\boldsymbol{y}}{t}\right)=0 \tag{3.23b}$$

$$\lambda\left(tg\left(\frac{\boldsymbol{y}}{t}\right)-1\right)=0 \tag{3.23c}$$

$$\mu_i c_i\left(\frac{\boldsymbol{y}}{t}\right)=0\ ,\ \forall\, i=1,\ldots,I \tag{3.23d}$$

$$\lambda\geq 0\ ,\ \mu_i\geq 0\ ,\ \forall\, i=1,\ldots,I \tag{3.23e}$$

$$tg\left(\frac{\boldsymbol{y}}{t}\right)\leq 1 \tag{3.23f}$$

$$c_i\left(\frac{\boldsymbol{y}}{t}\right)\leq 0\ ,\ \forall\, i=1,\ldots,I\ , \tag{3.23g}$$

wherein (3.23a) and (3.23b) are the Lagrangian stationarity conditions, (3.23c) and (3.23d) are the complementary slackness conditions, (3.23e) is the non-negativity of the multipliers, while (3.23f) and (3.23g) are the problem constraints. Exploiting Proposition 3.3, we know that at the optimum, $tg\left(\frac{\boldsymbol{y}}{t}\right)=1$. Then, $\lambda>0$, and we can decouple (3.23c) and (3.23f) from the rest of the system, which can be solved with respect to $\boldsymbol{x}=\boldsymbol{y}/t$, and then fulfilling (3.23c) and (3.23f) by setting $t=1/g(\boldsymbol{x})$. Moreover, due to (3.23d), the third summand in (3.23a) is zero, and due to (3.23b), the term in braces in (3.23a) is also zero. As a result, (3.23) becomes

$$-f\left(\boldsymbol{x}\right)+\lambda g\left(\boldsymbol{x}\right)=0\ ,\ \lambda\geq 0 \tag{3.24a}$$

$$-\nabla f\left(\boldsymbol{x}\right)+\lambda\nabla g\left(\boldsymbol{x}\right)+\sum_{i=1}^{I}\mu_i\nabla c_i\left(\boldsymbol{x}\right)=0 \tag{3.24b}$$

$$\mu_i c_i\left(\boldsymbol{x}\right)=0\ ,\ \forall\, i=1,\ldots,I \tag{3.24c}$$

$$c_i\left(\boldsymbol{x}\right)\leq 0\ ,\ \forall\, i=1,\ldots,I \tag{3.24d}$$

$$\mu_i\geq 0\ ,\ \forall\, i=1,\ldots,I \tag{3.24e}$$

Equations (3.24b), (3.24c), (3.24d), and (3.24e) are the KKT conditions of the problem

$$\max_{\boldsymbol{x}} f(\boldsymbol{x}) - \lambda g(\boldsymbol{x}) \tag{3.25a}$$

$$\text{s.t. } c_i(\boldsymbol{x}) \leq 0 \ , \forall \ i = 1, \ldots, I \ , \tag{3.25b}$$

which is convex because $\lambda \geq 0$. Then, any solution of (3.24) is also a global solution of (3.25). The objective (3.25a) can be recognized to be the auxiliary function employed by Dinkelbach's algorithm. Moreover, (3.24a) tells us that at the optimum we must have $f(\boldsymbol{x}) - \lambda g(\boldsymbol{x}) = 0$, which shows that any solution $\boldsymbol{x}^*$ of (3.24) must also be a limiting point of Dinkelbach's algorithm.

In this section we have shown that the KKT conditions of the equivalent convex problem (3.18) are equivalent to the optimality conditions stated by Dinkelbach's algorithm. The convexity of the reformulation in (3.18) can be exploited even further, and allows one to apply the duality theory available for convex problems. In particular, the connection between Dinkelbach's theorem and duality theory can be further strengthened by following a similar approach as in this section to show that the dual problem of (3.18) is formally equivalent to the dual problem of (3.25), [151].

3.3 Max-Min fractional programming

A MMFP has the form

$$\max_{\boldsymbol{x}} \min_{1 \leq k \leq K} \frac{f_k(\boldsymbol{x})}{g_k(\boldsymbol{x})} \tag{3.26a}$$

$$\text{s.t. } c_i(\boldsymbol{x}) \leq 0 \ , \forall \ i = 1, \ldots, I \tag{3.26b}$$

$$h_j(\boldsymbol{x}) = 0 \ , \forall \ j = 1, \ldots, J \ , \tag{3.26c}$$

As shown in Section 2.3.4, the objective of a MMFP is QC. This has paved the way to the development of a Dinkelbach-like procedure which is able to obtain the global solution of a MMFP by solving a sequence of convex problems. The algorithm is commonly referred to as *Generalized Dinkelbach's Algorithm* and has been introduced in [50] and [48].

3.3.1 Generalized Dinkelbach's Algorithm

The generalized Dinkelbach's algorithm can be seen as an extension of Dinkelbach's algorithm to the case in which a more general auxiliary function F is considered. Specifically, for a MMFP, the auxiliary function is defined as

$$F(\lambda) = \max_{\boldsymbol{x}\in\mathcal{S}} \left\{ \min_{1\leq k\leq K} \{f_k(\boldsymbol{x}) - \lambda_n g_k(\boldsymbol{x})\} \right\} . \tag{3.27}$$

The algorithm is formally stated as follows.

Algorithm 3 Generalized Dinkelbach's algorithm

$\epsilon > 0$; $n = 0$; $\lambda_n = 0$;
while $F(\lambda_n) > \epsilon$ **do**
  $\boldsymbol{x}_n^* = \arg\max_{\boldsymbol{x}\in\mathcal{S}} \left\{ \min_{1\leq k\leq K} \{f_k(\boldsymbol{x}) - \lambda_n g_k(\boldsymbol{x})\} \right\}$;
  $F(\lambda_n) = \min_{1\leq k\leq K} \{f_k(\boldsymbol{x}_n^*) - \lambda_n g_k(\boldsymbol{x}_n^*)\}$;
  $\lambda_{n+1} = \min_{1\leq k\leq K} \dfrac{f_k(\boldsymbol{x}_n^*)}{g_k(\boldsymbol{x}_n^*)}$;
  $n = n + 1$;
end while

We can observe that if $K = 1$, Algorithm 3 reduces to Dinkelbach's algorithm. When $K > 1$, following similar arguments as in Section 3.2.1, it can be shown that Algorithm 3 enjoys analogous convergence and optimality properties as Dinkelbach's algorithm, except for the fact that the convergence rate is linear instead of super-linear. However, despite this slightly slower convergence rate, Algorithm 3 still converts a MMFP into a sequence of convex problems, provided f_k is non-negative and concave for $k = 1, \ldots, K$, g_k positive and convex for all $k = 1, \ldots, K$, and $\mathcal{S}$ is defined by convex constraints.

3.4 Sum and product of ratios

Let us consider the SoRP

$$\max_{\boldsymbol{x}} \sum_{k=1}^{K} \frac{f_k(\boldsymbol{x})}{g_k(\boldsymbol{x})} \tag{3.28a}$$

$$\text{s.t. } c_i(\boldsymbol{x}) \leq 0 \ , \forall \ i = 1, \ldots, I \tag{3.28b}$$

$$h_j(\boldsymbol{x}) = 0 \ , \forall \ j = 1, \ldots, J \ . \tag{3.28c}$$

As mentioned in Section 2.3.5, a sum-of-ratios is in general neither PC nor QC, not even assuming f_k and g_k are affine for all $k = 1, \ldots, K$. This prevents the development of optimization algorithms able to solve (3.28) with limited complexity, and indeed finding the global solution of a SoRP with affordable complexity is still an open problem [64]. In [1] a Dinkelbach-like algorithm is proposed for SoRPs, which is reported here and labeled Algorithm 4.

Algorithm 4 Dinkelbach-like algorithm for SoRPs.

$\epsilon > 0$; $n = 0$; $\{\lambda_n^k\}_{k=1}^K = 0$;
while $F\left(\{\lambda_n^k\}_{k=1}^K\right) > \epsilon$ **do**
  $\boldsymbol{x}_n^* = \arg\max_{\boldsymbol{x} \in \mathcal{S}} \left\{ \sum_k^K f_i(\boldsymbol{x}) - \lambda_{n,k} g_k(\boldsymbol{x}) \right\}$;
  $F\left(\{\lambda_n^k\}_{k=1}^K\right) = \max_{\boldsymbol{x} \in \mathcal{S}} \left\{ \sum_k^K f_k(\boldsymbol{x}) - \lambda_{n,k} g_k(\boldsymbol{x}) \right\}$;
  $\lambda_{n+1,k} = \dfrac{f_k(\boldsymbol{x}_n^*)}{g_k(\boldsymbol{x}_n^*)}$, for all $k = 1, \ldots, K$;
  $n = n + 1$;
end while

We can see that Algorithm 4 requires only the solution of a sequence of convex problems, assuming f_k and g_k are respectively concave and convex for all $k = 1, \ldots, K$. However, the solution obtained upon convergence is not guaranteed to be globally optimal, as shown in [58] by a numerical counterexample. To date, the only methods available to globally solve a general SoRP or PoRP are based on global optimization algorithms [56, 18, 17]. The same is true for generic single-ratio

fractional problems in which the numerator and denominator are not respectively concave and convex functions, or with a non-convex feasible set. In general, global optimization methods require to explore the complete feasible set to determine the global maximum of the objective, which in general requires a too large complexity. However, recently it has been shown how the framework of monotonic optimization can be used to globally solve many non-convex problems, by exploring only the boundary of the feasible set, rather than the whole set [167, 146]. This method can also be applied to energy efficiency problems, as explained in the next section.

3.5 Global optimality in fractional programming

A brief review of monotonic optimization, its basic definitions and results, is provided in Appendix B. Here, we just mention that monotonic optimization can be described as a mathematical framework to optimize monotone functions over normal sets. The main problem in applying this mathematical tool to energy efficiency, is that, as we have seen, the energy efficiency is not a monotone function of the transmit power. This means that monotonic optimization algorithms can not be applied directly to energy efficiency problems, but some elaborations and transformations are needed. In this section we will see how fractional programming and monotonic optimization can be integrated to solve those fractional problems which can not be handled by the algorithms developed in previous sections. However, before entering into the mathematical details, we should stress that even if monotonic optimization requires to analyze only the boundary of the feasible set, thus exhibiting a lower complexity than standard global optimization methods, it can not claim to solve a non-convex problem in polynomial time. In fact, the complexity of generic monotonic optimization algorithms is still exponential, which limits its practical applications. Nevertheless, monotonic optimization can prove a valuable tool to derive benchmarks against which sub-optimal methods can be contrasted.

Single-ratio and max-min problems

Single-ratio problems can be solved with limited complexity by either Dinkelbach's algorithm or the Charnes-Cooper-Transform, provided the numerator and the denominator are respectively concave and convex functions, and the constraint set is convex. However, we have also seen that Dinkelbach's algorithm is able to converge to the global solution of the problem also when these requirements are not met, provided one is able to globally maximize the auxiliary sub-problems in each iteration to compute $\boldsymbol{x}_n^*$. The generic sub-problem is stated as

$$\max_{\boldsymbol{x}} f(\boldsymbol{x}) - \lambda g(\boldsymbol{x}) \tag{3.29a}$$

$$\text{s.t. } \boldsymbol{x} \in \mathcal{S} \, . \tag{3.29b}$$

which is not convex when either f and g are not concave and convex, or $\mathcal{S}$ is not a convex set. Nevertheless, it can be globally solved by means of monotonic optimization, provided the following assumptions are met

- f can be expressed as the difference of monotone functions $f(\boldsymbol{x}) = f_1(\boldsymbol{x}) - f_2(\boldsymbol{x})$.
- g is a monotone function.
- $\mathcal{S} = \mathcal{N} \cap \mathcal{C}$, with $\mathcal{N}$ and $\mathcal{C}$ a normal and co-normal set in the hyper-rectangle $[\mathbf{0}; \boldsymbol{m}]$, $\boldsymbol{m} \in \mathbb{R}^n$.

We observe that also under these assumptions, (3.29a) is not a monotone function, and, consequently, (3.29) is not a monotonic problem. However, requiring (3.29a) to be a monotone function would be a too strict assumption, which is not met in practical energy efficiency optimization problems. Instead, as it will be shown in Chapter 4, requiring (3.29a) to be the difference of increasing functions is a general enough assumption as far as energy efficiency optimization is concerned. To reformulate (3.29) into a monotonic problem, we follow [167] and apply

the substitution $t = -(f_2(\boldsymbol{x}) + \lambda g(\boldsymbol{x})) + f_2(\boldsymbol{m}) + g(\boldsymbol{m})$, which yields

$$\max_{t,\boldsymbol{x}} f_1(\boldsymbol{x}) + t \tag{3.30a}$$

$$\text{s.t. } \boldsymbol{x} \in \mathcal{S} \tag{3.30b}$$

$$t + f_2(\boldsymbol{x}) + \lambda g(\boldsymbol{x}) \leq f_2(\boldsymbol{m}) + g(\boldsymbol{m}) \tag{3.30c}$$

$$0 \leq t \leq f_2(\boldsymbol{m}) + g(\boldsymbol{m}) - (f_2(\boldsymbol{0}) + g(\boldsymbol{0})) \tag{3.30d}$$

Leveraging the results reviewed in Appendix B, Problem (3.30) can be shown to be a monotonic problem in canonical form. Then, we can globally solve a single-ratio problem by applying Dinkelbach's algorithm, solving each sub-problem by monotonic optimization tools, such as the polyblock algorithm, which is reviewed in Appendix B.

A similar technique can be applied to globally solve max-min fractional problems in which some ratios do not possess the concave/convex structure. The main difference is that now we employ the generalized Dinkelbach's algorithm as solution algorithm, leveraging monotonic optimization theory to solve each sub-problem. Recalling the structure of the sub-problems in the generalized Dinkelbach's algorithm, this can be accomplished by applying a similar variable substitution as for the single-ratio case, and recalling that the minimum function is increasing in each argument.

Sum and product of ratios

As we have seen in Section 3.4, SoRPs and PoRPs can not be globally solved with limited complexity, even if each ratio is pseudo-linear. However, following [167, 140], they can be recast as monotonic problems as follows. Let us consider the SoRP (3.28), and denote by $\mathcal{S}$ the set defining the feasible set. We assume that $f_k(\boldsymbol{x}) = f_{1,k}(\boldsymbol{x}) - f_{2,k}(\boldsymbol{x})$, with $f_{1,k}$, $f_{2,k}$, and g_k monotone functions for all $k = 1, \ldots, K$, and that $\mathcal{S} = \mathcal{N} \cap \mathcal{C}$, with $\mathcal{N}$ and $\mathcal{C}$ a normal and co-normal set in the

hyper-rectangle $[\mathbf{0}; \boldsymbol{m}]$, $\boldsymbol{m} \in \mathbb{R}^n$. First, we reformulate (3.28) as

$$\max_{\boldsymbol{x}, \{t_k\}_{k=1}^K} \sum_{k=1}^K t_k \tag{3.31a}$$

$$\text{s.t. } \boldsymbol{x} \in \mathcal{S} \tag{3.31b}$$

$$f_{1,k}(\boldsymbol{x}) - (f_{2,k}(\boldsymbol{x}) + t_k g_k(\boldsymbol{x})) \geq 0 \ , \ \forall \ k = 1, \ldots, K \tag{3.31c}$$

Clearly, (3.31a) is a monotone function, but (3.31c) does not define a monotone constraint because it is the difference of two monotone functions. However, it can be reformulated as a monotone constraint by introducing an additional variable s, and splitting (3.31c) into the two inequalities $f_{2,k}(\boldsymbol{x}) + t_k g_k(\boldsymbol{x}) + s \leq f_{2,k}(\boldsymbol{m}) + t_k g_k(\boldsymbol{m})$ and $f_{1,k}(\boldsymbol{x}) + s \geq f_{2,k}(\boldsymbol{m}) + t_k g_k(\boldsymbol{m})$. This allows one to rewrite (3.31a) as

$$\max_{\boldsymbol{x}, \{t_k\}_{k=1}^K} \sum_{k=1}^K t_k \tag{3.32a}$$

$$\text{s.t. } \boldsymbol{x} \in \mathcal{S} \ , 0 \leq s \leq f_{2,k}(\boldsymbol{m}) + t_k g_k(\boldsymbol{m}) - f_{2,k}(\mathbf{0}) - t_k g_k(\mathbf{0}) \tag{3.32b}$$

$$f_{1,k}(\boldsymbol{x}) + s \geq f_{2,k}(\boldsymbol{m}) + t_k g_k(\boldsymbol{m}) \ , \ \forall \ k = 1, \ldots, K \tag{3.32c}$$

$$f_{2,k}(\boldsymbol{x}) + t_k g_k(\boldsymbol{x}) + s \leq f_{2,k}(\boldsymbol{m}) + t_k g_k(\boldsymbol{m}) \ , \ \forall \ k = 1, \ldots, K \tag{3.32d}$$

which is a monotone problem in canonical form, by virtue of the results in Appendix B, and therefore can be solved by means of the polyblock algorithm.

Clearly, the described method applies also to PoRPs, with the only difference of resulting in the objective $\prod_{k=1}^K t_k$.

4

Energy efficiency in wireless networks: centralized approaches

Equipped with the generalized concavity and fractional programming framework described in Chapters 2 and 3, now we turn our attention to showing how the developed techniques and algorithms prove instrumental in tackling practical energy-efficient resource allocation problems in wireless networks. The focus of this chapter will be on centralized resource allocation algorithms which design the network physical layer resources to maximize a common energy-efficient performance function, selected as one of the four network energy-efficient performance measures defined in Section 1.2: GEE, WSEE, WPEE, or WMEE.

The network resources to design depend on the particular system setup and on the type of nodes in the network. In Section 4.1 we will start with the simpler case in which only the transmit powers are allocated. We remark that, besides modeling single-antenna, single-carrier systems, this scenario also applies to multiple-antenna and MC system in which precoders, receive filters, and subcarriers are not optimized. Moreover, the results and methods described in Section 4.1 will serve as a necessary basis to tackle the scenario analyzed in Section 4.2, in which multiple-antenna systems are considered and the transmit powers are jointly allocated with the precoders and receive filters, as well as the

scenario considered in Section 4.3, wherein the focus is on MC systems and joint transmit power and subcarrier allocation is performed.

4.1 Power allocation in wireless networks

The network topology under analysis is that of a general interference network with K transmitters and M receivers, as depicted in the left illustration of Fig. 4.1. One relevant variation of the model in Fig. 4.1 is that in which the transmitters communicate with the receivers through an amplify-and-forward (AF) relay, as shown in the right illustration of Fig. 4.1.

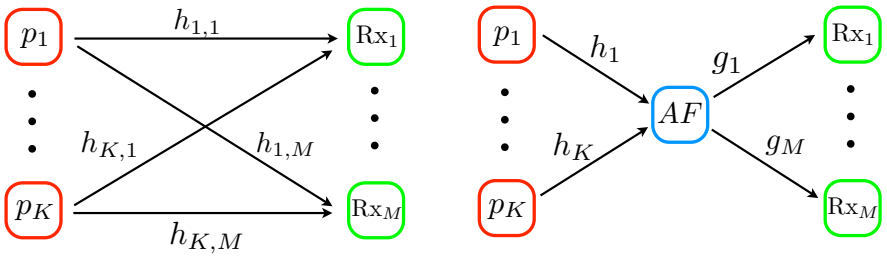

Figure 4.1: Left: interference network model with K transmitters and M receivers. Right: interference network model with AF relaying to enable communication between the K transmitters and the M receivers.

Clearly, the considered models can be readily specialized to other network topologies, such as interference channel (IC) (if $K = M$), multiple-access channel (MAC) (if $M = 1$), broadcast channel (BC) (if $K = 1$), interference multiple access channel (IMAC) in which different groups of transmitters intend to communicate with different receivers but interfere with one another, and interference broadcast channel (IBC) when each transmitter intends to communicate with a different subset of receivers, but its transmission causes interference to other receivers, too.

In the considered interference network setup, we consider two different models for the received SINR. In particular, we assume the SINR $\gamma_{k,m}$ of user k at receiver m can be expressed according to one of the following functional forms:

1. Linear SINR in the useful power.

$$\gamma_{k,m} = \frac{p_k \beta_{k,m}}{z_k + \sum_{j \neq k} p_j \beta_{j,m}} \, . \tag{4.1}$$

2. Concave fractional SINR in the useful power.

$$\gamma_{k,m} = \frac{p_k \alpha_{k,m}}{z_k + p_k \phi_{k,m} + \sum_{j \neq k} p_j \beta_{j,m}} \, . \tag{4.2}$$

In (4.1) and (4.2), p_k denotes the transmit power of user k, for all $k = 1, \ldots, K$, while all other coefficients are positive parameters which do not depend on the k-th users' transmit powers. The difference between (4.1) and (4.2) is the presence of a self-interference term in the denominator of (4.2).

4.1.1 Applications to present and future wireless networks.

As already mentioned, the considered network topology and SINR expressions can be readily applied to MAC and BC scenarios, which model uplink and downlink channels of conventional cellular networks. The focus of this section is to show that the considered system setup is much more general and applies to state-of-the-art and future wireless networks, too.

Multi-cell (relay-assisted) networks.

Consider M access points each serving one cell with K_m mobiles, and let $K = \sum_{m=1}^{M} K_m$. All terminals are equipped with a single antenna and operate on a single subcarrier. Denoting by $m = a(k)$ the access point associated to mobile k, for all $k = 1, \ldots, K$, and by $\sigma^2_{a(k)}$ the noise at access point $a(k)$, the SINR of user k is given by

$$\gamma_{k,a(k)} = \frac{|h_{k,a(k)}|^2 p_k}{\sigma^2_{a(k)} + \sum_{j \neq k} |h_{j,a(k)}|^2 p_j} \, , \tag{4.3}$$

which is formally equivalent to (4.1) by setting $\beta_{k,a(k)} = |h_{k,a(k)}|^2$, $z_k = \sigma^2_{a(k)}$, and $\beta_{j,a(k)} = |h_{j,a(k)}|^2$. Next, let us assume a half-duplex AF relay is deployed to help K cell-edge users, as shown in Fig. 4.2

for the case $M = 3$. Assuming the data symbols from the k users are statistically independent from the noise and with one another, the power of the signal received at the relay can be computed as

$$P_t = \sum_{k=1}^{K} p_k |h_k|^2 + \sigma_r^2 \ , \tag{4.4}$$

with σ_r^2 the noise power at the relay. Before being forwarded with power gain a^2, the signal received by the relay needs to be normalized by P_t, in order to ensure the relay amplifier does not operate in the saturation region. Since P_t depends on all of the users' powers, this result in the SINR of user k at its associated access point $a(k)$ to be expressed as

$$\gamma_{k,a(k)} = \frac{a^2 |g_{a(k)}|^2 |h_k|^2 p_k}{\sigma_{a(k)}^2 |h_k|^2 p_k + \sigma_r^2 (a^2 |g_{a(k)}|^2 + \sigma_{a(k)}^2) + \sum_{j \neq k} p_j |h_j|^2 (\sigma_{a(k)}^2 + a^2 |g_{a(k)}|^2)} \ , \tag{4.5}$$

which is formally equivalent to (4.2) upon setting $\alpha_{k,a(k)} = a^2 |g_{a(k)}|^2 |h_k|^2$, $\phi_{k,a(k)} = \sigma_{a(k)}^2 |h_k|^2$, $z_k = \sigma_r^2 (a^2 |g_{a(k)}|^2 + \sigma_{a(k)}^2)$, and $\beta_{j,a(k)} = |h_j|^2 (\sigma_{a(k)}^2 + a^2 |g_{a(k)}|^2)$.

All above derivations can be readily extended to MC systems and multiple-antenna systems with single stream transmission and linear reception by simply specifying accordingly the expressions of the coefficients $\alpha_{k,a(k)}$, $\phi_{k,a(k)}$, $\beta_{j,a(k)}$, and z_k, [187].

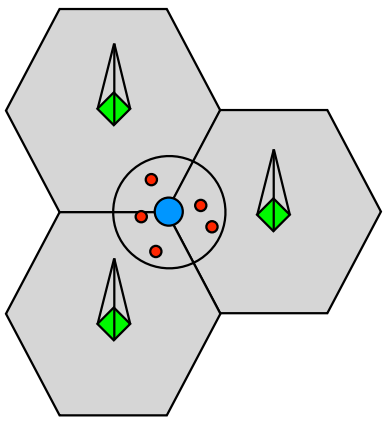

Figure 4.2: 3-cell relay-assisted network.

Small-cell (relay-assisted) networks.

Consider a wireless network in which K mobiles are located in an area served by M small-cell access points, where relays are possibly deployed at the border of the area to cover, in order to help cell-edge users, as shown in Fig. 4.3. The deployment of relays can be particularly convenient in case of small regions at the boundary of the area to cover, which are not reached by the small-cell access points. In such situations, it might be preferable to deploy relays instead of additional, more expensive small-cells. A user-scheduling protocol can be used to assign a group of cell-edge users to a given relay, which enables communication with the small cells. Conventional FDD or TDD techniques, as well as the use of directional antennas, can be used to separate the transmissions to or from the different relays. In all cases, as far as the received signal model is concerned, the small-cell (relay-assisted) scenario can be seen to be formally equivalent to the multi-cell (relay-assisted) scenario considered in the previous section.

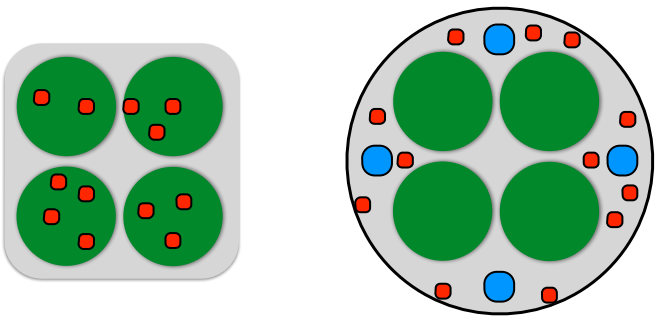

Figure 4.3: Left: A macro-cell served by 4 small cells; Right: Relays can be deployed at the macro-cell border to help edge-users.

Device-to-device (relay-assisted) networks.

In a cellular network, D2D communications can be activated by neighboring terminals, which then communicate directly with each other, bypassing the network infrastructure. This allows one to reduce the load of the network, as well as to increase the resource reuse factor.

As a result, when one or more D2D links are activated, a peer-to-peer network is established which underlays the cellular infrastructure. Assume K D2D links are activated in a cellular network which also contains K_C cellular users with interfering powers $\{p_{c,i}\}_{i=1}^{K_C}$. Denoting by $c_{i,k}$ the channel coefficient between cellular user i and device user k, the SINR enjoyed by the k-th device user at its intended receiver $a(k)$ can be expressed as

$$\gamma_{k,a(k)} = \frac{|h_{k,a(k)}|^2 p_k}{\sigma^2_{a(k)} + \sum_{j\neq k} |h_{j,a(k)}|^2 p_j + \sum_{i=1}^{K_C} |c_{i,k}|^2 p_{c,i}} , \tag{4.6}$$

which is formally equivalent to (4.1) by setting $\beta_{k,a(k)} = |h_{k,a(k)}|^2$, $z_k = \sigma^2_{a(k)} + \sum_{i=1}^{K_C} |c_{i,k}|^2 p_{c,i}$, and $\beta_{j,a(k)} = |h_{j,a(k)}|^2 p_j$.

Clearly, in order to activate a D2D communication, two mobiles need to be at a minimum distance below which it is more convenient to directly communicate rather than communicating through the base station. In order to increase such a minimum distance, the use of relays has been proposed [66]. In this context, the relay can implement a call admission control to select a subset of neighboring devices which are allowed to communicate bypassing the cellular infrastructure. If AF relaying is used, and defining $I_k = \sum_{i=1}^{K_C} |h_{i,k}|^2 p_{c,i}$ as the interference suffered by device user k due to the cellular users, and denoting by $g_{a(k)}$ the channel from the relay to the intended receiver of device user k, the resulting SINR experienced by the k-th device user is expressed as

$$\gamma_{k,a(k)} = \frac{a^2 |g_{a(k)}|^2 |h_k|^2 p_k}{\sigma_k^2 |h_k|^2 p_k + \sigma_r^2 (a^2 |g_{a(k)}|^2 + \sigma_k^2) + \sum_{j\neq k} p_j |h_j|^2 (\sigma_k^2 + a^2 |g_{a(k)}|^2) + I_k} , \tag{4.7}$$

which is formally equivalent to (4.2) upon setting $\alpha_{k,a(k)} = a^2 |g_{a(k)}|^2 |h_k|^2$, $\phi_{k,a(k)} = \sigma_k^2 |h_k|^2$, $z_k = \sigma_r^2 (a^2 |g_{a(k)}|^2 + \sigma_k^2) + I_k$, $\beta_{j,a(k)} = |h_j|^2 (\sigma_k^2 + a^2 |g_{a(k)}|^2)$.

Cognitive radio (relay-assisted) systems.

In its original formulation, cognitive radio takes advantage of the fact that not all licensed spectrum bands are used at the same time. Indeed,

several spectrum holes are present in the licensed spectrum band at a given point in time and geographical location [67]. So, it is possible for unlicensed users to temporarily use a spectrum hole for transmission, until the legitimate user needs to use it again. However, a higher resource reuse factor can be achieved using a spectrum sharing approach [157, 195], in which both the licensed and unlicensed users employ the same spectrum at the same time, provided the interference from the unlicensed users does not cause the QoS of the licensed users to drop below a predefined value. With this formulation, the cognitive radio system can be regarded as a peer-to-peer network underlaying the primary network, and is formally equivalent to the underlay D2D scenario described in the previous section.

Hardware-impaired networks.

The impact of non-ideal hardware on the performance of communication systems can be usually neglected in applications where high-quality hardware components can be afforded. However, recently the topic of hardware impairments in wireless communications is gaining momentum, mainly due to the rise of new transmission technologies such as massive MIMO, in which the use of expensive circuitry is not practical due to the large amount of required hardware. Recently, a model to account for hardware imperfections in wireless networks has been proposed in [23], where it is shown that the overall effect of hardware impairments can be modeled as an additional Gaussian interference term, whose power is proportional to the useful signal power. Applying this model to a multi-cell massive MIMO system wherein K transmitters communicate with L access points equipped with $N >> K/L$ antennas and low-power, low-cost circuitry, the signal vector received at access point $a(k)$ associated to user k, can be written as

$$\boldsymbol{r}_{a(k)} = \sum_{\ell=1}^{K} \boldsymbol{h}_{\ell,a(k)} x_\ell + \boldsymbol{w}_{a(k)} + \boldsymbol{\eta}_{a(k)} \ . \tag{4.8}$$

In (4.8), $\boldsymbol{h}_{\ell,a(k)}$ and x_ℓ are the ℓ-th user's channel to access point $a(k)$ and information symbol with power p_ℓ, $\boldsymbol{w}_{a(k)}$ is the white thermal noise at receiver $a(k)$ with covariance matrix $\sigma^2 \boldsymbol{I}_N$, while $\boldsymbol{\eta}_{a(k)}$ is the

hardware-impairment term, also modeled as a zero-mean Gaussian random vector, but with covariance matrix $\tau_{a(k)} \sum_{j=1}^{K} p_j \boldsymbol{D}_{j,a(k)}$, wherein $\boldsymbol{D}_{j,a(k)} = \mathrm{diag}(\{|h_{j,a(k)}(m)|^2\}_{m=1}^{M})$ and $\tau_{a(k)}$ is a proportionality coefficient related to the particular employed hardware. The resulting SINR enjoyed by the k-th user after linear reception by the filter $\boldsymbol{c}_k$, is thus written as

$$\gamma_{k,a(k)}=\frac{|\boldsymbol{c}_k^H \boldsymbol{h}_{k,a(k)}|^2 p_k}{\tau_{a(k)} \boldsymbol{c}_k^H \boldsymbol{D}_{k,a(k)} \boldsymbol{c}_k p_k + \sigma^2 \|\boldsymbol{c}_k\|^2 + \sum\limits_{j \neq k} p_j \left(|\boldsymbol{c}_k^H \boldsymbol{h}_{j,a(k)}|^2 + \tau_{a(k)} \boldsymbol{c}_k^H \boldsymbol{D}_{j,a(k)} \boldsymbol{c}_k \right)} \tag{4.9}$$

which is formally equivalent to (4.2), with $\alpha_{k,a(k)} = |\boldsymbol{c}_k^H \boldsymbol{h}_{k,a(k)}|^2$, $\phi_{k,a(k)} = \tau_{a(k)} \boldsymbol{c}_k^H \boldsymbol{D}_{k,a(k)} \boldsymbol{c}_k$, $z_k = \sigma^2 \|\boldsymbol{c}_k\|^2$, and $\beta_{j,a(k)} = |\boldsymbol{c}_k^H \boldsymbol{h}_{j,a(k)}|^2 + \tau_{a(k)} \boldsymbol{c}_k^H \boldsymbol{D}_{j,a(k)} \boldsymbol{c}_k$. A similar model applies to the downlink scenario [23].

Remark 4.1. Many other examples exist which fall under the umbrella of the system and signal model described in Fig. 4.1 and in Eqs. (4.1) and (4.2), but we omit details for the sake of brevity. We only remark that the SINR expression (4.2) also arises in ultra-wide-band systems [13], in networks affected by frequency-selective fading [31], and when the communication is impaired by inter-symbol interference [88].

In the rest of this section we enter into the mathematical details of power control for energy efficiency maximization via fractional programming. We will start by addressing the more widely investigated case of noise-limited scenarios, and then we will turn our attention to the more challenging interference-limited scenario.

4.1.2 Noise-limited scenarios

The general interference network model displayed in Fig. 4.1 reduces to a noise-limited scenario when a P2P channel is considered ($K = M = 1$), or when MACs and BCs are considered, in which successive interference cancellation (SIC) and dirty paper coding (DPC) techniques are used to remove multi-user interference. When no interference is present in a MAC, in both SINR models (4.1) and (4.2) we have $\beta_{j,m} = 0$, for all $j \neq k$.

Power control in (relay-assisted) P2P channels.

The P2P case has been already introduced in Section 1.1, and the energy efficiency maximization problem subject to a maximum power constraint is defined by

$$\max_{p} \frac{f(\gamma(p))}{\mu p + P_c} \tag{4.10a}$$

$$\text{s.t. } p \in [0; P_{max}] \tag{4.10b}$$

with $f(\gamma)$ being the so-called efficiency function. If f is concave as it happens for example when f is the channel capacity $f(\gamma) = \log_2(1+\gamma)$, then the numerator of the energy efficiency is concave provided also $\gamma(p)$ is concave in p, which holds for both the SINR expressions (4.1) and (4.2). As a result, the energy efficiency is the ratio between a concave and an affine function, and is therefore PC. In this case, (4.10) can be solved by means of any of the fractional programming algorithms developed in Chapter 3. Alternatively, since (4.10a) is PC, first-order optimality conditions are necessary and sufficient. Then, denoting by $\bar{p}$ the stationary point of (4.10a), the solution of (4.10) is obtained as $p^* = \min(\bar{p}, P_{max})$.

While the system capacity is the most widely used efficiency function, other choices are also possible, such as $f(\gamma) = R(1 - e^{-\gamma})^Q$, with R the communication rate and Q the data-packet length, which can be shown to be an approximation of the communication throughput. If $Q > 1$, $f(\gamma)$ is not concave, but S-shaped in γ. In this case, the second derivative of $f(\gamma(p))$ can be expressed as follows

$$\frac{\partial^2 f}{\partial p^2} = Q(1-e^{-\gamma(p)})^{Q-2} e^{-\gamma(p)} (\gamma'(p))^2 \left(Qe^{-\gamma(p)} - 1 + \frac{(1 - e^{-\gamma(p)})\gamma(p)''}{(\gamma(p)')^2} \right) \tag{4.11}$$

When (4.1) holds, (4.11) simplifies to

$$Q(1 - e^{-\gamma(p)})^{Q-2} e^{-\gamma(p)} (\gamma'(p))^2 \left(Qe^{-p\beta/z} - 1 \right) , \tag{4.12}$$

while when (4.2) holds, (4.11) becomes

$$Q(1-e^{-\gamma(p)})^{Q-2} e^{-\gamma(p)} (\gamma'(p))^2 \left(Qe^{-\gamma(p)} - 1 - \frac{2\phi}{z\alpha}(1 - e^{-\gamma(p)})(\phi p + z) \right) \tag{4.13}$$

In both cases, we can see that there exists a $\bar{p}$ such that $\frac{\partial^2 f}{\partial p^2}$ is positive for $p \leq \bar{p}$, and negative for $p \geq \bar{p}$, thereby implying that $f(\gamma(p))$ is S-shaped in p, too. Then, we can leverage Proposition 2.10 to claim the pseudo-concavity of the energy efficiency. Finally, the solution of (4.10) is once again obtained as $p^* = \min(\bar{p}, P_{max})$.

Power control in (relay-assisted) MACs and BCs

We will focus on a MAC in which SIC reception is implemented. Equivalent results can be obtained for a BC in which DPC is used by means of uplink-downlink duality. Moreover, we will assume the efficiency function is concave in γ, focusing on the most widespread choice $f(\gamma) = \log_2(1+\gamma)$. The energy-efficient power control problems will be formulated subject to a total transmit power constraint. We should remark that a similar power constraint is usually enforced in the BC case, while in the MAC scenario the typical power constraint is a per-transmitter constraint. Nevertheless, although focusing on a MAC, we consider a total power constraint with the aim of keeping the treatment as general as possible. All results can be readily specialized to the particular case of a per-transmitter power constraint[1].

The cooperative maximization of the network GEE can be cast as the fractional problem

$$\max_{\{p_k \geq 0\}_{k=1}^K} \frac{\sum_{k=1}^K \log_2(1+\gamma_k(p_k))}{\sum_{k=1}^K \mu_k p_k + P_{c,k}} \tag{4.14a}$$

$$\text{s.t.} \sum_{k=1}^K p_k \leq P_{max} \ , \tag{4.14b}$$

wherein each γ_k depends only on the useful power p_k, thanks to the SIC reception strategy. As a result, the numerator of (4.14a) is a sum of concave functions for both SINR expressions (4.1) and (4.2), and therefore is concave. On the other hand, the denominator is clearly affine, and we obtain that (4.14a) is a CLFP, which can be efficiently solved by the fractional programming tools described in Chapter 3.

[1]We should also remark that the results to be described also apply to the more general case in which the power constraint is expressed as $c(p_1, \ldots, p_K) \leq P_{max}$, with c a generic convex function of the transmit powers.

We obtain a similar result for the WMEE maximization problem,

$$\max_{\{p_k \geq 0\}_{k=1}^K} \min_{1 \leq k \leq K} w_k \frac{\log_2(1+\gamma_k(p_k))}{\mu_k p_k + P_{c,k}} \tag{4.15a}$$

$$\text{s.t.} \sum_{k=1}^K p_k \leq P_{max} \, . \tag{4.15b}$$

For both SINR expressions (4.1) and (4.2), each ratio has a concave numerator and an affine denominator, thus implying that (4.15) is a MMFP which can be efficiently solved by means of Algorithm 3.

The situation becomes more involved for WSEE and WPEE maximization. WSEE maximization can be cast as the SoRP

$$\max_{\{p_k \geq 0\}_{k=1}^K} \sum_{k=1}^K w_k \frac{\log_2(1+\gamma_k(p_k))}{\mu_k p_k + P_{c,k}} \tag{4.16a}$$

$$\text{s.t.} \sum_{k=1}^K p_k \leq P_{max} \, . \tag{4.16b}$$

As we have observed in Chapter 3, even if each summand has the concave-over-affine structure, no computationally efficient algorithm exists to solve a SoRP. However, for the particular case at hand, the global solution of (4.16) can still be determined with limited complexity, exploiting the fact that no multi-user interference is present. Indeed, this implies that the summands in (4.19a) are not coupled, each depending on a single transmit power. The only thing which couples the problem is the power constraint (4.16b). However, it is possible to reformulate (4.16) as a convex problem, exploiting the following result, which extends a result provided in [171].

Proposition 4.1. Assume $\gamma : p \in \mathbb{R}_+ \to \mathbb{R}_+$ is increasing, concave, and such that $\gamma(0) = 0$. Then, the function $r : p \in \mathbb{R}_+ \to r(p) = \frac{\log_2(1+\gamma(p))}{\mu p + P_c}$ is concave in the region $0 \leq p \leq p^*$, where p^* is the unique maximizer of $r(p)$.

Proof. Without loss of generality, we can assume $\mu = 1$. Then, since r is SPC, p^* is the unique solution of the equation

$$r^{'}(p) = 0 \leftrightarrow \frac{(p+P_c)\gamma^{'}(p)}{1+\gamma(p)} = \ln(1+\gamma(p)) \, . \tag{4.17}$$

Moreover, for $p \leq p^*$, the LHS of (4.17) is larger or equal than the RHS, whereas for $p > p^*$, the RHS is larger than the LHS. Next, all points in the concave region of r must satisfy the following condition [20]

$$r''(p) \leq 0 \leftrightarrow$$
$$\frac{(p+P_c)\gamma'(p)}{1+\gamma(p)} + \frac{\Big((p+P_c)\gamma'(p)\Big)^2}{2(1+\gamma(p))^2} - \frac{\gamma''(p)(p+P_c)^2}{2(1+\gamma(p))} \geq \ln(1+\gamma(p)). \tag{4.18}$$

Condition (4.18) is fulfilled for $p \to 0^+$, and since the second and third summands in the LHS of (4.18) are non-negative, we obtain that r is concave at least for all $0 \leq p \leq p^*$. □

By virtue of Proposition (4.1), there is no loss of generality in recasting Problem (4.16) as

$$\max_{\{p_k \geq 0\}_{k=1}^K} \sum_{k=1}^K w_k \frac{\log_2(1+\gamma_k(p_k))}{\mu_k p_k + P_{c,k}} \tag{4.19a}$$
$$\text{s.t.} \sum_{k=1}^K p_k \leq P_{max} \tag{4.19b}$$
$$p_k \leq p_k^* \ , \ \forall k = 1, \ldots, K \ , \tag{4.19c}$$

where the additional constraints (4.19c) ensure that (4.19) is a convex problem.

A similar approach can be used to solve the WPEE maximization problem, together with the observation that the exponentially weighted product of concave functions is log-concave.

4.1.3 Interference-limited scenarios

In many real-world wireless systems, interference suppression is not feasible or not practical. This makes energy-efficient power control significantly more difficult, and even the single-ratio GEE maximization problem becomes challenging. The main difficulty lies in the fact that the presence of a non-zero interference term in the SINR expressions makes the numerator of the energy efficiency of the each link

non jointly concave in all transmit powers, even when the efficiency function is concave in γ. To date, determining the global solutions of energy-efficient power control problems with limited complexity in interference-limited scenarios is still an open problem. Several different approaches have been recently proposed to compute suboptimal energy-efficient solutions. Some contributions adopt (semi)-orthogonal transmission schemes and/or linear interference neutralization techniques to remove multi-user interference, thus falling back to the noise-limited scenario [127, 177]. While leading to simple resource allocation algorithms, this approach has the drawback of reducing the resource reuse factor or of suffering from noise-enhancement effects. Several other contributions employ Dinkelbach's algorithm, proposing low-complexity, sub-optimal solutions for the auxiliary sub-problem to be solved in each iteration of Dinkelbach's algorithm. In [69, 55] the auxiliary sub-problem is tackled by means of alternating optimization, optimizing one transmit power at a time, while keeping the interference term fixed. This approach has a very limited complexity, even though convergence of the resulting algorithm can not be ensured, since Dinkelbach's algorithm is guaranteed to converge only if the global solution of each auxiliary problem is computed. In [70], an iterative algorithm is proposed, which is shown to yield a KKT point of the WSEE maximization problem.

A third, more recent approach is based on the framework of *sequential fractional programming*. The main idea is to tackle a difficult fractional program by solving a sequence of easier fractional problems. To this end, we need to introduce the following result, which will be used in combination with fractional programming theory.

Proposition 4.2. Let $\mathcal{P}$ be a maximization problem with continuous objective $r_0(\boldsymbol{x})$ and constraints $r_i(\boldsymbol{x}) \geq 0$, for $i = 1, \ldots, I$, defining a compact set. Let $\{\mathcal{P}_\ell\}_\ell$ be a sequence of maximization problems with objective $r_{0,\ell}(\boldsymbol{x})$, constraints $r_{i,\ell}(\boldsymbol{x}) \geq 0$, for $i = 1, \ldots, I$, and optimal solution $\boldsymbol{x}_\ell^*$. Assume that, for any ℓ and $i = 0, \ldots, I$, $r_{i,\ell}(\boldsymbol{x})$ enjoys the following properties.

P1) $r_{i,\ell}(\boldsymbol{x}) \leq r_i(\boldsymbol{x})$, for all $\boldsymbol{x}$.

P2) $r_{i,\ell}(\boldsymbol{x}^*_{\ell-1}) = r_i(\boldsymbol{x}^*_{\ell-1})$.

P3) $\nabla r_{i,\ell}(\boldsymbol{x}^*_{\ell-1}) = \nabla r_i(\boldsymbol{x}^*_{\ell-1})$.

Then, the sequence $\{\boldsymbol{x}^*_\ell\}_\ell$ of the solutions of $\{\mathcal{P}_\ell\}_\ell$ converges to a point satisfying the KKT optimality conditions of the original problem $\mathcal{P}$.

Proof. This result was first introduced in [113] and the proof can be obtained as follows. Due to Properties P1 and P2, for all ℓ and $i = 1, \ldots, I$ we have

$$r_{i,\ell+1}(\boldsymbol{x}^*_\ell) = r_i(\boldsymbol{x}^*_\ell) \geq r_{i,\ell}(\boldsymbol{x}^*_\ell) \geq 0 \,, \tag{4.20}$$

thus implying that $\boldsymbol{x}^*_\ell$ is feasible both for the original problem $\mathcal{P}$ and for next problem in the sequence $\mathcal{P}_{\ell+1}$. Next, exploiting again properties P1 and P2, we obtain

$$r_0(\boldsymbol{x}^*_\ell) \geq r_{0,\ell}(\boldsymbol{x}^*_\ell) \geq r_{0,\ell}(\boldsymbol{x}^*_{\ell-1}) = r_0(\boldsymbol{x}^*_{\ell-1}) \,, \tag{4.21}$$

thereby showing that the sequence $\{r_0(\boldsymbol{x}^*_\ell)\}_\ell$ of the values achieved by the objective of the original problem $\mathcal{P}$ is non-decreasing. In turn, this implies convergence because r_0 is continuous, and therefore admits a maximum on the compact feasible set. By a similar argument, exploiting also Property P3, it follows that upon convergence the KKT conditions of the original problem $\mathcal{P}$ are fulfilled. □

Proposition 4.2 allows one to find KKT points of a difficult problem to solve, by solving a sequence of approximate problems. The issue of course is to find suitable approximations of the objective and constraints that fulfill properties P1-P3, while at the same time resulting in an easier problem $\mathcal{P}_\ell$. The use of Proposition 4.2 coupled with fractional programming has been first proposed in [171, 190, 129], after it was successfully applied in the context of rate and SINR maximization problems [44, 170]. In the two coming sections we will show how Proposition 4.2 can be successfully integrated into the fractional programming framework, to develop algorithms which require an affordable complexity to converge to a KKT point of the resource allocation problem. Moreover, unlike most state-of-the-art approaches which are tailored for a particular system model, the advantage of this approach

is that it provides a general framework for energy-efficiency optimization, which can be used to solve a number of different problems in many different scenarios.

Power control with linear SINR

Let us consider the GEE maximization problem

$$\max_{\{p_k \geq 0\}_{k=1}^K} \frac{\sum_{k=1}^K \log_2 \left(1 + \frac{\beta_{k,a(k)} p_k}{z_k + \sum_{j \neq k} \beta_{j,a(k)} p_j}\right)}{\sum_{k=1}^K \mu_k p_k + P_{c,k}} \tag{4.22a}$$

$$\text{s.t.} \sum_{k=1}^K p_k \leq P_{max} \, . \tag{4.22b}$$

As anticipated, the numerator is not jointly concave in $\boldsymbol{p} = \{p_k\}_{k=1}^K$. Then, we search for a suitable lower-bound of (4.22a), so that we can employ the result in Proposition 4.2.

Lemma 4.1. For any non negative γ and γ_0, it holds $\log(1+\gamma) \geq a \log(\gamma) + b$, with

$$a = \gamma_0/(1+\gamma_0) \tag{4.23}$$

$$b = \log(1+\gamma_0) - \gamma_0 \log(\gamma_0)/(1+\gamma_0) \tag{4.24}$$

Moreover, the inequality is tight for $\gamma = \gamma_0$ and $\frac{\partial \log(1+\gamma)}{\partial \gamma}\Big|_{\gamma=\gamma_0} = \frac{\partial (a \log(\gamma)+b)}{\partial \gamma}\Big|_{\gamma=\gamma_0}$.

Proof. See [136, Section III.B]. □

Leveraging Lemma (4.1), we can lower-bound the GEE as

$$\text{GEE} \geq \frac{\sum_{k=1}^K a_k \left[\log_2 \beta_{k,a(k)} p_k - \log_2 \left(z_k + \sum_{j \neq k} p_j \beta_{j,a(k)}\right)\right] + b_k}{\sum_{k=1}^K \mu_k p_k + P_{c,k}} \tag{4.25}$$

and the bound is tight if $\{a_k, b_k\}_{k=1}^K$ are computed after (4.23) and (4.24). Finally, applying the variable substitution $p_k = 2^{q_k}$, (4.25) becomes

$$\frac{\sum_{k=1}^K a_k \left[\log_2 \beta_{k,a(k)} + q_k - \log_2 \left(z_k + \sum_{j\neq k} 2^{q_j} \beta_{j,a(k)}\right)\right] + b_k}{\sum_{k=1}^K \mu_k 2^{q_k} + P_{c,k}} \tag{4.26}$$

Recalling that the log-sum-exp function is convex, we can see that (4.26) now has a concave numerator and a convex denominator, and therefore can be maximized by means of Dinkelbach's algorithm with an affordable complexity[2]. Then, we can devise a power control algorithm which is guaranteed to converge to a KKT point of Problem (4.22) using Proposition 4.2, with Problem $\mathcal{P}_\ell$ given by

$$\max_{\{q_k\}_{k=1}^K} \frac{\sum_{k=1}^K a_k \left[\log_2 \beta_{k,a(k)} + q_k - \log_2 \left(z_k + \sum_{j\neq k} 2^{q_j} \beta_{j,a(k)}\right)\right] + b_k}{\sum_{k=1}^K \mu_k 2^{q_k} + P_{c,k}} \tag{4.27a}$$

$$\text{s.t.} \sum_{k=1}^K 2^{q_k} \leq P_{max} \ , \tag{4.27b}$$

and updating $\{a_k, b_k\}_{k=1}^K$ after each problem $\mathcal{P}_\ell$ is solved, so as to fulfill Properties P2 and P3 of Proposition 4.2. The pseudo-code of the final procedure is reported in Algorithm 5.

Using a similar approach it is possible to tackle the WMEE maximization problem, lower-bounding each of the transmitters energy efficiencies by Lemma 4.1, but then employing the generalized Dinkelbach's algorithm to globally solve each problem $\mathcal{P}_\ell$ of the sequence. A similar approach can also be used to find a KKT point of the WPEE maximization problem. However, in this case it is convenient to first apply the logarithmic function to simplify the problem. This converts the WPEE into the function

$$\sum_{k=1}^K w_k \ln\left[\log_2\left(1+\gamma_k\right)\right] - \sum_{k=1}^K w_k \ln(\mu_k p_k + P_{c,k}) \ . \tag{4.28}$$

[2]In general, the non-negativity of the numerator of (4.26) can not be guaranteed. However, we have shown in Chapter 3 that it is enough to ensure that the numerator has a non-negative maximum, which can be seen to hold.

Algorithm 5 Power control for GEE maximization with SINR (4.1)

$\ell = 0$; $\epsilon > 0$; Select a feasible $\boldsymbol{p}_0^{(0)}$;
while $\left|\text{GEE}\left(\boldsymbol{p}_0^{(\ell+1)}\right) - \text{GEE}\left(\boldsymbol{p}_0^{(\ell)}\right)\right| > \epsilon$ **do**
  $\ell = \ell + 1$;
  Compute $\gamma_{0,k}^{(\ell)}\left(\boldsymbol{p}_0^{(\ell)}\right)$, for all $k = 1, \ldots, K$;
  Compute $a_k^{(\ell)}, b_k^{(\ell)}$ according to (4.23) and (4.24);
  Compute $\boldsymbol{q}_0^{(\ell)}$ as the solution of Problem P_ℓ in (4.27);
  $\boldsymbol{p}_0^{(\ell)} = 2^{\boldsymbol{q}_0^{(\ell)}}$;
end while

At this point, applying the lower-bound in Lemma 4.1 to the $\log_2(\cdot)$ function and the the substitution $p_k = 2^{q_k}$, we obtain a concave lower-bound of (4.28), which can be maximized by ordinary convex programming and allows one to devise a similar algorithm as Algorithm 5 which converges to a KKT point of the WPEE maximization problem.

Finally, we deal with the power control problem for WSEE maximization. The problem is formulated as the SoRP

$$\max_{\{p_k \geq 0\}_{k=1}^K} \sum_{k=1}^{K} w_k \frac{\log_2\left(1 + \dfrac{\beta_{k,a(k)} p_k}{z_k + \sum_{j \neq k} \beta_{j,a(k)} p_j}\right)}{\mu_k p_k + P_{c,k}} \tag{4.29a}$$

$$\text{s.t.} \sum_{k=1}^{K} p_k \leq P_{max} \tag{4.29b}$$

In this case, the method outlined previously does not make the problem tractable. Indeed, even upon using a lower-bound to make the numerator of each ratio concave, we would be left with a sum of PC functions, which in general is not guaranteed to be PC. However, it is still possible to develop an algorithm which yields a KKT point of Problem (4.29), exploiting the sum-based nature of (4.29a). The KKT conditions of

(4.29) are expressed as

$$\frac{\mathrm{d}}{\mathrm{d}p_k}\mathrm{WSEE}(\boldsymbol{p}) + \nu_k - \lambda = 0,\ \forall\ k = 1, \ldots, K \tag{4.30a}$$

$$\nu_k \geq 0,\ \ \lambda \geq 0,\ \forall\ k = 1, \ldots, K \tag{4.30b}$$

$$-p_k \leq 0,\ \forall\ k = 1, \ldots, K \tag{4.30c}$$

$$\sum_{k=1}^{K} p_k \leq P_{max},\ k = 1, \ldots, K \tag{4.30d}$$

$$\nu_k p_k = 0,\ k = 1, \ldots, K \tag{4.30e}$$

$$\lambda \left(P_{max} - \sum_{k=1}^{K} p_k \right) = 0,\ k = 1, \ldots, K \tag{4.30f}$$

where λ and $\{\nu_k\}_{k=1}^{K}$ are the Lagrange multipliers associated to the maximum power constraint and to the non-negativity power constraints, respectively. After standard algebraic manipulations, it can be shown that

$$\frac{\mathrm{d}}{\mathrm{d}p_k}\mathrm{WSEE}(\mathbf{p}) = \frac{1}{\ln 2}\frac{\mathrm{Q}_k \beta_{k,a(k)}}{z_k + \mathrm{I}_k + p_k \beta_{k,a(k)}} - \mathrm{C}_k - \mathrm{L}_k \tag{4.31}$$

wherein

$$\mathrm{I}_k = \sum_{j \neq k}^{K} p_j \beta_{j,a(k)} \tag{4.32}$$

$$\mathrm{Q}_k = \frac{w_k}{P_{c,k} + \mu_k p_k} \tag{4.33}$$

$$\mathrm{C}_k = w_k \mu_k \frac{\log_2(1 + \gamma_{k,a(k)})}{(P_{c,k} + \mu_k p_k)^2} \tag{4.34}$$

$$\mathrm{L}_k = \frac{1}{\ln 2} \sum_{\ell \neq k}^{K} \mathrm{Q}_\ell \gamma_{\ell,a(\ell)} \frac{\beta_{k,a(\ell)}}{z_\ell + \sum_{j=1}^{K} p_j \beta_{j,a(\ell)}} \tag{4.35}$$

Finally, observing that some of the defined quantities depend themselves on p_k, (4.30a) can be rewritten as the fixed-point equation

$$p_k = \frac{(1/\ln 2) Q_k}{\lambda - \nu_k + \mathrm{C}_k + \mathrm{L}_k} - \frac{z_k + \mathrm{I}_k}{\beta_{k,a(k)}}. \tag{4.36}$$

Notice that I_k is the interference suffered by user k; Q_k is an equivalent weight for the rate achieved by user k scaled by the corresponding power consumption; C_k is a marginal power cost paid by user k; finally, L_k accounts for the interference caused by user k to unintended receivers. Then, an iterative algorithm to solve the KKT system (4.30) can be developed by starting from a feasible transmit power vector and iteratively updating the transmit powers as the solution of

$$\begin{cases} p_k = \max\left\{0, \dfrac{(1/\ln 2)\mathrm{Q}_k}{\lambda + \mathrm{C}_k + \mathrm{L}_k} - \dfrac{z_k + \mathrm{I}_k}{\beta_{k,a(k)}}\right\} \\ \displaystyle\sum_{k=1}^{K} p_k \leq P_{\max}\ , \end{cases} \tag{4.37}$$

which can be efficiently solved by bisection search on the multiplier λ. The resulting formal procedure can be stated as in Algorithm 6.

Algorithm 6 Power control for WSEE maximization

$\ell = 0$; $\epsilon > 0$; Select a feasible $\boldsymbol{p}^{(0)}$;
while $\|\boldsymbol{p}^{(\ell+1)} - \boldsymbol{p}^{(\ell)}\| > \epsilon$ **do**
  $\ell = \ell + 1$;
  Compute $\{\mathrm{I}_k, \mathrm{Q}_k, \mathrm{C}_k, \mathrm{L}_k\}_{k=1}^{K}$, after (4.32), (4.33), (4.34), (4.35);
  Compute $p_k^{(\ell)}$ according to (4.37), for all $k = 1, \ldots, K$;
end while

Power control with concave SINR

The approaches described in the previous section can be extended to the case in which the more general SINR expression (4.2) is considered. As an illustrative example, let us consider the maximization of the GEE. The problem to be solved is formulated as

$$\max_{\{p_k \geq 0\}_{k=1}^{K}} \frac{\sum_{k=1}^{K} \log_2\left(1 + \dfrac{\alpha_{k,a(k)} p_k}{z_k + \phi_{k,a(k)} p_k + \sum_{j \neq k} \beta_{j,a(k)} p_j}\right)}{\sum_{k=1}^{K} \mu_k p_k + P_{c,k}} \tag{4.38a}$$

$$\text{s.t.} \sum_{k=1}^{K} p_k \leq P_{max}\ . \tag{4.38b}$$

Applying the bound in Lemma 4.1, (4.38a) can be lower-bounded as

$$\text{GEE} \geq \frac{\sum_{k=1}^{K} a_k \left[\log_2 \beta_{k,a(k)} p_k - \log_2 \left(z_k + \phi_{k,a(k)} p_k + \sum_{j \neq k} p_j \beta_{j,a(k)}\right)\right] + b_k}{\sum_{k=1}^{K} \mu_k p_k + P_{c,k}} . \tag{4.39}$$

Also in this case, applying the variable change $p_k = 2^{q_k}$, for all $k = 1, \ldots, K$, turns (4.39) into a concave function of $\{q_k\}_{k=1}^{K}$, and a similar algorithm as Algorithm 5 can be designed to obtain a KKT point of Problem (4.38). More details on this will be provided in the next section, also considering QoS constraints.

In the following, we will instead consider an even more general concave SINR form than (4.2), which we will encounter in Section 4.2, in the context of resource allocation for multiple-antenna systems. Namely, let us assume the SINR is expressed as

$$\gamma_{k,a(k)} = \sum_{i=1}^{I} \frac{p_k \alpha_{k,a(k),i}}{z_{k,i} + p_k \phi_{k,a(k),i} + \sum_{j \neq k} p_j \beta_{j,a(k),i}} = \sum_{i=1}^{I} \gamma_{i,k} . \tag{4.40}$$

Then the GEE maximization problem becomes

$$\max_{\{p_k \geq 0\}_{k=1}^{K}} \frac{\sum_{k=1}^{K} \log_2 \left(1 + \sum_{i=1}^{I} \gamma_{i,k}\right)}{\sum_{k=1}^{K} \mu_k p_k + P_{c,k}} \tag{4.41a}$$

$$\text{s.t.} \sum_{k=1}^{K} p_k \leq P_{max} . \tag{4.41b}$$

In order to tackle Problem (4.41), it is still possible to employ the sequential approach described in Proposition 4.2, but the bound in Lemma 4.1 alone is not enough to make the numerator of the energy efficiency concave. To this end, let us introduce the following lemma, based on the arithmetic-geometric mean inequality.

Lemma 4.2. For any non negative $\{c_i\}_{i=1}^{n}$, with $\sum_{i=1}^{n} c_i = 1$, it holds $\gamma = \sum_{i=1}^{I} \gamma_i \geq \prod_{i=1}^{I} \left(\frac{\gamma_i}{c_i}\right)^{c_i}$. Moreover, for any non-negative $\{\gamma_{0,i}\}_{i=1}^{I}$, the bound is tight at $\gamma_0 = \sum_{i=1}^{I} \gamma_{i,0}$, and the first-order derivatives of the LHS and RHS of the bound are equal at γ_0, provided that

$$c_i = \frac{\gamma_{0,i}}{\gamma_0} , \tag{4.42}$$

for all $i = 1, \ldots, n$.

Proof. See [44] and [190]. □

Using first Lemma 4.2, and then Lemma 4.1, we can lower-bound (4.41a) as

$$\mathrm{GEE}(\boldsymbol{p}) \geq \frac{\sum_{k=1}^{K} a_k \log_2 \left(\prod_{i=1}^{I} \left(\frac{\gamma_{i,k}}{c_{i,k}} \right)^{c_{i,k}} \right) + b_k}{\sum_{k=1}^{K} p_k + P_{c,k}} \,. \tag{4.43}$$

Upon applying the substitution $p_k = 2^{q_k}$ in (4.43), the ℓ-th approximate Problem $\mathcal{P}_\ell$ can be formulated as

$$\max_{\{q_k\}_{k=1}^K} \frac{\varphi\left(\{q_k\}_{k=1}^K\right)}{\sum_{k=1}^{K} \mu_k 2^{q_k} + P_{c,k}} \tag{4.44a}$$

$$\text{s.t.} \sum_{k=1}^{K} 2^{q_k} \leq P_{max} \,, \tag{4.44b}$$

wherein

$$\varphi(\{q_k\}_{k=1}^K) = \sum_{k=1}^{K} \Bigg\{ a_k \sum_{i=1}^{I} c_{i,k} \Bigg[\log(\alpha_{k,a(k),i}) + q_k - \log_2 \left(z_{i,k} + \phi_{k,a(k),i} 2^{q_k} + \sum_{j \neq k}^{K} \beta_{j,a(k),i} 2^{q_j} \right) - \log_2 c_{i,k} \Bigg] + b_k \Bigg\} \tag{4.45}$$

The objective (4.44a) can be seen to be a jointly PC function of $\{q_k\}_{k=1}^K$, and therefore we can solve (4.44) by means of Dinkelbach's algorithm with affordable complexity. Leveraging this result, it is possible to develop Algorithm 7 in a similar fashion as done for Algorithm 5.

Algorithm 7 enjoys similar properties as Algorithm 5 and in particular it is guaranteed to converge to a KKT point of (4.41), requiring to solve only convex problems.

Algorithm 7 Power control for GEE maximization with SINR (4.40)

$\ell = 0$; $\epsilon > 0$; Select a feasible $\boldsymbol{p}_0^{(0)}$;
while $\left|\text{GEE}\left(\boldsymbol{p}_0^{(\ell+1)}\right) - \text{GEE}\left(\boldsymbol{p}_0^{(\ell)}\right)\right| > \epsilon$ **do**
  $\ell = \ell + 1$;
  Compute $\gamma_{0,i,k}^{(\ell)}$, for all $k = 1, \ldots, K$, as in (4.40);
  $\gamma_{0,k} = \sum_{i=1}^{I} \gamma_{0,i,k}$, for all $k = 1, \ldots, K$;
  Compute $c_{i,k}^{(\ell)}, a_k^{(\ell)}, b_k^{(\ell)}$ according to (4.42), (4.23), (4.24);
  Compute $\boldsymbol{q}_0^{(\ell)}$ as the solution of Problem P_ℓ in (4.44);
  $\boldsymbol{p}_0^{(\ell)} = 2^{\boldsymbol{q}_0^{(\ell)}}$;
end while

Power control with concave SINR and QoS constraints.

Assume the SINRs are expressed as in (4.2). In addition, assume that each user k in the network requires a QoS constraint in the form of a minimum achievable rate $R_{min,k}$. Then, the GEE maximization problem can be formulated as

$$\max_{\{p_k\}_{k=1}^K} \quad \frac{\sum_{k=1}^{K} \log_2\left(1 + \gamma_{k,a(k)}\right)}{p_c + \sum_{k=1}^{K} p_k} \tag{4.46a}$$

$$\text{s.t. } 0 \leq p_k \leq P_{max,k}\ , \forall k = 1, \ldots, K \tag{4.46b}$$

$$\log_2(1 + \gamma_{k,a(k)}) \geq R_{min,k}\ , \forall k = 1, \ldots, K\ . \tag{4.46c}$$

For later convenience, we also define

$$\gamma_{min,k} \triangleq 2^{R_{min,k}} - 1 \tag{4.47}$$

$$\gamma_{max,k} \triangleq \frac{\alpha_{k,a(k)}}{\phi_{k,a(k)}} \tag{4.48}$$

which represent the minimum SINR requirement and the maximum attainable SINR for user k. Therefore, a necessary condition such that (4.46) is feasible is

$$0 \leq \gamma_{min,k} \leq \gamma_{max,k} \quad \forall k \tag{4.49}$$

Condition (4.49) can be strengthened into a necessary and sufficient condition as shown in the following lemma, whose proof is available in [192].

Lemma 4.3. Let $\mathbf{F} \in \mathbb{C}^{K\times K}$ be a matrix whose (k,j)-th element is defined as

$$[\mathbf{F}]_{k,j} \triangleq \begin{cases} 0 & j = k \\ \frac{\beta_{j,a(k)}\gamma_{min,k}}{\alpha_{k,a(k)} - \phi_{k,a(k)}\gamma_{min,k}} & j \neq k \end{cases} \tag{4.50}$$

and denote by $\rho_{\mathbf{F}}$ its spectral radius. Problem (4.46) has a non-empty feasible set if and only if (4.49) holds and

$$\rho_{\mathbf{F}} < 1 \quad \text{and} \quad (\mathbf{I} - \mathbf{F})^{-1}\,\underline{\mathbf{s}} \leq \mathbf{P_{max}} \tag{4.51}$$

where $\mathbf{P_{max}} = [P_{max,1}, P_{max,2}, \ldots, P_{max,K}]^T \in \mathbb{R}_+^{K\times 1}$ and $\mathbf{s} \in \mathbb{R}_+^K$ has elements given by $[\underline{\mathbf{s}}]_k \triangleq z_k\gamma_{min,k}(\alpha_{k,a(k)} - \phi_{k,a(k)}\gamma_{min,k})^{-1}$.

After characterizing the feasibility of (4.46), we turn our attention to developing a solution algorithm. We can see that the objective of (4.46) is formally equivalent to that of (4.38), and therefore we can turn (4.46a) into a PC function resorting to the same lower-bound used for (4.38), coupled with the variable change $p_k = 2^{q_k}$. However, upon applying this variable change, the QoS constraint becomes

$$2^{q_k}(\alpha_{k,a(k)} - \gamma_{min,k}\phi_{k,a(k)}) \geq \gamma_{min,k}\left(z_k + \sum_{j\neq k}\beta_{j,a(k)}2^{q_j}\right). \tag{4.52}$$

Equation (4.52) is not a convex constraint, but since (4.49) must hold true, we can apply the logarithm function to both sides, which yields the convex inequality:

$$q_k - \log_2\left(z_k + \sum_{j\neq k}\beta_{j,a(k)}2^{q_j}\right) + \log_2\left(\frac{\alpha_{k,a(k)} - \gamma_{min,k}\phi_{k,a(k)}}{\gamma_{min,k}}\right) \geq 0\,. \tag{4.53}$$

Thus, we can employ again the sequential convex programming approach, in which the fractional problem to be solved in each iteration

is given by

$$\max_{\{q_k\}_{k=1}^K} \frac{\sum_{k=1}^K a_k \left[\log_2 \alpha_{k,a(k)} + q_k - \log_2 \left(z_k + \phi_{k,a(k)} 2^{q_k} + \sum_{j \neq k} 2^{q_j} \beta_{j,a(k)} \right) \right] + b_k}{\sum_{k=1}^K \mu_k 2^{q_k} + P_{c,k}} \tag{4.54a}$$

$$\text{s.t.} \sum_{k=1}^K 2^{q_k} \leq P_{max,k} \ , \forall k \tag{4.54b}$$

$$q_k - \log_2 \left(z_k + \sum_{j \neq k} \beta_{j,a(k)} 2^{q_j} \right) + \log_2 \left(\frac{\alpha_{k,a(k)} - \gamma_{min,k} \phi_{k,a(k)}}{\gamma_{min,k}} \right) \geq 0 \ , \forall k \tag{4.54c}$$

with coefficients $\{a_k, b_k\}_{k=1}^K$ given by (4.23) and (4.24). Problem (4.54) has a PC objective and convex constraints and therefore can be solved by fractional programming theory with polynomial complexity. The formal resource allocation algorithm is stated as in Algorithm 8.

Algorithm 8 Power control for GEE maximization with SINR (4.40) and QoS

Test feasibility by Proposition 4.3.
if Feasible **then**
  $\ell = 0$; $\epsilon > 0$; Select a feasible $\boldsymbol{p}_0^{(0)}$;
  while $\left| \text{GEE}\left(\boldsymbol{p}_0^{(\ell+1)}\right) - \text{GEE}\left(\boldsymbol{p}_0^{(\ell)}\right) \right| > \epsilon$ **do**
    $\ell = \ell + 1$;
    Compute $\gamma_{0,k}^{(\ell)}\left(\boldsymbol{p}_0^{(\ell)}\right)$, for all $k = 1, \ldots, K$;
    Compute $a_k^{(\ell)}, b_k^{(\ell)}$ according to (4.23) and (4.24);
    Compute $\boldsymbol{q}_0^{(\ell)}$ as the solution of Problem P_ℓ in (4.54);
    $\boldsymbol{p}_0^{(\ell)} = 2^{\boldsymbol{q}_0^{(\ell)}}$;
  end while
end if

Algorithm 8 enjoys similar properties as Algorithm 5, monotonically increasing the GEE value and converging to a point fulfilling the KKT

conditions of the original problem (4.46).

Before closing this section, we should remark that in this scenario it has been possible to reformulate the QoS constraint in convex form because we have considered individual QoS constraints. However, this is no longer possible when dealing with sum-QoS constraints. Nevertheless, in these scenarios it is still possible to obtain a KKT point of the resource allocation problem resorting to the sequential convex approximation tool. More details on this issue will be provided in Section 4.3.

4.2 Resource allocation in MIMO wireless networks

Spurred by the seminal work [161], over the years the use of multiple antennas has become an established means to improve the performance of wireless communication systems. Nowadays, the use of multiple antennas is standardized in LTE, and one candidate technology for 5G networks, massive MIMO, is based on the deployment of a great deal of antennas.

Equipping multiple-antennas provides new resources and signal dimensions other than the transmit powers that can be designed to increase the network energy efficiency. This leads to the problem of joint transmit power and transceiver design for energy efficiency maximization, which is addressed in this section. As it will be shown, this problem is more involved than the power control case addressed in Section 4.1, and fewer contributions have been made to date. In this section we will present state-of-the-art applications, starting from noise-limited scenarios and then moving on to the interference-limited case.

4.2.1 P2P MIMO channels.

Consider a MIMO channel with N_T transmit and N_R receive antennas. The energy efficiency of a P2P MIMO channel has been already introduced in (1.4), with the $N_R \times N_T$ matrix $\boldsymbol{P}$ denoting the transmitter precoding matrix. The energy-efficient resource allocation problem is

stated as

$$\max_{\boldsymbol{P}} \frac{W \log_2 \left| \boldsymbol{I}_N + \rho \boldsymbol{H} \boldsymbol{P} \boldsymbol{H}^H \right|}{\mu \mathrm{tr}(\boldsymbol{P}) + P_c} \tag{4.55a}$$

$$\text{s.t. } \mathrm{tr}(\boldsymbol{P}) \leq P_{max} \, . \tag{4.55b}$$

$$\boldsymbol{P} \succeq \boldsymbol{0} \, , \tag{4.55c}$$

with ρ being the inverse of the noise power. We observe that the precoding matrix $\boldsymbol{P}$ accounts for both the transmit power and transmit direction of the N_T data-streams. Depending on the implementation of the MIMO transceiver, the circuit power P_c may be a function of the number of active transmit and receive antennas, $P_c(\boldsymbol{P})$. If required, a QoS in the form of a minimum data-rate $R(\boldsymbol{P}) \geq R^*$ can be added to (4.55). Since the logarithm of the identity plus an Hermitian positive-semidefinite matrix is a matrix-concave function [91], the numerator of (4.55a) is concave in $\boldsymbol{P}$. As for the denominator, the trace of the transmit covariance matrix is a linear function and so it depends on the circuit power $P_c(\boldsymbol{P})$ whether the programming problem (4.55) can be solved with affordable complexity by means of the algorithms described in Chapter 3.

Circuit power $P_c(\boldsymbol{P})$	Problem Class
independent of $\boldsymbol{P}$, constant	CLFP
affine function of $\boldsymbol{P}$	CLFP
convex function of $\boldsymbol{P}$	CCFP
non-convex function of $\boldsymbol{P}$	Generic Fractional Program

Table 4.1: EE maximization of single-user MIMO link with different circuit power models.

The first three cases in Table 4.1 can be solved with affordable complexity by either Dinkelbach's algorithm or by using the Charnes-Cooper Transform, as described in Chapter 3. Instead, the fourth case requires the use of global programming methods, such as monotonic optimization.

Depending on the energy consumption model, the circuit power P_c can contain different terms. For the constant terms, a generic model

[84] contains the terms $n_T P_\gamma$ which corresponds to the power consumed for RF hardware per RF chain, i.e., per antenna, and P_{sta} is the static power consumption from baseband processing and battery unit. If all RF chains for all n_T antennas are used regardless of the precoding $\boldsymbol{P}$, we are in the first row in 4.1 and CLFP can be used to solve the corresponding energy-efficient problem. If the RF power consumption is modeled as a function of $\mathrm{tr}(\boldsymbol{P})$ only, again the CLFP method applies. If the power consumption of the RF hardware depends on the actual number of used antennas via the choice of $\boldsymbol{P}$, different expressions for $P_c(\boldsymbol{P})$ can occur, e.g., $P_c(\boldsymbol{P}) = \zeta \mathrm{tr}(\boldsymbol{P}^2) + \xi$ resulting in a convex function of $\boldsymbol{P}$. The corresponding GEE problem can be solved by CCFP. Finally, more complicated dependencies of the circuit power on the precoding matrix $\boldsymbol{P}$ lead to a generic fraction program.

4.2.2 P2P relay-assisted MIMO channels.

Now let us modify the scenario by considering a two-hop MIMO channel, as illustrated in Figure 4.4. Both wireless links are equipped with multiple transmit and receive antennas. The source node has N_S, the relay N_R, and the destination node has N_D antennas. The source chooses the transmit covariance matrix $\boldsymbol{P} \succeq 0$ under a transmit power constraint $\mathrm{tr}(\boldsymbol{P}) \leq P_S^{max}$. The non-regenerative AF relay multiplies the received vector by the AF matrix $\boldsymbol{A}$ under a relay power constraint P_R^{max}. The receiver performs a linear minimum mean square error (LMMSE) SIC reception. The whole system should run under a minimum rate constraint R^{min}. We consider four different CSI assumptions on the

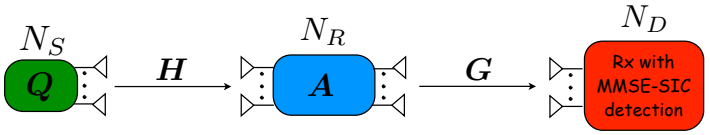

Figure 4.4: Single-user two-hop non-regenerative MIMO link.

channels $\boldsymbol{H}$ and $\boldsymbol{G}$ at the transmitter and relay node. First we assume that perfect CSI is available. Then the cases in which one of the two

channels is only statistically available is treated, and finally the scenario in which both channels are only statistically known is described.

Perfect CSI on both $\boldsymbol{H}$ and $\boldsymbol{G}$

The programming problem to solve is expressed as follows:

$$\max_{\boldsymbol{P},\boldsymbol{A}} \frac{R(\boldsymbol{P},\boldsymbol{A})}{\mu_S P_S(\boldsymbol{P}) + \mu_R P_R(\boldsymbol{P},\boldsymbol{A}) + P_c} \tag{4.56a}$$

$$\text{s.t. } P_S(\boldsymbol{P}) \leq P_S^{max},\ P_R(\boldsymbol{P},\boldsymbol{A}) \leq P_R^{max},\ R(\boldsymbol{P},\boldsymbol{A}) \geq R^{min}, \tag{4.56b}$$

with

$$\begin{aligned} R(\boldsymbol{P},\boldsymbol{A}) &= \log\det\left(\sigma_D^2\boldsymbol{I}_{N_D} + \boldsymbol{A}^H\boldsymbol{G}^H\boldsymbol{G}\boldsymbol{A}\left(\sigma_R^2\boldsymbol{I}_{N_R} + \boldsymbol{H}\boldsymbol{P}\boldsymbol{H}^H\right)\right) \\ &\quad - \log\det\left(\sigma_D^2\boldsymbol{I}_{N_D} + \sigma_R^2\boldsymbol{G}\boldsymbol{A}\boldsymbol{A}^H\boldsymbol{G}^H\right), \end{aligned} \tag{4.57}$$

and with amplifier non-ideality factors μ_R for the relay and μ_S for the source, and noise variances σ_R^2 at the relay, and σ_D^2 at the destination node, respectively. The source transmit power P_S is a function of the transmit covariance matrix $\boldsymbol{P}$ and it is given by $P_S(\boldsymbol{P}) = \mathrm{tr}(\boldsymbol{P})$, while the relay transmit power P_R is a function of the precoding matrix $\boldsymbol{P}$ and of the relay AF matrix $\boldsymbol{A}$ and is given by

$$P_R(\boldsymbol{P},\boldsymbol{A}) = \mathrm{tr}\left(\boldsymbol{A}^H\boldsymbol{A}\left(\sigma_R^2\boldsymbol{I}_{N_R} + \boldsymbol{H}\boldsymbol{P}\boldsymbol{H}^H\right)\right). \tag{4.58}$$

Tackling Problem (4.56) is quite more challenging that in the one-hop case. First of all, the numerator of (4.56a) is not jointly concave in $\boldsymbol{A}$ and $\boldsymbol{P}$, which prevents the direct use of fractional programming tools. Moreover, it is not immediately clear whether the optimal transmit directions should diagonalize the arguments of the determinant and of the trace. Indeed, while the numerator of (4.56a) is maximized by setting the transmit directions so as to diagonalize the channel matrices and arrange the eigenvalues in decreasing order, the same strategy would also maximize the denominator [114]. In the following we show that diagonalization is indeed optimal for Problem (4.56). We start with the following lemma.

Lemma 4.4. The function $\log|\boldsymbol{I}_N + \boldsymbol{T}^{-1}\boldsymbol{R}|$, where $\boldsymbol{T}$ is $N \times N$, Hermitian, and positive definite, while $\boldsymbol{R}$ is $N \times N$, Hermitian, and positive

semidefinite, is minimized when $\boldsymbol{T}$ and $\boldsymbol{R}$ commute and have eigenvalues arranged in the same order.

Proof. This result is a direct consequence of [22, VI.7.1, VI.7.2], where it is proved that $|\boldsymbol{T}+\boldsymbol{R}| \geq \prod_{j=1}^{N}(\lambda_j(T)+\lambda_j(R))$, with $\{\lambda_j(T)\}_{j=1}^{N}$ and $\{\lambda_j(R)\}_{j=1}^{N}$ the eigenvalues of $\boldsymbol{T}$ and $\boldsymbol{R}$, respectively, arranged in decreasing order. As a consequence, since $|\boldsymbol{T}+\boldsymbol{R}| = |\boldsymbol{T}||\boldsymbol{I}+\boldsymbol{T}^{-1}\boldsymbol{R}|$, we have

$$|\boldsymbol{T}||\boldsymbol{I}+\boldsymbol{T}^{-1}\boldsymbol{R}| \geq \prod_{j=1}^{N}(\lambda_j(T)+\lambda_j(R)) = |\boldsymbol{T}|\prod_{j=1}^{N}\left(1+\frac{\lambda_j(R)}{\lambda_j(T)}\right) \quad (4.59)$$

□

Next, we can determine the optimal source and relay transmit directions.

Proposition 4.3 (Proposition 1 in [185])**.** Let the singular value decomposition (SVD) of $\boldsymbol{H}$, $\boldsymbol{G}$, and $\boldsymbol{A}$ be $\boldsymbol{U}_H\boldsymbol{\Lambda}_H^{1/2}\boldsymbol{V}_H^H$, $\boldsymbol{U}_G\boldsymbol{\Lambda}_G^{1/2}\boldsymbol{V}_G^H$, and $\boldsymbol{U}_A\boldsymbol{\Lambda}_A^{1/2}\boldsymbol{V}_A^H$, and the eigen-value decomposition (EVD) of $\boldsymbol{P}$ be $\boldsymbol{U}_P\boldsymbol{\Lambda}_P\boldsymbol{U}_P^H$. Then, the optimal transmit covariance matrix $\boldsymbol{P}$ and relay matrix $\boldsymbol{A}$ for Problem (4.56a) are such that $\boldsymbol{U}_P = \boldsymbol{V}_H$, $\boldsymbol{U}_A = \boldsymbol{V}_G$, and $\boldsymbol{V}_A = \boldsymbol{U}_H$, respectively.

Proof. We start by rewriting the objective function as

$$\begin{aligned}&\frac{\log\left|\sigma_D^2\boldsymbol{I}_{N_D}+\boldsymbol{G}\boldsymbol{A}\left(\sigma_R^2\boldsymbol{I}_{N_R}+\boldsymbol{H}\boldsymbol{P}\boldsymbol{H}^H\right)\boldsymbol{A}^H\boldsymbol{G}^H\right|}{\mu_R\mathrm{tr}\left(\boldsymbol{A}(\boldsymbol{H}\boldsymbol{P}\boldsymbol{H}^H+\sigma_R^2\boldsymbol{I}_{N_R})\boldsymbol{A}^H\right)+\mu_S\mathrm{tr}(\boldsymbol{P})+P_c}\\ &-\frac{\log\left|\sigma_D^2\boldsymbol{I}_{N_D}+\sigma_R^2\boldsymbol{G}\boldsymbol{A}\boldsymbol{A}^H\boldsymbol{G}^H\right|}{\mu_R\mathrm{tr}\left(\boldsymbol{A}(\boldsymbol{H}\boldsymbol{P}\boldsymbol{H}^H+\sigma_R^2\boldsymbol{I}_{N_R})\boldsymbol{A}^H\right)+\mu_S\mathrm{tr}(\boldsymbol{P})+P_c}\end{aligned} \quad (4.60)$$

Now, defining the variables $\boldsymbol{Y} = \boldsymbol{H}\boldsymbol{P}\boldsymbol{H}^H$ and $\boldsymbol{X} = \boldsymbol{G}\boldsymbol{A}(\sigma_R^2\boldsymbol{I}_{N_R}+\boldsymbol{Y})^{1/2}$, (4.60) can be expressed as

$$\frac{\log\left|\sigma_D^2\boldsymbol{I}_{N_D}+\boldsymbol{X}\boldsymbol{X}^H\right|-\log\left|\sigma_D^2\boldsymbol{I}_{N_D}+\sigma_R^2\boldsymbol{X}(\boldsymbol{Y}+\sigma_R^2\boldsymbol{I}_{N_R})^{-1}\boldsymbol{X}^H\right|}{\mu_S\mathrm{tr}(\boldsymbol{H}^{-1}\boldsymbol{Y}\boldsymbol{H}^{-H})+\mu_R\mathrm{tr}\left(\boldsymbol{G}^{-1}\boldsymbol{X}\boldsymbol{X}^H\boldsymbol{G}^{-H}\right)+P_c} \quad (4.61)$$

Defining by $\boldsymbol{U}_x\boldsymbol{\Lambda}_x^{1/2}\boldsymbol{V}_x^H$ the SVD of $\boldsymbol{X}$ and by $\boldsymbol{U}_y\boldsymbol{\Lambda}_y\boldsymbol{U}_y^H$ the EVD of $\boldsymbol{Y}$, it follows that the first and second summand in the denominator of (4.61) are minimized when $\boldsymbol{U}_y = \boldsymbol{U}_H$ and $\boldsymbol{U}_x = \boldsymbol{U}_G$, respectively, because the trace of the product of two hermitian, positive semidefinite matrices is minimized for commuting matrices with eigenvalues arranged in opposite order [114, Lemma H.1.h]. Moreover, exploiting Lemma 4.4, it can also be seen that the numerator is maximized for $\boldsymbol{V}_x = \boldsymbol{U}_y = \boldsymbol{U}_H$. Therefore, such choices for $\boldsymbol{U}_x$, $\boldsymbol{V}_x$, and $\boldsymbol{U}_y$ simultaneously maximize the numerator and minimize the denominator of (4.61). Moreover, they are also feasible because the numerator of the objective is also the LHS of the QoS constraint, while the first and second summand in the denominator are the LHS of the power constraints. Next, from the expression of $\boldsymbol{Y}$ we have $\boldsymbol{Y} = \boldsymbol{U}_y\boldsymbol{\Lambda}_y\boldsymbol{U}_y^H = \boldsymbol{U}_H\boldsymbol{\Lambda}_H^{1/2}\boldsymbol{V}_H^H\boldsymbol{U}_P\boldsymbol{\Lambda}_P\boldsymbol{U}_P^H\boldsymbol{V}_H\boldsymbol{\Lambda}_H^{1/2}\boldsymbol{U}_H^H$, from which it follows that in order to achieve $\boldsymbol{U}_y = \boldsymbol{U}_H$, the relation $\boldsymbol{U}_P = \boldsymbol{V}_H$ needs to hold. Similarly, for $\boldsymbol{X}$ we have $\boldsymbol{X} = \boldsymbol{U}_x\boldsymbol{\Lambda}_x\boldsymbol{V}_x^H = \boldsymbol{U}_G\boldsymbol{\Lambda}_G^{1/2}\boldsymbol{V}_G^H\boldsymbol{U}_A\boldsymbol{\Lambda}_A^{1/2}\boldsymbol{V}_A^H\boldsymbol{U}_H(\boldsymbol{\Lambda}_H^{1/2}\boldsymbol{\Lambda}_P\boldsymbol{\Lambda}_H^{1/2}+\sigma_R^2\boldsymbol{I}_{N_R})^{1/2}\boldsymbol{U}_H^H$. Thus, in order to achieve $\boldsymbol{U}_x = \boldsymbol{U}_G$ and $\boldsymbol{V}_x = \boldsymbol{U}_H$, the relations $\boldsymbol{U}_A = \boldsymbol{V}_G$, and $\boldsymbol{V}_A = \boldsymbol{U}_H$ need to hold. □

In the proof we have assumed that the channel matrices are invertible. However, this assumption is not critical, and the result can be extended to generic channel matrices exploiting the fact that at the optimum $\boldsymbol{P}$ will have no component in the null space of $\boldsymbol{H}$ and $\boldsymbol{A}$ will have no component in the null space of $\boldsymbol{G}$. Therefore, we can reduce the system to an equivalent system with square and full-rank channels, and then apply the result in Proposition 4.3.

Upon plugging the optimal structure of $\boldsymbol{P}$ and $\boldsymbol{A}$ into (4.56), we can simplify the problem by reducing it to a power allocation problem with respect to the eigenvalues of the transmit covariance matrix and of the AF relay matrix, thereby significantly reducing the number of variables to optimize. Specifically, denote by $\lambda_{i,G}$, $\lambda_{i,A}$, $\lambda_{i,H}$, and $\lambda_{i,P}$, the generic (i,i) entry of the matrices $\left(\boldsymbol{\Lambda}_G^{1/2}\boldsymbol{\Lambda}_G^{H/2}\right)$, $\boldsymbol{\Lambda}_A$, $\left(\boldsymbol{\Lambda}_H^{1/2}\boldsymbol{\Lambda}_H^{H/2}\right)$, and $\boldsymbol{\Lambda}_P$, respectively, and by $\boldsymbol{\lambda}_P$ and $\boldsymbol{\lambda}_A$ the vectors $\{\lambda_{i,P}\}_{i=1}^{N_S}$ and $\{\lambda_{i,A}\}_{i=1}^{N_R}$.

Then, Problem (4.56a) becomes

$$\max_{\{\lambda_{i,P},\lambda_{i,A}\}_i} \frac{\sum_{i=1}^{N_S} \log\left(1+\frac{\lambda_{i,A}\lambda_{i,P}\lambda_{i,H}\lambda_{i,G}}{\sigma_D^2+\sigma_R^2\lambda_{i,A}\lambda_{i,G}}\right)}{\mu_S\sum_{i=1}^{N_S}\lambda_{i,P}+\mu_R\sum_{i=1}^{N_R}\lambda_{i,A}(\lambda_{i,H}\lambda_{i,P}+\sigma_R^2)+P_c} \tag{4.62a}$$

$$\text{s.t. } \sum_{i=1}^{N_S} \log\left(1+\frac{\lambda_{i,A}\lambda_{i,P}\lambda_{i,H}\lambda_{i,G}}{\sigma_D^2+\sigma_R^2\lambda_{i,A}\lambda_{i,G}}\right) \geq R_S^{min} \tag{4.62b}$$

$$\lambda_{i,P} \geq 0 \ \ \forall i=1,\ldots,N_S\ , \ \ \lambda_{i,A} \geq 0 \ \ \forall i=1,\ldots,N_R \tag{4.62c}$$

$$\sum_{i=1}^{N_S}\lambda_{i,P} \leq P_S^{max}\ , \ \ \sum_{i=1}^{N_R}\lambda_{i,A}(\lambda_{i,H}\lambda_{i,P}+\sigma_R^2) \leq P_R^{max}\ . \tag{4.62d}$$

Although we have simplified Problem (4.56) by determining the optimal transmit directions in closed-form, the numerator of (4.62a) is not jointly concave in $\boldsymbol{\lambda}_P$ and $\boldsymbol{\lambda}_A$, which prevents us from solving (4.62) with limited complexity by means of fractional programming tools. However, we observe that (4.62a) is PC in $\boldsymbol{\lambda}_P$ for fixed $\boldsymbol{\lambda}_A$, and PC in $\boldsymbol{\lambda}_A$ for fixed $\boldsymbol{\lambda}_P$. Therefore, one convenient approach is to use fractional programming in conjunction with the alternating optimization algorithm [20], alternatively solving (4.62) with respect to $\boldsymbol{\lambda}_P$, for fixed $\boldsymbol{\lambda}_A$, and with respect to $\boldsymbol{\lambda}_A$, for fixed $\boldsymbol{\lambda}_P$, until the objective converges. Each sub-problem can be conveniently solved by means of any of the tools described in Chapter 3 for CLFP. The formal procedure can be stated as in Algorithm 9.

Algorithm 9 EE maximization in two-hop P2P MIMO channels with perfect CSI.

$\ell = 0$; $\epsilon > 0$; Initialize $\boldsymbol{\lambda}_P^{(0)}$ to a feasible value;
while $\left|\text{GEE}^{(\ell+1)} - \text{GEE}^{(\ell)}\right| \geq \epsilon$ **do**
  $\ell = \ell + 1$;
  Given $\boldsymbol{\lambda}_P^{(\ell-1)}$, solve (4.62) with respect to $\boldsymbol{\lambda}_A$ to obtain $\boldsymbol{\lambda}_A^{(\ell)}$;
  Given $\boldsymbol{\lambda}_A^{(\ell)}$, solve Problem (4.62) with respect to $\boldsymbol{\lambda}_P$ to obtain the optimal $\boldsymbol{\lambda}_P^{(\ell)}$;
end while

Convergence of Algorithm 9 is ensured because after each iteration

the GEE is not decreased and is upper-bounded. In general, the solution obtained upon convergence is not guaranteed to be a point fulfilling the KKT conditions of (4.62), due to the fact that the constraints are coupled in $\boldsymbol{\lambda}_P$ and $\boldsymbol{\lambda}_A$. Instead, a KKT point can be obtained by a similar sequential approach as in Section 4.1.3, using Proposition 4.2 and Lemma 4.1 to lower-bound the rate function as

$$\sum_{i=1}^{N_S} \log\left(1+\frac{\lambda_{i,A}\lambda_{i,P}\lambda_{i,H}\lambda_{i,G}}{\sigma_D^2+\sigma_R^2\lambda_{i,A}\lambda_{i,G}}\right) \geq \sum_{i=1}^{N_S} a_i \log\left(\frac{\lambda_{i,A}\lambda_{i,P}\lambda_{i,H}\lambda_{i,G}}{\sigma_D^2+\sigma_R^2\lambda_{i,A}\lambda_{i,G}}\right)+b_i$$
$$= \sum_{i=1}^{N_S} a_i\left[\log(\lambda_{i,P})+\log\left(\frac{\lambda_{i,A}\lambda_{i,H}\lambda_{i,G}}{\sigma_D^2+\sigma_R^2\lambda_{i,A}\lambda_{i,G}}\right)\right]+b_i\ , \qquad (4.63)$$

which is a jointly concave function of $\boldsymbol{\lambda}_P$ and $\boldsymbol{\lambda}_A$. However, numerical results to be presented in the following suggest that the alternating optimization performs well in noise-limited scenarios.

Statistical CSI on H and perfect CSI on G

Assume that the relay-to-destination channel $\boldsymbol{G}$ is perfectly known but that only statistical CSI is available for the source-to-relay channel in the form of covariance feedback. This scenario is realistic in all situations in which the relay-to-destination channel is slowly time-varying, whereas the source-to-relay channel is rapidly time-varying and therefore more difficult to estimate and track. A typical example is the uplink of a communication system, in which the relay and destination are usually fixed, while the source is a mobile terminal.

Specifically, in this section the channel matrix $\boldsymbol{H}$ is expressed according to the Kronecker model [156], as $\boldsymbol{H}=\boldsymbol{Z}_H\boldsymbol{R}_{t,H}^{1/2}$, where $\boldsymbol{Z}_H$ is a random matrix with independent, zero-mean, unit-variance, proper complex Gaussian entries, whereas $\boldsymbol{R}_{t,H}$ is the positive semidefinite transmit correlation matrix associated to $\boldsymbol{H}$. The matrix $\boldsymbol{R}_{t,H}$ is assumed known whereas the matrix $\boldsymbol{Z}_H$ is unknown at the source and relay. The covariance feedback model has been widely used in the literature, [159, 158, 85, 90], and applies for example to scenarios in which the relay is surrounded by local scatterers that induce the matrix $\boldsymbol{R}_{t,H}$, whereas a rich multi-path environment is present between the relay and the destination, which is modeled by the matrix $\boldsymbol{Z}_H$. We also remark

that by letting the correlation matrix be the identity matrix, the special notable case in which $\boldsymbol{H}$ is completely unknown and modeled as a random matrix with independent, zero-mean, unit-variance, proper complex Gaussian entries is obtained.

In the considered statistical CSI scenario, the benefit and cost of the system in terms of data-rate and consumed energy are represented by the ergodic achievable rate and average consumed energy, which leads to defining the energy efficiency as the ratio between the system ergodic achievable rate, and average consumed power. Thus, the energy-efficient resource allocation problem to be considered is

$$\max_{\boldsymbol{P},\boldsymbol{A}} \frac{\mathbb{E}_{Z_H}\left[\log\left(\frac{\left|\sigma_D^2\boldsymbol{I}_{N_D}+\boldsymbol{G}\boldsymbol{A}\left(\boldsymbol{H}\boldsymbol{P}\boldsymbol{H}^H+\sigma_R^2\boldsymbol{I}_{N_R}\right)\boldsymbol{A}^H\boldsymbol{G}^H\right|}{\left|\sigma_D^2\boldsymbol{I}_{N_D}+\sigma_R^2\boldsymbol{G}\boldsymbol{A}\boldsymbol{A}^H\boldsymbol{G}^H\right|}\right)\right]}{\mu_R\mathbb{E}_{Z_H}\left[\mathrm{tr}(\boldsymbol{A}(\boldsymbol{H}\boldsymbol{P}\boldsymbol{H}^H+\sigma_R^2\boldsymbol{I}_{N_R})\boldsymbol{A}^H)\right]+\mu_S\mathrm{tr}(\boldsymbol{P})+P_c} \tag{4.64a}$$

$$\text{s.t. } \mathbb{E}_{Z_H}\left[\mathrm{tr}(\boldsymbol{A}(\boldsymbol{H}\boldsymbol{P}\boldsymbol{H}^H+\sigma_R^2\boldsymbol{I}_{N_R})\boldsymbol{A}^H)\right]\leq P_R^{max} \tag{4.64b}$$

$$\mathrm{tr}(\boldsymbol{P})\leq P_S^{max}\ ,\ \boldsymbol{P}\succeq 0 \tag{4.64c}$$

$$\mathbb{E}_{Z_H}\left[\log\left(\frac{\left|\sigma_D^2\boldsymbol{I}_{N_D}+\boldsymbol{G}\boldsymbol{A}\left(\boldsymbol{H}\boldsymbol{P}\boldsymbol{H}^H+\sigma_R^2\boldsymbol{I}_{N_R}\right)\boldsymbol{A}^H\boldsymbol{G}^H\right|}{\left|\sigma_D^2\boldsymbol{I}_{N_D}+\sigma_R^2\boldsymbol{G}\boldsymbol{A}\boldsymbol{A}^H\boldsymbol{G}^H\right|}\right)\right]\geq R^{min} \tag{4.64d}$$

We should mention that an alternative approach could be to maximize the average of the instantaneous energy efficiency namely

$$\mathbb{E}_{Z_H}\left[\frac{R(\boldsymbol{P},\boldsymbol{A})}{\mu_S P_S+\mu_R P_R+P_c}\right]\ . \tag{4.65}$$

However, (4.65) is not the ratio between the benefit produced by the system and the cost incurred to achieve such benefit, and therefore lacks physical meaning with respect to (4.64a). For this reason, (4.65) will not be considered as performance measure.

Coming back to Problem (4.64), the following proposition determines the optimal source eigenvector matrix $\boldsymbol{U}_P$ and the optimal relay left and right eigenvector matrices $\boldsymbol{U}_A$ and $\boldsymbol{V}_A$.

Proposition 4.4 (Propositions 3 and 4 in [185])**.** Define the EVD of $\boldsymbol{R}_{t,H}$ as $\boldsymbol{U}_{t,H}\boldsymbol{\Lambda}_{t,H}\boldsymbol{U}_{t,H}^H$. Then, the optimal $\boldsymbol{P}$ is such that $\boldsymbol{U}_P=\boldsymbol{U}_{t,H}$ and the optimal $\boldsymbol{A}$ is such that $\boldsymbol{U}_A=\boldsymbol{V}_G$ and $\boldsymbol{V}_A=\boldsymbol{I}_{N_R}$.

The proof of this result, as well a generalization to the case in which also a receive correlation matrix $\boldsymbol{R}_{r,H}$ is considered and the source-relay channel is modeled as $\boldsymbol{H} = \boldsymbol{R}_{r,H}^{1/2} \boldsymbol{Z}_H \boldsymbol{R}_{t,H}^{1/2}$, can be found in [185].

Plugging the optimal $\boldsymbol{U}_P$, $\boldsymbol{U}_A$, and $\boldsymbol{V}_A$ into (4.64), and defining $\boldsymbol{\Lambda}_y = \boldsymbol{\Lambda}_G^{H/2} \boldsymbol{\Lambda}_A \boldsymbol{\Lambda}_G^{1/2}$, and the matrix $\widetilde{\boldsymbol{\Lambda}}_G$ containing the upper-left $N_R \times N_R$ block of $(\boldsymbol{\Lambda}_G^{1/2})^{+H} (\boldsymbol{\Lambda}_G^{1/2})^{+}$, we can recast the problem as

$$\max_{\boldsymbol{\Lambda}_P, \boldsymbol{\Lambda}_y} \frac{\mathbb{E}_{Z_H} \left[\log \left| \boldsymbol{I}_{N_S} + \boldsymbol{\Lambda}_P \boldsymbol{\Lambda}_{t,H} \boldsymbol{Z}_H^H \boldsymbol{\Lambda}_y \left(\sigma_D^2 \boldsymbol{I}_{N_R} + \sigma_R^2 \boldsymbol{\Lambda}_y \right)^{-1} \boldsymbol{Z}_H \right| \right]}{\mu_R \mathrm{tr} \left(\boldsymbol{\Lambda}_P \boldsymbol{\Lambda}_{t,H} \right) \mathrm{tr} \left(\boldsymbol{\Lambda}_y \widetilde{\boldsymbol{\Lambda}}_G \right) + \mu_R \sigma_R^2 \mathrm{tr} \left(\boldsymbol{\Lambda}_y \widetilde{\boldsymbol{\Lambda}}_G \right) + \mu_S \mathrm{tr}(\boldsymbol{\Lambda}_P) + P_c} \tag{4.66a}$$

$$\text{s.t. } \mathrm{tr} \left(\boldsymbol{\Lambda}_P \boldsymbol{\Lambda}_{t,H} \right) \mathrm{tr} \left(\boldsymbol{\Lambda}_y \widetilde{\boldsymbol{\Lambda}}_G \right) + \sigma_R^2 \mathrm{tr} \left(\boldsymbol{\Lambda}_y \widetilde{\boldsymbol{\Lambda}}_G \right) \leq P_R^{max} \tag{4.66b}$$

$$\mathrm{tr}(\boldsymbol{\Lambda}_P) \leq P_S^{max} \ , \ \boldsymbol{\Lambda}_P \succeq 0 \ , \ \boldsymbol{\Lambda}_y \succeq 0 \tag{4.66c}$$

$$\mathbb{E}_{Z_H} \left[\log \left| \boldsymbol{I}_{N_S} + \boldsymbol{\Lambda}_P \boldsymbol{\Lambda}_{t,H} \boldsymbol{Z}_H^H \boldsymbol{\Lambda}_y \left(\sigma_D^2 \boldsymbol{I}_{N_R} + \sigma_R^2 \boldsymbol{\Lambda}_y \right)^{-1} \boldsymbol{Z}_H \right| \right] \geq R^{min} \tag{4.66d}$$

Unfortunately, as in the perfect CSI case, the numerator of (4.66a) is not jointly concave in $(\boldsymbol{\Lambda}_P, \boldsymbol{\Lambda}_y)$. However, it is again separately pseudo-concave in $\boldsymbol{\Lambda}_P$ and $\boldsymbol{\Lambda}_y$. The pseudo-concavity with respect to $\boldsymbol{\Lambda}_P$ for fixed $\boldsymbol{\Lambda}_y$ is apparent, whereas the pseudo-concavity with respect to $\boldsymbol{\Lambda}_y$ for fixed $\boldsymbol{\Lambda}_P$ follows by the fact that the matrix function $\boldsymbol{\Lambda}_y \left(\sigma_D^2 \boldsymbol{I}_{N_R} + \sigma_R^2 \boldsymbol{\Lambda}_y \right)^{-1}$ is matrix-concave in $\boldsymbol{\Lambda}_y$ [185, Lemma 5], and by the concavity and monotonicity of the function $E_{Z_H}[\log|\cdot|]$. Thus, a convenient way to tackle (4.66) is to resort again to the alternating maximization algorithm, alternatively optimizing $\boldsymbol{\Lambda}_P$ and $\boldsymbol{\Lambda}_y$. The pseudo-code of the algorithm is reported in Algorithm 10, which enjoys similar properties as Algorithm 9. It is guaranteed to converge since the energy efficiency is upper-bounded, it only requires the solution of CLFPs, and can be implemented either centrally or in a distributed way. A difference with respect to Algorithm 9 is that Algorithm 10 requires the evaluation of statistical expectations, due to the lack of perfect knowledge of the channel. In most applications, this can be easily accomplished numerically. Moreover, for those applications in which computational complexity is a critical issue, we remark that the proposed method can still be used by approximating the expectation with

a deterministic function. Several approaches exist in the literature to come up with suitable approximations of the $\mathbb{E}_{Z_H}\left[\log|\cdot|\right]$ function that would allow the computation of the expectations in (4.64) in closed-form. For example, the well-known WMMSE algorithm [155, 163] can be used to replace the rate function at the numerator of the objective by a sum of weighted traces, thus allowing the computation of the expectations by exchanging the statistical mean and trace operators. A second approach is to employ Jensen's inequality to come up with an approximation of the objective function. Such an approach will be used and described in more detail when dealing with the case in which both channels are only statistically known.

Algorithm 10 EE maximization in two-hop P2P MIMO channels with statistical CSI on the source-relay channel.

$\ell = 0$; $\epsilon > 0$; Initialize $\boldsymbol{\Lambda}_P^{(0)}$ to a feasible value;
while $\left|\mathrm{GEE}^{(\ell+1)} - \mathrm{GEE}^{(\ell)}\right| > \epsilon$ **do**
$\ell = \ell + 1$;
Given $\boldsymbol{\Lambda}_P^{(\ell-1)}$, solve Problem (4.64) with respect to $\boldsymbol{\Lambda}_y$ to obtain the optimal $\boldsymbol{\Lambda}_y^{(\ell)}$;
Given $\boldsymbol{\Lambda}_y^{(\ell)}$, solve Problem (4.64) with respect to $\boldsymbol{\Lambda}_P$ to obtain the optimal $\boldsymbol{\Lambda}_P^{(\ell)}$;
end while

Statistical CSI on G and perfect CSI on H

In this section, the opposite case of CSI knowledge is considered. The relay-to-destination channel will be assumed only statistically known and expressed according to the Kronecker model, whereas the source-to-relay channel will be assumed perfectly known. This scenario models all situations in which the source-to-relay channel is slowly time-varying, whereas the relay-to-destination channel is rapidly time-varying. A typical example is the downlink of a cellular system.

To elaborate, in this section the channel $\boldsymbol{G}$ is expressed as

$$\boldsymbol{G} = \boldsymbol{R}_{r,G}^{1/2} \boldsymbol{Z}_G \boldsymbol{R}_{t,G}^{1/2} \tag{4.67}$$

where $\boldsymbol{Z}_G$ is a random matrix with independent, zero-mean, unit-variance, proper complex Gaussian entries, whereas $\boldsymbol{R}_{r,G}$ and $\boldsymbol{R}_{t,G}$ are the positive semidefinite receive and transmit correlation matrices associated to $\boldsymbol{G}$. The matrices $\boldsymbol{R}_{r,G}^{1/2} = \boldsymbol{U}_{r,G}\boldsymbol{\Lambda}_{r,G}^{1/2}\boldsymbol{U}_{r,G}^H$ and $\boldsymbol{R}_{t,G}^{1/2} = \boldsymbol{U}_{t,G}\boldsymbol{\Lambda}_{t,G}^{1/2}\boldsymbol{U}_{t,G}^H$ are assumed known whereas the matrix $\boldsymbol{Z}_G$ is unknown. The problem can be formulated as

$$\max_{\boldsymbol{P},\boldsymbol{A}} \frac{\mathbb{E}_{Z_G}\left[\log\left(\frac{\left|\sigma_D^2\boldsymbol{I}_{N_D}+\boldsymbol{G}\boldsymbol{A}\left(\boldsymbol{H}\boldsymbol{P}\boldsymbol{H}^H+\sigma_R^2\boldsymbol{I}_{N_R}\right)\boldsymbol{A}^H\boldsymbol{G}^H\right|}{\left|\sigma_D^2\boldsymbol{I}_{N_D}+\sigma_R^2\boldsymbol{G}\boldsymbol{A}\boldsymbol{A}^H\boldsymbol{G}^H\right|}\right)\right]}{\mathrm{tr}\left(\boldsymbol{A}(\boldsymbol{H}\boldsymbol{P}\boldsymbol{H}^H+\sigma_R^2\boldsymbol{I}_{N_R})\boldsymbol{A}^H\right)+\mathrm{tr}(\boldsymbol{P})+P_c} \tag{4.68a}$$

$$\text{s.t. } \mathrm{tr}(\boldsymbol{A}(\boldsymbol{H}\boldsymbol{P}\boldsymbol{H}^H+\sigma_R^2\boldsymbol{I}_{N_R})\boldsymbol{A}^H) \le P_R^{max} \tag{4.68b}$$

$$\mathrm{tr}(\boldsymbol{P}) \le P_S^{max}\ ,\ \boldsymbol{P}\succeq 0 \tag{4.68c}$$

$$\mathbb{E}_{Z_G}\left[\log\left(\frac{\left|\sigma_D^2\boldsymbol{I}_{N_D}+\boldsymbol{G}\boldsymbol{A}\left(\boldsymbol{H}\boldsymbol{P}\boldsymbol{H}^H+\sigma_R^2\boldsymbol{I}_{N_R}\right)\boldsymbol{A}^H\boldsymbol{G}^H\right|}{\left|\sigma_D^2\boldsymbol{I}_{N_D}+\sigma_R^2\boldsymbol{G}\boldsymbol{A}\boldsymbol{A}^H\boldsymbol{G}^H\right|}\right)\right] \ge R^{min} \tag{4.68d}$$

As in previous sections, we will first determine the optimal source and relay transmit directions, and then we will address the resulting power control problem.

Proposition 4.5 (Propositions 5 in [185]). Consider Problem (4.68). The optimal $\boldsymbol{P}$ and $\boldsymbol{A}$ are such that $\boldsymbol{U}_P = \boldsymbol{V}_H$, $\boldsymbol{U}_A = \boldsymbol{U}_{t,G}$ and $\boldsymbol{V}_A = \boldsymbol{U}_H$.

The resulting power control problem is stated as

$$\max_{\boldsymbol{\Lambda}_P,\boldsymbol{\Lambda}_A} \frac{\mathbb{E}_{Z_G}\left[\log\left(\frac{\left|\sigma_D^2\boldsymbol{I}_{N_D}+\boldsymbol{\Lambda}_{r,G}\boldsymbol{Z}_G\boldsymbol{\Lambda}_{t,G}\boldsymbol{\Lambda}_A\left(\boldsymbol{\Lambda}_H^{1/2}\boldsymbol{\Lambda}_P\boldsymbol{\Lambda}_H^{H/2}+\sigma_R^2\boldsymbol{I}_{N_R}\right)\boldsymbol{Z}_G^H\right|}{\left|\sigma_D^2\boldsymbol{I}_{N_D}+\sigma_R^2\boldsymbol{\Lambda}_{r,G}\boldsymbol{Z}_G\boldsymbol{\Lambda}_{t,G}\boldsymbol{\Lambda}_A\boldsymbol{Z}_G^H\right|}\right)\right]}{\mathrm{tr}\left(\boldsymbol{\Lambda}_A\left(\boldsymbol{\Lambda}_H^{1/2}\boldsymbol{\Lambda}_P\boldsymbol{\Lambda}_H^{H/2}+\sigma_R^2\boldsymbol{I}_{N_R}\right)\right)+\mathrm{tr}(\boldsymbol{\Lambda}_P)+P_c} \tag{4.69a}$$

$$\text{s.t. } \mathrm{tr}\left(\boldsymbol{\Lambda}_A\left(\boldsymbol{\Lambda}_H^{1/2}\boldsymbol{\Lambda}_P\boldsymbol{\Lambda}_H^{H/2}+\sigma_R^2\boldsymbol{I}_{N_R}\right)\right) \le P_R^{max} \tag{4.69b}$$

$$\mathrm{tr}(\boldsymbol{\Lambda}_P) \le P_S^{max}\ ,\ \boldsymbol{\Lambda}_Q\succeq 0\ ,\ \boldsymbol{\Lambda}_A\succeq 0 \tag{4.69c}$$

$$\mathbb{E}_{Z_G}\left[\log\left(\frac{\left|\sigma_D^2\boldsymbol{I}_{N_D}+\boldsymbol{\Lambda}_{r,G}\boldsymbol{Z}_G\boldsymbol{\Lambda}_{t,G}\boldsymbol{\Lambda}_A\left(\boldsymbol{\Lambda}_H^{1/2}\boldsymbol{\Lambda}_P\boldsymbol{\Lambda}_H^{H/2}+\sigma_R^2\boldsymbol{I}_{N_R}\right)\boldsymbol{Z}_G^H\right|}{\left|\sigma_D^2\boldsymbol{I}_{N_D}+\sigma_R^2\boldsymbol{\Lambda}_{r,G}\boldsymbol{Z}_G\boldsymbol{\Lambda}_{t,G}\boldsymbol{\Lambda}_A\boldsymbol{Z}_G^H\right|}\right)\right] \ge R^{min} \tag{4.69d}$$

Again, the numerator of the objective is not jointly concave in $\mathbf{\Lambda}_P$ and $\mathbf{\Lambda}_A$, but it can be shown to be separately PC in $\mathbf{\Lambda}_P$ and $\mathbf{\Lambda}_A$ [185], which allows one to tackle Problem (4.69) by means of alternating optimization, in a similar fashion as in previous sections.

Algorithm 11 EE maximization in two-hop P2P MIMO channels with statistical CSI on the relay-destination channel.

$\ell = 0$; $\epsilon > 0$; Initialize $\mathbf{\Lambda}_P^{(0)}$ to a feasible value;
while $\left|\mathrm{GEE}^{(\ell+1)} - \mathrm{GEE}^{(\ell)}\right| > \epsilon$ **do**
$\ell = \ell + 1$;
Given $\mathbf{\Lambda}_P^{(\ell-1)}$, solve Problem (4.69) with respect to $\mathbf{\Lambda}_A$ to obtain the optimal $\mathbf{\Lambda}_A^{(\ell)}$;
Given $\mathbf{\Lambda}_A^{(\ell)}$, solve Problem (4.69) with respect to $\mathbf{\Lambda}_P$ to obtain the optimal $\mathbf{\Lambda}_P^{(\ell)}$;
end while

The properties of the optimal transmit precoding and the AF relaying matrix are further analyzed in [185]. The beamforming (or single-stream transmission) optimality range is characterized. It is shown that for small SNR values, only a single data stream is optimally supported by the two-hop MIMO link.

Statistical CSI on both $\boldsymbol{H}$ and $\boldsymbol{G}$

Assume that only statistical CSI is available for both channels $\boldsymbol{H}$ and $\boldsymbol{G}$. Specifically, both channel matrices $\boldsymbol{H}$ and $\boldsymbol{G}$ are expressed according to the Kronecker model as

$$\boldsymbol{H} = \boldsymbol{Z}_H \boldsymbol{R}_{t,H}^{1/2}\ , \quad \boldsymbol{G} = \boldsymbol{Z}_G \boldsymbol{R}_{t,G}^{1/2} \tag{4.70}$$

where the fading matrices $\boldsymbol{Z}_H$, $\boldsymbol{Z}_G$ are unknown to the source and relay, whereas the correlation matrices $\boldsymbol{R}_{t,H}$ and $\boldsymbol{R}_{t,G}$ are assumed known.

Then, the resource allocation problem is formulated as follows.

$$\max_{\boldsymbol{P},\boldsymbol{A}} \frac{\mathbb{E}_{H,G}\left[\log\left(\frac{\left|\sigma_D^2\boldsymbol{I}_{N_D}+\boldsymbol{G}\boldsymbol{A}\left(\boldsymbol{H}\boldsymbol{P}\boldsymbol{H}^H+\sigma_R^2\boldsymbol{I}_{N_R}\right)\boldsymbol{A}^H\boldsymbol{G}^H\right|}{\left|\sigma_D^2\boldsymbol{I}_{N_D}+\sigma_R^2\boldsymbol{G}\boldsymbol{A}\boldsymbol{A}^H\boldsymbol{G}^H\right|}\right)\right]}{\mu_R\mathbb{E}_H\left[\mathrm{tr}(\boldsymbol{A}(\boldsymbol{H}\boldsymbol{P}\boldsymbol{H}^H+\sigma_R^2\boldsymbol{I}_{N_R})\boldsymbol{A}^H)\right]+\mu_S\mathrm{tr}(\boldsymbol{P})+P_c} \tag{4.71a}$$

$$\text{s.t. } \mathrm{tr}(\boldsymbol{P}) \leq P_S^{max}\ , \boldsymbol{P}\succeq \boldsymbol{0} \tag{4.71b}$$

$$\mathbb{E}_H\left[\mathrm{tr}\left(\boldsymbol{A}\left(\boldsymbol{H}\boldsymbol{P}\boldsymbol{H}^H+\sigma_R^2\boldsymbol{I}_{N_R}\right)\boldsymbol{A}^H\right)\right] \leq P_R^{max} \tag{4.71c}$$

$$\mathbb{E}_{H,G}\left[\log\left(\frac{\left|\sigma_D^2\boldsymbol{I}_{N_D}+\boldsymbol{G}\boldsymbol{A}\left(\boldsymbol{H}\boldsymbol{P}\boldsymbol{H}^H+\sigma_R^2\boldsymbol{I}_{N_R}\right)\boldsymbol{A}^H\boldsymbol{G}^H\right|}{\left|\sigma_D^2\boldsymbol{I}_{N_D}+\sigma_R^2\boldsymbol{G}\boldsymbol{A}\boldsymbol{A}^H\boldsymbol{G}^H\right|}\right)\right] \geq R^{min} \tag{4.71d}$$

The optimal source and relay transmit directions are determined as follows.

Proposition 4.6 (Proposition 1 in [186]). Consider Problem (4.71). The optimal $\boldsymbol{P}$ is such that $\boldsymbol{U}_P = \boldsymbol{U}_{t,H}$, while the optimal $\boldsymbol{A}$ is such that $\boldsymbol{U}_A = \boldsymbol{U}_{t,G}$ and $\boldsymbol{V}_A = \boldsymbol{I}_{N_R}$.

Plugging the optimal $\boldsymbol{U}_P$, $\boldsymbol{U}_A$, and $\boldsymbol{V}_A$ into (4.71) we obtain a power control problem in $\boldsymbol{\Lambda}_P$ and $\boldsymbol{\Lambda}_A$. However, unlike previous scenarios, this time the resulting ergodic rate function turns out to be neither jointly, nor separately PC in $\boldsymbol{\Lambda}_P$ and $\boldsymbol{\Lambda}_A$, thus preventing the direct use of the alternating optimization algorithm. In order to circumvent this difficulty, we can apply Jensen's inequality, to find a simple approximation of the objective. Let us start by applying Jensen's inequality with respect to $\boldsymbol{Z}_H$, which yields

$$\frac{\mathbb{E}_{Z_G}\left[\log\left|\boldsymbol{I}_{N_D}+\mathrm{tr}(\boldsymbol{\Lambda}_P\boldsymbol{\Lambda}_{t,H})\boldsymbol{Z}_G\boldsymbol{\Lambda}_y\boldsymbol{Z}_G^H\left(\sigma_D^2\boldsymbol{I}_{N_D}+\sigma_R^2\boldsymbol{Z}_G\boldsymbol{\Lambda}_y\boldsymbol{Z}_G^H\right)^{-1}\right|\right]}{\mathrm{tr}\left(\boldsymbol{\Lambda}_{t,G}^{-1}\boldsymbol{\Lambda}_y\right)\left[\mathrm{tr}\left(\boldsymbol{\Lambda}_P\boldsymbol{\Lambda}_{t,H}\right)+\sigma_R^2\right]+\mathrm{tr}(\boldsymbol{\Lambda}_P)+P_c}\ , \tag{4.72}$$

with $\boldsymbol{\Lambda}_y = \boldsymbol{\Lambda}_{t,G}\boldsymbol{\Lambda}_A$.

Using similar techniques as in previous sections, (4.72) can be shown to be separately PC in $\boldsymbol{\Lambda}_y$ and $\boldsymbol{\Lambda}_P$, and therefore one could already devise an alternating optimization algorithm as done in previous sections.

However, if the goal is to devise a low-complexity resource allocation algorithm which does not require the computation of any expectation, Jensen's inequality can be applied again with respect to $\boldsymbol{Z}_G$, as detailed in [186], which leads to the following power control problem, which does not contain any statistical expectation.

$$\max_{\boldsymbol{\Lambda}_P,\boldsymbol{\Lambda}_y} \frac{N_D \log\left(1+\mathrm{tr}(\boldsymbol{\Lambda}_P\boldsymbol{\Lambda}_{t,H})\frac{1}{\sigma_R^2}\left(1-\frac{\sigma_D^2}{\sigma_D^2+\sigma_R^2\mathrm{tr}(\boldsymbol{\Lambda}_y)}\right)\right)}{\mathrm{tr}(\boldsymbol{\Lambda}_P\boldsymbol{\Lambda}_{t,H})\mathrm{tr}(\boldsymbol{\Lambda}_y\boldsymbol{\Lambda}_{t,G}^{-1})+\sigma_R^2\mathrm{tr}(\boldsymbol{\Lambda}_{t,G}^{-1}\boldsymbol{\Lambda}_y)+\mathrm{tr}(\boldsymbol{\Lambda}_P)+P_c} \quad (4.73a)$$

$$\text{s.t. } \mathrm{tr}(\boldsymbol{\Lambda}_P) \leq P_S^{max}\ , \Lambda_P \succeq \mathbf{0} \quad (4.73b)$$

$$\mathrm{tr}(\boldsymbol{\Lambda}_P\boldsymbol{\Lambda}_{t,H})\mathrm{tr}(\boldsymbol{\Lambda}_y\boldsymbol{\Lambda}_{t,G}^{-1})+\sigma_R^2\mathrm{tr}(\boldsymbol{\Lambda}_{t,G}^{-1}\boldsymbol{\Lambda}_y) \leq P_R^{max}\ , \Lambda_y \succeq \mathbf{0} \quad (4.73c)$$

$$N_D \log\left(1+\mathrm{tr}(\boldsymbol{\Lambda}_P\boldsymbol{\Lambda}_{t,H})\frac{1}{\sigma_R^2}\left(1-\frac{\sigma_D^2}{\sigma_D^2+\sigma_R^2\mathrm{tr}(\boldsymbol{\Lambda}_y)}\right)\right) \geq R^{min} \quad (4.73d)$$

We can see that Problem (4.73) is a CLFP with respect to $\boldsymbol{\Lambda}_P$ for fixed $\boldsymbol{\Lambda}_y$, and vice versa, and therefore can be tackled by means of the alternating optimization algorithm. In particular, denoting the objective (4.73a) by $\widetilde{\mathrm{GEE}}$ the resource allocation algorithm can be formulated as in Algorithm 12, which enjoys similar convergence properties as the algorithms developed for the previous CSI scenarios.

Algorithm 12 EE maximization in two-hop P2P MIMO channels with statistical CSI.

$\ell = 0$; $\epsilon > 0$; Initialize $\boldsymbol{\Lambda}_P^{(0)}$ to a feasible value;
while $\left|\widetilde{\mathrm{GEE}}^{(\ell+1)} - \widetilde{\mathrm{GEE}}^{(\ell)}\right| > \epsilon$ **do**
$\ell = \ell + 1$;
Given $\boldsymbol{\Lambda}_P^{(\ell-1)}$, solve Problem (4.73) with respect to $\boldsymbol{\Lambda}_y$ to obtain the optimal $\boldsymbol{\Lambda}_y^{(\ell)}$;
Given $\boldsymbol{\Lambda}_y^{(\ell)}$, solve Problem (4.73) with respect to $\boldsymbol{\Lambda}_P$ to obtain the optimal $\boldsymbol{\Lambda}_P^{(\ell)}$;
end while

Energy-efficient design in relay-assisted MACs and BCs

In this section the main focus will be on the MAC scenario. Corresponding results for the BC case can be obtained by means of duality theory, as done in [178]. Moreover, we will directly consider the relay-assisted case, as the less general one-hop case can be obtained by specializing the expression of the AF relay matrix accordingly.

The considered communication system is depicted in Fig. 4.5 and consists of K mobile transmitters that communicate with their service base station by means of a half-duplex AF relay. Each transmitter is equipped with N_S antennas, whereas N_R and N_D antennas are deployed at the relay and destination, respectively.

We consider the scenario in which the receiver employs LMMSE SIC reception, and consider the problem of allocating the transmitters covariance matrices $\{\boldsymbol{P}_k\}_{k=1}^K$ and the relay AF matrix $\boldsymbol{A}$ for GEE maximization. We will see that even resorting to the SIC reception strategy, the presence of multiple users makes the analysis more involved than in the previously considered P2P case. In particular, if $K > 1$ it will not be possible to determine the optimal transmit directions in closed-form. Nevertheless, we will show that the approach based on combining alternating optimization and fractional programming as in the P2P scenario, can be extended to the MAC case as well.

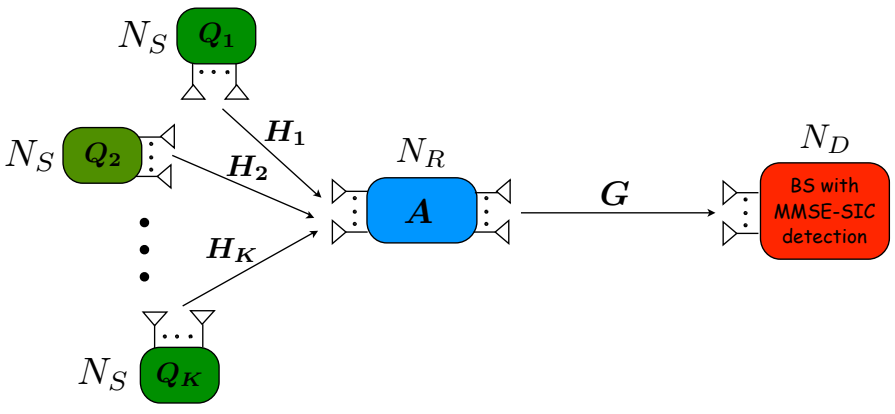

Figure 4.5: Non-regenerative Relay-Assisted MIMO MAC.

The resource allocation problem is formulated as the fractional program:

$$\max \frac{\log\left(\frac{\left|\sigma_D^2 \boldsymbol{I}_{N_R}+\left(\sum_{k=1}^K \boldsymbol{H}_k\boldsymbol{P}_k\boldsymbol{H}_k^H+\sigma_R^2\boldsymbol{I}_{N_R}\right)\boldsymbol{A}^H\boldsymbol{G}^H\boldsymbol{G}\boldsymbol{A}\right|}{\left|\sigma_D^2\boldsymbol{I}_{N_R}+\sigma_R^2\boldsymbol{A}^H\boldsymbol{G}^H\boldsymbol{G}\boldsymbol{A}\right|}\right)}{\sum_{k=1}^K \mu_k \mathrm{tr}(\boldsymbol{P}_k)+\mu_R \mathrm{tr}\left(\left(\sum_{k=1}^K \boldsymbol{H}_k\boldsymbol{P}_k\boldsymbol{H}_k^H+\sigma_R^2\boldsymbol{I}_{N_R}\right)\boldsymbol{A}^H\boldsymbol{A}\right)+P_c} \tag{4.74a}$$

$$\text{s.t. } \mathrm{tr}(\boldsymbol{P}_k) \leq P_k^{max}\ , \boldsymbol{P}_k \succeq \boldsymbol{0}\ , \forall k=1,\ldots,K \tag{4.74b}$$

$$\mathrm{tr}\left(\boldsymbol{A}^H\boldsymbol{A}\left(\sigma_R^2\boldsymbol{I}_{N_R}+\sum_{k=1}^K \boldsymbol{H}_k\boldsymbol{P}_k\boldsymbol{H}_k^H\right)\right) \leq P_R^{max} \tag{4.74c}$$

$$\log\left(\frac{\left|\sigma_D^2 \boldsymbol{I}_{N_R}+\left(\sum_{k=1}^K \boldsymbol{H}_k\boldsymbol{P}_k\boldsymbol{H}_k^H+\sigma_R^2\boldsymbol{I}_{N_R}\right)\boldsymbol{A}^H\boldsymbol{G}^H\boldsymbol{G}\boldsymbol{A}\right|}{\left|\sigma_D^2\boldsymbol{I}_{N_R}+\sigma_R^2\boldsymbol{A}^H\boldsymbol{G}^H\boldsymbol{G}\boldsymbol{A}\right|}\right) \geq R^{min} \tag{4.74d}$$

We can see that (4.74a) can be seen to be PC in $\{\boldsymbol{P}_k\}_{k=1}^K$ for fixed $\boldsymbol{A}$. Therefore, for any fixed $\boldsymbol{A}$, the problem of determining the optimal users' transmit covariance matrices is a CLFP. As for the optimization with respect to $\boldsymbol{A}$ for fixed $\{\boldsymbol{P}_k\}_{k=1}^K$, the following result holds.

Proposition 4.7 (Proposition 2 in [184]). Define $\boldsymbol{B} = \sum_{k=1}^K \boldsymbol{H}_k\boldsymbol{P}_k\boldsymbol{H}_k^H + \sigma_R^2\boldsymbol{I}_{N_R}$, with EVD $\boldsymbol{U}_B\boldsymbol{\Lambda}_B\boldsymbol{U}_B^H$. Then, the optimal $\boldsymbol{A}$ is such that $\boldsymbol{U}_A = \boldsymbol{V}_G$ and $\boldsymbol{V}_A = \boldsymbol{U}_B$.

The proof can be obtained with similar techniques as in Proposition 4.3. Upon optimizing with respect to $\boldsymbol{U}_A$ and $\boldsymbol{V}_A$, we are left with the relay power control problem

$$\max_{\{\lambda_{i,A}\}_{i=1}^{N_R}} \frac{\sum_{i=1}^{N_R}\log\left(1+\frac{\lambda_{i,A}\lambda_{i,B}\lambda_{i,G}}{\sigma_D^2+\sigma_R^2\lambda_{i,A}\lambda_{i,G}}\right)}{\sum_{i=1}^{N_R}\lambda_{i,A}\lambda_{i,B}+\sum_{k=1}^K \mathrm{tr}(\boldsymbol{P}_k)+P_c} \tag{4.75a}$$

$$\text{s.t. } \sum_{i=1}^{N_R}\lambda_{i,A}\lambda_{i,B} \leq P_R^{max}\ , \lambda_{i,A} \geq 0\ , \forall i=1,\ldots,N_R \tag{4.75b}$$

$$\sum_{i=1}^{N_R}\log\left(1+\frac{\lambda_{i,A}\lambda_{i,B}\lambda_{i,G}}{\sigma_D^2+\sigma_R^2\lambda_{i,A}\lambda_{i,G}}\right) \geq R^{min} \tag{4.75c}$$

We can see that Problem (4.75) is a CLFP, since $\sum_{i=1}^{N_R} \log\left(1+\frac{\lambda_{i,A}\lambda_{i,B}\lambda_{i,G}}{\sigma_D^2+\sigma_R^2\lambda_{i,A}\lambda_{i,G}}\right)$ is jointly concave in $\{\lambda_{i,A}\}_{i=1}^{N_R}$. Then, for fixed transmit covariance matrices, the optimal AF matrix can be determined by first setting $\boldsymbol{U}_A = \boldsymbol{V}_G$ and $\boldsymbol{V}_A = \boldsymbol{U}_B$, and then solving the CLFP (4.75). This means that once again a convenient way to tackle the GEE maximization problem is to employ the alternating optimization algorithm. The formal procedure can be stated as in Algorithm 13, which enjoys similar convergence properties as for the P2P case.

Algorithm 13 GEE maximization in two-hop MIMO MAC with perfect CSI.

$\ell = 0$; $\epsilon > 0$; Initialize $\left\{\boldsymbol{P}_k^{(0)}\right\}_{k=1}^K$ to feasible values;
while $\left|\text{GEE}^{(\ell+1)} - \text{GEE}^{(\ell)}\right| > \epsilon$ **do**
  $\ell = \ell + 1$;
  Given $\left\{\boldsymbol{P}_k^{(\ell-1)}\right\}_{k=1}^K$, compute $\boldsymbol{B}^{(\ell-1)} = \sum_{k=1}^K \boldsymbol{H}_k \boldsymbol{P}_k^{(\ell-1)} \boldsymbol{H}_k^H + \sigma_R^2 \boldsymbol{I}_{N_R} = \boldsymbol{U}_B^{(\ell-1)} \boldsymbol{\Lambda}_B^{(\ell-1)} \boldsymbol{U}_B^{H(\ell-1)}$;
  Set $\{\lambda_{i,A}^{(\ell)}\}_{i=1}^{N_R}$ as the solution of (4.75);
  $\boldsymbol{A}^{(\ell)} = \boldsymbol{V}_G \left(\text{diag}\left(\{\lambda_{i,A}^{(\ell)}\}_{i=1}^{N_R}\right)\right)^{1/2} \boldsymbol{U}_B^{H(\ell-1)}$;
  Given $\boldsymbol{A}^{(\ell)}$, and set $\{\boldsymbol{P}_k^{\ell}\}_{k=1}^K$ as the solution of (4.74);
end while

4.2.3 Relay-assisted MIMO IC

In the previous section we have seen how energy efficiency optimization in MIMO systems can prove to be a challenging problem even in noise-limited scenarios. Clearly, the task becomes even more complex in the interference-limited case. A typical approach to simplify the problem is to consider single-stream MIMO systems, in which each transmitter does not employ a possibly full-rank precoding matrix, but instead a beamforming vector, while linear multiuser detection is employed at the receiver to decode the data-streams from the different users. In

line with this approach, in this section we will focus on a single-stream MIMO IC. As for the MAC case, we will directly consider the more general two-hop scenario, which includes as a special case the one-hop case. To be more specific, the system model is that of Fig. 4.1-b, with $K = M$, and in which each receiver is interested in decoding the data of a different transmitter[3]. Communiation takes place over a two-hop channel with the help of a half-duplex node which has no decoding abilities but operates by amplifying the signal from the first hop and forwarding it over the second hop to the final destinations. In this setting, the typical choice is an AF relay, but it is also possible to employ light access points without decoding abilities. As far as the techniques to be described are concerned, the particular type of AF device is not important and the type of node that best suits the network requirements can be chosen.

Denote by N_T, N_R, and N_D the number of antennas deployed at each transmitter, at the relay, and at each receiver, respectively, by p_k, $\boldsymbol{q}_k$ and $\boldsymbol{H}_k$, the k-th user's transmit power, beamforming vector, and channel to the relay, and by $\boldsymbol{G}_k$ the channel from the relay to the k-th receiver. In order to avoid amplifier saturation at the relay, the received signal needs to be normalized by the square root of its power P_t, before being amplified. Assuming that the noise is uncorrelated from the information symbols, and that information symbols from different users are uncorrelated with each other, we have

$$P_t = N_R\sigma_R^2 + \sum_{\ell=1}^{K} p_\ell \|\boldsymbol{H}_\ell \boldsymbol{q}_\ell\|^2 \, . \tag{4.76}$$

After normalization, the received signal is precoded by the $N_R \times N_R$ amplification matrix $\boldsymbol{A}$, subject to the power constraint $\mathrm{tr}(\boldsymbol{A}\boldsymbol{A}^H) \leq P_r$, with P_r denoting the available power at the relay, and then forwarded to the destinations. Assuming a direct link between transmitters and receivers is not available, and denoting by $\boldsymbol{c}_k$ the k-th user's linear receive filter, for all $k = 1, \ldots, K$, the SINR achieved by the k-th

[3]The results to follow can be straightforwardly extended to the more general case of a multicast network in which each transmitter is interested in communicating with more than one receiver, which also includes the case in which the number of transmitters is lower than the number of receivers.

communication link is[4]

$$\gamma_k = \frac{p_k |\boldsymbol{c}_k^H \boldsymbol{G}_k \boldsymbol{A} \boldsymbol{H}_k \boldsymbol{q}_k|^2}{\sigma_R^2 \|\boldsymbol{c}_k^H \boldsymbol{G}_k \boldsymbol{A}\|^2 + P_t \sigma_D^2 \|\boldsymbol{c}_k\|^2 + \sum_{\ell \neq k} p_\ell |\boldsymbol{c}_k^H \boldsymbol{G}_k \boldsymbol{A} \boldsymbol{H}_\ell \boldsymbol{q}_\ell|^2} \ , \quad (4.77)$$

and the GEE maximization problem is expressed as

$$\max \ \frac{\sum_{k=1}^K \log_2(1+\gamma_k(\boldsymbol{A}, \boldsymbol{c}_k, \{p_k, \boldsymbol{q}_k\}_{k=1}^K))}{\sum_{k=1}^K \mu_k p_k + P_{c,k}} \quad (4.78a)$$

$$\text{s.t. } \|\boldsymbol{q}_k\| = 1; \ \boldsymbol{c}_k \in \mathbb{C}^{N_D} \ , \forall \ k = 1, \ldots, K \quad (4.78b)$$

$$\text{tr}(\boldsymbol{A}\boldsymbol{A}^H) \leq P_r \ , p_k \in [0; P_{max,k}] \ , \forall \ k = 1, \ldots, K \quad (4.78c)$$

Plugging (4.76) into (4.77), we can see that (4.77) is expressed as in (4.2). Therefore, if only the transmit powers were to be allocated, we could readily re-use the results presented in Section 4.1 to solve (4.78). However, besides the transmit powers, the goal here is to allocate also the relay AF matrix $\boldsymbol{A}$, the linear receive filters $\{\boldsymbol{c}_k\}_{k=1}^K$, and the beamforming vectors $\{\boldsymbol{q}_k\}_{k=1}^K$.

Relay Matrix AF Design

We see that the AF matrix affects only the numerator of the GEE. However, finding the GEE-maximizing $\boldsymbol{A}$ appears to be a difficult matrix-valued, non-convex problem, which would therefore require a high computational complexity to be solved. Moreover, even if we could solve it, the optimal $\boldsymbol{A}$ would inevitably depend on the users' transmit powers, receive filters, and beamforming vectors, thus coupling relay design with the design of the other resources. This means that the non-convex relay design problem should be solved again any time any of the other resources is updated. This level of complexity is not feasible for low-cost devices with ordinary computing abilities such as layer-1 relays. Therefore, an alternative approach to relay design is sought. The approach to be described here has been introduced in [190], and is based on allocating the relay matrix so as to null out multi-user interference

[4]When dealing with IC, we drop the double subscript $(k, a(k))$ in γ, recalling that in an IC we have $a(k) = k$.

at each receiver. This interference neutralization scheme has at least three advantages:

1. As it will be described, it completely decouples relay design from the design of the other resources, thereby significantly reducing the complexity of the overall resource allocation algorithm.

2. Neutralizing multi-user interference allows for simpler single-user data decoding at the receivers.

3. The interference-neutralizing AF matrix can be determined in closed-form, as we show next.

Before determining the interference-neutralizing AF matrix, we observe that if one is not interested in beamforming and receive filter allocation, then, provided $N_R \geq K$, interference neutralization can be achieved by defining the matrices $\boldsymbol{U} = [\boldsymbol{H}_1\boldsymbol{q}_1, \ldots, \boldsymbol{H}_K\boldsymbol{h}_K]$ and $\boldsymbol{V} = [\boldsymbol{G}_1^H\boldsymbol{c}_1, \ldots, \boldsymbol{G}_K^H\boldsymbol{c}_K]$ and setting $\boldsymbol{A} = a(\boldsymbol{V}^H)^+\boldsymbol{U}^+$, with a such that the relay power constraint is met [75]. However, this approach requires the transmit and receive filters to be fixed and does not work if the vectors $\{\boldsymbol{q}_k, \boldsymbol{c}_k\}_{k=1}^K$ are also varying during the optimization process. In this case, relay design would once again be coupled with the other resources. Instead, in order to obtain a universal interference neutralization scheme that does not depend on the other network resources, we proceed as follows. For any choice of the receive filters, beamforming vectors, and transmit powers, interference neutralization at the relay can be achieved by enforcing the conditions

$$\boldsymbol{G}_k\boldsymbol{A}\boldsymbol{H}_\ell = \boldsymbol{0}_{N_D,N_T} \ , \ \forall\, \ell \neq k \ . \tag{4.79}$$

Additionally, in order to guarantee a desired effective channel for each user k, the following conditions should also be enforced.

$$\boldsymbol{G}_k\boldsymbol{A}\boldsymbol{H}_k = a\widetilde{\boldsymbol{A}}_k \ , \ \forall\, k \ , \tag{4.80}$$

with the scalar a to be set so as to meet the relay power constraint, and with the $N_D \times N_T$ matrices $\widetilde{\boldsymbol{A}}_k$ to be adjusted according to some QoS policy among the users. Conditions (4.80) can be regarded as a form of channel equalization among the users. If $\widetilde{\boldsymbol{A}}_1 = \widetilde{\boldsymbol{A}}_2 = \ldots = \widetilde{\boldsymbol{A}}_K$, each

transmitter-receiver pair k has the same equivalent channel $\boldsymbol{G}_k\boldsymbol{A}\boldsymbol{H}_k$. Instead, if some users belong to a different priority class, the corresponding $\widetilde{\boldsymbol{A}}_k$ can be tuned to grant these users a better equivalent channel. A simple way to allocate the matrices $\{\widetilde{\boldsymbol{A}}_k\}_{k=1}^K$ is according to a channel-matching criterion [145]. Specifically, denoted by $\boldsymbol{U}_{H,k}\boldsymbol{\Lambda}_{H,k}^{1/2}\boldsymbol{V}_{H,k}^H$ and $\boldsymbol{U}_{G,k}\boldsymbol{\Lambda}_{G,k}^{1/2}\boldsymbol{V}_{G,k}^H$ the SVDs of $\boldsymbol{H}_k$ and $\boldsymbol{G}_k$, respectively, for all $k = 1, \ldots, K$ we impose

$$\boldsymbol{G}_k\boldsymbol{A}\boldsymbol{H}_k = a\boldsymbol{U}_{G,k}\boldsymbol{\Lambda}_{G,k}^{1/2}\boldsymbol{\Lambda}_{H,k}^{1/2}\boldsymbol{V}_{H,k}^H = a\widetilde{\boldsymbol{A}}_k \ . \tag{4.81}$$

Next, applying the vectorization operator, and defining $\boldsymbol{a}_k = vec(\widetilde{\boldsymbol{A}}_k)$ for all $k = 1, \ldots, K$, (4.79) and (4.80) can be equivalently rewritten as

$$vec(\boldsymbol{G}_k\boldsymbol{A}\boldsymbol{H}_k) = a\boldsymbol{a}_k \tag{4.82}$$

$$vec(\boldsymbol{G}_k\boldsymbol{A}\boldsymbol{H}_\ell) = \boldsymbol{0}_{N_D N_T} \ , \tag{4.83}$$

which, exploiting the identity $vec(\boldsymbol{X}\boldsymbol{Y}\boldsymbol{Z}) = (\boldsymbol{Z}^T \otimes \boldsymbol{X})vec(\boldsymbol{Y})$, in turn become

$$(\boldsymbol{H}_k^T \otimes \boldsymbol{G}_k)vec(\boldsymbol{A}) = a\boldsymbol{a}_k \tag{4.84}$$

$$(\boldsymbol{H}_\ell^T \otimes \boldsymbol{G}_k)vec(\boldsymbol{A}) = \boldsymbol{0}_{N_D N_T} \ . \tag{4.85}$$

Stacking together the equations for each user k, we obtain the linear system

$$\boldsymbol{C}vec(\boldsymbol{A}) = a\boldsymbol{v} \ , \tag{4.86}$$

with $\boldsymbol{v}^T = [\boldsymbol{a}_1^T, \boldsymbol{0}_{(K-1)N_D N_T}^T, \ldots, \boldsymbol{0}_{(K-1)N_D N_T}^T, \boldsymbol{a}_K^T]$ and

$$\boldsymbol{C} = \begin{bmatrix} \widetilde{\boldsymbol{H}}_1 \\ \vdots \\ \widetilde{\boldsymbol{H}}_K \end{bmatrix} \ , \ \widetilde{\boldsymbol{H}}_k = \begin{bmatrix} \boldsymbol{H}_k^T \otimes \boldsymbol{G}_1 \\ \vdots \\ \boldsymbol{H}_k^T \otimes \boldsymbol{G}_K \end{bmatrix} \ . \tag{4.87}$$

Thus, the interference neutralization problem can be equivalently reformulated as the system of linear equations (4.86), which admits at least one solution if the $K^2 N_D N_T \times N_R^2$ matrix $\boldsymbol{C}$ has rank $r = K^2 N_D N_T$. Under such an assumption, from (4.86) we obtain

$$vec(\boldsymbol{A}) = a\boldsymbol{C}^+\boldsymbol{v} \ , \tag{4.88}$$

where $a \leq \frac{\sqrt{P_R}}{\|\boldsymbol{C}^{+}\boldsymbol{v}\|}$ ensures that the relay power constraint is met, because $\mathrm{tr}(\boldsymbol{A}\boldsymbol{A}^H) = \|vec(\boldsymbol{A})\|^2$.

Remark 4.2. It should be stressed that the considered approach is different from interference alignment techniques which design the beamforming vectors and AF matrix to constrain the interference at each receiver in a suitable vector space, in order to eliminate it by zero forcing reception. Here, we neither assume nor impose any particular configuration of the interference at each receiver. The beamforming vectors and receive filters can be allocated for energy efficiency maximization, or according to any other criterion, and the resulting interference is nulled out by the relay precoding.

Remark 4.3. It should be noted that even if the entries of the coefficient matrix $\boldsymbol{C}$ are obtained from independent channel realizations, in order to ensure that $\boldsymbol{C}$ has rank $K^2N_DN_T$ with probability one, it is not enough to have $N_R^2 \geq K^2N_DN_T$. To see this, note that, for all $k = 1, \ldots, K$, the $KN_DN_T \times N_R^2$ matrix $\widetilde{\boldsymbol{H}}_k$ can be written as $\widetilde{\boldsymbol{H}}_k = \boldsymbol{H}_k^T \otimes \widetilde{\boldsymbol{G}}$, wherein $\widetilde{\boldsymbol{G}}$ is the $KN_D \times N_R$ matrix obtained by stacking together the channel matrices $\{\boldsymbol{G}_k\}_{k=1}^K$. Now, since the rank of a Kronecker product is equal to the product of the ranks of the factors, we obtain

$$\mathrm{rank}(\widetilde{\boldsymbol{H}}_k) = \mathrm{rank}(\boldsymbol{H}_k)\mathrm{rank}(\widetilde{\boldsymbol{G}}) = \min(N_T, N_R)\min(N_R, KN_D) \;, \tag{4.89}$$

where the last equality holds with probability one, since the entries of $\boldsymbol{H}_k$ and $\widetilde{\boldsymbol{G}}$ are realizations of independent random variables. Consequently, in order to guarantee that the rank of $\boldsymbol{C}$ is $r = K^2N_DN_T$ with probability 1, it is necessary to have $N_R \geq KN_D$ and $N_R \geq N_T$ so that each block $\widetilde{\boldsymbol{H}}_k$ in $\boldsymbol{C}$ provides KN_DN_T independent equations. Then, the condition for the achievability of interference neutralization can be expressed in compact form as $N_R \geq \max\{K\sqrt{N_DN_T}, KN_D, N_T\}$. If we consider the special case $N_T = N_D = 1$ we obtain $N_R \geq K$, which is known to hold in the particular case of single-antenna terminals [75].

Remark 4.4. It is seen that the number of relay antennas that are required in order to achieve interference neutralization grows linearly in the system parameters. This appears as the key factor in the choice of

what AF device to employ. Depending on the number of users K and of equipped transmit and receive antennas N_T and N_D, a layer-1 relay or a light access point which can host more antennas should be selected. Moreover, with this respect we should also mention that having light infrastructure nodes with tens of antennas is not only technically feasible, but also appears as a likely scenario in future wireless networks. Two popular trends in wireless communications go in this direction: massive MIMO systems, where a large number of antennas is used, and mmWave communications, which allows one to reduce antenna sizes, thereby allowing to deploy a larger number of antennas.

Remark 4.5. Finally, we should stress that even if not enough antennas are deployed to exactly solve (4.86), still, computing (4.88) is always possible and yields the least squares solution of (4.86), i.e. the element in the column span of $\boldsymbol{C}$ that is at minimum Euclidean distance from $\boldsymbol{v}$. In light of this consideration, it is expected that allocating the relay matrix according to (4.88) performs well even when perfect interference neutralization can not be achieved, as confirmed by numerical results.

Receive filters design.

From (4.78) we see that the design of the receive filters can be decoupled over the users, because the SINR of one user does not depend on the receive filters of the other users. Then, each receiver k will set $\boldsymbol{c}_k$ as the vector which maximizes γ_k and it is well-known that the SINR maximizing linear receive filter is the LMMSE receiver [172]. Therefore, the optimal $\boldsymbol{c}_k$ is expressed as

$$\boldsymbol{c}_k^{LMMSE} = \sqrt{\frac{p_k}{P_t}} \boldsymbol{Z}_k^{-1} \boldsymbol{G}_k \boldsymbol{A} \boldsymbol{H}_k \boldsymbol{q}_k \,, \tag{4.90}$$

and the corresponding k-th user's SINR is given by

$$\gamma_k^{LMMSE} = \frac{p_k}{P_t} \boldsymbol{q}_k^H \boldsymbol{H}_k^H \boldsymbol{A}^H \boldsymbol{G}_k^H \boldsymbol{Z}_k^{-1} \boldsymbol{G}_k \boldsymbol{A} \boldsymbol{H}_k \boldsymbol{q}_k \,. \tag{4.91}$$

with $\boldsymbol{Z}_k = \frac{1}{P_t} \boldsymbol{G}_k \boldsymbol{A} \left(\sum_{i \neq k} p_i \boldsymbol{H}_i \boldsymbol{q}_i \boldsymbol{q}_i^H \boldsymbol{H}_i^H + \sigma_R^2 \boldsymbol{I}_{N_R} \right) \boldsymbol{A}^H \boldsymbol{G}_k^H + \sigma_D^2 \boldsymbol{I}_{N_D}$ being the interference-plus-noise covariance matrix at receiver k. Setting the relay matrix to the interference-neutralizing matrix $\boldsymbol{A}_{IN}$, $\boldsymbol{Z}_k$

simplifies to

$$\boldsymbol{Z}_k = \frac{\sigma_R^2}{P_t}\boldsymbol{G}_k\boldsymbol{A}_{IN}\boldsymbol{A}_{IN}^H\boldsymbol{G}_k^H + \sigma_D^2\boldsymbol{I}_{N_D} \ , \tag{4.92}$$

which is still colored due to the fact that $\boldsymbol{A}_{IN}$ in general is not a scaled identity matrix. Now, defining for all $k = 1, \ldots, K$, $\boldsymbol{v}_k = \boldsymbol{G}_k\boldsymbol{A}_{IN}\boldsymbol{H}_k\boldsymbol{q}_k$, and $\boldsymbol{R}_k = \sigma_R^2\boldsymbol{G}_k\boldsymbol{A}_{IN}\boldsymbol{A}_{IN}^H\boldsymbol{G}_k^H + \sigma_D^2\left(\sigma_R^2 N_R + \sum_{\ell\neq k} p_\ell\|\boldsymbol{H}_\ell\boldsymbol{q}_\ell\|^2\right)\boldsymbol{I}_{N_D}$, (4.91) can be simplified to

$$\begin{aligned}\gamma_k^{LMMSE} &= p_k\boldsymbol{v}_k^H\left(\sigma_R^2\boldsymbol{G}_k\boldsymbol{A}_{IN}\boldsymbol{A}_{IN}^H\boldsymbol{G}_k^H + P_t\sigma_D^2\boldsymbol{I}_{N_D}\right)^{-1}\boldsymbol{v}_k \\ &= p_k\boldsymbol{v}_k^H\left(\boldsymbol{R}_k + \phi_k p_k\boldsymbol{I}_{N_D}\right)^{-1}\boldsymbol{v}_k \ ,\end{aligned} \tag{4.93}$$

Transmit powers design

In order to design a power control routine, let us further elaborate on (4.93) by performing the EVD of $\boldsymbol{R}_k = \sum_{i=1}^{N_D} r_{i,k}\boldsymbol{u}_{i,k}\boldsymbol{u}_{i,k}^H$. Noticing that the eigenvectors of $\boldsymbol{R}_k$ do not depend on the transmit powers, being the eigenvectors of $\sigma_R^2\boldsymbol{G}_k\boldsymbol{A}_{IN}\boldsymbol{A}_{IN}^H\boldsymbol{G}_k^H$, whereas the eigenvalues of $\boldsymbol{R}_k$ are equal to $r_{i,k} = \lambda_{i,k} + \sigma_D^2\left(\sigma_R^2 N_R + \sum_{\ell\neq k} p_\ell\|\boldsymbol{H}_\ell\boldsymbol{q}_\ell\|^2\right)$, with $\lambda_{i,k}$ the eigenvalues of $\sigma_R^2\boldsymbol{G}_k\boldsymbol{A}_{IN}\boldsymbol{A}_{IN}^H\boldsymbol{G}_k^H$, (4.93) as a function of the users' transmit powers can be expressed as

$$\gamma_k^{LMMSE} = \sum_{i=1}^{N_D}\frac{\alpha_{i,k}p_k}{z_{i,k} + \phi_k p_k + \sum_{\ell\neq k} p_\ell\beta_\ell} \ , \tag{4.94}$$

wherein $\alpha_{i,k} = |\boldsymbol{v}_k^H\boldsymbol{u}_{i,k}|^2$, $\phi_k = \sigma_D^2\|\boldsymbol{H}_k\boldsymbol{q}_k\|^2$, $z_{i,k} = \sigma_D^2\sigma_R^2 N_R + \lambda_{i,k}$ and $\beta_\ell = \sigma_D^2\|\boldsymbol{H}_\ell\boldsymbol{q}_\ell\|^2$, for all $i, k = 1, \ldots, K$, $i = 1, \ldots, N_D$. Equation (4.94) shows that, although spatial multi-user interference has been suppressed by the relay precoding, each SINR still depends on all of the users' transmit powers, which appear in the relay power normalization term P_t. In order to design a power control routine, we observe that (4.94) is formally equivalent to (4.40). Therefore, when interference neutralization is performed at the relay, and the optimum LMMSE receive filters are used, the resulting energy-efficient power control problem can be tackled by means of Algorithm 7, which employs the sequential method described in Proposition 4.2.

Algorithm 14 Cooperative GEE maximization by transmit power and receive filters allocation with relay interference neutralization.

Set $vec(\boldsymbol{A})$ as in (4.88) and obtain the corresponding $\boldsymbol{A}_{IN}$;
$\ell = 0$; $\epsilon > 0$; Initialize $\boldsymbol{p}_0^{(0)}$ to a feasible value;
while $|\mathrm{GEE}^{(\ell+1)} - \mathrm{GEE}^{(\ell)}| > \epsilon$ **do**
  $\ell = \ell + 1$;
  Given $\boldsymbol{p}_0^{(\ell)}$, for all $k = 1, \ldots, K$, $i = 1, \ldots, N_D$ compute $a_k^{(\ell)}, b_k^{(\ell)}, c_{i,k}^{(\ell)}$ according to (4.23), (4.24), and (4.42);
  Compute $\boldsymbol{q}_0^{(\ell)}$ as the solution of Problem P_ℓ in (4.44);
  $\boldsymbol{p}_0^{(\ell)} = 2^{\boldsymbol{q}_0^{(\ell)}}$;
end while
For all $k = 1, \ldots, K$, $\boldsymbol{c}_k = \boldsymbol{c}_k^{LMMSE}$;

Finally, we can formulate a general resource allocation algorithm for GEE maximization as follows.

Algorithm 14 is designed to be implemented in a centralized fashion. Based on global CSI, a computational center runs Algorithm 14 and then enforces the resulting resource allocation on the users. In the considered system, this role can be carried out by the relay, which can estimate the first-hop channels by training sequences and the second-hop channels either exploiting channel reciprocity in case of TDD operation, or by having the receivers estimate and feedback the channels.

4.2.4 Numerical illustrations

Here we present numerical illustrations of the GEE achieved by the described algorithms in the noise-limited scenario, for the different CSI and spatial correlation scenarios. The numerical illustrations for the interference-limited scenario will be provided in Section 5.2 in the next chapter, in order to have a comparison with the distributed case.

We set $N_S = N_R = N_D = 3$, $\sigma_D^2 = \sigma_R^2 = \sigma^2$, $P_S^{max} = P_R^{max} = P^{max}$, $P_c = 5\,\mathrm{W}$, $\mu = 1$, and we have considered no rate requirement, i.e. $R^{min} = 0$. The transmit and receive correlation matrices have been generated according to the exponential correlation model, with equal correlation index ρ, whereas the matrices $\boldsymbol{Z}_H$ and $\boldsymbol{Z}_G$ have been gen-

erated as realizations of Gaussian matrices with zero-mean and unit-variance proper complex Gaussian entries. In Fig. 4.6, we set $\rho = 0.5$, and compared the achieved instantaneous energy efficiency, normalized to the communication bandwidth $W = 1\,\text{MHz}$, versus SNR $= P_{max}/\sigma^2$ with the pair $(\boldsymbol{P}, \boldsymbol{A})$ obtained from the following resource allocation algorithms:

- Algorithm 9, with perfect CSI on both $\boldsymbol{H}$ and $\boldsymbol{G}$
- Algorithm 10, with perfect CSI on $\boldsymbol{G}$ and statistical CSI on $\boldsymbol{H}$
- Algorithm 11, with perfect CSI on $\boldsymbol{H}$ and statistical CSI on $\boldsymbol{G}$

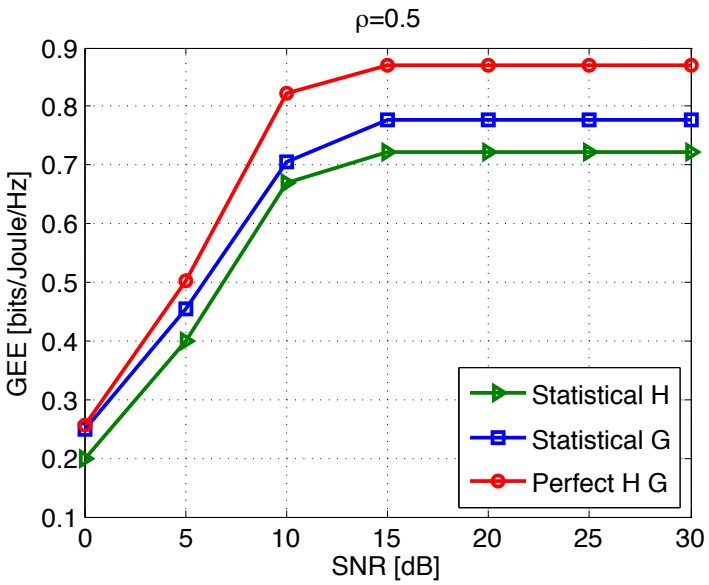

Figure 4.6: $\rho = 0.5$. Achieved GEE normalized to the communication bandwidth for: a) Algorithm 9 with perfect CSI; b) Algorithm 10 with statistical CSI on $\boldsymbol{H}$; c) Algorithm 11 with statistical CSI on $\boldsymbol{G}$.

As expected, better performance is obtained when perfect CSI is available. Interestingly, it is also seen that having perfect knowledge of $\boldsymbol{H}$ grants better performance than having perfect knowledge of $\boldsymbol{G}$. This can be explained noticing that the source-to-relay channel $\boldsymbol{H}$ affects both the numerator and the denominator of the GEE, whereas the relay-to-destination channel $\boldsymbol{G}$ affects only the numerator. Moreover, in a multi-hop communication the first hop is the most critical one and a poor estimate of the first-hop channel negatively affects the following hop.

In Fig. 4.7 a similar scenario as in Fig. 4.6 has been considered, with the difference that the performance achieved for $\rho = 0.1$ and $\rho = 0.9$ is contrasted. As for $\rho = 0.5$, having perfect knowledge of $\boldsymbol{H}$ allows one to achieve a higher instantaneous GEE than when $\boldsymbol{G}$ is perfectly available. Moreover, the results indicate that the gap to the perfect CSI case is bigger when $\rho = 0.1$ than when $\rho = 0.9$. This is also expected because the correlation index ρ is a measure of how much information the channel covariance matrices convey on the channels.

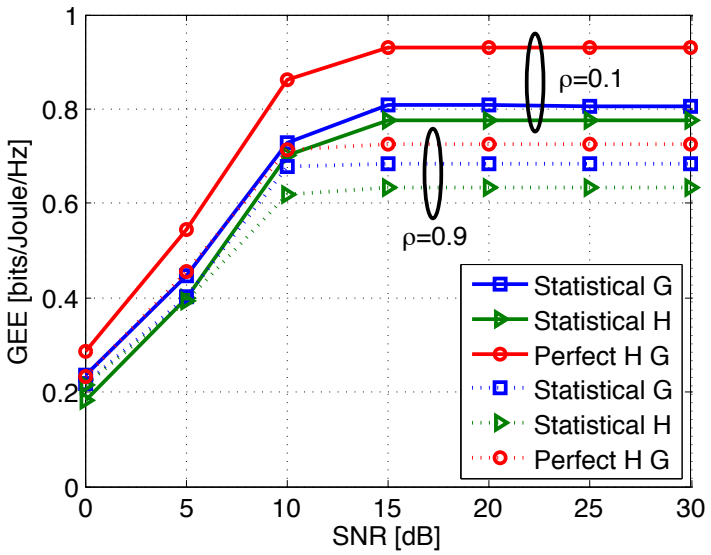

Figure 4.7: $\rho = 0.1; 0.9$. Achieved GEE normalized to the communication bandwidth for: a) Algorithm 9 with perfect CSI; b) Algorithm 10 with statistical CSI on $\boldsymbol{H}$; c) Algorithm 11 with statistical CSI on $\boldsymbol{G}$.

4.3 Resource allocation in multi-carrier wireless networks

The use of multiple transmit subcarriers is nowadays a well-established technique in modern wireless networks, which is efficiently implemented in modern digital signal processors by the use of the discrete Fourier transform. The use of multiple subcarriers for transmission has several attractive features. For example, dividing a large bandwidth into smaller sub-bands centered around orthogonal subcarriers, effectively converts a frequency-selective fading channel into a set of parallel flat-fading channels. Moreover, in a multiple-user system, the orthogonal subcarriers can be allocated to different users, leading to the popular OFDMA scheme. The use of MC and OFDMA represents one of the major components of the LTE standard for 4G networks, and is anticipated to remain a key feature in future wireless networks, too.

In this section we show how fractional programming proves essential in the energy-efficient design of MC networks. As in MIMO systems we could exploit the additional degrees of freedom granted by the use of multiple-antennas, in MC systems the goal will be to perform joint subcarrier and transmit power allocation.

4.3.1 P2P MC systems.

The energy efficiency of a P2P MC system with N available subcarriers was already introduced in (1.5), and is given by

$$\mathrm{EE} = \frac{W \sum_{n=1}^{N} \log_2(1+\gamma_n(p_n))}{\mu \sum_{n=1}^{N} p_n + P_c} \ , \tag{4.95}$$

wherein $\gamma_n(p_n)$ is the SNR on subcarrier n, which depends only on the power p_n on subcarrier n. The energy efficiency maximization problem can be formulated as

$$\max_{\{p_n\}_{n=1}^{N}} \ \frac{W \sum_{n=1}^{N} \log_2(1+\gamma_n(p_n))}{\mu \sum_{n=1}^{N} p_n + P_c} \tag{4.96a}$$

$$\text{s.t. } p_n \geq 0 \ , \ \forall \ n = 1, \ldots, N \tag{4.96b}$$

$$\sum_{n=1}^{N} p_n \leq P_{max} \tag{4.96c}$$

If the SNR γ_n is a concave function of p_n, then (4.96) is a CLFP and can be solved by the techniques developed in Chapter 3. This is the case for the SINR expressions (4.1), (4.2), and (4.40), (with β coefficients all equal to zero for the P2P scenario).

We observe that in this case subcarrier allocation is automatically included in Problem (4.96), since the optimal set of subcarriers to use will be the set of subcarriers for which the optimal transmit powers are strictly positive, as dictated by the solution of (4.96). However, subcarrier allocation can be much more involved when a constraint is enforced to use only a subset of the available subcarriers. In such a scenario the resource allocation problem will in general be a mixed-integer program, for which efficient solution methods are lacking. Nevertheless, in some cases it is possible to find the solution with limited complexity, as described in the next example.

4.3.2 Downlink MC interference network.

In this section we consider a one-hop CoMP system in which M base stations serve a total of K users using N subcarriers. Within one cell, each subcarrier can be assigned to only one user, but one user can be served using more than one subcarrier. Moreover, multi-user, out-of-cell interference is present because subcarriers are reused in the different cells of the cluster. Let us denote by $\mathcal{B}_m$ the set of users associated to base station m, and let $k(m,n)$ indicate the user scheduled by base station m on subcarrier n, $\boldsymbol{k}^{[n]} = (k(1,n), \ldots, k(M,n))^T$, and $\boldsymbol{k} = \text{vec}\{\mathbf{k}^{[1]} \ldots, \mathbf{k}^{[N]}\}$. Also, denote by $p_m^{[n]}$ the transmit power of base station m on subcarrier n, and define $\boldsymbol{p}^{[n]} = (p_1^{[n]}, \ldots, p_M^{[n]})^T$ and $\mathbf{p} = \text{vec}\{\mathbf{p}^{[1]}, \ldots, \mathbf{p}^{[N]}\}$. With this notation, the SINR enjoyed by user $k(m,n)$ is expressed as

$$\gamma_{m,k(m,n)}^{[n]}(\boldsymbol{p}^{[n]}) = \frac{p_m^{[n]} |h_{m,k(m,n)}^{[n]}|^2}{\sigma_{k(m,n)}^2 + \sum_{j \neq m} p_j^{[n]} |h_{j,k(m,n)}^{[n]}|^2} \,, \tag{4.97}$$

and the GEE maximization problem is formulated as

$$\max_{\boldsymbol{k},\boldsymbol{p}} \frac{\sum_{m=1}^{M}\sum_{n=1}^{N}\log_2\left(1+\gamma_{m,k(m,n)}^{[n]}(\boldsymbol{p}^{[n]})\right)}{\sum_{m=1}^{M}\sum_{n=1}^{N}P_{c,m}^{[n]}+\mu_m^{[n]}p_m^{[n]}} \tag{4.98a}$$

$$\text{s.t. } p_m^{[n]} \geq 0 \ ,\forall\ m=1,\ldots,M\ ,n=1,\ldots,N \tag{4.98b}$$

$$k(m,n)\in\mathcal{B}_m\ ,\forall\ m=1,\ldots,M\ ,n=1,\ldots,N \tag{4.98c}$$

$$\sum_{n=1}^{N} p_m^{[n]} \leq P_{max,m}\ ,\forall m=1,\ldots,M \tag{4.98d}$$

At a first sight it might seem that Problem (4.98) is a mixed-integer problem due to subcarrier scheduling. However, this is not the case, and, given any feasible power vector $\boldsymbol{p}$, the optimal subcarrier scheduling can be efficiently determined. Indeed, for any feasible power vector $\boldsymbol{p}$, the optimization over $\boldsymbol{k}$ affects only the numerator of (4.98a). Moreover, for fixed $\boldsymbol{p}$, and for any m and n, the corresponding SINR depends only on $k(m,n)$ and not on the scheduling of other users. Therefore, for fixed $\boldsymbol{p}$, subcarrier allocation is separable across base stations and subcarriers, and the optimal scheduling is computed as

$$\hat{k}(m,n)=\arg\max_{s\in\mathcal{B}_m}\log_2(1+\gamma_{m,s}^{[n]}) \tag{4.99}$$

for $m=1,\ldots,M$ and $n=1,\ldots N$. We should stress that solving (4.99) does not involve an exhaustive search of all possible subcarrier assignment, but only requires each base station m to make $|\mathcal{B}_m|$ comparisons in order to determine the best user to schedule over subcarrier n. Therefore, subcarrier assignment can be performed by making $MN\,|\mathcal{B}_m|$ comparisons in total. Otherwise stated, in order to determine the best user to schedule over a given subcarrier n, base station m does not need to know what users the other base station have scheduled over subcarrier n, but only the amount of interference power on subcarrier n, which is known once the power vector $\boldsymbol{p}$ is fixed.

Being able to efficiently solve the subcarrier assignment problem for any fixed power vector, suggests that joint subcarrier and power allocation can be conveniently performed by means of alternating optimization, iteratively optimizing the transmit powers for fixed subcarriers and the subcarrier scheduling for fixed transmit powers. Moreover, this

approach leads to obtaining a resource allocation policy which fulfills the KKT conditions of Problem (4.98).

To elaborate, (4.99) shows how to determine the optimal subcarrier scheduling for fixed transmit powers. To complete the resource allocation algorithm, we need to perform power allocation for fixed subcarrier assignment. When the vector $\boldsymbol{k}$ is fixed, the power control problem reduces to the maximization of the GEE

$$\frac{\sum_{m=1}^{M}\sum_{n=1}^{N}\log_2\left(1+\gamma_{m,k(m,n)}^{[n]}\right)}{\sum_{m=1}^{M}\sum_{n=1}^{N}P_{c,m}^{[n]}+\mu_m^{[n]}p_m^{[n]}}\,, \tag{4.100}$$

with $\gamma_{m,k(m,n)}^{[n]}$ given by (4.97). The numerator of (4.100) is non-concave in the transmit powers, which prevents the direct use of fractional programming. However, $\gamma_{m,k(m,n)}^{[n]}$ is formally equivalent to (4.1), with $\beta_{m,k(m,n)}^{[n]}=|h_{m,k(m,n)}^{[n]}|^2$, for $m=1,\ldots,M$, and $z_m^{[n]}=\sigma_{k(m,n)}^2$, which, for fixed subcarrier assignment, become constant parameters. Then, for any $\boldsymbol{k}$, a power vector fulfilling the KKT conditions of Problem (4.98) can be determined leveraging again the sequential method provided by Proposition 4.2. More in detail, we use Lemma 4.1 to lower-bound (4.100) as

$$\text{GEE}\geq\frac{\sum_{m=1}^{M}\sum_{n=1}^{N}\left[a_m^{[n]}\log_2\left(\gamma_{m,k(m,n)}^{[n]}\right)+b_m^{[n]}\right]}{\sum\limits_{m=1}^{M}\sum\limits_{n=1}^{N}\left(P_{c,m}^{[n]}+\mu_m^{[n]}p_m^{[n]}\right)}\,, \tag{4.101}$$

Next, upon applying the substitution $p_m^{[n]}=2^{q_m^{[n]}}$, we obtain the power control problem

$$\max_{\boldsymbol{q}}\frac{\sum\limits_{m=1}^{M}\sum\limits_{n=1}^{N}\left\{a_m^{[n]}\left[\log_2\beta_{m,k(m,n)}^{[n]}+q_m^{[n]}-\log_2\left(z_m^{[n]}+\sum\limits_{j\neq m}\beta_{j,k(m,n)}^{[n]}2^{q_j^{[n]}}\right)\right]+b_m^{[n]}\right\}}{\sum\limits_{m=1}^{M}\sum\limits_{n=1}^{N}\left(P_{c,m}^{[n]}+\mu_m^{[n]}2^{q_m^{[n]}}\right)} \tag{4.102a}$$

$$\text{s.t.}\sum_{n=1}^{N}2^{q_m^{[n]}}\leq P_{max,m}\,,\forall m=1,\ldots,M\,. \tag{4.102b}$$

Problem (4.102) is a CCFP and therefore can be efficiently solved by fractional programming algorithms. Finally, a joint power and subcarrier resource allocation algorithm can be formulated as in Algorithm 15, in which the power control subroutine is carried out in a similar way as in Algorithm 5.

Algorithm 15 Power control and subcarrier scheduling for GEE maximization in OFDMA downlink CoMP.

$\ell = 0$; $\epsilon > 0$; Select a feasible $\boldsymbol{p}_0^{(0)}$;
while $\left|\text{GEE}\left(\boldsymbol{k}^{(\ell+1)}, \boldsymbol{p}_0^{(\ell+1)}\right) - \text{GEE}\left(\boldsymbol{k}^{(\ell)}, \boldsymbol{p}_0^{(\ell)}\right)\right| > \epsilon$ **do**
  $\ell = \ell + 1$;
  Set $\boldsymbol{k}^{(\ell)}$ as in (4.99);
  Compute $\gamma_{0,m}^{[n],(\ell)}\left(\boldsymbol{p}_0^{(\ell)}\right)$, for all $m = 1, \ldots, M$, $n = 1, \ldots, N$;
  Compute $a_m^{[n],(\ell)}, b_m^{[n],(\ell)}$ for all $m = 1, \ldots, M$, $n = 1, \ldots, N$, after Lemma 4.1;
  Compute $\boldsymbol{q}_0^{(\ell)}$ as the solution of Problem (4.102);
  $\boldsymbol{p}_0^{(\ell)} = 2^{\boldsymbol{q}_0^{(\ell)}}$;
end while

Algorithm 15 enjoys the following optimality claim.

Proposition 4.8 (Proposition 1 in [171])**.** Algorithm 15 monotonically improves the GEE value at each iteration and converges. Moreover, the solution obtained at convergence satisfies the KKT conditions for Problem (4.98).

The described method can be successfully applied for the maximization of other energy efficiency metrics than the GEE.

In [171] it is shown that subcarrier allocation for WSEE maximization is again performed by computing (4.99), and then an alternating optimization algorithm can be developed, in which the power allocation sub-routine iteratively updates the transmit powers in order to fulfill the KKT conditions of the power control sub-problem, in a similar fashion as in Algorithm 6. Upon convergence, a KKT point of the original WSEE maximization problem is obtained. In the following, we will label this algorithm as **Sum-EE-maximization**.

In [171], the problem of power and subcarrier allocation for WPEE maximization is also studied. Upon applying the logarithmic function to the product, thereby converting it into a sum to simplify the problem, optimal sub-carrier allocation for fixed transmit power can be performed by computing

$$k(m,n) = \arg \max_{s \in \mathcal{B}_m} w_{m,s}^{[n]} \ln \frac{\log_2(1+\gamma_{m,s}^{[n]})}{P_{c,m}^{[n]} + \mu_m^{[n]} p_m^{[n]}} \ . \tag{4.103}$$

On the other hand, power allocation for fixed user-scheduling can be performed by resorting again to sequential convex optimization. The resulting power and sub-carrier allocation algorithm is guaranteed to converge to a point fulfilling the KKT conditions of the WPEE maximization problem [171]. In the following, we will label this algorithm as **Prod-EE-maximization**.

In this section we have considered a SINR expression which, as a function of the transmitters' powers, followed (4.1). However, the presented framework can also be applied to more involved SINR expressions, such as (4.2) and (4.40). In addition, it is also possible to deal with other energy efficiency metrics, such as the WMEE, and with the uplink scenario. More details on these issues will be provided in the coming section.

4.3.3 Uplink MC interference network with QoS constraints.

Let us consider the uplink channel of a multi-cell OFDMA network with K transmitters, M receivers, and N available subcarriers. Assume that the SINR experienced by transmitter k at its intended receiver on subcarrier n follows (4.2). Assuming that each transmitter is allowed to use all of the available subcarriers, the WMEE maximization problem

with QoS rate constraints can be cast as

$$\max_{\boldsymbol{p}} \min_{1\leq k\leq K} w_k \frac{\sum_{n=1}^{N}\log_2\left(1+\gamma_{k,a(k)}^{[n]}\right)}{\sum_{n=1}^{N}P_{c,k}^{[n]}+\mu_k^{[n]}p_k^{[n]}} \tag{4.104a}$$

$$\text{s.t. } \sum_{n=1}^{N} p_k^{[n]} \leq P_{max,k}\ ,\forall\ k=1,\ldots,K \tag{4.104b}$$

$$\sum_{n=1}^{N}\log_2(1+\gamma_{k,a(k)}^{[n]}) \geq R_{min,k}\ ,\forall\ k=1,\ldots,K \tag{4.104c}$$

Each ratio in (4.104a) has a non-concave numerator due to the presence of multi-user interference. However, exploiting the fact that the $\min(\cdot)$ function is increasing, we can lower-bound (4.104a) by lower-bounding each ratio. Leveraging Lemma 4.1, and applying the substitution $p_k^{[n]} = 2^{q_k^{[n]}}$, yields

$$\mathrm{EE}_k \geq \widetilde{\mathrm{EE}}_k = \frac{\sum_{n=1}^{N}\left[b_k^{[n]}+a_k^{[n]}\left(\log_2\alpha_{k,a(k)}^{[n]}+q_k^{[n]}-\log_2\left(z_k^{[n]}+\phi_{k,a(k)}^{[n]}2^{q_k^{[n]}}+\sum_{j\neq k}\beta_{j,a(k)}^{[n]}2^{q_j^{[n]}}\right)\right)\right]}{\sum_{n=1}^{N}P_{c,k}^{[n]}+\mu_k^{[n]}2^{q_k^{[n]}}} \tag{4.105}$$

A second challenge is represented by the QoS constraints, which are not convex. Moreover, unlike the single-carrier scenario, it is not possible to reformulate the QoS constraints in convex form upon applying the substitution $p_k^{[n]} = 2^{q_k^{[n]}}$. However, we can use the same trick used to lower-bound the objective, to obtain a lower-bound of the LHS of the QoS constraints, which yields

$$\sum_{n=1}^{N}\log_2(1+\gamma_{k,a(k)}^{[n]}) \geq \sum_{n=1}^{N}\left[b_k^{[n]}+a_k^{[n]}\log_2\left(\alpha_{k,a(k)}^{[n]}\right)+a_k^{[n]}q_k^{[n]}\right] - \sum_{n=1}^{N}\left[a_k^{[n]}\log_2\left(z_k^{[n]}+\phi_{k,a(k)}^{[n]}2^{q_k^{[n]}}+\sum_{j\neq k}\beta_{j,a(k)}^{[n]}2^{q_j^{[n]}}\right)\right] = \widetilde{R}_k \tag{4.106}$$

Then, a suitable approximation of Problem (4.104), in the sense of Proposition 4.2, is given by

$$\max_{\boldsymbol{q}} \min_{1\leq k\leq K} w_k \widetilde{\mathrm{EE}}_k \tag{4.107a}$$

$$\text{s.t.} \sum_{n=1}^{N} 2^{q_k^{[n]}} \leq P_{max,k} \,, \forall\, k = 1, \ldots, K \tag{4.107b}$$

$$\widetilde{R}_k \geq R_{min,k} \,, \forall\, k = 1, \ldots, K \tag{4.107c}$$

Given the expressions of $\widetilde{\mathrm{EE}}_k$ and $\widetilde{R}_k$, it follows that (4.107) is a MMFP, which can therefore be solved by the generalized Dinkelbach's algorithm. Then, a resource allocation algorithm for WMEE maximization can be stated as in Algorithm 16.

Algorithm 16 Resource allocation for WMEE maximization in MC interference networks.

$\epsilon = 0$; $\ell = 0$; Initialize $\boldsymbol{p}_0^{(0)}$ to a feasible value;
while $\left|\mathrm{WMEE}^{(\ell+1)} - \mathrm{WMEE}^{(\ell)}\right| > \epsilon$ **do**
  $\ell = \ell + 1$;
  Compute $\gamma_{0,m}^{[n],(\ell)}(\boldsymbol{p}_0^{(\ell)})$ for all $k = 1, \ldots, K$ and $n = 1, \ldots, N$;
  Compute $a_k^{[n],(\ell)}$ and $b_k^{[n],(\ell)}$, for all $k = 1, \ldots, K$ and $n = 1, \ldots, N$ after Lemma 4.1;
  Compute $\boldsymbol{q}_0^{(\ell)}$ as the solution of Problem (4.107);
  $\boldsymbol{p}_0^{(\ell)} = 2^{\boldsymbol{q}_0^{(\ell)}}$;
end while

Algorithm 16 can be shown to enjoy the following optimality claim [192].

Proposition 4.9. Algorithm 16 monotonically increases the value of (4.104a) and converges to a point which fulfills the KKT conditions of the epigraph-form[5] of (4.104).

[5] In this case it is not possible to directly claim the convergence to a KKT point of (4.104), because (4.104a) is not differentiable. If GEE maximization were the goal, a similar approach could be used to obtain a KKT point of the original resource allocation problem.

We observe that in this section subcarrier allocation was implicitly performed by the power control algorithm, since Algorithm 16 automatically switches off the subcarriers which should not be used by setting the corresponding transmit powers to zero. The scenario in which each transmitter is allowed to use only a subset $\mathcal{N}_k \subset \{1, 2, \ldots, N\}$ of subcarriers, with $1 < |\mathcal{N}_k| < N$ is still an open problem and in general requires an exhaustive search. A viable approach is to use relaxation techniques, to convert the integer variables of the problem into continuous variables. Upon doing this, the problem can be solved as described in this section, and then the solution can be rounded-off to make it feasible for the original problem.

4.3.4 Numerical illustrations

In this section, we present numerical results to illustrate the performance of the described algorithms. We consider the wireless cellular network in Figure 4.8.

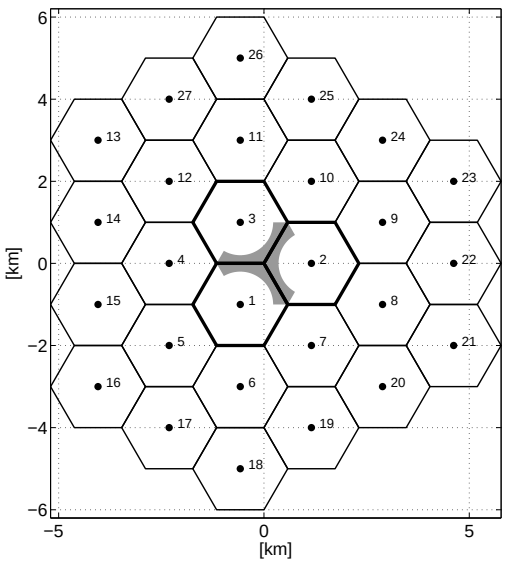

Figure 4.8: Simulated cellular network: Base Stations 1, 2, and 3 are coordinated, and users are randomly dropped in the grey area.

Three base stations coordinate their transmission on $N = 16$ subcarriers with bandwidth $W = 180\,\text{kHz}$. Each base station serves three users, which are uniformly distributed in the grey area. As to the power model, $P_{c,1}^{[n]} = 0.25\,\text{W}$, $P_{c,2}^{[n]} = 0.5\,\text{W}$, $P_{c,3}^{[n]} = 0.75\,\text{W}$, and $\mu_1^{[n]} = \mu_2^{[n]} = \mu_3^{[n]} = 3.8$, for $n = 1, \ldots, N$, which are typical values for LTE systems [8]. On each subcarrier, we consider Rayleigh fading, Log-Normal shadowing with standard deviation 8 dB, and the path-loss model $\text{PL(d)} = \text{PL}_0\,(d_0/d)^4$, where $d \geq d_0$ is the distance in meters, and PL_0 is the free-space attenuation at the reference distance $d_0 = 100\,\text{m}$ with a carrier frequency of 1800 MHz [62].

The noise term $z_m^{[n]}$ accounts for both the thermal noise and the out-of-cluster interference, and following [108], is modeled as

$$z_m^{[n]} = \underbrace{F\mathcal{N}_0 B}_{\text{thermal noise}} + \underbrace{\mathcal{P}_{\text{out}}\text{PL}_0 \sum_{j\in\mathcal{I}} \left(\frac{d_0}{d_{j,s}}\right)^4 \xi_{j,s}^{[n]}}_{\text{out-of-cluster interference}}$$

where $F = 3\,\text{dB}$ is the noise figure of the receiver, $\mathcal{N}_0 = -174\,\text{dBm/Hz}$ is the noise power spectral density, $\mathcal{I} = \{4, 5, \ldots, 27\}$ is the set of uncoordinated base stations in Figure 4.8, $\mathcal{P}_{\text{out}}$ is the average power radiated by the uncoordinated base stations on each subcarrier, $d_{j,s}$ is the distance from base station j to user s, and $\xi_{j,s}^{[n]}$ is the Log-Normal shadowing[6]. Notice that $\mathcal{P}_{\text{out}} = 0$ corresponds to the case in which the cluster of coordinated base stations is isolated. The presented results have been obtained by averaging over 1000 independent user drops. All algorithms are initialized by assuming that the base stations transmit at the maximum power on each subcarrier and the convergence tolerance is set to $\epsilon = 10^{-4}$.

Figures 4.9–4.12 show the value of the GEE, WSEE, WPEE, and sum-rate achieved by the following resource allocation policies:

- $\boldsymbol{p}$ and $\boldsymbol{k}$ resulting from GEE maximization by Algorithm 15.
- $\boldsymbol{p}$ and $\boldsymbol{k}$ resulting from WSEE maximization by the Sum-EE-maximization Algorithm.

[6]We assume that users only track long-term interference levels from uncoordinated base stations and, hence, short-term fading is averaged out

- $\boldsymbol{p}$ and $\boldsymbol{k}$ resulting from WPEE maximization by the Prod-EE-maximization Algorithm.
- $\boldsymbol{p}$ and $\boldsymbol{k}$ resulting from sum-rate maximization as done in [170].
- $\boldsymbol{p}$ and $\boldsymbol{k}$ obtained by uniformly spreading all the available power over the N subcarriers.

The weights for the WSEE and WPEE are taken all equal. In each figure, the subplot on the left refers to an isolated cluster, and the results are shown versus $P_{\max}$, while the subplot on the right refers to a non-isolated cluster, and the results are shown versus $\mathcal{P}_{\text{out}}$, for $P_{\max} = 35$ dBm. For an isolated cluster, all solutions provide similar performance when $P_{\max} \leq 10\,\text{dBm}$, since the radiated power consumption is negligible with respect to the circuit power consumption and, also, the co-channel interference is small compared to the noise power. For larger values of $P_{\max}$, instead, the considered figures of merit lead to different resource allocation strategies and, consequently, system performance. In this regime, the maximization of the sum-rate is obtained at the price of a heavy degradation in the system energy efficiency, no matter which definition of energy efficiency is considered (GEE, WSEE, or WPEE). On the other hand, GEE, WSEE, and WPEE maximization exhibit a floor as $P_{\max}$ increases, since they do not use the excess available power to further increase the rate. For a non-isolated cluster, the value of GEE, WSEE, WPEE, and sum-rate degrade for increasing values of the out-of-cluster interference, irrespectively of the considered optimization criterion. Also, the performance gap among the considered solutions reduces as $\mathcal{P}_{\text{out}}$ increases, since the out-of-cluster interference becomes dominant, making coordinated resource allocation less and less beneficial.

Next, we address the impact that maximizing the WSEE or the WPEE can have on the resulting resource allocation policy, with respect to the maximization of the GEE.

Figure 4.13 considers an isolated cluster and shows the empirical CDF of the energy efficiency achieved on each subcarrier for $P_{\max} = 20$ dBm (top) and the standard deviation of the energy efficiency achieved on each subcarrier versus $P_{\max}$ (bottom), for GEE, WSEE, and WPEE

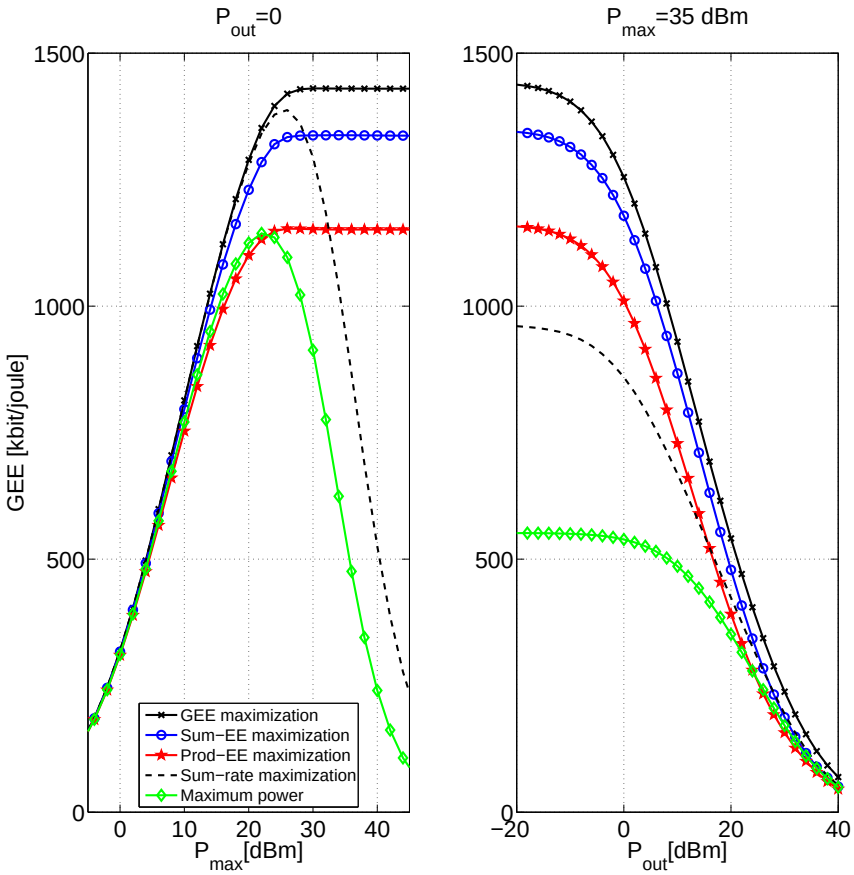

Figure 4.9: GEE vs $P_{\max}$ for $\mathcal{P}_{\text{out}} = 0$ (left); GEE vs $\mathcal{P}_{\text{out}}$ for $P_{\max} = 35$ dBm (right).

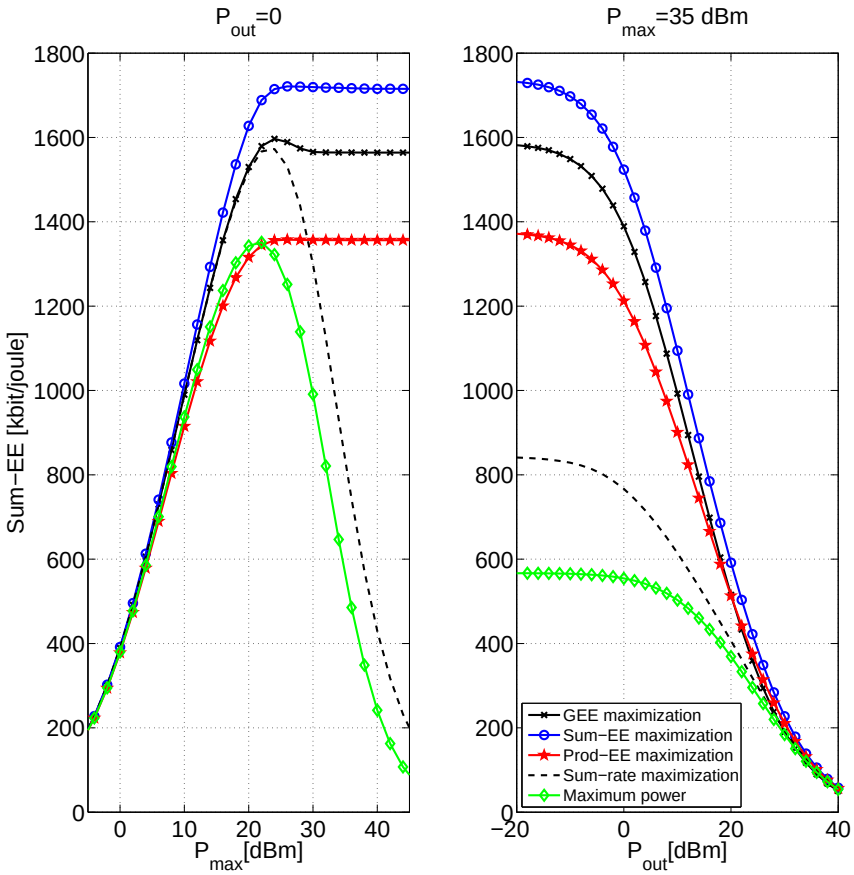

Figure 4.10: Sum-EE vs $P_{\max}$ for $\mathcal{P}_{\text{out}} = 0$ (left); Sum-EE vs $\mathcal{P}_{\text{out}}$ for $P_{\max} = 35$ dBm (right).

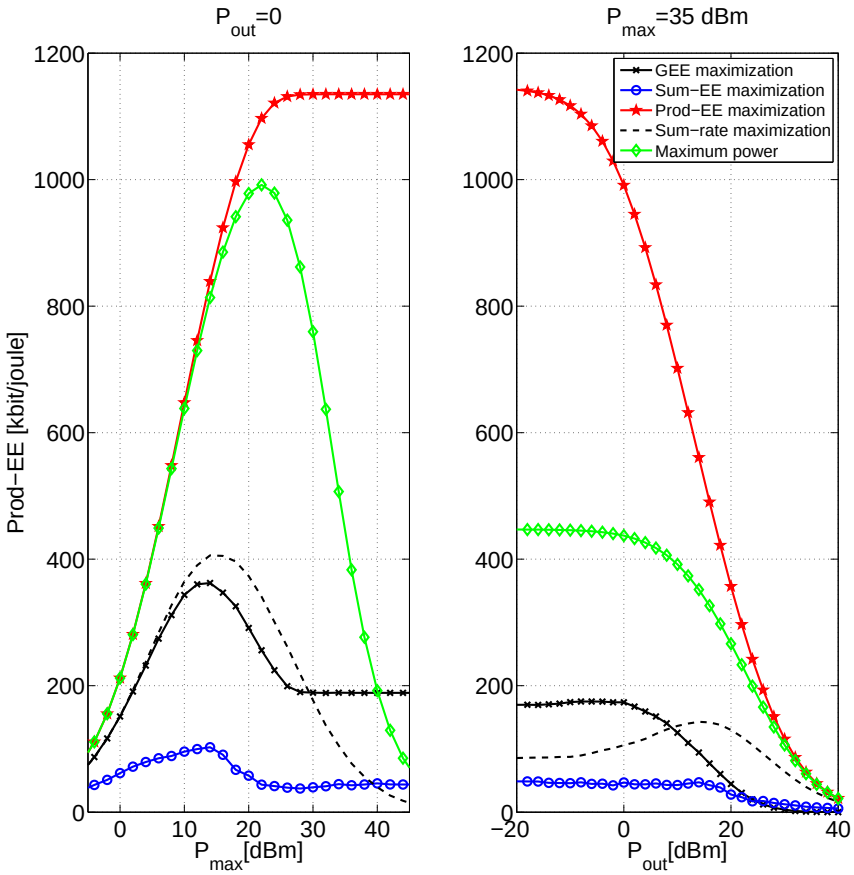

Figure 4.11: Prod-EE vs $P_{\max}$ for $\mathcal{P}_{\text{out}} = 0$ (left); Prod-EE vs $\mathcal{P}_{\text{out}}$ for $P_{\max} = 35$ dBm (right).

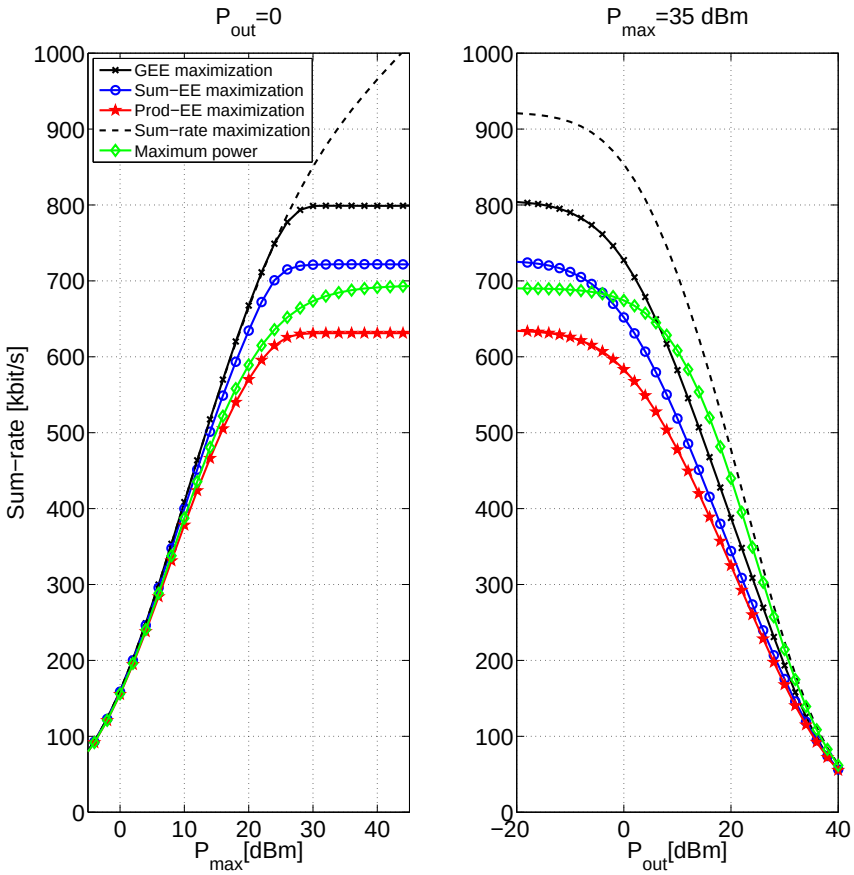

Figure 4.12: Sum-rate vs $P_{\max}$ for $\mathcal{P}_{\text{out}} = 0$ (left); sum-rate vs $\mathcal{P}_{\text{out}}$ for $P_{\max} = 35$ dBm (right).

maximization. Results show that the energy efficiency achieved on the individual subcarriers is less dispersed if WPEE is maximized, thus confirming that this performance metric is able to yield a more balanced use of the available subcarriers.

The weights in the definition of WSEE and WPEE may be used to give priority to specific subcarriers and/or base stations. This is an attractive feature, especially in heterogeneous scenarios, which is analyzed in Figure 4.14, with reference to the WSEE. We consider WSEE maximization in an isolated cluster, for two choices of the weights: a) $w_{1,s}^{[n]} = 0.7$, $w_{2,s}^{[n]} = 0.5$, and $w_{3,s}^{[n]} = 0.3$; b) $w_{1,s}^{[n]} = 0.3$, $w_{2,s}^{[n]} = 0.5$, and $w_{3,s}^{[n]} = 0.7$, for $n = 1, \ldots, N$, and we illustrate the average energy efficiency of base station m, defined as

$$\frac{1}{N} \sum_{n=1}^{N} \frac{\log_2 \left(1 + \gamma_{m,k(m,n)}^{[n]}\right)}{P_{c,m}^{[n]} + \mu_m^{[n]} p_m^{[n]}} ,$$

for $m = 1, 2, 3$. Since $P_{c,1}^{[n]} = 0.25\,\mathrm{W}$, $P_{c,2}^{[n]} = 0.5\,\mathrm{W}$, and $P_{c,3}^{[n]} = 0.75\,\mathrm{W}$, the first base station is the most energy-efficient, while the third one is the most energy-inefficient. In the first scenario, Base Station 1 achieves an average energy-efficiency much larger than that of other base stations, as it has the largest priority and the best energy efficiency. Instead, Base Station 3 is extremely penalized, as it has the worst energy efficiency and the smallest priority. In the second scenario, a more balanced resource allocation is obtained by assigning a higher priority to Base Station 3 and a lower priority to Base Station 1. Notice that the performance of Base Station 2 remains approximately unchanged, as its weights are kept fixed.

Finally, we provide results as to the computational complexity required to maximize the GEE, WSEE, and WPEE, showing in Fig. 4.15 the evolution of the achieved GEE, WSEE, and WPEE versus the iteration index of the corresponding resource allocation procedure. The upper plots refer to an isolated cluster, while the lower plots to a non-isolated cluster. All algorithms reach a steady value in a few iterations in all considered scenarios, with the number of iterations increasing for larger $P_{\max}$ and lower P_{out}. This is expected since a larger $P_{\max}$ means a larger feasible set to search, while a larger P_{out} makes interfer-

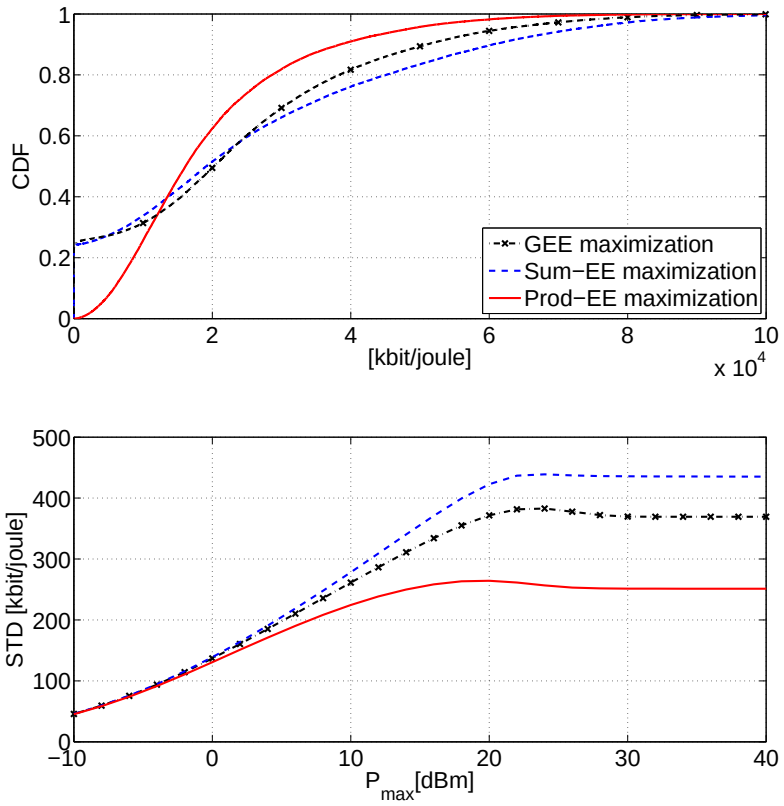

Figure 4.13: Empirical CDF of the energy efficiency achieved on each subcarrier when $P_{\max} = 20$ dBm and $P_{\text{out}} = 0$ (top); standard deviation of the energy efficiency achieved on each subcarrier versus $P_{\max}$ (bottom) when $P_{\text{out}} = 0$.

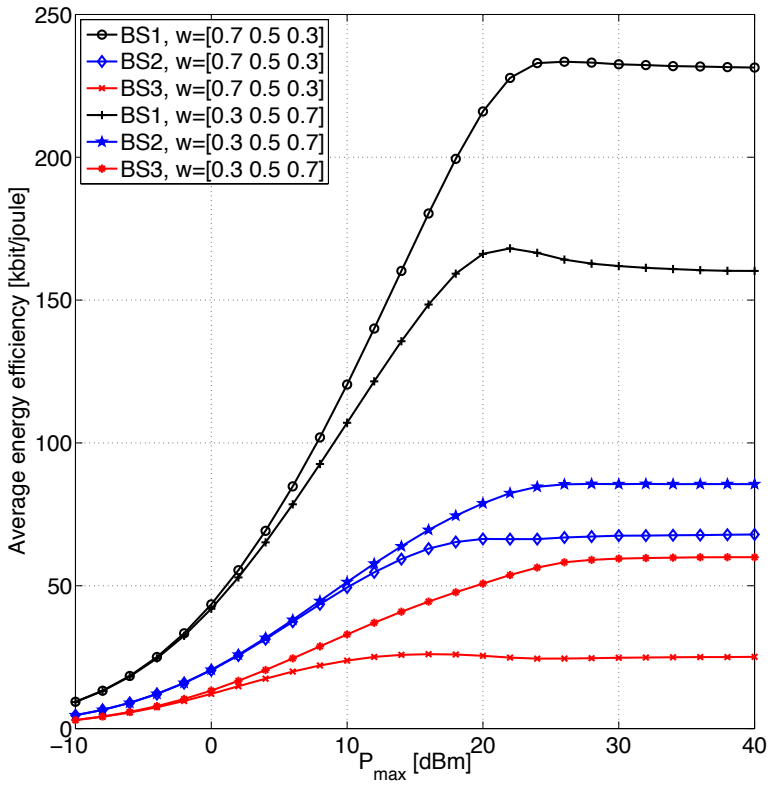

Figure 4.14: Average energy efficiency of each coordinated BS versus $P_{\max}$. The maximization of the WSEE is considered in an isolated cluster, for different choices of the weights.

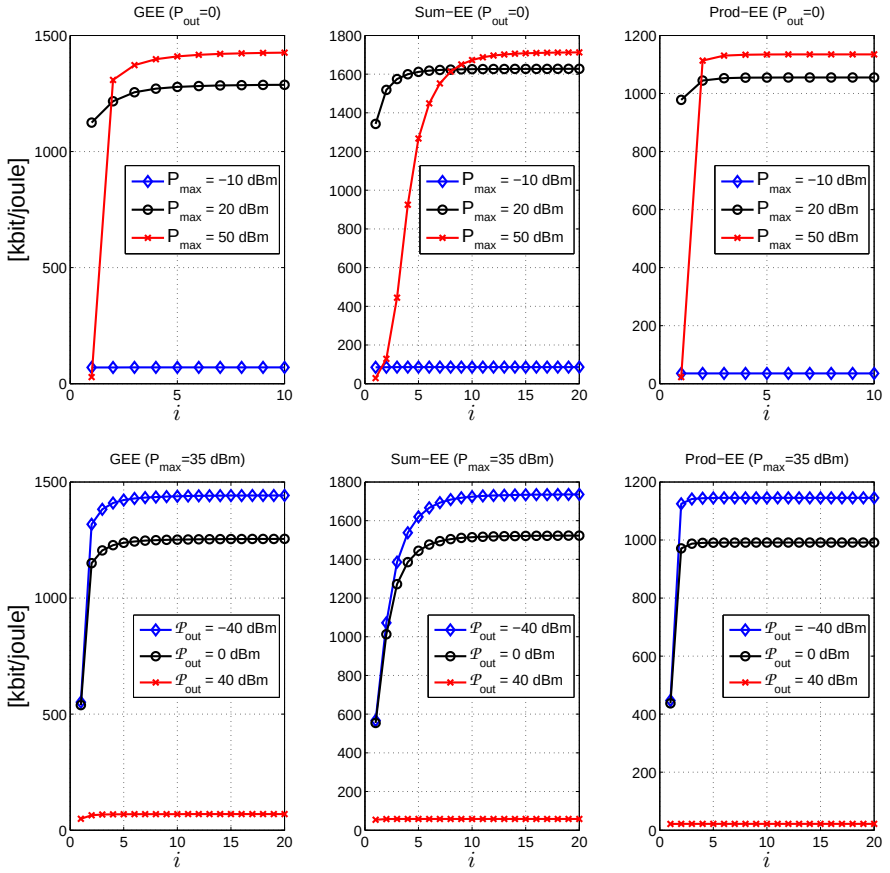

Figure 4.15: GEE, WSEE, and WPEE versus the number of iterations required for convergence. Top: $P_{\max} = -10, 20, 50$ dBm and $P_{\text{out}} = 0$. Bottom: $P_{\text{out}} = -40, 0, 40$ dBm and $P_{\max} = 35$ dBm.

ence management within the cluster less relevant, and causes a faster convergence to a power allocation which employs all available power.

4.4 Summary

This chapter has developed a unified framework for network energy efficiency maximization in cooperative wireless systems via fractional programming. Considering a general interference network model and signal

model, which can be specialized to many relevant instances of wireless networks, we have shown how fractional programming allows one to successfully perform the maximization of the four network energy-efficient metrics defined in Section 1.2.

We have started by developing energy-efficient power control algorithms, which forms the basic building block to tackle more involved resource allocation problems where more resources than the transmit powers are to be allocated. We have first analyzed the noise-limited regime, showing that in this case it is possible to achieve global optimality of the network energy efficiency with affordable complexity. Then, we turned our attention to the more difficult scenario of interference-limited networks, which has been tackled by integrating the fractional programming framework with the tool of sequential convex optimization. This makes it possible to develop a general sequential fractional programming framework, which provides resource allocation algorithms guaranteed to converge and to fulfill the KKT first-order optimality conditions of the GEE, WPEE, and WMEE maximization problems. As for the WSEE, we have taken a different approach, developing an iterative algorithm which also finds a local optimum of the WSEE, by iteratively solving the KKT conditions of the WSEE maximization problem.

Next, we have described how to extend the developed power control algorithms to the case in which the transmit powers are to be jointly allocated with the precoders and receive filters in a MIMO system, or with the transmit subcarriers in a MC system. As a representative of the former scenario, we have considered a relay-assisted MIMO interference network, while as an example of the latter scenario, we have considered an OFDMA-based CoMP system with and without QoS constraints. The approaches developed for the power control case can be successfully extended, preserving the pleasant KKT optimality claim.

5

Energy efficiency in wireless networks: distributed approaches

The focus of this chapter is on distributed resource allocation methods for energy efficiency. As opposed to centralized approaches in which all of the network resources are optimized to maximize a common, system-wide performance function, in a distributed scenario, the network nodes behave in a competitive, self-organizing way, aiming at maximizing their individual energy efficiency through the allocation of their own resources, without considering possible negative effects that this behavior might have on the other nodes in the network. As intuition suggests, the resulting resource allocation policy will in general suffer a performance gap with respect to a centralized allocation, from a social welfare point of view. However, competitive resource allocation is attractive since it allows for distributed resource allocation, requiring less feedback overhead and computational complexity than cooperative approaches. Besides, it allows for self-organizing networks which can operate without the presence of a central authority that dictates and coordinates the resource allocation policy. This is a quite attractive feature, which is becoming more and more a major issue in present wireless networks, due to the exponential growth of connected devices. For a more focused analysis of advantages and disadvantages

of cooperative and competitive resource allocation methods, we refer to [100].

From a mathematical point of view, the most suitable framework to model and analyze competitive interactions among autonomous decision makers is *game theory*, which has indeed become a standard approach in developing competitive resource allocation algorithms [81, 7, 94, 93]. Following this line of research, this chapter will describe how fractional programming integrates into the game-theoretic framework, thereby allowing to formulate and solve competitive resource allocation problems for energy efficiency, and to devise algorithms which are the competitive counterparts of the cooperative ones described in Chapter 4. Section 5.1 deals with the problem of competitive power control for energy efficiency, while competitive resource allocation for MIMO and MC networks will be addressed in Sections 5.2 and 5.3, respectively. We will focus on interference-limited scenarios, since typically in noise-limited scenarios there is no coupling among the nodes individual resource allocation and the competitive power allocation problem reduces to a set of separate P2P resource allocations which can be dealt with by the tools illustrated in Chapter 4.

5.1 Power allocation in wireless networks

The competitive energy-efficient power control problem is described as the scenario in which each transmitter k aims at maximizing its own energy efficiency EE_k, and in order to do so it can tune its own transmit power p_k. Mathematically, this translates into considering the K coupled fractional problems

$$\max_{p_k} \frac{f(\gamma_k(p_k, \boldsymbol{p}_{-k})}{\mu_k p_k + P_{c,k}} \ , \forall\ k = 1, \ldots, K \tag{5.1a}$$

$$\text{s.t. } 0 \leq p_k \leq P_{max,k} \ , \forall\ k = 1, \ldots, K \ , \tag{5.1b}$$

where $\boldsymbol{p}_{-k} = \{p_i\}_{i \neq k}$. The coupling among the K problems in (5.1) is due to the SINRs, which depend on all of the transmit powers. Therefore, when transmitter k maximizes its own EE_k by setting p_k as the solution of the k-th problem in (5.1), this modifies the energy efficiencies of all the other transmitters, which will then react by setting their

transmit powers as the new maximizers of their own energy efficiencies. Thus, (5.1) defines an iterative power update process which should be analyzed in terms of existence of equilibria points and of convergence to an equilibrium. Game theory provides the mathematical tools to perform such analysis. A brief review of the main results from game theory is provided in Appendix C.1.

From a game-theoretic perspective, the energy-efficient, competitive power allocation problem can be formulated as the non-cooperative game in normal form,

$$\mathcal{G}_p = \{\mathcal{K}, \{\mathcal{S}_k\}_{k=1}^K, \{u_k\}_{k=1}^K\} \ , \tag{5.2}$$

wherein $\mathcal{K} = \{1, 2, \ldots, K\}$ is the set of players, who can select a strategy p_k in a strategy set $\mathcal{S}_k = [0; P_{max,k}]$, so as to maximize the utility function $u_k = \mathrm{EE}_k$. In the game-theoretic jargon, the generic k-th problem in (5.1) is the best response (BR) of player k to the strategies taken by the other players, and it can be seen to be a fractional problem. The iteration represented by the K coupled problems (5.1) is called the best response dynamics (BRD) of the game and an equilibrium point of (5.1) is called Nash equilibrium (NE). For a generic non-cooperative game, the existence of an NE and the convergence of the BRD is not guaranteed. In the rest of this section we will study the NE existence and the BRD convergence for the game (5.2), for both linear and concave SINR expressions.

5.1.1 Competitive power control with linear SINR

Let us consider the BRD (5.1), with γ_k expressed as in (4.1). For notational ease, let us define $b_k = \frac{\beta_{k,a(k)}}{z_k + \sum_{j \neq k} p_j \beta_{j,a(k)}}$, which allows us to express (4.1) in the more compact form

$$\gamma_k = p_k b_k \ . \tag{5.3}$$

Then, (5.1) becomes

$$\max_{p_k} \frac{f\left(p_k b_k(\boldsymbol{p}_{-k})\right)}{\mu_k p_k + P_{c,k}} \ , \forall \ k = 1, \ldots, K \tag{5.4a}$$

$$\text{s.t. } 0 \leq p_k \leq P_{max,k} \ , \forall \ k = 1, \ldots, K \ , \tag{5.4b}$$

where we have highlighted the fact that the dependence on the other transmit powers appears only in the coefficient b_k. In order to determine the existence of an NE, we recall from Appendix C.1 that a sufficient condition for the existence of an NE is to require that, for all $k = 1, \ldots, K$, $\mathcal{S}_k$ is closed and compact, while $u_k(p_k, \boldsymbol{p}_{-k})$ is continuous in $\{p_k\}_{k=1}^K$ and QC with respect to p_k. This result makes the connection between game theory and generalized concavity even stronger. Besides the fact that each BR problem is a fractional problem, we will need fractional programming and generalized concavity theory to show the quasi-concavity of the utility functions and ensure the existence of an NE.

Proposition 5.1. If $f(\gamma)$ is either increasing and concave, or $f(\gamma) = R(1 - e^{-\gamma})^Q$, with R a positive parameter, then $\mathcal{G}_p$ admits an NE. Moreover, for all $k = 1, \ldots, K$, the solution of the k-th player's BR problem is $p_k^* = \min(\bar{p}_k, P_{max,k})$, with $\bar{p}_k$ the solution to the equation

$$\mu_k p_k + P_{c,k} = \frac{\mu_k}{b_k} \frac{f(\gamma_k)}{f'(\gamma_k)} \, . \tag{5.5}$$

Proof. For all $k = 1, \ldots, K$, the strategy sets S_k are closed intervals in $\mathbb{R}$ and therefore are also compact, while (5.1a) is continuous in $\{p_k\}_{k=1}^K$. Next, for all $k = 1, \ldots, K$, we can see that the k-th player's BR problem is formally equivalent to the energy-efficient power control problem in P2P channels analyzed in Section 4.1.2. As a consequence, following a similar argument we obtain that (5.1a) is SPC, and hence also QC, in p_k. This also implies that (5.1a) has a unique maximizer which can be found from first-order stationarity conditions. Setting the first-order derivative of (5.1a) to zero we obtain (5.5) and, accounting for the maximum power constraint we obtain that the solution to the k-th player's BR problem is $p_k^* = \min(\bar{p}_k, P_{max,k})$, for all $k = 1, \ldots, K$. □

After establishing the existence of an NE, the next issue is to determine whether there exists a unique NE and if the BRD is always guaranteed to converge to an NE. It turns out that the answer to both questions is affirmative, provided some additional conditions are fulfilled. Specifically, the following results have been obtained so far.

Proposition 5.2. Assume the SINR γ_k is expressed as in (5.3) for all $k = 1, \ldots, K$. The non-cooperative game $\mathcal{G}_p$ admits a unique NE, and the BRD is guaranteed to converge to the unique NE whenever one of the following conditions holds:

(a) $f(\gamma_k) = R(1 - e^{-\gamma_k})^Q$ and $P_{c,k} = 0$.

(b) $f(\gamma_k) = \log_2(1 + \gamma_k)$.

(c) $f(\gamma_k) = R(1 - e^{-\gamma_k})$.

Assertion (a) was the first one to be proved [63, 148], whereas (b) and (c) have been proved only recently in [122] and [187], respectively. The case in which $f(\gamma_k) = R(1 - e^{-\gamma_k})^Q$ with $Q > 1$ and $P_{c,k} > 0$ has been analyzed in [21], but a conclusive proof for the uniqueness of the NE and the convergence of the BRD is still missing. We do not provide here the details of the proof of Proposition 5.2, as it does not require the use of fractional programming, but instead makes use of the framework of standard functions [180], which is reviewed in Appendix C.1.

Based on Proposition 5.2, we can formulate a competitive power control algorithm for energy efficiency, which is guaranteed to converge to the unique NE of $\mathcal{G}_p$. The algorithm works by letting the players iteratively update their radiated power according to their BR, and can be formally stated as in Algorithm 17.

Algorithm 17 Competitive power control with SINR (5.3)

$\ell = 0$; $\epsilon > 0$; Select a feasible $\boldsymbol{p}^{(0)}$;
while $\max_k \left| \mathrm{EE_k}(\boldsymbol{p}^{(\ell+1)}) - \mathrm{EE_k}(\boldsymbol{p}^{(\ell)}) \right| > \epsilon$ **do**
  $\ell = \ell + 1$;
  for $k = 1$ to K **do**
    Compute $\bar{p}_k$ as the solution of (5.5);
    $p_k^{(\ell)} = \min\{\bar{p}_k, P_{max,k}\}$;
  end for
end while

At first sight, it would seem that Algorithm 17 requires each player k to know the channels and current transmit powers of the other players

in order to compute $\bar{p}_k$ and to determine its BR. This would make the distributed implementation of Algorithm 17 problematic, thus losing one of the main advantages of competitive resource allocation. However, this is not the case, because in order to compute its BR, a player does not need to know the individual powers and channels of the other players, but only the aggregate parameter b_k. In order to accomplish this, it is sufficient that each transmitter k knows only its experienced SINR γ_k, which is typically locally available to transmitter k, as γ_k can be measured at the intended receiver and then fed back to the transmitter [134, 154, 133, 122, 187]. This only requires feedback information to be exchanged between each transmitter and its intended receiver, and not between a transmitter and non-intended receivers. Once γ_k is known, player k can simply compute $b_k = \gamma_k/p_k$, with p_k being its current transmit power before the update, and then obtain the new transmit power p_k.

5.1.2 Competitive power control with concave SINR

Let us consider the BRD (5.1), with γ_k expressed as in (4.2). For notational ease, let us define $\omega_k = z_k + \sum_{j \neq k} p_j \beta_{j,a(k)}$, which allows us to express (4.2) in the more compact form[1]

$$\gamma_k = \frac{p_k \alpha_k}{\phi_k p_k + \omega_k} \, . \tag{5.6}$$

Then, (5.1) becomes

$$\max_{p_k} \frac{f\left(\dfrac{p_k \alpha_k}{\phi_k p_k + \omega_k(\boldsymbol{p}_{-k})}\right)}{\mu_k p_k + P_{c,k}} \, , \forall \, k = 1, \ldots, K \tag{5.7a}$$

$$\text{s.t. } 0 \leq p_k \leq P_{max,k} \, , \forall \, k = 1, \ldots, K \, , \tag{5.7b}$$

where the dependence on the other transmit powers is concentrated in the coefficient ω_k. Leveraging the fact that (5.6) is a concave function of p_k, it is possible to extend the result in Proposition 5.1, thus establishing the existence of an NE for (5.7). Specifically, we have the following result.

[1] We have omitted the double subscript $(k, a(k))$ in α_k and ϕ_k.

Proposition 5.3 (Proposition 1 in [187]). If $f(\gamma)$ is either increasing and concave, or $f(\gamma) = R(1 - e^{-\gamma})^Q$, with R a positive parameter, then $\mathcal{G}_p$ admits an NE. Moreover, for all $k = 1, \ldots, K$, the solution of the k-th player's BR problem is $p_k^* = \min(\bar{p}_k, P_{max,k})$, with $\bar{p}_k$ the unique, positive solution of the equation

$$\frac{\mu_k p_k + P_{c,k}}{(\phi_k p_k + \omega_k)^2} = \frac{\mu_k}{\alpha_k \omega_k} \frac{f(\gamma_k)}{f'(\gamma_k)} \, . \tag{5.8}$$

As for the uniqueness of the NE and the convergence of the BRD, the following result holds.

Proposition 5.4 (Proposition 2 in [187]). Assume the SINR γ_k is expressed as in (5.6) for all $k = 1, \ldots, K$. The non-cooperative game $\mathcal{G}_p$ admits a unique NE, and the BRD is guaranteed to converge to the unique NE if $f(\gamma_k)$ is increasing, concave, and fulfills the condition

$$\left(f'(\gamma_k)\right)^2 - f''(\gamma_k) f(\gamma_k) \geq \frac{f'(\gamma_k) f(\gamma_k)}{\gamma_k} \, , \quad \forall \gamma_k \geq 0 \, . \tag{5.9}$$

The proof of this result can be found in [187] and is once again based on the standard function framework developed in [180]. It can be easily checked that both $f(\gamma_k) = \log_2(1 + \gamma_k)$ and $f(\gamma) = R(1 - e^{-\gamma_k})$ fulfill the assumptions of Proposition 5.4. Based on Proposition 5.4, we can formulate a competitive power control algorithm for energy efficiency, which is guaranteed to converge to the unique NE of $\mathcal{G}_p$, as shown in Algorithm 18.

Algorithm 18 Competitive power control with SINR (5.6)

$\ell = 0$; $\epsilon > 0$; Select a feasible $\boldsymbol{p}^{(0)}$;
while $\max_k \left| \mathrm{EE_k}(\boldsymbol{p}^{(\ell+1)}) - \mathrm{EE_k}(\boldsymbol{p}^{(\ell)}) \right| > \epsilon$ **do**
  $\ell = \ell + 1$;
  for $k = 1$ to K **do**
    Compute $\bar{p}_k$ as the solution of (5.8);
    $p_k^{(\ell)} = \min\{\bar{p}_k, P_{max,k}\}$;
  end for
end while

Similarly to what has been observed for the linear SINR case, each player k does not need to know the other players' channels and transmit powers in order to compute its BR. It is only required that each transmitter k knows its own channel to its intended receiver, from which α_k and ϕ_k can be directly computed. Then, it is possible to solve for ω_k in (5.6), thus obtaining $\omega_k = \frac{\alpha_k p_k}{\gamma_k} - \phi_k p_k$. Again, this approach only requires feedback information to be exchanged between each transmitter and its intended receiver, and not between a transmitter and non-intended receivers.

We conclude this section mentioning that the results derived when considering the SINR expression (5.6) have been recently extended to the more general case in which the SINR is expressed as in (4.40). In particular, [190] shows that in such a scenario, a unique NE exists and that the BRD of the game is guaranteed to converge to such unique equilibrium, provided the same assumptions of Proposition 5.4 hold.

5.1.3 Competitive power control with concave SINR and QoS constraints

Let us consider again the BRD (5.1), with γ_k expressed as in (5.6), and in addition let us assume that each player requires a minimum rate $R_{min,k}$. Then, (5.1) can be formulated as

$$\max_{p_k} \frac{f\left(\frac{p_k \alpha_k}{\phi_k p_k + \omega_k(\boldsymbol{p}_{-k})}\right)}{\mu_k p_k + P_{c,k}} \,, \forall\, k = 1, \ldots, K \tag{5.10a}$$

$$\text{s.t. } 0 \leq p_k \leq P_{max,k} \,, \forall\, k = 1, \ldots, K \tag{5.10b}$$

$$\log_2\left(1 + \frac{p_k \alpha_k}{\phi_k p_k + \omega_k(\boldsymbol{p}_{-k})}\right) \geq R_{min,k} \,, \tag{5.10c}$$

where the dependence on the other transmit powers is concentrated in the coefficient ω_k, which appears not only in (5.10a), but also in (5.10c). This means that the strategy set of player k can be written as

$$\mathcal{S}_k(\boldsymbol{p}_{-k}) = \left\{ p_k : 0 \leq p_k \leq P_{max,k},\ \log_2\left(1 + \frac{p_k \alpha_k}{\phi_k p_k + \omega_k(\boldsymbol{p}_{-k})}\right) \geq R_{min,k} \right\}, \tag{5.11}$$

thus depending on the other players' strategies. A non-cooperative game in which not only the utility functions, but also the strategy sets are coupled in the players' strategies, is called a *generalized* non-cooperative game, and its analysis is more involved than for regular non-cooperative games. In particular, in order to establish the existence of a generalized Nash equilibrium (GNE), the following stricter conditions are required: [5, 57]:

1. The players' strategy sets $\mathcal{S}_k(\boldsymbol{p}_{-k})$ are nonempty, closed, convex, and contained in some compact set $\mathcal{C}_k$ for all $\boldsymbol{p}_{-k} \in \mathcal{S}_{-k} \equiv \prod_{\ell \neq k} \mathcal{S}_\ell$.

2. The sets $\mathcal{S}_k(\boldsymbol{p}_{-k})$ vary continuously with $\boldsymbol{p}_{-k}$ (in the sense that the graph of the set-valued correspondence $\boldsymbol{p}_{-k} \mapsto \mathcal{S}_k(\boldsymbol{p}_{-k})$ is closed).

3. For all k, EE_k is QC in p_k for all admissible $\boldsymbol{p}_{-k}$.

For the case at hand, the following result can be proved [192].

Proposition 5.5. Assume $f(\gamma)$ is either increasing and concave, or $f(\gamma) = R(1 - e^{-\gamma})^Q$, with R a positive parameter. If

$$\underline{\gamma}_{min,k} \leq \frac{\alpha_k}{\phi_k} \quad \forall k \tag{5.12}$$

$$P_{max,k} \geq \gamma_{min,k} \frac{\sigma_k^2 + \sum_{j \neq k} \beta_{j,a(k)} P_{max,j}}{\alpha_k - \phi_k \gamma_{min,k}} \quad \forall k \,, \tag{5.13}$$

then $\mathcal{G}_p$ admits a GNE. Moreover, for all $k = 1, \ldots, K$, the solution of the k-th player's BR problem is

$$p_k^*(\boldsymbol{p}_{-k}) = \min\left\{P_{max,k}, \max\left\{\bar{p}_k, P_{min,k}\right\}\right\} \,, \tag{5.14}$$

wherein $\bar{p}_k$ is the unique solution of (5.8), and

$$P_{min,k}(\boldsymbol{p}_{-k}) = \gamma_{min,k} \frac{\sigma_k^2 + \sum_{j \neq k} \beta_{j,a(k)} p_j}{\alpha_k - \phi_k \gamma_{min,k}} \tag{5.15}$$

Next, assuming that (5.12) and (5.13) hold, it is possible to use the standard function framework to show that a unique GNE exits and that the BRD is always guaranteed to converge. More formally, we have the following result from [192].

Proposition 5.6. If (5.12) and (5.13) hold, then the game $\mathcal{G}_p$ admits a unique GNE point, which can be obtained by starting from any feasible power vector $\{p_k\}_{k=1}^K$ and iteratively updating the transmit powers according to (5.10).

Based on Propositions 5.5 and 5.6, we can formulate a competitive power control algorithm for energy efficiency, which is guaranteed to converge to the unique NE of $\mathcal{G}_p$ assuming (5.12) and (5.13) hold. The formal algorithm is labeled as Algorithm 19.

Algorithm 19 Competitive power control with SINR (5.6) and QoS

$\ell = 0$; $\epsilon > 0$; Select a feasible $\boldsymbol{p}^{(0)}$;
while $\max_k \left| \mathrm{EE_k}(\boldsymbol{p}^{(\ell+1)}) - \mathrm{EE_k}(\boldsymbol{p}^{(\ell)}) \right| > \epsilon$ **do**
  $\ell = \ell + 1$;
  for $k = 1$ to K **do**
    Compute p_k^* as in (5.14);
  end for
end while

As in the case without QoS, the algorithm can be implemented in a fully distributed fashion, since it only requires each player to know local information.

5.2 Resource allocation in MIMO wireless networks

In this section, we extend the competitive power control algorithm analyzed in the previous section to the MIMO scenario. The problem is always formulated as a non-cooperative game, with the node energy efficiencies as utility functions, but now the strategy set of each player includes also the choice of the precoder and receive filter.

5.2.1 Resource allocation in MIMO IC

Let us consider a K-user MIMO IC in which each transmitter k allocates its precoding matrix $\boldsymbol{P}_k$ for individual energy efficiency optimization. The problem is formulated as the non-cooperative game

$\mathcal{G} = \{\mathcal{K}, \{\mathcal{S}_k\}_{k=1}^K, \{u_k\}_{k=1}^K\}$, wherein, for all $k = 1, \ldots, K$ we have

$$\begin{aligned} \mathcal{S}_k &= \left\{ \boldsymbol{P}_k \in \mathbb{C}^{N_T \times N_T} \, , \boldsymbol{P}_k \succeq \boldsymbol{0} \, , \mathrm{tr}(\boldsymbol{P}_k) \leq P_{k,max} \right\} \\ u_k &= \mathrm{EE}_k = \frac{\log_2 \left| \boldsymbol{I}_{N_D} + \boldsymbol{Z}_k^{-1/2} \boldsymbol{H}_k \boldsymbol{P}_k \boldsymbol{H}_k^H \boldsymbol{Z}_k^{-1/2} \right|}{\mu_k \mathrm{tr}(\boldsymbol{P}_k) + P_{c,k}} \, , \end{aligned} \tag{5.16}$$

with $\boldsymbol{Z}_k = \sum_{i \neq k} \boldsymbol{H}_i \boldsymbol{P}_i \boldsymbol{H}_i^H + \sigma_{N_D}^2 \boldsymbol{I}_{N_D}$. The BRD of the game is thus formulated as

$$\max_{\boldsymbol{P}_k \succeq \boldsymbol{0}} \frac{\log_2 \left| \boldsymbol{I}_{N_D} + \boldsymbol{Z}_k^{-1/2} \boldsymbol{H}_k \boldsymbol{P}_k \boldsymbol{H}_k^H \boldsymbol{Z}_k^{-1/2} \right|}{\mu_k \mathrm{tr}(\boldsymbol{P}_k) + P_{c,k}} \, , \forall \, k = 1, \ldots, K \tag{5.17a}$$

$$\text{s.t. } \mathrm{tr}(\boldsymbol{P}_k) \leq P_{max,k} \, , \forall \, k = 1, \ldots, K \, , \tag{5.17b}$$

By a similar argument as for the MIMO P2P case, we can recognize that (5.17a) is a PC function of $\boldsymbol{P}_k$, and that each BR problem is a CLFP. Moreover, the pseudo-concavity of the utility functions, together with the fact that all utility functions are continuous in $\{\boldsymbol{P}_k\}_{k=1}^K$ and each $\mathcal{S}_k$ is closed and compact, implies that $\mathcal{G}$ admits an NE. Instead, the uniqueness of the NE and the convergence of the BRD do not hold in general. They are not guaranteed even in the simpler case of achievable rate maximization, as shown in [154], where general conditions on the system parameters and channels matrices are derived such that the NE is unique and the BRD converges. Similar conditions for the energy-efficient scenario are not available to date. A first result in this direction is provided in [89], for the special case of square and invertible channel matrices.

5.2.2 Resource allocation in relay-assisted MIMO IC

We study the same scenario as in Section 4.2.3. The relay matrix is still allocated so as to achieve interference neutralization, but the difference is that now each user k allocates its transmit power p_k, its receive filter $\boldsymbol{c}_k$, and its beamforming vector $\boldsymbol{q}_k$ for individual energy efficiency maximization. Since the relay interference neutralization matrix does not depend on the rest of the network resources, the resource allocation phase can be regarded as a two-stage process. First, the relay designs its AF matrix for interference neutralization, setting $\boldsymbol{A} = \boldsymbol{A}_{IN}$. Afterwards,

given $\boldsymbol{A} = \boldsymbol{A}_{IN}$, the competitive allocation of the users' powers, receive filters, and beamforming vectors takes place, which can be modeled as a non-cooperative game in normal form $\mathcal{G} = \{\mathcal{K}, \{\mathcal{S}_k\}_{k=1}^K, \{u_k\}_{k=1}^K\}$, wherein

$$\begin{aligned} \mathcal{S}_k &= [0; P_{k,max}] \times \mathbb{C}^{N_D} \times \mathbb{C}_1^{N_T} \\ u_k &= \mathrm{EE}_k = \frac{f(\gamma_k)}{\mu_k p_k + P_{c,k}} \ , \end{aligned} \tag{5.18}$$

with $\mathbb{C}_1^{N_T}$ the set of N_T-dimensional unit-norm vectors, and γ_k given by (4.77). The corresponding BRD is formulated as

$$\max_{(p_k, \boldsymbol{c}_k, \boldsymbol{q}_k)} \frac{f(\gamma_k)}{\mu_k p_k + P_{c,k}} \ , \forall \ k = 1, \ldots, K \tag{5.19a}$$

$$\text{s.t. } (p_k, \boldsymbol{c}_k, \boldsymbol{q}_k) \in \mathcal{S}_k \ , \forall \ k = 1, \ldots, K \ , \tag{5.19b}$$

If all network resources except for the transmit power are fixed, we see that γ_k as a function of p_k can be expressed as in (5.6). In this case, the game admits a unique NE and (5.19) is guaranteed to converge by virtue of Propositions 5.3 and 5.4 [2]. If instead, other resources are jointly allocated with the transmit powers, analyzing (5.19) can not be carried out by exploiting previous results.

Competitive receive filters allocation

As already observed in the cooperative case, the SINR of link k depends only on the receive filter $\boldsymbol{c}_k$, and not on the receive filters of the other links. Moreover, each player's utility function is maximized by setting the receive filter so as to maximize the SINR. Then, for all $k = 1, \ldots, K$, the BR of player k is to set $\boldsymbol{c}_k$ as the LMMSE receiver (4.90). Thus, exploiting the relay interference neutralization, each player's SINR can be expressed as in (4.94). Setting $\omega_k = \sum_{\ell \neq k} \beta_\ell p_\ell + \sigma_D^2 \sigma_R^2 N_R$, (4.94) can be expressed more compactly as

$$\gamma_k^{LMMSE} = p_k \sum_{i=1}^{N_D} \frac{\alpha_{i,k}}{\lambda_{i,k} + \omega_k + \phi_k p_k} \ . \tag{5.20}$$

[2] This result holds even if the relay matrix is not allocated for interference neutralization

Plugging (5.20) into (5.19), the BRD of the game is equivalently reformulated as

$$\max_{p_k, \boldsymbol{q}_k} \frac{f(\gamma_k^{LMMSE})}{\mu_k p_k + P_{c,k}} \, , \forall \, k = 1, \ldots, K \tag{5.21a}$$

$$\text{s.t. } (p_k, \boldsymbol{q}_k) \in [0; P_{max,k}] \times \mathbb{C}_1^{N_T} \, , \forall \, k = 1, \ldots, K \, . \tag{5.21b}$$

Competitive transmit power allocation

We observe that even if spatial multi-user interference has been suppressed by the relay interference neutralization precoding, the users' SINRs are still coupled in the transmit powers, as evidenced by the expression of the generic k-th user's SINR (5.20). This is due to the power normalization factor P_t, which depends on all transmit powers. As a result, the competitive power control problem defined by (5.21) differs from previously analyzed problems because of the different expression of the SINR of the players. However, it is possible to extend previously derived results to this scenario as well. We start by ensuring the existence of an NE.

Proposition 5.7 (Proposition 1 in [190]). If $f(\gamma)$ is non-negative, increasing, and concave, then $\mathcal{G}$ admits an NE. Moreover, for all $k = 1, \ldots, K$, the solution of the k-th player's BR problem is $p_k^* = \min(\bar{p}_k, P_{max,k})$, with $\bar{p}_k$ the unique, positive solution of the equation

$$\frac{f\left(\gamma_k^{LMMSE}(p_k)\right)}{\frac{\partial \gamma_k^{LMMSE}}{\partial p_k} \frac{\partial f\left((\gamma_k^{LMMSE}(p_k)\right)}{\partial \gamma_k^{LMMSE}}} - p_k = P_c \, . \tag{5.22}$$

The proof is contained in [190] and exploits the key-observation that (5.20) is a concave function of p_k, from which it follows that the k-th player's utility function is SPC in p_k and hence first-order optimality conditions are necessary and sufficient.

Establishing the uniqueness of the NE and convergence of BRD leverages once again the framework of standard functions [180] and leads to the following result.

Proposition 5.8 (Proposition 2 in [190]). Assume the SINR γ_k is expressed as in (5.20) for all $k = 1, \ldots, K$. The non-cooperative game $\mathcal{G}$ admits a unique NE, and the BRD is guaranteed to converge to the unique NE if $f(\gamma_k)$ is non-negative, increasing, concave, and fulfills the condition

$$\left(f^{'}(\gamma_k)\right)^2 - f^{''}(\gamma_k) f(\gamma_k) \geq \frac{f^{'}(\gamma_k) f(\gamma_k)}{\gamma_k} , \quad \forall \gamma_k \geq 0 . \tag{5.23}$$

Based on the derived results, a competitive resource allocation algorithm for energy efficiency maximization can be formulated as Algorithm 20.

Algorithm 20 Competitive transmit power and receive filters allocation for energy efficiency with relay interference neutralization.

Set $vec(\boldsymbol{A})$ as in (4.88) and obtain the corresponding $\boldsymbol{A}_{IN}$.
$\ell = 0$; $\epsilon > 0$; Select a feasible $\boldsymbol{p}^{(0)}$;
while $\max_k \left| \mathrm{EE_k}(\boldsymbol{p}^{(\ell+1)}) - \mathrm{EE_k}(\boldsymbol{p}^{(\ell)}) \right| > \epsilon$ **do**
  $\ell = \ell + 1$;
  for $k = 1$ to K **do**
    Compute $\bar{p}_k$ as the solution of (5.22);
    $p_k^{(\ell)} = \min\{\bar{p}_k, P_{max,k}\}$;
  end for
end while
For all $k = 1, \ldots, K$, set $\boldsymbol{c}_k$ to the LMMSE receiver

Algorithm 20 converges by virtue of Proposition 5.8 and has a limited computational complexity, since relay design requires only to solve a linear system while the power update routine involves only the solution of the scalar non-linear equation (5.22). Moreover, it can be implemented in a distributed fashion as explained in the following remark.

Remark 5.1. Even if the parameter ω_k which is needed to compute (5.22) depends on the other players' powers and channels, Algorithm 20 can still be implemented in a distributed way and each player k is required to know only his own channels $\boldsymbol{H}_k$ and $\boldsymbol{G}_k$, as well as the AF

matrix $\boldsymbol{A}_{IN}$. Two approaches for the distributed computation of ω_k can be employed. The first approach is based on the observation that $\omega_k = \sigma_D^2(P_t - p_k\|\boldsymbol{H}_k\boldsymbol{q}_k\|^2)$ and that P_t is the received power at the relay. Therefore, the relay can simply measure and broadcast P_t to the transmitters, which can then compute ω_k. Each time a player updates his transmit power, this results in a change of the received power P_t measured by the relay, which will then broadcast the new value.

The second distributed implementation of Algorithm 20 is based on the fact that each receiver k can locally measure the SINR γ_k and then solve for ω_k in (5.20). Afterwards, ω_k is fed back to transmitter k which can compute its BR. This only requires feedback information to be exchanged between each transmitter-receiver pair and not between a receiver and other transmitters.

Beamforming design

So far, we have kept the beamforming vectors fixed. In this section we describe how they can be incorporated into the derived algorithms. To begin with, let us observe that the beamforming vectors do not affect the denominators of the energy efficiencies. Thus, each player k will allocate $\boldsymbol{q}_k$ in order to maximize its own SINR γ_k^{LMMSE}, and its BR problem is formulated as

$$\max_{\boldsymbol{q}_k} \; p_k \boldsymbol{q}_k^H \boldsymbol{H}_k^H \boldsymbol{A}_{IN}^H \boldsymbol{G}_k^H \left(\sigma_R^2 \boldsymbol{G}_k \boldsymbol{A}_{IN} \boldsymbol{A}_{IN}^H \boldsymbol{G}_k^H + \sigma_D^2 P_t \boldsymbol{I}_{N_D}\right)^{-1} \boldsymbol{G}_k \boldsymbol{A}_{IN} \boldsymbol{H}_k \boldsymbol{q}_k \tag{5.24a}$$

$$\text{s.t. } \|\boldsymbol{q}_k\| = 1 \tag{5.24b}$$

where the optimization variable appears also in P_t which depends on all beamforming vectors. The following proposition provides the solution to (5.24).

Proposition 5.9. For all $k = 1, \ldots, K$, the BF vector $\boldsymbol{q}_k^*$ that solves Problem (5.24) is the dominant eigenvector of the matrix $\boldsymbol{H}_k^H \boldsymbol{H}_k$.

The proof can be found in [190] and exploits the structure of $\boldsymbol{A}_{IN}$. From Proposition (5.9) we have that the optimal beamforming vectors are not coupled with each other and do not depend on the users'

transmit powers. Thus, we can incorporate beamforming design into Algorithm 20 by setting $\boldsymbol{q}_k = \boldsymbol{q}_k^*$ for all $k = 1, \ldots, K$, after relay design.

5.2.3 Numerical illustrations

In this section we present numerical results to assess the performance of the developed competitive and cooperative algorithms. We start with Algorithm 20, compared with its cooperative counterpart Algorithm 14. For all $k = 1, \ldots, K$, the channel matrices have been generated as $\boldsymbol{H}_k = \mathrm{PL}_{k,t}\widetilde{\boldsymbol{H}}_k$ and $\boldsymbol{G}_k = \mathrm{PL}_{k,r}\widetilde{\boldsymbol{G}}_k$, with $\mathrm{PL}_{k,t}$ and $\mathrm{PL}_{k,r}$ the path losses of the k-th transmitter-relay link, and of the k-th relay-receiver link, respectively, and with $\widetilde{\boldsymbol{H}}_k$ and $\widetilde{\boldsymbol{G}}_k$ realizations of zero-mean Gaussian random matrices whose entries have unit-variance. As for the path-losses, following [62] they have been modeled as $\mathrm{PL}_{k,t} = \mathrm{PL}_0 \left(\frac{d_{k,t}}{d_0}\right)^4$ and $\mathrm{PL}_{k,r} = \mathrm{PL}_0 \left(\frac{d_{k,r}}{d_0}\right)^4$, respectively, where PL_0 is the free-space attenuation at the reference distance $d_0 = 100\,\mathrm{m}$ with a carrier frequency of 1800 MHz, while $d_{k,t}$ and $d_{k,r}$ are the distances between the k-th transmitter and the relay and between the relay and the k-th receiver, which have been randomly generated between 100 m and 500 m. The users' maximum transmit powers and circuit powers have been set to $P_{max,k} = 0\,\mathrm{dBW}$, $P_{c,k} = 10\,\mathrm{dBm}$, and $\mu_k = 1$ for all $k = 1, \ldots, K$, while the available relay power is $P_r = 10\,\mathrm{dBW}$. It has been assumed $\sigma_D^2 = \sigma_R^2 = \sigma^2 = F\mathcal{N}_0 W$, with $W = 180\,\mathrm{kHz}$ being the communication bandwidth, $F = 3\,\mathrm{dB}$ the receiver noise figure and $\mathcal{N}_0 = -174\,\mathrm{dBm/Hz}$ the receive power spectral density, which are typical values of LTE networks [8]. The presented results have been obtained upon averaging over 10^4 independent system scenarios and initialization points.

In Fig. 5.1, single-antenna transmitters have been considered, whereas $N_D = 2$ and $N_R = 16$, with the number of active transmit-receive pairs K ranging from 1 to 10. With these parameters, it is possible to achieve perfect interference neutralization for $K \leq 8$. The GEE achieved in the following scenarios is reported:

- competitive resource allocation with relay interference neutralization, namely Algorithm 20.

- competitive power control with LMMSE reception, but without relay interference neutralization. The AF matrix is set as the discrete Fourier Transform (DFT) matrix of order N_R scaled to meet the relay power constraint, as proposed in [145].
- competitive power control with matched filter reception and without interference neutralization, namely Algorithm 18 with scaled DFT relay matrix of order N_R.
- cooperative resource allocation with relay interference neutralization, namely Algorithm 14.

The results indicate that the proposed interference neutralization scheme is able to grant significant performance gains over other schemes. Moreover, the competitive Algorithm 20 exhibits virtually the same performance as the cooperative Algorithm 14 when perfect interference neutralization can be achieved, while it suffers a limited gap when interference neutralization is no longer possible. This can be explained observing that suppressing spatial multi-user interference reduces the coupling among the users and reducing the coupling in a non-cooperative scenario tends to close the performance gap between competitive and cooperative approaches. This is also confirmed by the fact that a non-negligible gap emerges when perfect interference neutralization is not achieved.

In Fig. 5.2, we consider multiple antennas at the transmitters, too, setting $N_T = 2$. For the rest, the system parameters and illustrated algorithms are the same as in Fig. 5.1 and similar remarks as for Fig. 5.1 hold. In addition, an interesting observation is that unlike the single-antenna case, a small gap between Algorithm 20 and 14 appears also at the boundary of the interference neutralization region, for $K = 8$ users. This can be explained noticing that, although the number of interferers that can be neutralized is the same, the number of interfering streams has doubled since $N_T = 2$. Thus, interference neutralization is still achievable for $K \leq 8$, but more power is required to suppress all interfering streams, which reduces the power that can be given to the intended channels, and in turn degrades a little the performance of the competitive Algorithm 20.

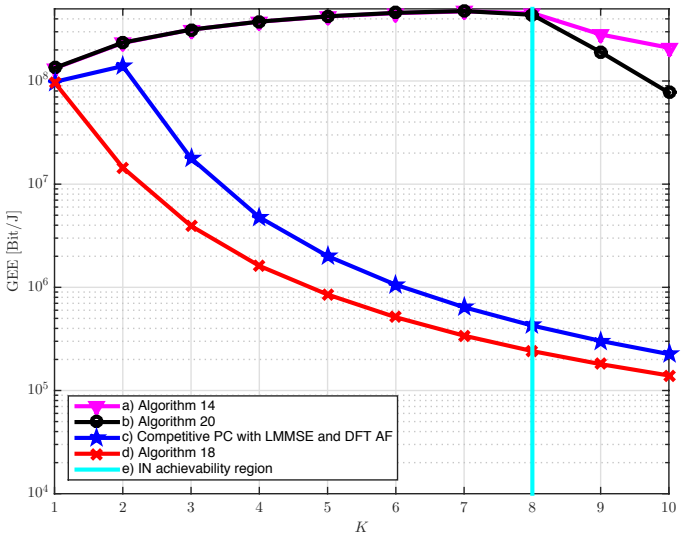

Figure 5.1: $N_T = 1$, $N_R = 16$, $N_D = 2$; GEE for: a) Algorithm 14; b) Algorithm 20; c) Competitive power control with LMMSE reception and DFT relay matrix; d) Algorithm 18; e) Interference neutralization is perfectly achieved for $K \leq 8$.

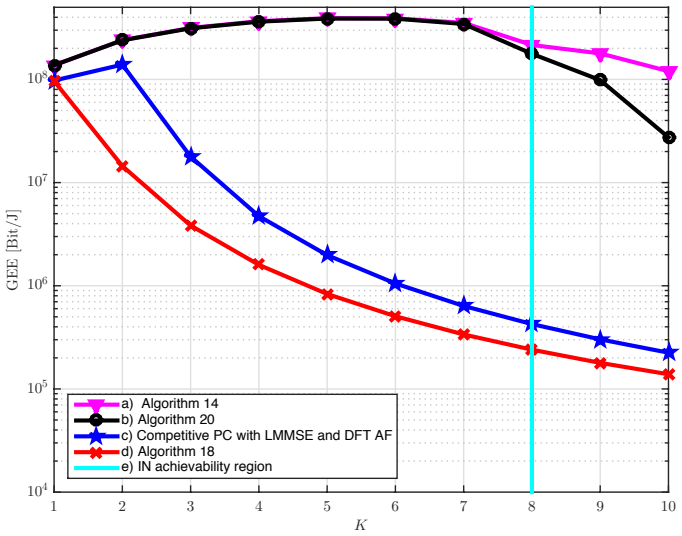

Figure 5.2: $N_T = 2$, $N_R = 16$, $N_D = 2$; GEE for: a) Algorithm 14; b) Algorithm 20; c) Competitive power control with LMMSE reception and DFT relay matrix; d) Algorithm 18; e) Interference neutralization is perfectly achieved for $K \leq 8$.

Next, we analyze the impact of QoS constraints on the energy-efficient resource allocation problems. We consider a single-cell massive MIMO system, with $K = 5$ users and a hardware-impaired base station where $M = 50$ antennas are deployed. The hardware impairment factor is set to $\tau = 10^{-2}$ and the users are randomly placed in a square of edge 1000 m with a minimum distance of 50 m from the base station. For all k, $P_{max,k} = \overline{P}$ and $p_{c,k} = 10\,\text{dBm}$. The receive noise power is $\sigma^2 = FB\mathcal{N}_0$, with $F = 3\,\text{dB}$ and $\mathcal{N}_0 = -174\,\text{dBW/Hz}$. The communication bandwidth is set to $W = 1\,\text{MHz}$. All channels are generated according to the Rayleigh fading model with path-loss model as in [36]. The minimum rate constraint $R_{min,k}$ is set as a percentage R_k of the maximum rate that user k can achieve when $p_k \to \infty$, while the other users' powers are finite, namely $\lim_{p_k \to \infty} \log_2(1 + \gamma_k) = \log_2\left(1 + \frac{\alpha_k}{\phi_k}\right)$. For simplicity, we assume $R_1 = R_2 = \ldots = R_K = R$.

Fig. 5.3 analyzes the feasibility probability P_f of the GEE maximization problem as a function of $\overline{P}$, for different values of R. The results are obtained by averaging over $5 \cdot 10^4$ independent scenarios of users' drops and channel coefficients.

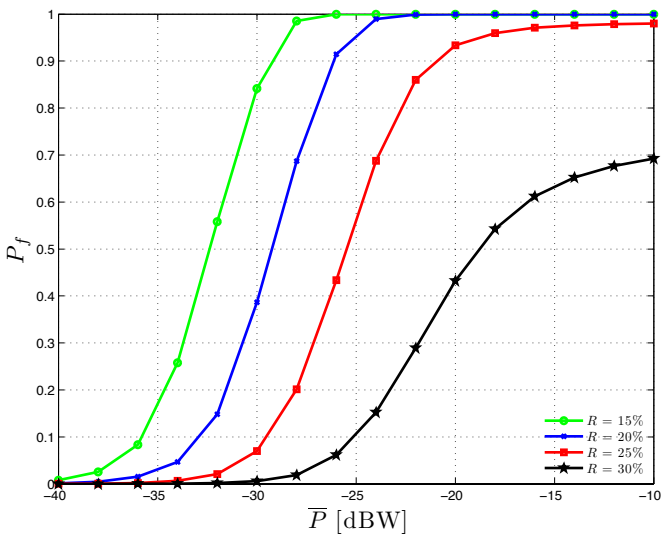

Figure 5.3: $K = 5; M = 50; \tau = 10^{-2}$. P_f versus $\overline{P}$ with minimum per-user rate constraints: (a) $R = 15\%$; (b) $R = 20\%$; (c) $R = 25\%$; (d) $R = 30\%$.

We can see that P_f approaches 1 for realistic values of $\overline{P}$ up to $R = 25\%$, whereas for $R = 30\%$ the typical transmit power levels which are used in the uplink of present cellular systems are not enough to ensure a high P_f.

Next, we analyze the energy-efficient performance of the cooperative Algorithm 8 with QoS constraints. Fig. 5.4 compares the achieved GEE by the following schemes:

- (a) Algorithm 8 with $R = 20\%$;
- (b) Algorithm 8 without QoS constraints, i.e. $R = 0\%$;
- (c) Sum-rate maximization[3];
- (d) Maximum power allocation, i.e. $p_k = \overline{P}$ for all k, considered as a baseline scheme.

In scheme (a), if the problem turns out to be unfeasible, the QoS constraint is relaxed and the solution from scheme (b) is taken. For low values of $\overline{P}$, this circumstance is frequent, and indeed schemes (a) and (b) perform similarly. At the same time, schemes (b) and (c) also perform similarly for low $\overline{P}$, thus suggesting that in this range of $\overline{P}$, GEE and sum-rate maximization are equivalent. Instead, different performance are achieved for larger values of $\overline{P}$. Indeed, increasing $\overline{P}$ eventually allows attaining the peak of the GEE. At this point, the GEE achieved by scheme (b) remains constant, as using the excess transmit power would only decrease the GEE, while the GEE achieved by scheme (c) decreases, because this scheme makes use of the excess transmit power to maximize the sum-rate. Instead, scheme (a) strikes a balance between these two extremes. Some of the excess power is used to fulfill the QoS constraints, which slightly decreases the GEE, but once the constraints are met, the transmit power is not further increased and the achieved GEE keeps constant. We remark that this slight reduction of the GEE grants a higher minimum rate. In particular, in the saturation region of the GEE, the average minimum rate granted by scheme

[3]Algorithm 8 can be straightforwardly specialized to maximize the sum-rate instead, of the GEE.

(b) is 1.594 bit/s/Hz/user, whereas it increases to 2.358 bit/s/Hz/user when scheme (a) is used.

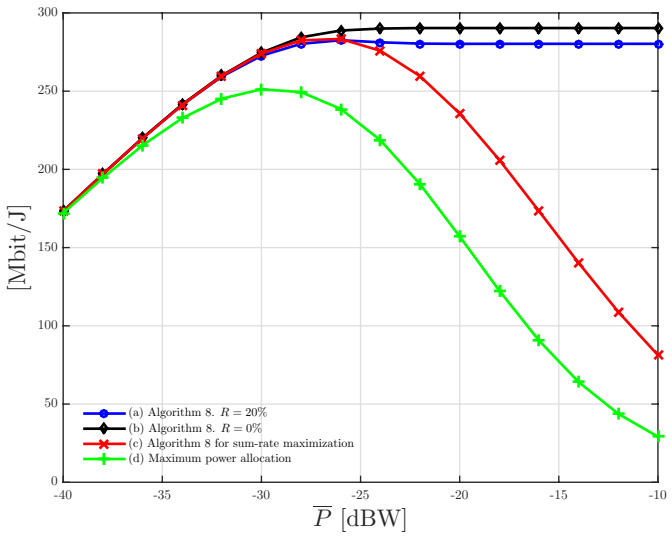

Figure 5.4: $K = 5; M = 50; \tau = 10^{-2}$. Average achieved GEE versus $\overline{P}$ for: (a) Algorithm 8 for GEE maximization with $R = 20\%$; (b) Algorithm 8 for GEE maximization with $R = 0\%$; (c) sum-rate maximization; (d) Maximum transmit power allocation.

Fig. 5.5 compares the GEE performance of the centralized Algorithm 8 and of its distributed counterpart Algorithm 19 for $R = 0\%$ and $R = 20\%$. Again, in case the QoS constraints make the problem unfeasible, they are relaxed and the solution for $R = 0\%$ is taken. The results show that, while the centralized scheme suffers a little performance gap in terms of GEE when QoS constraints are introduced, having minimum rate requirements causes a larger GEE degradation in the distributed scenario, especially for increasing $\overline{P}$. This is expected because the distributed scheme does not jointly manage the interference as the centralized one does, which results in high multi-user interference, especially for large $\overline{P}$.

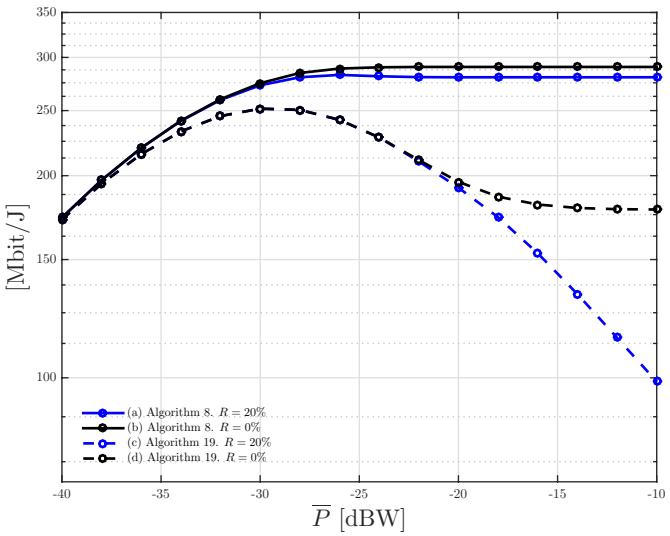

Figure 5.5: $K = 5; M = 50; \tau = 10^{-2}$. Average achieved GEE versus $\overline{P}$ for: (a) Algorithm 8 for GEE maximization with $R = 20\%$; (b) Algorithm 8 for GEE maximization with $R = 0\%$; (c) Algorithm 19 for distributed resource allocation with $R = 20\%$; (d) Algorithm 19 for distributed resource allocation with $R = 0\%$.

Finally, Table 5.1 shows the average number of iterations required by Algorithms 8 and 19 to converge, with $R = 0\%$ and $R = 20\%$, respectively, for $\epsilon = 10^{-3}$. It is seen that both algorithms converge after a small number of iterations, which slightly increases for larger $\overline{P}$. This is expected since increasing $\overline{P}$ results in a larger feasible set.

Table 5.1: $K = 5; M = 50; \tau = 10^{-2}$. Average number of required iterations to reach convergence versus P_{max} for: (a) Algorithm 8 for GEE maximization with $R = 20\%$; (b) Algorithm 8 for GEE maximization with $R = 0\%$; (c) Algorithm 19 for distributed resource allocation with $R = 20\%$; (d) Algorithm 19 for distributed resource allocation with $R = 0\%$.

[dBW]	$\overline{P} = -34$	$\overline{P} = -26$	$\overline{P} = -18$	$\overline{P} = -10$
Algorithm 8. $R = 0\%$	3.69	6.30	6.49	6.51
Algorithm 8. $R = 20\%$	3.67	6.68	6.76	6.77
Algorithm 19. $R = 0\%$	1.01	1.42	3.66	4.50
Algorithm 19. $R = 20\%$	1.01	1.42	3.67	6.71

5.3 Resource allocation in multi-carrier wireless networks

In this section, we extend the competitive power control algorithms analyzed in Section 5.1 to MC, OFDMA-based systems, in which joint subcarrier and transmit power allocation is to be performed. In this context, the energy efficiency of each user is given by

$$\mathrm{EE}_k = \frac{W \sum_{n=1}^{N} f\left(\gamma_k^{[n]}(p_k^{[n]}, \boldsymbol{p}_{-k}^{[n]})\right)}{\mu \sum_{n=1}^{N} p_k^{[n]} + P_{c,k}}\,, \tag{5.25}$$

wherein $\gamma_k^{[n]}$ is the SINR enjoyed by user k on subcarrier n, which depends on the power $p_k^{[n]}$ that user k transmits on subcarrier n, but also on the powers that the other users are transmitting on the same subcarrier, as denoted by the vector $\boldsymbol{p}_{-k}^{[n]}$.

From a game-theoretic perspective, the competitive power and subcarrier allocation problem is formulated as the non-cooperative game in normal form, in which each user k selects the set $\mathcal{N}_k$ of subcarriers to employ, and the transmit power level on each subcarrier, so as to maximize (5.25). Unfortunately, as it happens for MIMO systems when precoding design is included in the resource allocation game, also in this scenario, the inclusion of subcarrier allocation causes the non-cooperative game to have a BRD which is not guaranteed to always converge, even when the SINR $\gamma_k^{[n]}$ is linear in the useful power $p_k^{[n]}$. Moreover, in some scenarios, the players are not allowed to use all the available subcarriers, which means that the cardinality of $\mathcal{N}_k$ is constrained to be strictly less than N. In this case, the BR problems are in general mixed-integer problems and not even the existence of an NE can be guaranteed [13]. In order to simplify the problem, we consider the case in which the players are allowed to select any subset $\mathcal{N}_k$ of the subcarrier set. Then, subcarrier selection is automatically performed by power allocation, by allocating zero power to the subcarriers that a given user does not wish to use. However, also this case is quite challenging. The existence of an NE is only guaranteed if the efficiency function f is concave, as this results in a PC utility function. Instead, if $f(\gamma)$ is not concave, but for example S-shaped, the utility function will not be PC in general, since the sum of S-shaped functions need

not be S-shaped. Moreover, in both cases, the convergence of the BRD and the uniqueness of the NE can not be guaranteed [122, 12], thus preventing us form developing best-response-based resource allocation algorithms. One approach is to modify the players utility functions so as to guarantee the convergence of the BRD for any realization of the system parameters [182, 30]. An alternative approach is to derive conditions on the system parameters such that the non-cooperative game admits a convergent BRD. This is done in [122] for the SINR expression (4.1), in [12] always assuming the SINR is expressed as in (4.1), but considering QoS rate constraints, too, and in [192], considering the SINR expression (4.2) and accounting for QoS rate constraints. In the following, we will describe in more detail this last scenario.

5.3.1 MC interference network with QoS constraints.

Consider the uplink of a MC multi-cell network with K transmitters, L receivers, and N available subcarriers and assume that the users SINRs are expressed as in (4.2). Assuming that each user requires a minimum achievable rate of $R_{min,k}$, the energy-efficient competitive resource allocation problem leads to the BRD

$$\max_{\{p_k^{[n]}\geq 0\}_{n=1}^N} \mathrm{EE}_k \ , \forall\ k=1,\ldots,K \tag{5.26a}$$

$$\text{s.t.} \sum_{n=1}^{N} p_k^{[n]} \leq P_{max,k} \ , \forall\ k=1,\ldots,K \tag{5.26b}$$

$$\sum_{n=1}^{N} \log_2(1+\gamma_k^{[n]}(p_k^{[n]}, \boldsymbol{p}_{-k}^{[n]})) \geq R_{min,k} \ , \forall\ k=1,\ldots,K \tag{5.26c}$$

with EE_k given by (5.25) and $f(\gamma)=\log_2(1+\gamma)$.

The presence of multiple sub-carriers does not pose new significant challenges as far as solving the individual BR-problems is concerned. Indeed, we see that (5.26a) is PC in $\{p_k^{[n]}\}_{n=1}^N$, while the constraints are convex. So, the individual BR-problem can still be solved by means of fractional programming theory. However, as in the single-carrier case, the presence of the QoS constraints turns the game into a generalized non-cooperative game, and the strategy set of the generic player k can

be written as

$$\mathcal{S}_k(\boldsymbol{p}_{-k}) = \Big\{ \{p_k^{[n]}\}_{n=1}^N \ : \ p_k^{[n]} \geq 0 \ \forall \ n \ , \sum_{n=1}^N p_k^{[n]} \leq P_{max,k} \ , \\ \sum_{n=1}^N \log_2(1+\gamma_k^{[n]}(p_k^{[n]}, \boldsymbol{p}_{-k}^{[n]})) \geq R_{min,k} \Big\} \ , \tag{5.27}$$

with $\boldsymbol{p}_{-k} = \{\boldsymbol{p}_{-k}^{[n]}\}_{n=1}^N$. In the multi-carrier scenario, the analysis of this generalized non-cooperative game is much more involved than in the single-carrier setting. Nevertheless, it is possible to come up with sufficient conditions which ensure the uniqueness of a GNE and the convergence of the BRD. The resulting expressions are rather involved and their derivation is not related to fractional programming, but is instead based on the theory of block-norm contractions. For this reason we do not report here the resulting conditions, referring to [192] for the details.

Finally, in those scenarios for which the BRD is guaranteed to converge, a competitive resource allocation algorithm can be developed similarly to Algorithm 18, performing a distributed implementation of the BRD in (5.26).

5.3.2 Numerical illustrations

In our numerical results we consider the uplink of a 3-cell OFDMA network with $N = 16$ available subcarriers, equally spaced by $\Delta f = 180\,\text{kHz}$, in which $K = 3$ cell-edge single-antenna users, communicate with their associated base stations, each equipped with $M = 3$ antennas, via a single-antenna AF relay. The mobile users are placed at a distance from the relay randomly generated in the interval $[100; 300]\,\text{m}$ and the propagation channels are subject to path-loss and fast-fading.

We have compared the performance of the competitive approach described in the previous section, to the cooperative approach which maximizes the GEE subject to QoS constraints. Specifically, the cooperative approach has been developed in a similar way as Algorithm 16, replacing the WMEE with the GEE as objective to maximize [192]. Fig. 5.6 shows the achieved GEE versus $\overline{P}$ for the following resource allocation algorithms:

- (a) Centralized GEE maximization with $R = 20\%$ and $R = 0\%$;
- (b) Competitive resource allocation with $R = 20\%$ and $R = 0\%$;
- (c) Cooperative sum-rate maximization.

If the problems with QoS constraints are unfeasible, we take the solution of the corresponding scheme with $R = 0\%$. As in the single-carrier scenario, introducing QoS constraints enables to trade-off a slight reduction in GEE with a significant increase of the users' minimum rate, which increases from 3.8194 bit/s/Hz/user when $R = 0\%$, to 7.1683 bit/s/Hz/user when $R = 20\%$. Moreover, the gap suffered by the distributed scheme is smaller than in the single-carrier setting. This is due to both the beneficial effect of the MC transmission format and CoMP reception, and to the lower number of players, $K = 3$, than in the single-carrier case, where $K = 5$. Having a larger number of players in a non-cooperative game is known to result in a larger gap to cooperative settings [102].

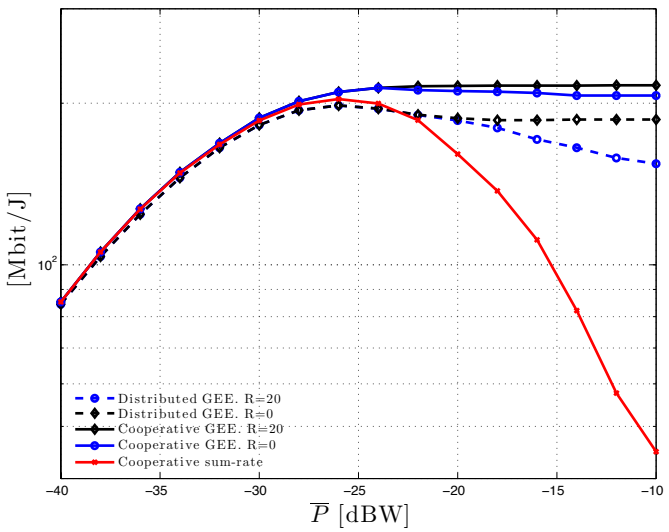

Figure 5.6: $K = 3; N = 16$. Average GEE versus $\overline{P}$ for: (a) Distributed resource allocation. $R = 20\%$; (b) Distributed resource allocation. $R = 0\%$; (c) GEE maximization. $R = 20\%$; (d) GEE maximization. $R = 0\%$; (e) sum-rate maximization.

5.4 Summary

In this chapter we have presented competitive algorithms for resource allocation in wireless interference networks. The problem has been formulated as a non-cooperative game in normal form with the transmitters as players trying to maximize their individual energy efficiencies by allocating their own resources. At first, several competitive power control games have been analyzed, for increasingly general SINR expressions, using a game-theoretic approach. Fractional programming and generalized concavity have proved useful in this context, too. Exploiting the results in Chapters 2 and 3 has allowed us to solve the players' BR problems and to establish the existence of an NE for the considered games. Moreover, exploiting also the framework of standard functions we have shown that a unique NE exists for the considered power control games and that their BRD is guaranteed to converge to such unique NE. Leveraging these results, we have designed competitive BR-based power allocation algorithms, which are guaranteed to converge to a unique equilibrium, have low-complexity, and require low overhead, thereby lending themselves to practical implementation in self-organizing networks.

The resource allocation problem becomes more involved when precoders in MIMO systems, and subcarriers in OFDMA systems, are also to be allocated. In these scenarios, convergence of the BRD can no longer be ensured, thus preventing to come up with BR-based resource allocation algorithms. Typical approaches to deal with this issue include deriving conditions on the system parameters such that the non-cooperative game admits a unique NE and its BRD converges, using interference neutralization techniques so as to reduce the coupling among the players' utility functions and obtain a convergent BRD, or modifying the game formulation by a suitable design of the players' utilities so as to guarantee the convergence of the BRD. Examples for these approaches have been mentioned, describing in detail the interference neutralization technique and the derivation of sufficient convergence conditions for the BRD in one-hop and two-hop MIMO and MC interference networks, also considering QoS constraints.

6

Extensions and future lines of research

In this monograph we have developed a unified framework to tackle different classes of fractional problems, and we have presented many applications to energy efficiency maximization in wireless networks. The purpose of this chapter is to show how the considered framework can be extended in several directions, mentioning some of the main lines of research and open problems to be addressed in the area of energy efficiency.

6.1 Global optimality in energy efficiency problems

As we have seen, in the relevant scenario of interference-limited networks, finding the global optimum of the network energy efficiency with affordable computational complexity is an open problem. All available, practical algorithms apply sub-optimal methods with different trade-offs between optimality and complexity. The framework we have described is no exception, guaranteeing the convergence to a local optimum by solving a sequence of convex problems, but without any claim on global optimality.

However, while the goal of globally solving network energy effi-

ciency maximization problems with limited complexity still appears ambitious, we have described in Section 3.5 how monotonic optimization can be used together with fractional programming to globally solve a wider class of fractional problems than CCFPs and MMFPs. Although the complexity of this approach is still too large for practical applications, it provides an efficient way to test the performance of low-complexity, suboptimal algorithms. While monotonic optimization in wireless networks has been previously applied to rate maximization problems [92, 168, 26, 106], its use for energy efficiency maximization is still an almost unexplored research area. The main difference when using monotonic optimization for GEE maximization is that the GEE is not a monotone function in the transmit powers. Preliminary results to overcome this difficulty and apply the framework of Section 3.5 are provided in [117], for GEE maximization problems. Consider for example the cooperative power control problem (4.22) with a per-transmitter power constraint. Applying Dinkelbach's algorithm, in each iteration, for a given $\lambda \geq 0$ we have to solve the auxiliary problem

$$\max_{\{p_k \geq 0\}_{k=1}^K} \sum_{k=1}^{K} \left[\log_2 \left(z_k + \sum_{j=1}^{K} \beta_{j,a_k} p_j \right) - \left(\log_2 \left(z_k + \sum_{j \neq k} \beta_{j,a_k} p_j \right) + \lambda(\mu_k p_k + P_{c,k}) \right) \right] \tag{6.1a}$$

$$\text{s.t. } p_k \leq P_{max,k} \ , \forall \ k = 1, \ldots, K \ . \tag{6.1b}$$

Since (6.1a) is the difference of concave functions, (6.1) is not a convex problem. However, observing that (6.1a) is the difference of monotone functions of $\{p_k\}_{k=1}^K$, we can apply the method outlined in Section 3.5 with

$$f_1(\boldsymbol{p}) = \sum_{k=1}^{K} \log_2 \left(z_k + \sum_{j=1}^{K} \beta_{j,a_k} p_j \right), f_2(\boldsymbol{p}) = \sum_{k=1}^{K} \log_2 \left(z_k + \sum_{j \neq k} \beta_{j,a_k} p_j \right) \tag{6.2}$$

$$g(\boldsymbol{p}) = \lambda \left(\sum_{k=1}^{K} \mu_k p_k + P_{c,k} \right) \tag{6.3}$$

$$\mathcal{N} = [0; P_{max,1}] \times \ldots, \times [0; P_{max,K}] \ , \ \mathcal{C} = \mathbb{R}^K \ . \tag{6.4}$$

Many more scenarios and applications remain to be investigated considering this approach, such as the maximization of different energy-efficient metrics, more involved SINR expressions and power constraints, scenarios with QoS constraints.

6.2 Resource allocation with imperfect CSI

Most of the examples that we have presented in Chapters 4 and 5 have considered the case in which perfect CSI is available to the network nodes. However, It is anticipated that future cellular networks will have to serve such a large number of connected devices, that it will be impossible to have global CSI knowledge. This issue becomes even more compelling in MC or multiple-antenna networks, where each user has a vector or matrix channel. Accordingly, a well-motivated research direction is to address energy efficiency maximization problems assuming that only imperfect CSI is available, either in the form of statistical CSI, or in the form of a rough channel estimate, subject to a non-negligible estimation error.

Also in these scenarios, fractional programming appears as an essential tool to solve the resulting optimization problems. Indeed, a scenario in which fractional programming can be successfully applied to perform energy-efficient resource allocation based only on statistical CSI, was analyzed in Section 4.2, when dealing with energy efficiency optimization in the two-hop P2P MIMO system. Instead, if partial CSI is available, considering the two-hop P2P MIMO system as an example, we model the channels as

$$\boldsymbol{H} = \widehat{\boldsymbol{H}} + \boldsymbol{\Delta}_H \ , \ \boldsymbol{G} = \widehat{\boldsymbol{G}} + \boldsymbol{\Delta}_G \ , \tag{6.5}$$

with $\widehat{\boldsymbol{H}}$ and $\widehat{\boldsymbol{G}}$ the channel estimates, while $\boldsymbol{\Delta}_H$ and $\boldsymbol{\Delta}_G$ are the estimation errors. Two main approaches can be individuated to deal with the error terms $\boldsymbol{\Delta}_H$ and $\boldsymbol{\Delta}_G$. The first approach is to perform a worst-case resource allocation, in which the estimation errors are constrained such that $\|\boldsymbol{\Delta}_H\| \leq \epsilon_H$ and $\|\boldsymbol{\Delta}_G\| \leq \epsilon_G$. Then, the worst-case GEE

maximization problem can be formulated as the fractional problem

$$\max_{\boldsymbol{P}\succeq\mathbf{0},\boldsymbol{A}} \min_{\boldsymbol{\Delta}_G,\boldsymbol{\Delta}_H} \frac{\log_2 \frac{\left|\sigma_D^2\boldsymbol{I}_{N_D}+\boldsymbol{A}^H\boldsymbol{G}^H\boldsymbol{G}\boldsymbol{A}\left(\sigma_R^2\boldsymbol{I}_{N_R}+\boldsymbol{H}\boldsymbol{P}\boldsymbol{H}^H\right)\right|}{\left|\sigma_D^2\boldsymbol{I}_{N_D}+\sigma_R^2\boldsymbol{G}\boldsymbol{A}\boldsymbol{A}^H\boldsymbol{G}^H\right|}}{\mu_S\mathrm{tr}(\boldsymbol{P})+\mu_R\mathrm{tr}(\boldsymbol{A}(\boldsymbol{H}\boldsymbol{P}\boldsymbol{H}^H+\sigma_R^2\boldsymbol{I}_{N_R})\boldsymbol{A}^H)+P_c} \tag{6.6a}$$

$$\text{s.t. } \mathrm{tr}(\boldsymbol{P})\leq P_S^{max}\ ,\mathrm{tr}(\boldsymbol{A}(\boldsymbol{H}\boldsymbol{P}\boldsymbol{H}^H+\sigma_R^2\boldsymbol{I}_{N_R})\boldsymbol{A}^H)\leq P_R^{max} \tag{6.6b}$$

$$\|\boldsymbol{\Delta}_H\|\leq\epsilon_H\ ,\|\boldsymbol{\Delta}_G\|\leq\epsilon_G\ . \tag{6.6c}$$

Instead, a different approach is to assume a distribution for the error terms $\boldsymbol{\Delta}_H$ and $\boldsymbol{\Delta}_G$, thus optimizing the statistical average of the GEE. In both cases, the optimization appears challenging and remains an open problem.

6.3 Energy efficiency in networks with stochastic topologies

In this monograph, we have focused on energy-efficient resource allocation in wireless networks with finite dimensions, where the word dimensions refers to the number of connected nodes and deployed antennas.

However, the next generation of wireless cellular networks will have to cope with an unprecedented number of connected devices, so that a natural approach is to increase the amount of deployed resources, in terms of infrastructure nodes and/or of equipped antennas. This trend is rapidly causing present networks to evolve into *dense* networks, where the word dense does not simply mean that more nodes and antennas are present, but, more importantly, that the nodes location, as well as the SINR they experience, become impossible to compute deterministically and should rather be modeled as random variables. As an immediate consequence, the approach which deterministically defines the energy efficiency of a link as the benefit/cost ratio in terms of achieved throughput and consumed power, does not apply anymore, because the interference levels suffered by the network nodes become also random variables which depend on the random behavior of the network. In such a scenario, in order to define the energy-efficient benefit-cost ratio of

the network, it is necessary to develop new models which are able to statistically characterize the interference in the network.

This requires the use of mathematical tools like RMT [47, 165] and SG [11, 175]. SG models the locations of the network nodes as random variables which follow specific spatial distributions. Among the different distributions, the most widely used is the Poisson-Point-Process (PPP), which has been shown to strike the best compromise between mathematical tractability, and faithful modeling of real-world systems. Given a spatial distribution, SG provides the framework to statistically characterize the interference levels.

On the other hand, RMT analyses large networks performing a limiting analysis, which provides asymptotic expressions of the users SINRs, wherein the randomness of the network is averaged out. Indeed, the asymptotic expressions are sometimes referred to as *deterministic equivalents*.

Based on these statistical characterizations, it is possible to define the energy efficiency of a network with random topology, as the average or asymptotic benefit-cost ratio, which should then be optimized by fractional programming theory. Therefore, energy efficiency optimization in networks with random topologies involves an interplay of different mathematical tools to be combined with fractional programming. However, the tools and techniques developed in this monograph remain an essential component of the resource allocation process, as they provide the theoretical basis to optimize the resulting average or asymptotic energy efficiency.

Appendices

A

Fundamentals of linear algebra

Most of the material can be found in [76, 77, 22]. Since this section contributes basic results, the proofs are omitted.

Proposition A.1 (Singular value decomposition)**.** Every non-zero matrix $\boldsymbol{A}$ of dimension $n \times m$ can be decomposed into

$$\boldsymbol{A} = \boldsymbol{V}\boldsymbol{\Sigma}\boldsymbol{W}^H$$

where $\boldsymbol{V}, \boldsymbol{W}$ are unitary square matrices of sizes $n \times n$ and $m \times m$ and $\boldsymbol{\Sigma}$ is an $n \times m$ pseudo-diagonal matrix with nonnegative main diagonal entries, and the same rank as $\boldsymbol{A}$.

Proposition A.2 (Eigenvalue decomposition)**.** Let $\boldsymbol{A}$ be a square matrix of dimension n. Then $\boldsymbol{A}$ is Hermitian if and only if there is a square unitary matrix $\boldsymbol{U}$ of size n and a real diagonal matrix $\boldsymbol{\Lambda}$ of size $n \times n$ such that

$$\boldsymbol{A} = \boldsymbol{U}\boldsymbol{\Lambda}\boldsymbol{U}^H.$$

Lemma A.1 (Matrix inversion lemma)**.** Suppose $\boldsymbol{A}, \boldsymbol{B}$ are square and invertible matrices. It holds

$$\left(\boldsymbol{A} + \boldsymbol{X}\boldsymbol{B}\boldsymbol{X}^H\right)^{-1} = \boldsymbol{A}^{-1} - \boldsymbol{A}^{-1}\boldsymbol{X}\left[\boldsymbol{B}^{-1} + \boldsymbol{X}^H\boldsymbol{A}^{-1}\boldsymbol{X}\right]^{-1}\boldsymbol{X}^H\boldsymbol{A}^{-1} \quad \text{(A.1)}$$

Lemma A.2 (Trace and determinant relations.)**.** Let $\boldsymbol{A} \in \mathbb{C}^{n\times m}$ and $\boldsymbol{B} \in \mathbb{C}^{m\times n}$, then the following equalities hold:

$$\mathrm{tr}(\boldsymbol{AB}) = \mathrm{tr}(\boldsymbol{BA}) \tag{A.2}$$

$$|\boldsymbol{I}_n + \boldsymbol{AB}| = |\boldsymbol{I}_m + \boldsymbol{BA}| \tag{A.3}$$

Moreover, when $\boldsymbol{A}$ and $\boldsymbol{B}$ are two Hermitian, $n \times n$, positive semi-definite matrices, with eigenvalues $\{\lambda_i(\boldsymbol{A})\}_{i=1}^n$ and $\{\lambda_i(\boldsymbol{B})\}_{i=1}^n$, arranged in decreasing order, it holds

$$\sum_{i=1}^{n} \lambda_i(\boldsymbol{A})\lambda_{n-i+1}(\boldsymbol{B}) \leq \mathrm{tr}(\boldsymbol{AB}) \leq \sum_{i=1}^{n} \lambda_i(\boldsymbol{A})\lambda_i(\boldsymbol{B}) \tag{A.4}$$

$$\prod_{i=1}^{n} (\lambda_i(\boldsymbol{A}) + \lambda_i(\boldsymbol{B})) \leq |\boldsymbol{A} + \boldsymbol{B}| \leq \prod_{i=1}^{n} (\lambda_i(\boldsymbol{A}) + \lambda_{n-i+1}(\boldsymbol{B})) \tag{A.5}$$

The above eigenvalue inequalities can be extended to the case of generic complex matrices, upon replacing eigenvalues with singular values.

Definition A.1 (Kronecker product)**.** Let $\boldsymbol{A} \in \mathbb{C}^{n\times m}$ and $\boldsymbol{B} \in \mathbb{C}^{p\times q}$. The Kronecker product between $\boldsymbol{A}$ and $\boldsymbol{B}$ is defined as the $np \times mq$ matrix $\boldsymbol{C} = \boldsymbol{A} \otimes \boldsymbol{B}$, with generic (i, j) element given by

$$\boldsymbol{C}_{i,j} = a_{i,j}\boldsymbol{B} \ , \tag{A.6}$$

with $i = 1, \ldots, n$ and $j = 1, \ldots, m$.

Lemma A.3. If $\boldsymbol{A}$ and $\boldsymbol{B}$ are square matrices of order n and p, respectively, and with eigenvalues $\lambda_i(\boldsymbol{A})$ and $\mu_j(\boldsymbol{B})$, with $i = 1, \ldots, n$ and $j = 1, \ldots, p$, then the eigenvalues of $\boldsymbol{A} \otimes \boldsymbol{B}$ are

$$\lambda_i(\boldsymbol{A})\mu_j(\boldsymbol{B}) \ , \forall i = 1, \ldots, n \ , \ j = 1, \ldots, p \ . \tag{A.7}$$

From the above lemma, the following relations follow:

$$\mathrm{tr}(\boldsymbol{A} \otimes \boldsymbol{B}) = \mathrm{tr}(\boldsymbol{A})\mathrm{tr}(\boldsymbol{B}) \tag{A.8}$$

$$|\boldsymbol{A} \otimes \boldsymbol{B}| = |\boldsymbol{A}|^p \, |\boldsymbol{A}|^n \tag{A.9}$$

$$\mathrm{rank}(\boldsymbol{A} \otimes \boldsymbol{B}) = \mathrm{rank}(\boldsymbol{A})\mathrm{rank}(\boldsymbol{B}) \tag{A.10}$$

$$(\boldsymbol{A} \otimes \boldsymbol{B})^{-1} = \boldsymbol{A}^{-1} \otimes \boldsymbol{B}^{-1} \ , \text{if } \boldsymbol{A} \text{ and } \boldsymbol{B} \text{ are invertible} \tag{A.11}$$

The Kronecker product proves very useful in the solution of matrix equations, thanks to the following identity

$$vec(\boldsymbol{AXB}) = (\boldsymbol{B}^T \otimes \boldsymbol{A})vec(\boldsymbol{X}) \ , \tag{A.12}$$

with $vec(\cdot)$ denoting the vectorization operator which produces a vector by stacking the columns of a matrix one under the other. The identity in (A.12) allows one to solve matrix equations of the form $\boldsymbol{AXB} = \boldsymbol{C}$, by converting them into the linear system of equations

$$(\boldsymbol{B}^T \otimes \boldsymbol{A})vec(\boldsymbol{X}) = vec(\boldsymbol{C}) \ . \tag{A.13}$$

B

Fundamentals of optimization theory

In this appendix, a brief review of convex programming is provided. Furthermore, the main theoretical results of monotonic optimization are provided, together with one solution algorithm, namely the outer polyblock algorithm.

B.1 Convex optimization

The book [28] provides a very good overview on convex optimization. In this section, we review selected results that are either prerequisites for the fractional programming theory developed in Chapter 2, or useful for immediate application. The material is mainly from [28, Chapter 5].

B.1.1 Lagrange dual function

Consider the following optimization problem given in standard form

$$\begin{aligned} p^* = \min f_0(x) \quad \text{s.t.} \quad & f_k(x) \leq 0 \text{ for } k = 1, \ldots, m \\ & \text{and } h_k(x) = 0 \text{ for } k = 1, \ldots, p \end{aligned} \tag{B.1}$$

for $x \in \mathcal{X} \subseteq \mathbb{R}^n$.

Definition B.1 (Lagrangian)**.** The **Lagrangian** $\mathrm{L} : \mathcal{X} \times \mathbb{R}^m \times \mathbb{R}^p \to \mathbb{R}$ for problem (B.1) is

$$L(x, \boldsymbol{\lambda}, \boldsymbol{\nu}) = f_0(x) + \sum_{k=1}^{m} \lambda_k f_k(x) + \sum_{k=1}^{p} \nu_k h_k(x).$$

The **Lagrangian multiplier** λ_i is associated with the i-th inequality constraint, whereas ν_i is associated with the i-th equality constraint. The vectors $\boldsymbol{\lambda}$ and $\boldsymbol{\nu}$ are called the **dual variables** or **Lagrange multiplier vectors** for Problem (B.1).

The **Lagrange dual function** $g : \mathbb{R}^m \times \mathbb{R}^p \to \mathbb{R}$ is the minimum value of the Lagrangian over x

$$g(\boldsymbol{\lambda}, \boldsymbol{\nu}) = \inf_{x \in \mathcal{X}} L(x, \boldsymbol{\lambda}, \boldsymbol{\nu}).$$

Remark B.1. Since the dual function is the pointwise infimum of a famliy of affine functions of $(\boldsymbol{\lambda}, \boldsymbol{\nu})$, it is concave, even if the problem in (B.1) is not convex.

Lemma B.1 (Section 5.1.3 [28])**.** The dual function yields lower bounds on the optimal value of the problem (B.1). For any $\boldsymbol{\lambda} \succeq \mathbf{0}$ and any $\boldsymbol{\nu}$ we have

$$g(\boldsymbol{\lambda}, \boldsymbol{\nu}) \leq p^*.$$

Proof. Suppose $\bar{x}$ is a feasible point for the problem (B.1), i.e. $f_i(\bar{x}) \leq 0$ and $h(\bar{x}) = 0$, and $\boldsymbol{\lambda} \succeq \mathbf{0}$. Obviously

$$\sum_{k=1}^{m} \lambda_k f_k(\bar{x}) + \sum_{k=1}^{p} \nu_k h_k(\bar{x}) \leq 0,$$

since the terms in the first sum are nonpositive and terms in the second sum are all zero. As a result,

$$g(\boldsymbol{\lambda}, \boldsymbol{\nu}) = \inf_{x \in \mathcal{X}} L(x, \boldsymbol{\lambda}, \boldsymbol{\nu}) \leq L(\bar{x}, \boldsymbol{\lambda}, \boldsymbol{\nu}) \leq f_0(\bar{x}).$$

This lower bound holds for all feasible points $\bar{x} \in \mathcal{X}$. □

Remark B.2. In the Lagrangian function, a constraint violation is weighted linearly by its corresponding multiplier. Since the constraints

are to be fulfilled in any way, the first approach would be to define the function outside the feasible range as ∞. This hard punishment of constraint violation is replaced by the linear one in the Lagrangian multiplier L.

Definition B.2 (Langrange dual problem)**.** A natural question regarding the Lagrange dual function is about the best lower bound that can be obtained from the Lagrange dual function

$$d^* = \max g(\boldsymbol{\lambda}, \boldsymbol{\nu}) \qquad \text{s.t.} \quad \boldsymbol{\lambda} \succeq \mathbf{0}. \tag{B.2}$$

This is called the **Langrange dual problem** associated with Problem (B.1).

Remark B.3. The Lagrange dual problem (B.2) is always a convex optimization problem, since the objective to be maximized is concave and the constraint is convex. This is independent of whether the primal problem in (B.1) is convex or not. Furthermore, the optimal value of the dual problem is always smaller than or equal to the value of the primal problem

$$d^* \leq p^*.$$

The difference $p^* - d^*$ is the **optimal duality gap**, and is always non-negative.

B.1.2 Strong duality

Definition B.3 (Strong duality)**. Strong duality** holds if the duality gap $p^* - d^* = 0$. This means that the best bound that can be obtained from the Lagrange dual function is tight.

Remark B.4. Strong duality does not, in general, hold. Even convexity of the primal problem is not sufficient. The conditions under which strong duality holds are called constraint qualifications. One simple constraint qualification is **Slater's condition**: There is an $x \in \mathcal{X}$ s.t. $f_i(x) < 0$ for all $i = 1, ..., m$ and $h_i(x) = 0$ for all $i = 1, ..., p$. Slater's theorem says that strong duality holds, if Slater's condition holds (and the problem is convex).

Consider in the following the optimization problem with only inequality constraints

$$\max f_0(x) \qquad \text{s.t.} \quad f_i(x) \leq 0 \text{ for } i = 1, ..., m.$$

Denote the Lagrangian multiplier for the inequality constraints by λ_k. A connection to max-min problems can be explained by the following representations: Weak duality can be expressed as the inequality

$$\sup_{\boldsymbol{\lambda} \succeq \mathbf{0}} \inf_x L(x, \boldsymbol{\lambda}) \leq \inf_x \sup_{\boldsymbol{\lambda} \succeq \mathbf{0}} L(x, \boldsymbol{\lambda})$$

and strong duality as the equality

$$\sup_{\boldsymbol{\lambda} \succeq \mathbf{0}} \inf_x L(x, \boldsymbol{\lambda}) = \inf_x \sup_{\boldsymbol{\lambda} \succeq \mathbf{0}} L(x, \boldsymbol{\lambda})$$

This can be generalized to arbitrary functions $f(x, y)$. In order to decide whether the min-max expressions satisfy the saddle-point property

$$\min_{x \in X} \max_{y \in Y} f(x, y) = \max_{y \in Y} \min_{x \in X} f(x, y) \tag{B.3}$$

we use Theorem 1 in [59]. According to [59, Theorem 1], (B.3) is fulfilled if, X and Y are two compact Hausdorff spaces, f is lower semi-continuous for every $y \in Y$, f is upper semi-continuous for every $x \in X$, f is convex in x and concave in y, and if the sets X and Y are convex. The following saddle-point interpretation can also be applied

$$f(x^*, y) \leq f(x^*, y^*) \leq f(x, y^*),$$

for all $x \in X$ and $y \in Y$. In other words, x^* minimizes $f(x, y^*)$ and y^* maximizes $f(x^*, y)$

$$f(x^*, y^*) = \inf_{x \in X} f(x, y^*) \qquad \text{and} \qquad f(x^*, y^*) = \sup_{y \in Y} f(x^*, y).$$

This also implies that the strong maxmin property holds (and therefore the strong duality).

Example B.1. Consider the following convex programming problem

$$\min x^2 \qquad \text{s.t.} \quad x \leq -3.$$

In standard form (B.1) we have $f_0(x) = x^2$ and $f_1(x) = x + 3$. The Lagrangian is given by

$$L(x, \lambda) = x^2 + \lambda(x + 3).$$

The dual function is given by

$$g(\lambda) = -\frac{1}{4}\lambda^2 + 3\lambda$$

The maximum of the dual function is found to be at $\lambda^* = 6$ and yields the value of the dual problem $d^* = 9$. The solution of the primal problem is then $x^* = -\frac{1}{2}\lambda = -3$ and the value of the primal problem is $p^* = 9$. Since the problem is convex, strong duality holds, i.e. $p^* = d^*$.

B.1.3 Optimality conditions

Assume that strong duality holds. Let x^* be a primal optimal and $(\boldsymbol{\lambda}^*, \boldsymbol{\nu}^*)$ be a dual optimal point. This means that

$$\begin{aligned} f_0(x^*) = g(\boldsymbol{\lambda}^*, \boldsymbol{\nu}^*) &= \inf_x \left(f_0(x) + \sum_{k=1}^{m} \lambda_i^* f_i(x) + \sum_{k=1}^{p} \nu_i^* h_i(x) \right) \\ &\leq f_0(x^*) + \sum_{k=1}^{m} \lambda_i^* f_i(x) + \sum_{k=1}^{p} \nu_i^* h_i(x) \leq f_0(x^*) \ , \end{aligned}$$

and the two inequalities in this chain hold with equality. Therefore, it follows that the minimizer of the Lagrangian with respect to x is x^*. In addition to this, $\sum_{k=1}^{m} \lambda_i^* f_i(x^*) = 0$, which leads to the so called **complementary slackness** condition

$$\lambda_i^* f_i(x^*) = 0 \qquad \text{for all } i = 1, ...m.$$

This means that the i-th optimal Lagrange multiplier is zero unless the i-th constraint is active at the optimum. Finally, we arrive at the Karush-Kuhn-Tucker optimality conditions (KKT conditions).

Definition B.4 (KKT conditions)**.** The KKT conditions for the opti-

mization problem in (B.1) are given by

$$\begin{aligned} \nabla f_0(x^*) + \sum_{i=1}^{m} \lambda_i^* \nabla f_i(x^*) + \sum_{i=1}^{p} \nu_i^* \nabla h_i(x^*) &= 0 \,, \\ f_i(x^*) &\leq 0 \,, i=1,...,m \\ h_i(x^*) &= 0 \,, i=1,...,p \\ \lambda_i^* &\succeq \mathbf{0} \,, i=1,...,m \\ \lambda_i^* f_i(x^*) &= 0 \,, i=1,...,m \,. \end{aligned} \tag{B.4}$$

Lemma B.2 (KKT optimality conditions)**.** The KKT conditions are necessary optimality conditions for any nonlinear optimization problem under the assumption that the constraints are regular. If the primal problem is convex, the KKT conditions are also sufficient. If a convex optimization problem with differentiable objective and constraint functions satisfies Slater's condition, then the KKT conditions provide necessary and sufficient conditions for optimality.

B.2 Monotonic optimization

Monotonic optimization problems occur in resource allocation, power control, and precoding problems in wireless interference networks. They can be solved using various approaches depending on their specific properties. In this section, we focus on the basic properties of monotonic programming and the solution by the outer polyblock algorithm. For further results and references, the interested reader is referred to [167, 146, 196, 24].

B.2.1 Increasing functions and normal sets

At first, we introduce the basic concepts of *increasing functions* and *normal sets*.

Definition B.5. For two vectors $\boldsymbol{x}', \boldsymbol{x} \in \mathbb{R}^n$ we write $\boldsymbol{x}' \geq \boldsymbol{x}$ and say that $\boldsymbol{x}'$ dominates $\boldsymbol{x}$ if $x_i' \geq x_i$ for all $i = 1, ..., n$. We write $\boldsymbol{x}' > \boldsymbol{x}$ and say that $\boldsymbol{x}'$ strictly dominates $\boldsymbol{x}$ if $x_i' > x_i$ for all $i = 1, ..., n$.

Note that the domination only induces a partial ordering because not all vectors can be compared. For example, if $\boldsymbol{x} = [1, 2]$ and

$\boldsymbol{x}' = [2, 1]$ then we have neither $\boldsymbol{x} \geq \boldsymbol{x}'$ nor $\boldsymbol{x}' \geq \boldsymbol{x}$. The order in Definition B.5 can be used to define the class of order preserving functions as follows.

Definition B.6. A function $f : \mathbb{R}^n \to \mathbb{R}$ is said to be increasing on $\mathbb{R}^n_+$ if $f(\boldsymbol{x}) \leq f(\boldsymbol{x}')$ whenever $0 \leq \boldsymbol{x} \leq \boldsymbol{x}'$. The function is said to be increasing in the hyper-rectangle $[a, b]^n \subset \mathbb{R}^n_+$ if $f(\boldsymbol{x}) \leq f(\boldsymbol{x}')$ whenever $a\mathbf{1} \leq \boldsymbol{x} \leq \boldsymbol{x}' \leq b\mathbf{1}$. A function is said to be strictly increasing if for $\boldsymbol{x}' \geq \boldsymbol{x} \geq 0$ and $\boldsymbol{x}' \neq \boldsymbol{x}$ follows that $f(\boldsymbol{x}') > f(\boldsymbol{x})$. (Here $\mathbf{1} = [1, ..., 1]^T$.)

Many functions encountered in resource allocation problems are increasing in the sense of Definition B.6. For example, the sum-rate capacity of a MAC [164] is increasing in the vector of powers allocated to the users: $f(\boldsymbol{p}) = \log\left(1 + \mathrm{SNR} \cdot \sum_{k=1}^{K} p_k a_k\right)$ where $a_1, ..., a_K$ are squared channel gains.

If the domain of these increasing functions is a so-called normal set (to be defined next), we will later obtain a characterization of the set on which the maximum is achieved.

A set $\mathcal{N}$ is said to be *normal* if for all $\boldsymbol{x} \in \mathcal{N}$ all points in the box $[\mathbf{0}, \boldsymbol{x}]$ are also in $\mathcal{N}$. More precisely:

Definition B.7. A set $\mathcal{N} \subset \mathbb{R}^n_+$ is called normal if for any two points $\boldsymbol{x}, \boldsymbol{x}' \in \mathbb{R}^n_+$ such that $\boldsymbol{x}' \leq \boldsymbol{x}$, if $\boldsymbol{x} \in G$, then $\boldsymbol{x}' \in G$, too.

The empty set, the singleton $\{0\}$, and $\mathbb{R}^n_+$ are special normal sets. We refer to them as trivial normal subsets of $\mathbb{R}^n_+$.

Definition B.8 (Conormal set)**.** A set $\mathcal{C} \subset \mathbb{R}^n_+$ is said to be *conormal* in $[\mathbf{0}, \boldsymbol{x}]$ if for any $\boldsymbol{y} \in \mathcal{C}$, all $\boldsymbol{z} \in [\boldsymbol{y}, \boldsymbol{x}]$ also belong to $\mathcal{C}$.

Proposition B.1. The set $\mathcal{N} = \{\boldsymbol{x} \in \mathbb{R}^n_+ \ : \ g(\boldsymbol{x}) \leq 0\}$ is normal and closed if $g : \mathbb{R}^n_+ \to \mathbb{R}$ is lower semi-continuous and increasing.

The set $\mathcal{C} = \{\boldsymbol{x} \in \mathbb{R}^n_+ \ : \ h(\boldsymbol{x}) \geq 0\}$ is conormal and closed if $h : \mathbb{R}^n_+ \to \mathbb{R}$ is upper semi-continuous and increasing.

For the characterization of the maximum of an increasing function over a normal set, we need the notion of *upper boundary*.

Definition B.9. A point $\boldsymbol{y} \in \mathbb{R}^n_+$ is called an upper boundary point of a bounded closed normal set $\mathcal{N}$ if $\boldsymbol{y} \in \mathcal{N}$ while the set $K_{\boldsymbol{y}} = \boldsymbol{y} + \mathbb{R}^n_{++} = \{\boldsymbol{y}' \in \mathbb{R}^n_+ \mid \boldsymbol{y}' > \boldsymbol{y}\}$ lies outside $\mathcal{N}$, i.e.

$$K_{\boldsymbol{y}} \subset \mathbb{R}^n_+ \setminus \mathcal{N}.$$

The set of upper boundary points of $\mathcal{N}$ is called the upper boundary of $\mathcal{N}$ and it is denoted by $\partial^+\mathcal{N}$.

The following result shows that the maximum of a strictly increasing function over a normal set is always achieved on the upper boundary of the normal set. The statement is somewhat weaker than Proposition 7 in [167]. However, for our purposes we only need the following version and provide an alternative proof by contradiction.

Lemma B.3. The global maximum of a strictly increasing function $f(\boldsymbol{x})$ over a normal set $\mathcal{N}$, if it exists, is attained on $\partial^+\mathcal{N}$.

Proof. Suppose $\boldsymbol{x} \in \mathcal{N}$ is a point where $f(\boldsymbol{x})$ attains a global maximum and that $\boldsymbol{x} \notin \partial^+\mathcal{N}$. Then there exists a $\boldsymbol{y} \in \mathcal{N}$ with $\boldsymbol{x} \leq \boldsymbol{y}$ and for which at least one component in $\boldsymbol{y}$ is larger than in $\boldsymbol{x}$. Since $f(\boldsymbol{x})$ is strictly increasing, we must have $f(\boldsymbol{x}) < f(\boldsymbol{y})$. □

B.2.2 Monotonic optimization and outer polyblock approximation

We next give some background on monotonic optimization. A monotonic optimization problem in standard form [146] is given by

$$\max_{\boldsymbol{x}} f(\boldsymbol{x}) \qquad \text{s.t.} \quad \boldsymbol{x} \in \mathcal{N} \tag{B.5}$$

where $\mathcal{N}$ is a normal, but not necessarily convex set. It is also possible to give a more general definition by considering the feasible set as $\mathcal{N} \cap \mathcal{C}$, with $\mathcal{C}$ a conormal set. However, we will limit our review of monotonic optimization to the case of (B.5). We assume that $\mathcal{N}$ is normalized such that the smallest box containing $\mathcal{N}$ is the unit box.

The main difficulty involved in solving Problem (B.5) is that the constraint set is non-convex. However, using the polyblock approach it turns out that there is an interesting duality between optimization of increasing functions over normal sets and optimization of convex functions over convex sets [166].

From Lemma B.3 we know that the maximum of $f(\boldsymbol{x})$ over $\mathcal{N}$ is attained at the upper boundary $\partial^+\mathcal{N}$. The main idea to solve the non-convex optimization problem (B.5) is to approximate $\partial^+\mathcal{N}$ by a shrinking sequence of polyblocks.

Definition B.10. A set $\mathcal{P} \subset \mathbb{R}^n_+$ is called a polyblock if it is the union of a finite number of hyper-rectangles.

The polyblock $\mathcal{P}$ is generated by a set of vertices T. The minimal set of vertices consists of only proper vertices, i.e., vertices which are not dominated by any other vertex is T. It follows that for all $\boldsymbol{z}, \boldsymbol{z}' \in T$ with $\boldsymbol{z} \neq \boldsymbol{z}'$ it does not hold $\boldsymbol{z} > \boldsymbol{z}'$ or $\boldsymbol{z} < \boldsymbol{z}'$. Another important consequence of Lemma B.3 is that the maximum of an increasing function over a polyblock is achieved at a proper vertex.

The main idea of the outer polyblock algorithm is as follows: construct a nested sequence of polyblocks which approximate the normal set $\mathcal{N}$ from above

$$P_1 \supset P_2 \supset ... \supset \mathcal{N} \qquad \text{such that} \quad \max_{\boldsymbol{x} \in P_k} f(\boldsymbol{x}) \searrow \max_{\boldsymbol{x} \in \mathcal{N}} f(\boldsymbol{x}) \tag{B.6}$$

where $x_k \searrow x$ means that $x_k \to x$ when $k \to \infty$ and that $x_k \geq x_l \geq x$ for all $l \geq k$. The main steps of the outer polyblock algorithm are described next. Define the maximizer at iteration k as

$$\tilde{\boldsymbol{x}}^{(k)} \in \arg\max_{\boldsymbol{x} \in T_k} f(\boldsymbol{x}), \tag{B.7}$$

where T_k is the minimal vertex set of P_k. The first step is to construct the nested sequence in (B.6), i.e., to construct a new polyblock $\mathcal{P}_{k+1}$ contained in $\mathcal{P}_k \setminus \{\tilde{\boldsymbol{x}}^{(k)}\}$ but still containing $\mathcal{N}$. This step is motivated in Propositions 17 and 18 in [167]. However, we provide an alternative description for convenience and completeness.

Let the set of vertices in step k be $T_k = \{\boldsymbol{x}_1^{(k)}, ..., \boldsymbol{x}_{K^{(k)}}^{(k)}\}$. Denote $\bar{\boldsymbol{x}}^{(k)}$ as the unique intersection point of $\partial^+\mathcal{N}$ and $\delta\tilde{\boldsymbol{x}}^{(k)}$ with $\delta \in [0, 1]$. Then the set of (not necessarily minimal) vertices in step $k+1$ is constructed as follows

$$T_{k+1} = T_k \setminus \{\tilde{\boldsymbol{x}}^{(k)}\} \bigcup_{\nu=1}^{n} \{\tilde{\boldsymbol{x}}^{(k)} - [\tilde{x}_\nu^{(k)} - \bar{x}_\nu^{(k)}]\boldsymbol{e}_\nu\} \tag{B.8}$$

where $\boldsymbol{e}_n$ is the nth column of the identity matrix. The construction of the vertices in step $k+1$ is illustrated in Figure B.1. The new vertices are $\boldsymbol{x}_{+1}^{(k)} = \tilde{\boldsymbol{x}}^{(k)} - [\tilde{x}_\nu^{(k)} - \bar{x}_1^{(k)}]\boldsymbol{e}_1$, $\boldsymbol{x}_{+2}^{(k)} = \tilde{\boldsymbol{x}}^{(k)} - [\tilde{x}_\nu^{(k)} - \bar{x}_2^{(k)}]\boldsymbol{e}_2$, and $\boldsymbol{x}_{+3}^{(k)} = \tilde{\boldsymbol{x}}^{(k)} - [\tilde{x}_\nu^{(k)} - \bar{x}_3^{(k)}]\boldsymbol{e}_3$ as described in (B.8).

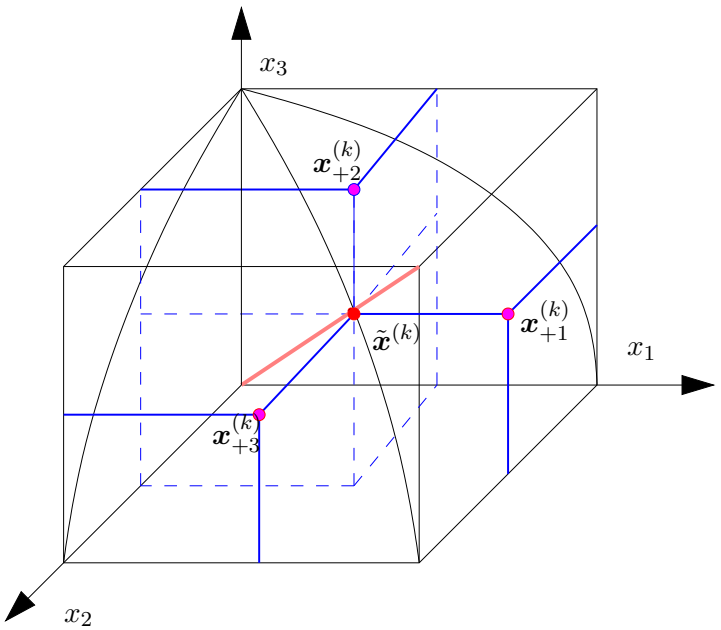

Figure B.1: Construction of vertices in step $k+1$ in (B.8).

Let $\mathcal{P}_k$ and $\mathcal{P}_{k+1}$ be the polyblocks induced by the minimal set of vertices T_k and T_{k+1}, respectively.

Proposition B.2. The constructed polyblocks $\mathcal{P}_k$ and $\mathcal{P}_{k+1}$ fulfill

$$\mathcal{N} \subset \mathcal{P}_{k+1} \subset \mathcal{P}_k \setminus \{\tilde{\boldsymbol{x}}^{(k)}\}. \tag{B.9}$$

Proof. In order to show the second relation $\mathcal{P}_{k+1} \subset \mathcal{P}_k \setminus \{\tilde{\boldsymbol{x}}^{(k)}\}$ it suffices to verify that for each vertex $\boldsymbol{x}_\ell^{(k)}$ in T_k with $1 \leq \ell \leq K^{(k)}$ there exists a vertex $\boldsymbol{x}_{\tilde{\ell}}^{(k+1)}$ in T_{k+1} such that $\boldsymbol{x}_\ell^{(k)} \geq \boldsymbol{x}_{\tilde{\ell}}^{(k+1)}$. Let $\bar{\ell}$ be the index which belongs to the maximal vertex in T_k, i.e., $\bar{\ell} = \arg\max_{1\leq\ell\leq K^{(k)}} f(\boldsymbol{x}_\ell^{(k)})$. For all $\ell \neq \bar{\ell}$ there is a $\boldsymbol{x}_{\tilde{\ell}}^{(k+1)} = \boldsymbol{x}_\ell^{(k)}$ because T_{k+1} still contains these non-maximum vertices (or after removing of all

dominated vertices they are dominated). For $\bar{\ell}$ there are n new vertices $\boldsymbol{x}_{\check{\nu}}^{(k+1)} = \{\tilde{\boldsymbol{x}}^{(k)} - [\tilde{x}_\nu^{(k)} - \bar{x}_\nu^{(k)}]\boldsymbol{e}_\nu\}$ for $1 \leq \nu \leq n$ with $\boldsymbol{x}_{\check{\nu}}^{(k+1)} \geq \boldsymbol{x}_{\bar{\ell}}^{(k)}$.

In order to prove the first relation $\mathcal{N} \subset \mathcal{P}_{k+1}$ we have to find for all boundary points $\boldsymbol{d} \in \partial^+\mathcal{N}$ a vertex $\boldsymbol{x}_\ell^{(k+1)}$ in T_{k+1} such that $\boldsymbol{d} \leq \boldsymbol{x}_\ell^{(k+1)}$. For all upper boundary points $\boldsymbol{d} \in \partial^+\mathcal{N}$ with $\boldsymbol{d} \leq \boldsymbol{x}_\ell^{(k)}$ and $\ell \neq \bar{\ell}$ we find immediately the corresponding vertex in T_{k+1} because these vertices were not removed in (B.8). For the upper boundary points $\boldsymbol{d} \in \partial^+\mathcal{N}$ for which $\boldsymbol{d} \leq \boldsymbol{x}_\ell^{(k)}$ we find one of the n new vertices $\boldsymbol{x}_{\check{\nu}}^{(k+1)} = \{\tilde{\boldsymbol{x}}^{(k)} - [\tilde{x}_\nu^{(k)} - \bar{x}_\nu^{(k)}]\boldsymbol{e}_\nu\}$ for $1 \leq \nu \leq n$ such that $\boldsymbol{d} \leq \boldsymbol{x}_{\check{\nu}}^{(k+1)}$. □

Finally, we can remove all dominated vertices of T_{k+1} to obtain the minimal vertex set needed for the next step $k+2$.

B.2.3 Outer polyblock algorithm and stopping criteria

The general outer polyblock algorithm is described in Algorithm 21. There are three stopping criteria ϵ-, and η-accuracy reached, or maximum number of steps exceeded.

In Line 7, the search for the intersection point is a scalar optimization problem in $0 \leq \delta \leq 1$ and simple Newton methods could be used. In the implementation, we used Bolzano's bisection procedure as suggested in [146, Section 8] to compute the intersection point.

Given a tolerance $\epsilon > 0$, denote

$$\mathcal{N}^\epsilon = \{\boldsymbol{x} \in \mathcal{N} | x_i \geq \epsilon, \quad i = 1, ..., n\}.$$

Assuming ϵ is small but positive such that $\mathcal{N}^\epsilon \neq \emptyset$, a global solution of the problem

$$\max_{\boldsymbol{x}} f(\boldsymbol{x}) \qquad \text{s.t.} \quad \boldsymbol{x} \in \mathcal{N}^\epsilon \tag{B.10}$$

will be called an ϵ-optimal solution of (B.5). A solution $\bar{\boldsymbol{x}} \in \mathcal{N}$, such that $f(\bar{\boldsymbol{x}})$ differs from the optimal value of (B.10) by at most $\eta > 0$, will be referred to as an (ϵ, η)-approximate optimal solution of (B.10).

For any positive (ϵ, η), Theorem 1 in [146] shows that the algorithm terminates after a finite number of steps.

Algorithm 21 Generalized outer polyblock algorithm

Constraint set $\mathcal{D}$, $\epsilon > 0$; $\eta > 0$; $T = \mathbf{1}$; $k = 1$;
while ϵ, η-accuracy and maximum number of steps is not reached **do**
$\boldsymbol{x}^{(k)} = \arg\max\{f(\boldsymbol{x}) | \boldsymbol{x} \in T, \boldsymbol{x} \geq \epsilon\mathbf{1}\}$;
if $\boldsymbol{x}^{(k)} \in \mathcal{D}$ **then**
$\boldsymbol{x}^* = \boldsymbol{x}^{(k)}$ is ϵ-optimal solution
Compute the intersection point $\boldsymbol{y}^{(k)}$ of $\partial^+\mathcal{D}$ with $\delta\boldsymbol{x}^{(k)}$ with $0 \leq \delta \leq 1$ $\bar{\boldsymbol{y}}^{(k)} = \arg\max\{f(\bar{\boldsymbol{y}}^{(k-1)}), f(\boldsymbol{y}^{(k)})\}$
else$f(\bar{\boldsymbol{y}}^{(k)}) \geq f(\boldsymbol{x}^{(k)}) - \eta$
$\boldsymbol{x}^* = \bar{y}^{(k)}$ is an (ϵ, η)-approximate solution of (B.5);
Compute n extreme points of the rectangle $[\boldsymbol{y}^{(k)}, \boldsymbol{x}^{(k)}]$ that are adjacent to $\boldsymbol{x}^{(k)}$: $\boldsymbol{x}^{(k),i} = \boldsymbol{x}^{(k)} - (\boldsymbol{x}_i^{(k)} - \boldsymbol{y}_i^{(k)})\boldsymbol{e}^i$ for $1 \leq i \leq n$ $Z = [T \setminus \{\boldsymbol{x}^{(k)}\}] \cup \{\boldsymbol{x}^{(k),1}, ..., \boldsymbol{x}^{(k),n}\}$ T is obtained from Z after dropping all vectors which are dominated by others
end if
$k = k + 1$;
end while
Solution $\boldsymbol{x}^*$ to (B.5);

C

Fundamentals of game theory

In this section, we provide some basic background on non-cooperative games in strategic normal form and their solution concepts. For a more in-depth review, we refer to the textbooks and book chapters about game theory in general [132, 61, 15, 130, 138, 125] as well as about engineering applications of game theory in communications and networking [110, 65, 2, 95, 96].

C.1 Games in strategic normal form

Definition C.1. A game in strategic normal form is described by a triple $\mathcal{G} = \{\mathcal{K}, \mathcal{S}, \mathcal{U}\}$ consisting of the set of players $\mathcal{K} = \{1, 2, ..., K\}$, the strategy space $\mathcal{S}$, and the set of utility functions $\mathcal{U} = \{u_1, u_2, ..., u_K\}$ mapping from the strategy space $\mathcal{S}$ to the real numbers.

In many cases, the strategy space $\mathcal{S}$ is the Cartesian product of the individual strategy spaces $\mathcal{S} = \mathcal{S}_1 \times \ldots \times \mathcal{S}_K$.

The game $\mathcal{G}$ is played once and the players need to decide on their strategies $s_1, ..., s_K$ depending on the information they have about the game and the other players. If the players know all components of the game perfectly, the game is called a game with complete information. If

each player decides deterministically on the strategy s_k, we talk about pure strategies, while if the players decide stochastically on their strategy choices, we talk about mixed strategies.

There are certain solution concepts which arguably find strategy tuples $\boldsymbol{s} = [s_1, ..., s_K]$[1] which describe reasonable outcomes of the game in normal form under the assumption that the players behave rationally. The easiest and best motivated solution concept is the solution in dominant strategies.

Definition C.2. A dominant strategy s'_k of player k is the BR to any strategy vector $\boldsymbol{s}_{-k}$ of the other players, i.e.,

$$s'_k = br_k(\boldsymbol{s}_{-k}) = \arg\max_{s_k \in \mathcal{S}_k} u_k(s_k, \boldsymbol{s}_{-k}) \quad \text{for all } \boldsymbol{s}_{-k} \in \mathcal{S} \setminus \mathcal{S}_k. \tag{C.1}$$

The advantage of the dominant strategies is that it is a very reasonable solution. The disadvantage is that it does not always exist. In this case, another solution concept is the Nash equilibrium (NE).

Definition C.3. An NE strategy profile is a tuple $\boldsymbol{s}^* = [s_1^*, ..., s_K^*]$ such that each user k cannot improve the utility by changing the strategy from s_k^* to any other strategy $s_k \in \mathcal{S}_k$ unilaterally, i.e.,

$$u_k(s_k^*, \boldsymbol{s}_{-k}^*) \geq u_k(s_k, \boldsymbol{s}_{-k}^*) \quad \text{for all } k \in \mathcal{K} \text{ and } s_k \in \mathcal{S}_k. \tag{C.2}$$

Definition C.4 (Best response dynamics (BRD))**.** The BRD of a non-cooperative game in normal form $\mathcal{G}$, is defined as the iteration

$$\max_{s_k \in \mathcal{S}_k} u_k(s_k, \boldsymbol{s}_{-k}) \, , \forall \, k \in \mathcal{K} \, . \tag{C.3}$$

We can see that by construction the fixed points of (C.3) are the NE of the game.

The NE is a selfish solution concept leading to an outcome of the game which is not necessarily Pareto optimal, i.e., which cannot be improved for one player without decreasing the utility of at least one other player. The distance between the NE and the Pareto boundary is called the *Price of anarchy* [135, 130].

The applicability of the NE as a solution concept depends on the following three properties:

[1] We denote the vector of strategies without strategy of user k by $\boldsymbol{s}_{-k} = [s_1, ..., s_{k-1}, s_{k_1}, ..., s_K]$.

1. Does there exist an NE in pure strategies? It is known that every finite game in strategic form has an NE in mixed strategies. However, the existence of a pure strategy NE is not always guaranteed.

2. Is the NE unique? If the NE exists, then the operational meaning is much stronger if it is unique. Furthermore, the players do not need to argue or find a mechanism for choosing the *right* NE as in the case in which multiple equilibria exist.

3. Does the BRD converge to the unique NE? The best response dynamics as introduced in (C.3) can be implemented as a distributed iterative algorithm in which the players play the best response iteratively, keeping the strategies of the others fixed. However, in general a BRD is not guaranteed to always converge, not even if one or more NE exist. Therefore, studying the convergence properties of the BRD is of great interest to design distributed implementations of resource allocation algorithm. If the iterative BRD is convergent from any starting point, it is said to be globally stable.

In order to answer the three questions, there are results and sufficient conditions available which are collected and summarized below.

Theorem C.1 ([53, 5])**.** A non-cooperative game in normal form admits at least one NE in pure strategies, if the strategy sets are non-empty, convex, and compact, if the utility function u_k is continuous in $\boldsymbol{s}$ and quasi-concave in s_k, for all $k \in \mathcal{K}$.

One way to prove global stability is to show that the best response is a standard function [180]. In order to qualify for a standard function, the players' best responses should satisfy the following properties:

1. Positivity: The best response of player k should be non-negative for all strategies of the other players, i.e., $br_k(\boldsymbol{s}_{-k}) \geq 0$ for all $\boldsymbol{s}_{-k} \in \mathcal{S} \setminus \mathcal{S}_k$ and for all $k \in \mathcal{K}$.

2. Monotonicity: The best response should be monotonic increasing in the strategies of the other players, i.e., $br_k(\boldsymbol{s}_{-k}) \geq br_k(\boldsymbol{t}_{-k})$ whenever $\boldsymbol{s}_{-k} \geq \boldsymbol{t}_{-k}$ (component-wise).

3. Scalability: The scaled best response should be larger than the best response of the scaled strategies of the other players, i.e., for all $\boldsymbol{s}_{-k} \in \mathcal{S} \setminus \mathcal{S}_k$ and all $k \in \mathcal{K}$ and $\mu > 1$ it should hold

$$\mu br_k(\boldsymbol{s}_{-k}) \geq br_k(\mu \boldsymbol{s}_{-k}). \tag{C.4}$$

Theorem C.2 ([180])**.** If the best response of a non-cooperative game is a standard function, and provided that one NE exists, then the NE is unique and the BRD is guaranteed to converge to the unique NE.

To conclude, we introduce a particular class of non-cooperative games, namely potential games [124], which under very mild assumptions have the pleasant property of being guaranteed to admit at least one NE and to have a convergent BRD.

Definition C.5. A non-cooperative game in normal form $\mathcal{G} = \{\mathcal{K}, \{\mathcal{S}_k\}_k, \{u_k\}_k\}$ is called an *exact potential game* if there exists a function $V : \mathcal{S}_1 \times \mathcal{S}_2 \times \ldots \mathcal{S}_K \to \mathbb{R}$ such that for any $k \in \mathcal{K}$ and for any $(s_k, \boldsymbol{s}_{-k}), (s_k^*, \boldsymbol{s}_{-k}) \in \mathcal{S}_1 \times \mathcal{S}_2 \times \ldots \mathcal{S}_K$, we have

$$u_k(s_k, \boldsymbol{s}_{-k}) - u_k(s_k^*, \boldsymbol{s}_{-k}) = V(s_k, \boldsymbol{s}_{-k}) - V(s_k^*, \boldsymbol{s}_{-k}) \, . \tag{C.5}$$

From the definition, it follows that in a potential game, for all $k = 1, \ldots, K$, the k-th player's BR problem is equivalent to the maximization of the potential function V with respect to the k-th player's strategy s_k, and thus the BRD can be regarded as an alternating maximization performed on the potential function V, in which the different strategies $s_1, \ldots, s_k$ are iteratively optimized. This observation leads to the following result.

Theorem C.3. Consider a potential game with compact strategy set $\mathcal{S}_1 \times \mathcal{S}_2 \times \ldots \mathcal{S}_K$, and assume the potential function V is continuous in $s_1, \ldots, s_K$. The the game admits at least one NE, and the BRD is guaranteed to converge[2].

[2]Here, convergence is meant in the value of the objective

Acknowledgements

Part of this work has formed the basis for the tutorial [188], and has been presented during lectures at the Technische Universität Dresden, within the course "Advancements of communications and information theory".

The work of Alessio Zappone has been supported by the German Research Foundation (DFG), within the framework of the project CEMRIN, under grants ZA 747/1-2 and ZA 747/1-3. The work of Eduard Jorswieck has been supported by the German Research Foundation (DFG) in the Collaborative Research Center 912 "Highly Adaptive Energy-Efficient Computing" (HAEC), and within the Cluster of Excellence "Center for Advancing Electronics Dresden" (cfaed), and by the European research project DIWINE, which is partly funded by the European Union under its FP7 ICT Objective 1.1 - The Network of the Future.

The authors wish to thank Prof. Stefano Buzzi and Prof. Luca Venturino (University of Cassino and Southern Lazio), Dr. Giusi Alfano and Prof. Michela Meo (Politecnico di Torino), Dr. Pan Cao, Zhijiat Chong, and Bho Matthiesen (Technische Universität Dresden), for helpful discussions and joint work on some of the research papers presented in this monograph.

References

[1] Y. Almogy and O. Levin. A class of fractional programming problems. *Operations Research*, 19:57–67, 1971.

[2] E. Altman, T. Boulogne, R. El-Azouzi, T. Jimenez, and L. Wynter. A survey of networking games in telecommunications. *Comput. Oper. Res.*, 33:286–311, 2006.

[3] J. Andrews, S. Buzzi, W. Choi, S. Hanly, A. Lozano, A. C. K. Soong, and J. C. Zhang. What will 5G be? *IEEE Journal on Selected Areas in Communications*, 32(6):1065–1082, June 2014.

[4] J. G. Andrews. Seven ways that HetNets are a cellular paradigm shift. *IEEE Communications Magazine*, 51(3):136–144, March 2013.

[5] K. J. Arrow and G. Debreu. Existence of an equilibrium for a competitive economy. *Econometrica*, 22(3):265–290, July 1954.

[6] K. J. Arrow and K .J. Enthoven. Quasi-concave programming. *Econometrica*, 29:779–800, 1961.

[7] A. Attar, T. Basar, M. Debbah, H. V. Poor, and Q. Zhao. Special issue on game theory in communications. *IEEE Journal on Selected Areas in Communications*, 30(1), January 2012.

[8] G. Auer, V. Giannini, C. Desset, I. Godor, P. Skillermark, M. Olsson, M. A. Imran, D. Sabella, M. J. Gonzalez, O. Blume, et al. How much energy is needed to run a wireless network? *IEEE Wireless Communications*, 18(5):40–49, 2011.

[9] M. Avriel, W. E. Diewert, S. Schaible, and I. Zang. *Generalized concavity*. SIAM, 1988.

[10] Mordecai Avriel. *Nonlinear Programming: Analysis and Methods*. Prentice Hall, 2003.

[11] F. Baccelli and B. Błaszczyszyn. Stochastic geometry and wireless networks: Volume I theory. *Now Publishers: Foundations and Trends in Networking*, 3(3–4):249–449, March 2009.

[12] G. Bacci, E. V. Belmega, P. Mertikopoulos, and L. Sanguinetti. Energy-aware competitive power allocation in heterogeneous networks with QoS constraints. *IEEE Transactions on Wireless Communications, in press, available: http://arxiv.org/abs/1408.7004*, 2014.

[13] G. Bacci, H. V. Poor, M. Luise, and A. M. Tulino. Energy efficient power control in impulse radio UWB wireless networks. *IEEE Journal of Selected Topics in Signal Processing*, 1(3):508–520, October 2007.

[14] R. G. Bartle. *The elements of real analysis*. 2nd ed. John Wiley & Sons, New York, 1976.

[15] T. Basar and G. J. Olsder. *Dynamic Noncooperative Game Theory*. Classics In Applied Mathematics. SIAM, second edition, 1999.

[16] E. V. Belmega and S. Lasaulce. Energy-efficient precoding for multiple-antenna terminals. *IEEE Transactions on Signal Processing*, 59(1):329–340, January 2011.

[17] H. P. Benson. Global optimization of nonlinear sums of ratios. *Journal of Mathematical Analysis and Applications*, 263:301–315, 2001.

[18] H. P. Benson. Global optimization algorithm for the nonlinear sum of ratios problem. *Journal of Optimization Theory and Applications*, 112:1–29, 2002.

[19] H. P. Benson. Solving sum of ratios fractional programs via concave minimization. *Journal of Optimization Theory and Applications*, 135:1–17, 2007.

[20] D. P. Bertsekas. *Nonlinear Programming*. Athena Scientific, 1999.

[21] S. M. Betz and H. V. Poor. Energy efficient communications in CDMA networks: A game theoretic analysis considering operating costs. *IEEE Transactions on Signal Processing*, 56(10):5181–5190, October 2008.

[22] R. Bhatia. *Matrix Analysis*. Springer, 1997.

[23] E. Björnson, J. Hoydis, M. Kountouris, and M. Debbah. Massive MIMO systems with non-ideal hardware: Energy efficiency, estimation, and capacity limits. *IEEE Transaction Information Theory*, in press, 2014.

[24] E. Björnson and E. A. Jorswieck. Optimal resource allocation in coordinated multi-cell systems. *Now Publishers: Foundations and Trends in Communications and Information Theory*, 9(2-3):113–381, January 2013.

[25] E. Björnson, L. Sanguinetti, J. Hoydis, and M. Debbah. Optimal design of energy-efficient multi-user MIMO systems: Is massive MIMO the answer? *IEEE Transactions on Wireless Communications*, in press, 2014.

[26] E. Björnson, G. Zheng, M. Bengtsson, and B. Ottersten. Robust monotonic optimization framework for multicell MISO systems. *IEEE Transactions on Signal Processing*, 60(5):2508–2523, May 2012.

[27] F. Boccardi, R. W. Heath, A. Lozano, T. L. Marzetta, and P. Popovski. Five disruptive technology directions for 5G. *IEEE Communications Magazine*, 52(2):74–80, February 2014.

[28] S. P. Boyd and L. Vandenberghe. *Convex optimization*. Cambridge Univ Press, 2004.

[29] G. Brante, I. Stupia, R. D. Souza, and L. Vandendorpe. Outage probability and energy efficiency of cooperative MIMO with antenna selection. *IEEE Transactions on Wireless Communications*, 12(11):5896–5907, November 2013.

[30] S. Buzzi, G. Colavolpe, D. Saturnino, and A. Zappone. Potential games for energy-efficient power control and subcarrier allocation in uplink multicell OFDMA systems. *IEEE Journal of Selected Topics in Signal Processing*, 6(2):89 –103, April 2012.

[31] S. Buzzi, V. Massaro, and H. V. Poor. Energy-efficient resource allocation in multipath CDMA channels with band-limited waveforms. *IEEE Transactions on Signal Processing*, 57(4):1494–1510, April 2009.

[32] S. Buzzi and H. V. Poor. Joint receiver and transmitter optimization for energy-efficient CDMA communications. *IEEE Journal on Selected Areas in Communications*, 26(3):459–472, April 2008.

[33] S. Buzzi, H. V. Poor, and D. Saturnino. Noncooperative waveform adaptation games in multiuser wireless communications. *IEEE Signal Processing Magazine*, 26(5):64–76, September 2009.

[34] S. Buzzi, H. V. Poor, and A. Zappone. Transmitter waveform and widely-linear receiver design: Non-cooperative games for wireless multiple-access networks. *IEEE Transactions on Information Theory*, 56(10):4874–4892, October 2010.

[35] S. Buzzi and D. Saturnino. A game-theoretic approach to energy-efficient power control and receiver design in cognitive CDMA wireless networks. *IEEE Journal of Selected Topics in Signal Processing*, 5(1):137–150, February 2011.

[36] G. Calcev, D. Chizhik, B. Goransson, S. Howard, H. Huanga, A. Kogiantis, A. Molisch, A. Moustakas, D. Reed, and H. Xu. A wideband spatial channel model for system-wide simulations. *IEEE Transactions on Vehicular Technology*, 56(2), March 2007.

[37] A. Cambini and L. Martein. *Generalized convexity and optimization: theory and applications*. Springer-Verlag: lecture notes in economics and mathematical systems, 2009.

[38] A. Charnes and W. W. Cooper. Programming with linear fractional functionals. *Naval Research Logistics Quarterly*, 9:181–186, 1962.

[39] X. Chen and L. Lei. Energy-efficient optimization for physical layer security in multi-antenna downlink networks with QoS guarantee. *IEEE Communications Letters*, 17(4):637–640, 2013.

[40] X. Chen, X. Wang, and X. Chen. Energy-efficient optimization for wireless information and power transfer in large-scale MIMO systems employing energy beamforming. *IEEE Wireless Communications Letters*, 2(6):667–670, December 2013.

[41] X. Chen, X. Xu, and X. Tao. Energy efficient power allocation in generalized distributed antenna system. *IEEE Communications Letters*, 16(7):1022–1025, July 2012.

[42] Y. Chen, S. Zhang, S. Xu, and G. Y. Li. Fundamental trade-offs in green wireless networks. *IEEE Communications Magazine*, 49(6):30–37, June 2011.

[43] K. T. K. Cheung, S. Yang, and L. Hanzo. Achieving maximum energy-efficiency in multi-relay OFDMA cellular networks: A fractional programming approach. *IEEE Transactions on Communications*, 61(7):2746–2757, 2013.

[44] M. Chiang, C. Wei, D. P. Palomar, D. O'Neill, and D. Julian. Power control by geometric programming. *IEEE Transactions on Wireless Communications*, 6(7):2640–2651, July 2007.

[45] Z. Chong and E. A. Jorswieck. Energy-efficient power control for MIMO time-varying channels. In *Online Conference on Green Communications (GreenCom), 2011 IEEE*, pages 92–97, 2011.

[46] Z. Chong, N. Zorba, and E. A. Jorswieck. Energy-efficient modulation selection and feedback quantization. In *2012 IEEE 17th International Workshop on Computer Aided Modeling and Design of Communication Links and Networks (CAMAD)*, pages 75–79, Sept 2012.

[47] R. Couillet and M. Debbah. *Random matrix methods for wireless communications*. Cambridge University Press, Cambridge, New York, 2011.

[48] J. P. Crouzeix and J. A. Ferland. Algorithms for generalized fractional programming. *Mathematical Programming*, 52:191–207, 1991.

[49] J. P. Crouzeix and J. A. Ferland. Criteria for quasi-convexity and pseudo-convexity: relationships and comparisons. *Mathematical Programming*, 56:223–232, 1992.

[50] J. P. Crouzeix, J. A. Ferland, and S. Schaible. An algorithm for generalized fractional programs. *Journal of Optimization Theory and Applications*, 47(1):35–49, 1985.

[51] S. Cui, A. J. Goldsmith, and A. Bahai. Energy-efficiency of MIMO and cooperative MIMO techniques in sensor networks. *IEEE Journal on Selected Areas in Communications*, 22(6):1089–1098, August 2004.

[52] N. Dan, L.-N. Tran, P. Pirinen, and M. Latva-aho. Precoding for full duplex multiuser MIMO systems: Spectral and energy efficiency maximization. *IEEE Transactions on Signal Processing*, 61(16):4038–4050, August 2013.

[53] G. Debreu. A social equilibrium existence theorem. In *National Academy of Sciences*, volume 38, pages 886–893, 1952.

[54] W. Dinkelbach. On nonlinear fractional programming. *Management Science*, 13(7):492–498, March 1967.

[55] B. Du, C. Pan, W. Zhang, and M. Chen. Distributed energy-efficient power optimization for CoMP systems with max-min fairness. *IEEE Communications Letters*, 18(6):999–1002, 2014.

[56] M. Dür, R. Horst, and N. V. Thoai. Solving sum-of-ratios fractional programs using efficient points. *Optimization*, 49:447–466, 2001.

[57] F. Facchinei and C. Kanzow. Generalized Nash equilibrium problems. *Springer 4OR*, 5:173–210, 2007.

[58] J. E. Falk and S. W. Palocsay. *Optimizing the sum of linear fractional functions*. C. A. Floudas and P. M. Pardalos (eds.), Kluwer Academic Publishers, Dordrecht, 1992.

[59] K. Fan. Minimax theorems. *Proc. N. A. S.*, 39:42–47, 1953.

[60] D.-Q. Feng, C.-Z. Jiang, G.-B. Lim, L. J. Cimini, G. Feng, and G. Y. Li. A survey of energy efficient wireless communications. *IEEE Communications Surveys and Tutorials*, 15(1):167–178, 2013.

[61] D. Fudenberg and J. Tirole. *Game Theory*. MIT Press, 1993.

[62] A. Goldsmith. *Wireless Communications*. Cambridge University Press, 2005.

[63] D. J. Goodman and N. B. Mandayam. Power control for wireless data. *IEEE Personal Communications*, 7:48–54, 2000.

[64] N. Hadjisavvas, S. Komlósi, and S. Schaible (eds.). *Handbook of Generalized Convexity*. Springer, 2005.

[65] Z. Han, D. Niyato, W. Saad, T. Basar, and A. Hjorungnes. *Game Theory in Wireless and Communication Networks: Theory, Models, and Applications*. Cambridge University Press, 2011.

[66] M. Hasan, E. Hossain, and D. I. Kim. Resource allocation under channel uncertainties for relay-aided device-to-device communication underlaying LTE-A cellular networks. *IEEE Transactions on Wireless Communications*, 13(4):2322–2338, April 2014.

[67] S. Haykin. Cognitive radio: Brain-empowered wireless communications. *IEEE Journal on Selected Areas in Communications*, 23(2):201–220, February 2005.

[68] C. He, G. Y. Li, F.-C. Zheng, and X. You. Energy-efficient resource allocation in OFDM systems with distributed antennas. *IEEE Transactions on Vehicular Technology*, 63(3):1223–1231, March 2014.

[69] S. He, Y. Huang, S. Jin, and L. Yang. Coordinated beamforming for energy efficient transmission in multicell multiuser systems. *IEEE Transactions on Communications*, 61(12):4961–4971, December 2013.

[70] S. He, Y. Huang, L. Yang, and B. Ottersten. Coordinated multicell multiuser precoding for maximizing weighted sum energy efficiency. *IEEE Transactions on Signal Processing*, 62(3):741–751, February 2014.

[71] F. Heliot. Low-complexity energy-efficient joint resource allocation for two-hop MIMO-AF systems. *IEEE Transactions on Wireless Communications*, 13(6):3088–3099, June 2014.

[72] C. Hellings and W. W. Utschick. Energy efficiency optimization in MIMO broadcast channels with fairness constraints. In *IEEE 14th Workshop on Signal Processing Advances in Wireless Communications (SPAWC 2013)*, pages 599–603, 2013.

[73] A. Helmy, L. Musavian, and L.-N. Tho. Energy-efficient power adaptation over a frequency-selective fading channel with delay and power constraints. *IEEE Transactions on Wireless Communications*, 12(9):4529–4541, September 2013.

[74] P.-H. Ho, G. Shen, S. Subramaniam, H. T. Mouftah, C. Qiao, and L. Wosinska. Special issue on energy-efficiency in optical networks. *IEEE Journal of Selected Topics in Signal Processing*, 2013.

[75] Z. K. M. Ho and E. Jorswieck. Instantaneous relaying: Optimal strategies and interference neutralization. *IEEE Transactions on Signal Processing*, 60(12):6655–6668, December 2012.

[76] R. A. Horn and C. R. Johnson. *Matrix Analysis*. Cambridge University Press, 1985.

[77] R. A. Horn and C. R. Johnson. *Topics in Matrix Analysis*. Cambridge University Press, 1991.

[78] E. Hossain, V. K. Bhargava, and G. Fettweis, editors. *Green Radio Communication Networks*. Cambridge University Press, 2012.

[79] J. Hoydis, M. Kobayashi, and M. Debbah. Green small-cell networks: a cost- and energy-efficient way of meeting the future traffic demands. *IEEE Vehicular Technology Magazine*, 6(1):37–43, March 2011.

[80] Y. Hu, B. Ji, Y. Huang, F. Yu, and L. Yang. Energy-efficiency resource allocation of very large multi-user MIMO systems. *Wireless Networks*, 20(6):1421–1430, August 2014.

[81] J. Huang, D. P. Palomar, N. Mandayam, J. Walrand, S. B. Wicker, and T. Basar. Special issue on game theory in communication systems. *IEEE Journal on Selected Areas in Communications*, 26(7), September 2008.

[82] I. Hwang, S. Song, and S. S. Soliman. A holistic view on hyper-dense heterogeneous and small cell networks. *IEEE Communications Magazine*, 51(6):20–27, June 2013.

[83] C.-L. I, C. Rowell, S. Han, Z. Xu, G. Li, and Z. Pan. Toward green and soft: a 5G perspective. *IEEE Communications Magazine*, 52(2):66–73, February 2014.

[84] C. Isheden, Z. Chong, E. A. Jorswieck, and G. Fettweis. Framework for link-level energy efficiency optimization with informed transmitter. *IEEE Transactions on Wireless Communications*, 11(8):2946–2957, August 2012.

[85] S. A. Jafar and A. Goldsmith. Transmitter optimization and optimality of beamforming for multiple antenna systems. *IEEE Transactions on Wireless Communications*, 3(4):1165–1175, July 2004.

[86] R. Jagannathan. On some pproperties of programming problems in parametric form pertaining to fractional programming. *Management Science*, 12(7), 1966.

[87] R. Jagannathan. Duality for nonlinear fractional programs. *Mathematical Methods of Operations Research*, 17(1):1–3, 1973.

[88] M. Jang, Y. Kwon, H. Park, and T. Hwang. Energy-efficient uplink power control for multiuser SIMO systems with imperfect channel state information. *EURASIP Journal on Wireless Communications and Networking*, 166(10.1186/1687-1499-2014-166), October 2014.

[89] C. Jiang and L. Cimini. Energy-efficient transmission for MIMO interference channels. *IEEE Transactions on Wireless Communications*, 12(6):2988–2999, June 2013.

[90] E. A. Jorswieck and H. Boche. Channel capacity and capacity-range of beamforming in MIMO wireless systems under correlated fading with covariance feedback. *IEEE Transactions on Wireless Communications*, 3(5):1543–1553, September 2004.

[91] E. A. Jorswieck and H. Boche. Majorization and matrix-monotone functions in wireless communications. *Now Publishers: Foundations and Trends in Communications and Information Theory*, 3(6):553–701, 2006.

[92] E. A. Jorswieck and E. G. Larsson. Monotonic optimization framework for the two-user MISO interference channel. *IEEE Transactions on Communications*, 58(7):2159–2168, July 2010.

[93] E. A. Jorswieck, E. G. Larsson, M. Luise, and H. V. Poor. Special issue on game theory in signal processing and communications. *IEEE Signal Processing Magazine*, 26(5), September 2009.

[94] E. A. Jorswieck, E. G. Larsson, M. Luise, H. V. Poor, and A. Leshem. Special issue on game theory in signal processing. *IEEE Journal of Selected Topics in Signal Processing*, 6(2), April 2012.

[95] E. A. Jorswieck and R. Mochaourab. *Mechanisms and games for dynamic spectrum allocation*, chapter Walrasian Model for Resource Allocation and Transceiver Design in Interference Networks. T. Alpcan, H. Boche, M. Honig, H. V. Poor (eds.), Cambridge University Press, 2013.

[96] E. A. Jorswieck, R. Mochaourab, and K. M. Ho. *Physical layer security in wireless communications*, chapter Game Theory for Physical Layer Security on Interference Channels. Sean Zhou, et al. (eds.), CRC Press, Boca Raton, FL, 2013.

[97] S. Kim, B. G. Lee, and D. Park. Energy-per-bit minimized radio resource allocation in heterogeneous networks. *IEEE Transactions on Wireless Communications*, 13(4):1862–1873, April 2014.

[98] I. Ku, C.-X. Wang, and J. Thompson. Spectral-energy efficiency tradeoff in relay-aided cellular networks. *IEEE Transactions on Wireless Communications*, 12(10):4970–4982, October 2013.

[99] E. G. Larsson, O. Edfors, F. Tufvesson, and T. L. Marzetta. Massive MIMO for next generation wireless systems. *IEEE Communications Magazine*, 52(2):186–195, February 2014.

[100] E. G. Larsson and E. A. Jorswieck. Competition versus cooperation on the MISO interference channel. *IEEE Journal on Selected Areas in Communications*, 26(7):1059–1069, September 2008.

[101] S. Lasaulce, Y. Hayel, R. El Azouzi, and M. Debbah. Introducing hierarchy in energy games. *IEEE Transactions on Wireless Communications*, 8(7):3833–3843, 2009.

[102] S. Lasaulce and H. Tembine. *Game Theory and Learning for Wireless Networks: Fundamentals and Applications.* Academic Press. Elsevier, 2011.

[103] L. Lei, Z. Zhong, C. Lin, and X. (S.) Shen. Operator controlled device-to-device communications in LTE-Advanced networks. *IEEE Wireless Communications*, 19(3):96–104, June 2012.

[104] G. Y. Li, S. Xu, A. Swami, N. Himayat, and G. Fettweis. Special issue on energy-efficient wireless communications. *IEEE Journal on Selected Areas in Communications*, 29(8), September 2011.

[105] G. Y. Li, Z.-K. Xu, C. Xiong, C.-Y. Yang, S.-Q. Zhang, Y. Chen, and S.-G. Xu. Energy-efficient wireless communications: tutorial, survey, and open issues. *IEEE Wireless Communications*, 18(6):28–35, December 2011.

[106] L. Liu, R. Zhang, and K. C. Chua. Achieving global optimality for weighted sum-rate maximization in the K-User Gaussian interference channel with multiple antennas. *IEEE Transactions on Wireless Communications*, 11(5):1933–1945, May 2012.

[107] R. A. Loodaricheh, S. Mallick, and V. Bhargava. Energy efficient resource allocation for OFDMA cellular networks with user cooperation and QoS provisioning. *IEEE Transactions on Wireless Communications*, 13(11):6132–6146, November 2014.

[108] A. Lozano, R. W. Heath, and J. G. Andrews. Fundamental limits of cooperation. *IEEE Transaction Information Theory*, 59(9):5213–5226, September 2013.

[109] J. Lv, A. Zappone, and E. A. Jorswieck. Energy-efficient MIMO underlay spectrum sharing with rate splitting. In *15th IEEE International Workshop on Signal Processing Advances in Wireless Communications (SPAWC 14)*, Toronto, Canada, June 2014.

[110] A. MacKenzie and L. DaSilva. *Game Theory for Wireless Engineers*. Morgan & Claypool Publishers, 2006.

[111] O. L. Mangasarian. Pseudo-convex functions. *SIAM Journal on Control*, 3(2):281–290, 1965.

[112] J. Mao, G. Xie, J. Gao, and Y. Liu. Energy efficiency optimization for cognitive radio MIMO broadcast channels. *IEEE Communications Letters*, 17(2):337–340, February 2013.

[113] B. R. Marks and G. P. Wright. A general inner approximation algorithm for non-convex mathematical programs. *Operations Research*, 26(4):681–683, 1978.

[114] A. W. Marshall and I. Olkin. *Inequalities: theory of majorization and its applications*. Academic Press New York, 1979.

[115] B. Martos. Hyperbolic programming. *Naval research logistic quarterly*, 11:135–165, 1964.

[116] T. L. Marzetta. Noncooperative cellular wireless with unlimited numbers of base station antennas. *IEEE Transactions on Wireless Communications*, 9(11):3590–3600, November 2010.

[117] B. Matthiesen, A. Zappone, and E. A. Jorswieck. Design of 3-way relay channels for throughput and energy efficiency. *IEEE Transactions on Wireless Communications*, PP(99), 2014.

[118] F. Meshkati, M. Chiang, H. V. Poor, and S. C. Schwartz. A game-theoretic approach to energy-efficient power control in multicarrier CDMA systems. *IEEE Journal on Selected Areas in Communications*, 24(6):1115–1129, June 2006.

[119] F. Meshkati, A. J. Goldsmith, H. V. Poor, and S. C. Schwartz. A game-theoretic approach to energy-efficient modulation in CDMA networks with delay QoS constraints. *IEEE Journal on Selected Areas in Communications*, 25(6):1069–1078, August 2007.

[120] F. Meshkati, H. V. Poor, S. C. Schwartz, and N. B. Mandayam. An energy-efficient approach to power control and receiver design in wireless data networks. *IEEE Transactions on Communications*, 53(11):1885–1894, November 2005.

[121] F. Meshkati, S. C. Schwartz, and H. V. Poor. Energy-efficient resource allocation in wireless networks. *IEEE Signal Processing Magazine*, 24(3):58–68, May 2007.

[122] G. Miao, N. Himayat, G. Y. Li, and S. Talwar. Distributed interference-aware energy-efficient power optimization. *IEEE Transactions on Wireless Communications*, 10(4):1323–1333, April 2011.

[123] J. Mo and J. Walrand. Fair end-to-end window-based congestion control. *IEEE/ACM Transactions on Networking*, 8(5):556–567, October 2000.

[124] D. Monderer and L. S. Shapley. Potential games. *Games and economic behavior*, 14:124–143, 1996.

[125] R. B. Myerson. *Game theory: analysis of conflict*. Harvard University Press, 1997.

[126] D. W. K. Ng, E. S. Lo, and R. Schober. Energy-efficient resource allocation for secure OFDMA systems. *IEEE Transactions on Vehicular Technology*, 61(6):2572–2585, July 2012.

[127] D. W. K. Ng, E. S. Lo, and R. Schober. Energy-efficient resource allocation in multi-cell OFDMA systems with limited backhaul capacity. *IEEE Transactions on Wireless Communications*, 11(10):3618–3631, October 2012.

[128] D. W. K. Ng, E. S. Lo, and R. Schober. Energy-efficient resource allocation in OFDMA systems with large numbers of base station antennas. *IEEE Transactions on Wireless Communications*, 11(9):3292–3304, September 2012.

[129] D. Nguyen, L.-N. Tran, P. Pirinen, and M. Latva-aho. Precoding for full duplex multiuser MIMO systems: Spectral and energy efficiency maximization. *IEEE Transactions on Signal Processing*, 61(16):4038–4050, August 2013.

[130] N. Nisan, T. Roughgarden, E. Tardos, and V. V. Vazirani. *Algorithmic Game Theory*. Cambridge University Press, 2007.

[131] O. Onireti, F. Heliot, and M. A. Imran. On the energy efficiency-spectral efficiency trade-off of distributed MIMO systems. *IEEE Transactions on Communications*, 61(9):3741–3753, September 2013.

[132] M. J. Osborne and A. Rubinstein. *A Course in Game Theory*. The MIT Press, 1994.

[133] J. S. Pang, G. Scutari, F. Facchinei, and C. Wang. Distributed power allocation with rate constraints in Gaussian parallel interference channels. *IEEE Transactions on Information Theory*, 54(8):3471–3489, August 2008.

[134] J. S. Pang, G. Scutari, D. P. Palomar, and F. Facchinei. Design of cognitive radio systems under temperature-interference constraints: A variational inequality approach. *IEEE Transactions on Signal Processing*, 58(6):3251–3271, June 2010.

[135] C. Papadimitriou. Algorithms, games, and the internet. In *STOC '01: Proceedings of the thirty-third annual ACM symposium on Theory of computing*, pages 749–753, New York, NY, USA, 2001. ACM.

[136] J. Papandriopoulos and J. S. Evans. Low-complexity distributed algorithms for spectrum balancing in multi-user DSL networks. In *Proc. 2006 IEEE International Conference on Communications*, pages 3270–3275, Istanbul, Turkey, June 2006.

[137] Y. Pei, Y.-C. Liang, K. C. Teh, and K. H. Li. Energy-efficient design of sequential channel sensing in cognitive radio networks: Optimal sensing strategy, power allocation, and sensing order. *IEEE Journal on Selected Areas in Communications*, 29(8):1648–1659, September 2011.

[138] H. J. M. Peters. *Axiomatic Bargaining Game Theory*. Kluwer Academic Publishers, 1992.

[139] P. Phunchongharn, E. Hossain, and D. I. Kim. Resource allocation for device-to-device communications underlaying LTE-Advanced networks. *IEEE Wireless Communications*, 20(4):91–100, August 2013.

[140] N. T. H. Phuong and H. Tuy. A unified monotonic approach to generalized linear fractional programming. *Journal of Global Optimization*, 26:229–259, 2003.

[141] P. S. Raghavendra and B. Daneshrad. An energy-efficient water-filling algorithm for OFDM systems. In *2010 IEEE International Conference on Communications (ICC)*, pages 1–5, May 2010.

[142] P. Ren, Y. Wang, and Q. Du. CAD-MAC: A channel-aggregation diversity based MAC protocol for spectrum and energy efficient cognitive ad hoc networks. *IEEE Journal on Selected Areas in Communications*, 32(2):237–250, February 2014.

[143] S. Ren and M. van der Schaar. Pricing and distributed power control in wireless relay networks. *IEEE Transactions on Signal Processing*, 59(6):2913–2926, June 2011.

[144] R. Ródenas, M. López, and D. Verastegui. Extensions of Dinkelbach's algorithm for solving non-linear fractional programming problems. *Springer Top: An Official Journal of the Spanish Society of Statistics and Operations Research*, 7(1):33–70, June 1999.

[145] F. Roemer, M. Haardt, and E. A. Jorswieck. Efficient spatial processing and resource allocation for amplify and forward two-way relaying. In *Cross Layer Designs in WLAN Systems*. Troubador Publishing Ltd, June 2011.

[146] A. Rubinov, H. Tuy, and H. Mays. An algorithm for monotonic global optimization problems. *Optimization*, 49:205–221, 2001.

[147] F. Rusek, D. Persson, B. K. Lau, E. G. Larsson, T. L. Marzetta, O. Edfors, and F. Tufvesson. Scaling up MIMO: Opportunities and challenges with very large arrays. *IEEE Signal Processing Magazine*, 30(1):40–60, January 2013.

[148] C. U. Saraydar, N. B. Mandayam, and D. J. Goodman. Pricing and power control in a multicell wireless data network. *IEEE Journal on Selected Areas in Communications*, 19(10):1883–1892, October 2001.

[149] S. Schaible. Parameter-free convex equivalent and dual programs of fractional programming problems. *Zeitschrift für Operations Research*, 18(5):187–196, October 1974.

[150] S. Schaible. Duality in fractional programming: A unified approach. *Operations Research*, 24:452–461, 1976.

[151] S. Schaible. Fractional programming. I, duality. *Management Science*, 22(8):858–867, 1976.

[152] S. Schaible. Fractional programming. II, on Dinkelbach's algorithm. *Management Science*, 22(8):868–873, 1976.

[153] S. Schaible. Bibliography in fractional programming. *Zeitschrift für Operations Research*, 26(7), 1982.

[154] G. Scutari, D. P. Palomar, and S. Barbarossa. The MIMO iterative waterfilling algorithm. *IEEE Transactions on Signal Processing*, 57(5):1917–1935, May 2009.

[155] Q. Shi, M. Razaviyayn, Z. Q. Luo, and C. He. An Iteratively Weighted MMSE Approach to Distributed Sum-Utility Maximization for a MIMO Interfering Broadcast Channel. *IEEE Transactions on Signal Processing*, 59(9):4331–4340, September 2011.

[156] D. S. Shiu, G. J. Foschini, M. J. Gans, and J. M. Kahn. Fading correlation and its effect on the capacity of multielement antenna systems. *IEEE Transactions on Communications*, 48(3):502–513, March 2000.

[157] S. Sirinivasa and S. A. Jafar. Cognitive radios for dynamic spectrum access - the throughput potential of cognitive radio: a theoretical perspective. *IEEE communications Magazine*, 45(5):73–79, 2007.

[158] A. Soysal and S. Ulukus. Optimum power allocation for single-user MIMO and multi-user MIMO-MAC with partial CSI. *IEEE Journal on Selected Areas in Communications*, 25(7):1402–1412, September 2007.

[159] A. Soysal and S. Ulukus. Optimality of beamforming in fading MIMO multiple access channels. *IEEE Transactions on Communications*, 57(4):1171–1183, April 2009.

[160] C. Sun and C. Yang. Energy efficiency analysis of one-way and two-way relay systems. *EURASIP Journal on Wireless Communications and Networking*, pages 1–18, February 2012.

[161] I. E. Telatar. Capacity of multi-antenna Gaussian channels. *European Transactions on Telecommunications*, 10(6):585–595, 1999.

[162] M. L. Treust and S. Lasaulce. A repeated game formulation of energy-efficient decentralized power control. *IEEE Transactions on Wireless Communications*, 9(9):2860–2869, September 2010.

[163] K. T Truong, P. Sartori, and R. W. Heath. Cooperative algorithms for MIMO amplify-and-forward relay networks. *IEEE Transactions on Signal Processing*, 61(5):1272–1287, March 2013.

[164] D. Tse and P. Viswanath. *Fundamentals of Wireless Communications*. Cambridge University Press, 2005.

[165] A. M. Tulino and S. Verdú. Random matrix theory and wireless communications. *Now Publishers: Foundations and Trends in Communications and Information Theory*, 1(1):1–182, June 2004.

[166] H. Tuy. *Convex Analysis and Global Optimization (Nonconvex Optimization and Its Applications)*. Kluwer Academic Publishers, Dordrecht, 1998.

[167] H. Tuy. Monotonic optimization. *SIAM Journal on Optimization*, 11(2):464–494, 2000.

[168] W. Utschick and J. Brehmer. Monotonic optimization framework for coordinated beamforming in multicell networks. *IEEE Transactions on Signal Processing*, 60(4):1899–1909, April 2012.

[169] V. Varma, S. Lasaulce, M. Debbah, and S. Elayoubi. An energy efficient framework for the analysis of MIMO slow fading channels. *IEEE Transactions on Signal Processing*, 61(10):2647–2659, May 2013.

[170] L. Venturino, N. Prasad, and X. Wang. Coordinated scheduling and power allocation in downlink multicell OFDMA networks. *IEEE Transactions on Vehicular Technology*, 58(6):2835–2848, July 2009.

[171] L. Venturino, A. Zappone, C. Risi, and S. Buzzi. Energy-efficient scheduling and power allocation in downlink OFDMA networks with base station coordination. *IEEE Transactions on Wireless Communications*, 14(1):1–14, January 2015.

[172] S. Verdú. *Multiuser detection*. Cambridge Univ Press, 1998.

[173] S. Verdú. Spectral efficiency in the wideband regime. *IEEE Transactions on Information Theory*, 48(6):1319–1343, June 2002.

[174] Y. Wang, W. Xu, K. Yang, and J. Lin. Optimal energy-efficient power allocation for OFDM-based cognitive radio networks. *IEEE Communications Letters*, 16(9):1420–1423, 2012.

[175] S. Weber and J. G. Andrews. Transmission capacity of wireless networks. *Now Publishers: Foundations and Trends in Communications and Information Theory*, 5(2–3):109–281, 2012.

[176] X. Xiao, X. Tao, and J. Lu. QoS-aware energy-efficient radio resource scheduling in multi-user OFDMA systems. *IEEE Communications Letters*, 17(1):75–78, January 2013.

[177] X. Xiao, X. Tao, and J. Lu. Energy-efficient resource allocation in LTE-based MIMO-OFDMA systems with user rate constraints. *IEEE Transactions on Vehicular Technology*, PP(99):1–1, 2014.

[178] J. Xu and L. Qiu. Energy efficiency optimization for MIMO broadcast channels. *IEEE Transactions on Wireless Communications*, 12(2):690–701, February 2013.

[179] Q. Xu, X. Li, H. Ji, and X. Du. Energy-efficient resource allocation for heterogeneous services in OFDMA downlink networks: Systematic perspective. *IEEE Transactions on Vehicular Technology*, 63(5):2071–2082, June 2014.

[180] R. D. Yates. A framework for uplink power control in cellular radio systems. *IEEE Journal on Selected Areas in Communications*, 13(7):1341–1347, September 1995.

[181] F. R. Yu, X. Zhang, and V. C. Leung. *Green Communications and Networking*. CRC Press, 2012.

[182] A. Zappone, G. Alfano, S. Buzzi, and M. Meo. Distributed energy-aware resource allocation in multi-antenna multi-carrier interference networks with statistical CSI. *EURASIP Journal on Wireless Communications and Networking*, 1:1–16, 2013.

[183] A. Zappone, S. Buzzi, and E. A. Jorswieck. Energy-Efficient power control and receiver design in relay-assisted DS/CDMA wireless networks via game theory. *IEEE Communications Letters*, 15(7):701–703, July 2011.

[184] A. Zappone, P. Cao, and E. A. Jorswieck. Energy Efficiency Optimization in Multiuser Relay-Assisted MIMO Systems. In *Asilomar Conference on Signals, Systems, and Computers*, Pacific Grove, CA, USA, November 2013.

[185] A. Zappone, P. Cao, and E. A. Jorswieck. Energy efficiency optimization in relay-assisted MIMO systems with perfect and statistical CSI. *IEEE Transactions on Signal Processing*, 62(2):443–457, January 2014.

[186] A. Zappone, P. Cao, and E. A. Jorswieck. Energy efficiency optimization with statistical CSI in two-hop MIMO systems. *IEEE Signal Processing Letters*, 21(11):1398–1402, November 2014.

[187] A. Zappone, Z. Chong, E. A. Jorswieck, and S. Buzzi. Energy-aware competitive power control in relay-assisted interference wireless networks. *IEEE Transactions on Wireless Communications*, 12(4):1860–1871, April 2013.

[188] A. Zappone and E. A. Jorswieck. Tutorial: Energy efficiency in 5G heterogeneous and small-cell wireless networks. In *11th International Symposium on Wireless Communication Systems (ISWCS 14)*, Barcelona, Spain, August 2014.

[189] A. Zappone, E. A. Jorswieck, and S. Buzzi. Competitive energy-aware resource allocation in two-hop multiple-antenna interference networks. In *IEEE Wireless Communications and Networking Conference (WCNC 14)*, Istanbul, Turkey, April 2014.

[190] A. Zappone, E. A. Jorswieck, and S. Buzzi. Energy efficiency and interference neutralization in two-hop MIMO interference channels. *IEEE Transactions on Signal Processing*, 62(24):6481–6495, December 2014.

[191] A. Zappone, P. H. Lin, and E. A. Jorswieck. Energy efficiency in secure multi-antenna systems. *IEEE Transactions on Signal Processing, submitted, http://arxiv.org/abs/1505.02385*, 2015.

[192] A. Zappone, L. Sanguinetti, G. Bacci, E. A. Jorswieck, and M. Debbah. Energy-efficient power control: A look at 5G wireless technologies. *IEEE Transactions on Signal Processing, submitted, http://arxiv.org/abs/1503.04609*, 2015.

[193] E. Zhang, S. Yin, L. Yin, and S. Li. Energy-efficient link adaptation for cognitive radios with heterogeneous QoS requirements. In *8th International Conference on Cognitive Radio Oriented Wireless Networks (CROWNCOM 2013)*, pages 263–268, July 2013.

[194] H. Zhang, A. Gladisch, M. Pickavet, Z. Tao, and W. Mohr. Special issue on energy efficiency in communications. *IEEE Communications Magazine*, 48(11), November 2010.

[195] R. Zhang, Y.-C. Liang, and S. Cui. Dynamic resource allocation in cognitive radio networks. *IEEE Signal Processing Magazine*, 27(3):102–114, May 2010.

[196] Y. J. Zhang, L. Qian, and J. Huang. Monotonic optimization in communication and networking systems. *Now Publishers: Foundations and Trends in Networking*, 7(1):1–75, 2012.

[197] Z. Zhou, M. Dong, K. Ota, J. Wu, and T. Sato. Distributed interference-aware energy-efficient resource allocation for device-to-device communications underlaying cellular networks. In *Proc. IEEE Global Communication Conference (GLOBECOM)*, 2014.